CONTROLLED OXIDATIVE LEACHING TECHNIQUE FOR ARSENIFEROUS URANIUM AND OTHER ORES

Final Report

by

G.P. Demopoulos and P. Kondos
Department of Mining and Metallurgical Engineering
McGill University
Montreal, Quebec

Work on the project was conducted under the auspices of the Canada Centre for Mineral and Energy Technology, Energy, Mines and Resources Canada.

DSS File No. 22ST. 23440-4-9067

DSS Contract Serial No. OST84 - 00138

MICROMEDIA

202 pp

TABLE OF CONTENTS

Page

Executive Summary

Resumé

1. INTRODUCTION 1
    1.1 The Radium Problem in Uranium Milling 1
    1.2 The Pressure Chloride Leaching System 3
    1.3 Objectives and Project Elements 5

2. LEACHING CHEMISTRY OF ARSENIC 7
    2.1 Scope 7
    2.2 Solution Chemistry 8
    2.3 Experimental Results 11
        2.3.1 Ferric Ion Leaching System 11
        2.3.2 Pressure Leaching System 15
    2.4 Discussion 19
        2.4.1 Ferric Ion Leaching System 19
        2.4.2 Pressure Leaching System 21
    2.5 Summary 24

3. PRESSURE CHLORIDE LEACHING OF THE KEY LAKE URANIUM ORE 26
    3.1 Scope 26
    3.2 Statistical Design and Modelling 27
        3.2.1 Selection of Process Variables 27
        3.2.2 Selection of Statistical Design 30

Page

3.3 Experimental 37

3.3.1 Ore 37
3.3.2 Apparatus 39
3.3.3 Procedure 40

3.4 Results and Discussion 42

3.4.1 Ore Reactivity 45
3.4.2 Model Equations 54
3.4.3 Metallurgical Analysis 63

3.4.3.1 Study of the Response: % Uranium Extraction 65
3.4.3.2 Study of the Response: % Radium Extraction 87
3.4.3.3 Study of the Response: % Nickel Extraction 101
3.4.3.4 Study of the Response: % Arsenic Extraction 116
3.4.3.5 Study of the Response: Acid Consumption (moles/l) 126
3.4.3.6 Study of the Response: Pressure Leach EMF (mV) 137
3.4.3.7 Optimum Leaching Conditions and Conceptual Flowsheet 141

4. RADIUM EXTRACTION: THE ROLE OF CALCIUM CHLORIDE 153

4.1 Scope 153
4.2 Estimation of the Solubility of $RaSO_4$ 154
4.3 The Role of $CaCl_2$ 160

5. CONCLUSIONS - RECOMMENDATIONS 168

5.1 Conclusions 168
5.2 Recommendations 171

Page

6. APPENDICES 173

- 6.1 Innovations in Chemical Analysis 173
  - 6.1.1 Determination of Arsenic (III) 173
  - 6.1.2 Free Acid Determination 175
- 6.2 The "Reduced Activity Coefficient" Method 176

7. REFERENCES 188

Executive Summary

The present uranium leaching practice results only in uranium recovery with the other radionuclides and in particular Ra^{226} - the most notorious of all - remaining in the leach residues. Serious concerns arise from the presence of these radionuclides in the millions of tons of tailings produced every year and the possibility of gradual escape to the environment. The problem of long-term management of radioactive tailings is even more acute in the case of high grade arseniferous uranium ores of N. Saskatchewan. A radical solution to this problem is to modify the uranium milling process with the purpose of solubilizing radium along with uranium and isolating the former within the mill complex. This approach has been investigated here.

In particular the simultaneous extraction of uranium and radium from a complex (U-Ra-Ni-As) and high grade uranium ore (Key Lake deposit) has been investigated by employing a novel leaching system: O_2-$CaCl_2$-HCl. The experimental programme has involved (i) the experimental study of the aqueous chemistry of arsenic relevant to the present leaching system, (ii) the execution of a series of statistically designed experiments and the development of comprehensive model equations for optimization purposes. The experiments were conducted in the following region of conditions: 0.33 kg solids/1 soln. $\leqslant$ slurry density $\leqslant$ 1.0 kg/1; 0.5 N $\leqslant [HCl]_o \leqslant$ 1.5 N; 1.5 M $\leqslant [CaCl_2]_o \leqslant$ 3.5 M and 2 hrs

$\leq$ Time $\leq$ 6 hrs. Temperature and oxygen pressure were kept constant at 68°C and 75 psi respectively.

The following optimum leaching conditions were identified offering almost complete (> 99%) U and Ra co-extraction: 0.33 kg solids/l, 1.0 M $[HCl]_o$, 1.5 M $[CaCl_2]_o$ and 2 hours. For these conditions nickel and arsenic extractions were 64% and 58% respectively while the following reagent consumptions were found: 12 kg HCl/ton ore and 1.4 kg CaO/ton ore. Further increase in nickel extraction is not justified since it results in excessively high acid consumption values and long leaching times. This being due to the different leachability of the U/Ra and Ni carrier minerals.

The solubility of $RaSO_4$ has been estimated and the role of calcium chloride in enhancing radium extraction has been quantified. The potential usefulness of applying this leaching system to the treatment of other arseniferous materials has been indicated. Further work on the removal of arsenic from the leach liquor by H_2S precipitation and the recycling of the leach medium $CaCl_2$/HCl is recommended.

Résumé

Le procédé actuel de lixiviation des minerais d'uranium ne permet que la récupération de l'uranium, les autres radioéléments, tels que le Radium 226, restant dans les résidus de la lixiviation.

La présence de ces composés radioactifs dans des millions de tonnes de déchets, pouvant graduellement se disperser dans l'environnement, pose de sérieux problèmes.

Le problème de la gestion à long terme de ces déchets radioactifs devient même grave dans le cas des minerais arséneferreux provenant du nord de la province de Saskatchewan car its contiennent de hauts niveaux d'uranium.

Une solution radicale à ce problème consiste à modifier le procédé de traitement de l'Uranium afin de solubiliser le radium avec l'uranium et d'isoler ce dernier dans une usine de concentrateurs. Cette approche est envisagée dans cette étude.

En particulier, l'extraction simultanée de l'Uranium et du radium à partir d'un minerai complexe d'Uranium (U-Ra-Ni-As), provenant du dépot de Key Lake, est étudiée à l'aide du nouveau système de lixiviation O_2-$CaCl_2$-HCl.

Le programme de recherches expérimentales impliqua d'une part l'étude des solutions chimiques aqueuses d'arsenic en rapport avec le système de lixiviation mentionné ci dessus, et d'autre part la réalisation d'une série d'expériences planifiées selon une méthodologie statistique choisies et le développement d'équations rendant compte du modèle, ceci dans le but d'optimiser le procédé.

Les expériences furent faites dans les conditions suivantes:

.33 kg solide/l $\leqslant$ densité de la pulp $\leqslant$ 1 kg solide/l
$0.5N \leqslant |HCl|_o \leqslant 1.5$ N
1.5 M $\leqslant |CaCl_2|_o \leqslant 3.5$ M
2 heures $\leqslant$ temps $\leqslant$ 6 heures

La température et la pression furent maintenues constantes à 68°C et 75 psi respectivement.

Les conditions offrants une extraction presque complète de l'Uranium et du Radium (supérieure à 99%) sont les suivantes:
.33 kg de composés solide par litre
concentration initiale de HCl de 1 M
concentration initiale de $CaCl_2$ de 1.5 M
durée de la lixiviation: deux heures.

Dans ces conditions, les pourcentages d'extraction du Nickel et de l'Arsenic sont 64% et 58% respectivement tandis que la

consommation des réactifs est de 12kg par tonne de minerai pour HCl et 1.4 kg par tonne de minerai pour CaO. Un pourcentage d'extration du Nickel plus élevé ne se justifie par dans la mesure su il en résulterait une consommation excessivement importante d'acide et des temps de lixiviation trop longs. Ceci provient de la lixiviabilité différente des minerais U-Ra et Ni.

La solubilité du $RaSO_4$ est estimée et le role de $CaCl_2$ dans l'augmentation du pourcentage d'extraction du Radium est quantifiée. L'utilité et l'application potentielles de ce nouveau système de lixiviation pour le traitement d'autres minerais arsenoferreux sont mentionnées. L'extension des recherches vers la possibilité d'enlever l'As des solutions de lixiviation par précipitation de H_2S et le recyclage du milieu de lixiviation sont recommandées.

1. INTRODUCTION

1.1 The Radium Problem in Uranium Milling

Present methods of extracting uranium from its ores involve leaching with sulphuric acid or alkaline solutions, depending upon the ore mineralogy (1). In fact, the sulphuric acid leaching route is the preferred one among most of the world-wide uranium extraction plants and the sole method used in Canada. Present practice though, using H_2SO_4 leaching (either atmospheric or pressure), results only in uranium recovery with the other radionuclides (Ra^{226}, Th^{230}, Pb^{210}) and in particular Ra^{226} - the most notorious of all - remaining largely in the leach residue (2). Serious concerns arise from the presence of these radionuclides in the millions of tons of tailings produced every year and the possibility of their gradual escape to the environment. During the operating life of the mill complex, containment of the radionuclides is accomplished with the application of improved tailings management techniques (3)(4). However due to the long half-life of radium-226 (1620 years) these radioactive tailings need to be managed for centuries after the closure of the producing mills. This remains as yet an unsolved problem. In response to these serious environmental issues the Canadian Government established the National Uranium Tailings Program (5) to look into the overall problem. In Canada today there are over 100 million tonnes of uranium tailings, a figure that could triple by the end of the century. Most of these tailings are located in the Elliot Lake area of Ontario. The problem of long-term management of radioactive tailings is even more acute in the case of the high grade ores (~2% U) which were discovered in the early 1970's in Northern Saskatchewan. Thus the Key Lake uranium mill, the largest in the world (6)(7), produces tailings containing radium at a level of about 6000 pCi/g while the Elliot Lake tailings contain 300-400 pCi/g. The environmentally acceptable limit for solids is 25-30 pCi/g (8)(9).

To overcome the problem of long-term tailings management, modification of the uranium milling process has been proposed with the objective of developing an alternative leaching system capable of achieving simultaneous extraction of uranium and radium (10)(11). By solubilizing radium along with uranium, it would then be possible to isolate radium within the mill complex in a small mass concentrate that could be subsequently disposed of in a more controlled manner. For example in 1982 there were approximately 8,000,000 tonnes of uranium tailings produced in Canada. These tailings will be a continual source of radioactivity for centuries to come. If, alternatively, radium had been isolated through a solubilization process a concentrate of only about 3.0 kg would have been produced which could then be disposed of along with the high level radioactive wastes originating from nuclear plants. Disposal of the latter wastes in deep geologic formations is considered, on a long-term basis, as being less of a hazard than uranium mill tailings disposal on the surface (12). In addition the amount of radium to be isolated from uranium milling operations is very small as compared to the quantities of high level wastes produced every year by the nuclear industry.

Due to the insolubility of $RaSO_4$ it is apparent that an appropriate leaching system would have to use a different leachant than H_2SO_4 to achieve simultaneous solubilization of uranium and radium. Nitrate and chloride media are the logical alternatives to conventional sulphuric acid. Both routes have been attempted in the past, but only with limited success. References 13 to 16 describe nitrate leaching investigations. The majority of the investigations though have used HCl based media; thus references 8, 13 and 17 to 19 describe HCl leaching investigations while reference 20 describes the use of $FeCl_3$ as Ra leachant. Those references reported varying degrees of success. In general it was found that sulphide minerals present in the U-ore adversely affect Ra extraction on one hand while on the other, very poor Ra recoveries were obtained in the case of the complex U-Ra-Ni-As ores of N. Saskatchewan.

1.2 The Pressure Chloride Leaching System

In addition to ambient pressure leaching systems, leaching under oxygen over-pressure could be an alternative system too. Investigations initiated by Demopoulos back in 1982 when he was working at CANMET as a visiting scientist, have in fact examined this approach as a possible route for achieving simultaneous extraction of uranium and radium. In the initial stage of these investigations involving treatment of a pyritic uranium ore from Elliot Lake, Ontario, it was found that pressure leaching in a calcium chloride medium was a very effective method for U and Ra coextraction in a single stage (21). Subsequently the same leaching approach was successfully applied to an arseniferous high grade U ore (Midwest) of N. Saskatchewan (22). Leach residues containing less than 40 pCi/g Ra were produced from both ores. In view of the omnivorous nature of the new leaching approach a patent application was recently filed in Canada (23).

The pressure chloride leaching ($O_2/CaCl_2/HCl$) though of the complex ores of N. Saskatchewan is greatly complicated due to their high As content. Arsenic is present in the form of nickel arsenide minerals. During leaching arsenic gets oxidized and reports in the solution. In view of the limited solubility enjoyed by this element several metal-arsenic compounds might precipitate creating thus serious processing problems. As a result high acid additions are required to maintain oxidized arsenic soluble during leaching. Thus the earlier investigations (22) involving leaching of Midwest ore had to employ very high HCl concentrations to overcome the As precipitation problem. Furthermore from these early investigations it became apparent that a complex correlation existed among the process parameters (HCl conc, $CaCl_2$ conc, slurry density, etc.) and U, Ra, and Ni co-extraction, that rendered optimisation of the process a very difficult task.

1.3 Objectives and Project Elements

In view of these unique processing problems encountered with the pressure chloride leaching of the arseniferous U ores of N. Saskatchewan on one hand and the economic and ecological importance of these ores on the other, it was decided the work described in this report to be undertaken with the overall objective of optimizing the coextraction of U and Ra. Process optimization was sought via two complementary routes:

(1) By studying the speciation (i.e. formation of As(III) and/or As(V) species in solution) of arsenic under simulated U-leaching conditions with the purpose of devising possible control action in order to alleviate the As(V) precipitation problem - Phase I.

(2) By applying response surface methodology (computer-aided statistical design) with the purpose of developing mathematical models to simulate and optimize the process - Phase II.

The findings of Phase I are discussed in Chapter 2 of this report while the findings of Phase II are discussed in Chapter 3. In relation to the above project elements innovative work was done in two additional fronts: (a) theoretical studies were done to elucidate the role of $CaCl_2$ on radium extraction (Chapter 4) and (b) development of special analytical techniques for the determination of As(III) and free acid concentration in concentrated leach solutions (Appendix 6). Finally a number of conclusions-recommendations are made (Chapter 5) concerning the treatment of arseniferous uranium (in particular) and other ores (in general) with pressure chloride leaching.

2. LEACHING CHEMISTRY OF ARSENIC

2.1 Scope

In this part of the work, particulate samples of several nickel arsenide minerals (niccolite, $NiAs$; rammelsbergite, $NiAs_2$; and gersdorffite, $NiAsS$) were subjected to oxidative leaching using sulphate and chloride media. These minerals were chosen since they represent most of the arsenic content of the complex U ores of N. Saskatchewan. Conditions simulating the atmospheric ($Fe(III)$) and pressure (O_2) leaching stages of the process flowsheet currently operated at the Key Lake plant (6) were investigated. Both the conventional sulphate and the alternative chloride (advocated here) leaching systems were evaluated for comparison purposes.

The purpose of this work was twofold: (i) to establish the relative leachability of these minerals and (ii) to determine the oxidation state of the dissolved arsenic as a function of the applied conditions. These two aspects of the solution chemistry of arsenic had to be understood prior to attempting to control the respective oxidation reactions as a means of avoiding the troublesome arsenic precipitation problem. In particular arsenic precipitation during leaching could result among others in the following processing problems: loss of valuable metal, loss of oxidant, difficulties in solid/liquid separation, and solution purification complications.

2.2 Solution Chemistry

The term solution chemistry as it is used here encompasses the dissolution behaviour of arsenide minerals, the distribution of As(III) and As(V) species in solution (speciation), and the solubility of various metal-arsenic compounds. The latter aspect of aqueous chemistry of arsenic has been extensively studied in recent years primarily by Robins in Australia and Nishimura and Tozawa in Japan and lately by Ettel et al of INCO. The solubilities of a number of As(V) and As(III) compounds have been determined and appropriate thermodynamic diagrams were constructed (24). Moreover the significance of these diagrams to the environmental stability of arsenic has been one of the major themes in a recent hydrometallurgical meeting in Canada (25). However, considerably less work has been reported in literature on the other two aspects of the aqueous chemistry of arsenic, i.e. dissolution and speciation.

The leaching of niccolite (NiAs) in $FeCl_3$ media has been studied by Dutrizac and Morrison (26), who reported this arsenide mineral to dissolve readily yielding As(III) instead of As(V) in solution. No similar studies appear to have been reported in literature for the other arsenide minerals. Weir and Masters (6) in their report describing the developmental work for the Key Lake uranium process have postulated that NiAs and NiAsS are oxidized in both ferric sulphate and O_2/H_2SO_4 systems to yield primarily As(V) in solution. No direct experimental evidence though was provided. They also reported NiAs to be readily leached again, in contrast to NiAsS which was found to dissolve only at elevated temperatures and pressures. No information as to the dissolution of rammelsbergite ($NiAs_2$) has been reported.

The acidic-oxidizing portion of the Eh-pH diagram for the As-H_2O system is shown in Fig. 1. As can be seen, the two aqueous arsenic species of interest to the present work are H_3AsO_3 and H_3AsO_4. In dilute (0.1 - 1.0 N) acid solutions (H_2SO_4 or HCl) such as those used in the present study no complexes of As(III) and As(V) with the matrix anion are known to form (27)(28).

The standard reduction potential for H_3AsO_4/H_3AsO_3 is 0.56 volts, therefore at least according to thermodynamics, for oxidative leaching systems with higher potentials, H_3AsO_4 would be expected to form. To evaluate the oxidizing power of the three oxidants used here (i.e. Fe(III), $NaClO_3$, and O_2) the oxidation state diagram of Fig. 2 was constructed. It is evident that all three oxidants are expected to favour the formation of As(V).

As was discussed earlier the oxidation state of arsenic has a direct impact on the ease of precipitation of this element. To illustrate this behaviour the solubility diagram of Fig. 3 was constructed with the use of data reported by Robins (24,25). In this diagram the precipitation domains for the As(III) and As(V) compounds of Fe(II and III) and Ni(II) are compared. It can be

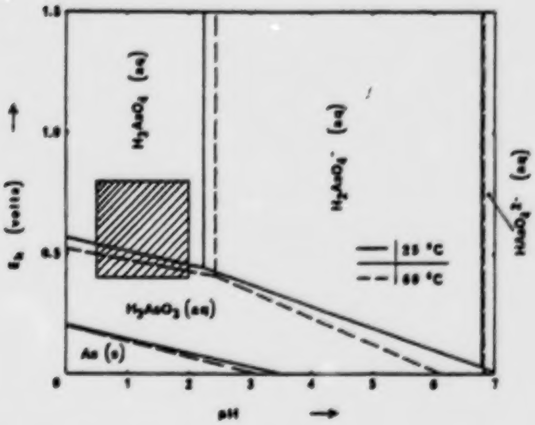

Fig. 1 E_h-pH diagram for the As-H_2O system (10^{-2}M).

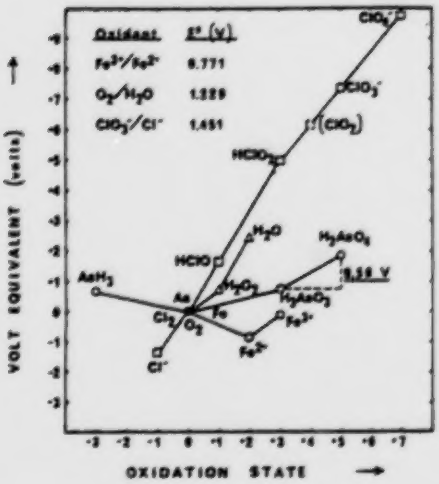

Fig. 2 Oxidation state diagram for As, Fe, O and Cl.

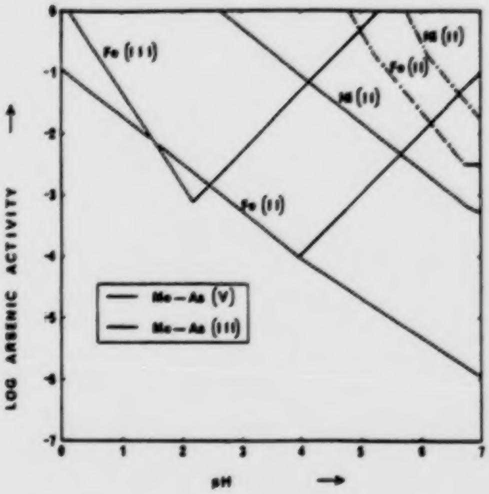

Fig. 3 The stability regions for the arsenites and arsenates of Fe and Ni at equal activities (25°C).

clearly seen that the As(III) compounds are soluble in the acidic region as opposed to the corresponding As(V) compounds and especially those of iron. Since the formation of iron arsenate is endothermic in nature (29) more severe precipitation is expected at the elevated temperatures employed in actual leaching processes.

2.3 Experimental Results

Characterization information on the arsenide minerals used in this study are given in Table 1. All other chemicals used were of analytical grade. 1-2g/l of closely sized particulate mineral samples were subjected to leaching. AA spectrophotometry was used for total element solution analysis while for the determination of As(III), an analytical technique was established using ion exchange resins for the separation of the arsenic species from the metal cations followed by titration of As(III) with potassium bromate (see Appendix 6.1.1). The EMF of the leach solutions was directly monitored in both atmospheric and pressure systems using redox combination electrodes. All potentials are reported here with reference to SHE (i.e. E_h).

2.3.1 Ferric Ion Leaching System

Typical dissolution curves obtained for the three arsenide minerals are shown in Fig. 4. In this series of tests temperature was varied from 30 to 90°C, Fe(III) concentration

Table 1. Description of minerals used in this investigation

	Niccolite	Rammelsbergite	Gersdorffite
Source	Moose Horn Mine Elk Lake, Ontario	Bischophofen Austria	Bischophofen Austria
XRD pattern	NiAs-Hexagonal	$NiAs_2$-Orthorhombic	NiAsS-Cubic
Ni:As molar ratio	1:1.034	1:2	1:1.054
Purity (%)	97%	82%	71%
Impurities	+ minor carbonates	5% SiO_2 0.17% Fe 1.84% Co + minor carbonates	25% SiO_2 1.24% Fe 0.28% Co + minor carbonates

Table 2. Ferric ion leaching of nickel arsenide minerals - additional data on arsenic speciation (1.0 M Fe(III))

		% As(III) FORMATION				
		NiAs		$NiAs_2$		NiAsS
Temp. (°C)	Time (min)	H_2SO_4	HCl	H_2SO_4	HCl	HCl
45	30	97.9	-	90.6	92.1	n.d.
	120	-	-	-	-	n.d.
	180	-	-	93.4	100	-
	360	-	-	92.9	96.2	-
60	30	100	100	-	-	n.d.
	120	-	-	-	87.0	3.4
	180	98.0	92.0	-	-	-
	360	93.9	85.1	-	-	-

n.d.: not detected

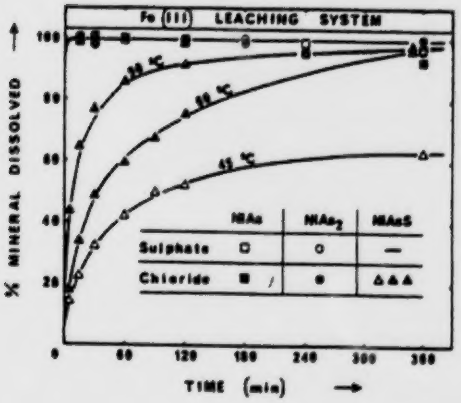

Fig. 4 Ferric ion leaching of nickel arsenide minerals (1.0 M Fe(III); NiAs/NiAs$_2$: 60°C and -200 + 270 mesh;NiAsS : -325 + 400 mesh).

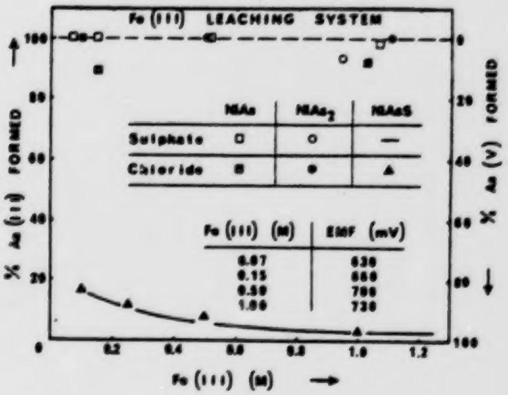

Fig. 5 Arsenic speciation in ferric ion leaching (60°C ; 120 min.).

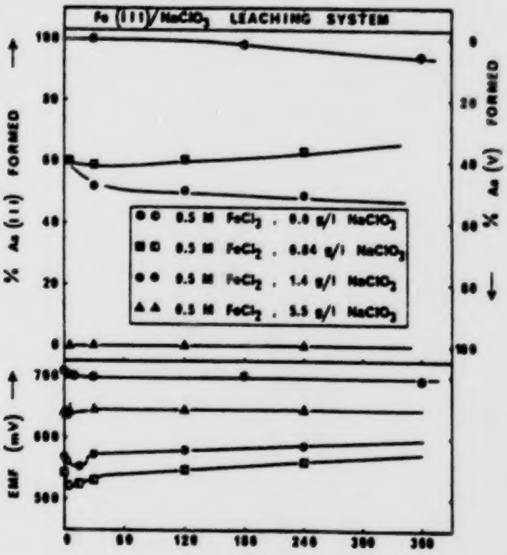

Fig. 6. Arsenic speciation in ferric ion/sodium chlorate system (60°C).

from 0.1 to 1.0 M while the acid concentration was kept constant at 0.4 N. The dissolution of niccolite and rammelsbergite was very fast under all tested conditions (100% dissolution in less than 15 min.), while gersdorffite dissolution was much slower.

By analysing systematically for As(III) and $As_{(total)}$ several solution samples during the various leaching runs the speciation picture for arsenic was established. Typical results obtained are presented in Fig. 5 in the form of % As(III) formed (in comparison to total dissolved arsenic) vs. Fe(III) concentration. As can be seen NiAs and $NiAs_2$ yield As(III) in solution as opposed to NiAsS which yields As(V). The matrix anion appears not to have any measurable effect on arsenic speciation within the range of conditions investigated. Additional results are presented in Table 2.

In uranium leaching it is known that chemical oxidants have to be added to regenerate ferric ion which is the actual oxidant for U(IV). Among the oxidants used are $NaClO_3$, MnO_2, or more recently H_2SO_5 (Caro's acid), while oxygen is employed in pressure leaching. The effect of $NaClO_3$ on arsenic speciation was investigated in conjunction with the ferric ion leaching system. Particulate samples of NiAs were leached in 0.5 M $FeCl_2$ solutions in which different amounts of $NaClO_3$ were added in an effort to correlate the prevailing redox potential to the arsenic species formed. The results obtained are illustrated in Fig. 6. The recorded EMF (E_h) is also plotted. For all these tests complete dissolution of NiAs was observed within the first 30 min. of reaction. These results clearly show that the addition of increasing amounts of $NaClO_3$ to the leach solution results in progressive elimination of As(III) even in potentials lower than those prevailing in direct Fe(III) leaching. (For comparison purposes, the corresponding curves for 0.5 M $FeCl_3$ are given in Fig. 6). Evidently upon formation of As(III) by the action of Fe(III) ions, $NaClO_3$ oxidizes subsequently As(III) to As(V) in solution. This view is supported by the results of a test in which partial dissolution of NiAs was effected first by using sub-stoichiometric amounts of Fe(III) and then complete dissolution was brought upon with the addition of $NaClO_3$. Analysis of the final leach solution showed all arsenic to be present as As(V).

2.3.2 Pressure Leaching System

Typical pressure leaching curves obtained for the three arsenide minerals are shown in Fig. 7. In this series of tests temperature was varied from 45 to 90°C and the oxygen pressure from 175 to 2100 kPa (25 to 300 psi) while the acid concentration was kept constant at 0.4 N. Again niccolite and rammelsbergite were found to dissolve at relatively fast rates as opposed to gersdorffite. However the overall observed kinetics appear to be slower than those in the corresponding Fe(III) system (Fig. 4). Furthermore it appears the O_2-H_2SO_4 system to give slightly better results than the corresponding O_2-HCl system. The

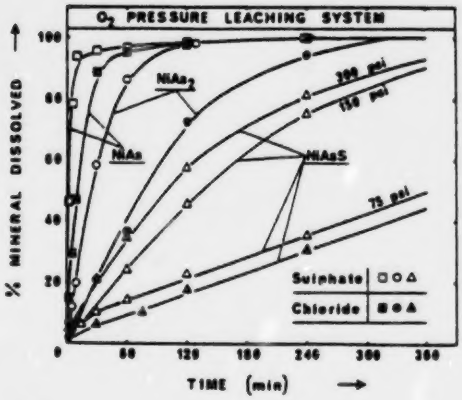

Fig. 7 Pressure leaching of nickel arsenide minerals (60°C; NiAs : -325 + 400 mesh and 525 kPa ; $NiAs_2$: -270 + 325 mesh and 525 kPa;NiAsS:-200 + 270 mesh and 90°C).

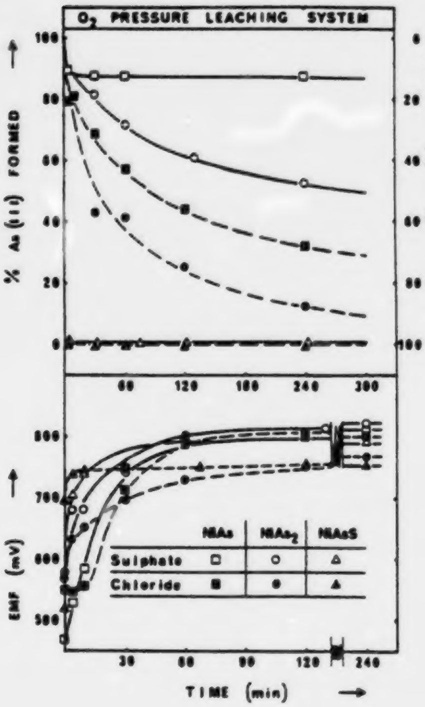

Fig. 8 Arsenic speciation in pressure leaching (60°, 525 kPa O_2; for NiAsS T = 90°C).

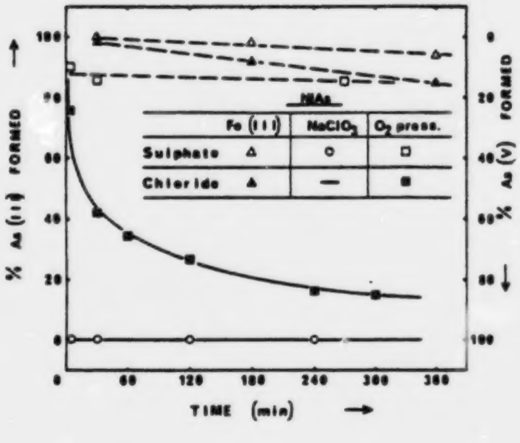

Fig. 9 Arsenic speciation in niccolite leaching - comparison of the different oxidants (60°C; 1 M Fe(III) ; 5.5 g/ℓ $NaClO_3$; 525 kPa O_2)

dissolution kinetics of NiAsS were found to be greatly accelerated by the elevation of temperature and pressure.

Representative arsenic speciation results for the pressure leaching system are illustrated in Fig. 8. Additional experimental measurements are given in Table 3. The speciation picture is becoming now quite complicated. In general it can be stated that a greater tendency towards As(V) formation is observed in pressure leaching. Moreover it appears, for reasons not yet understood, that the chloride system yields more As(V) than the respective sulphate system. As(III) was found to be kinetically stable only in the O_2-H_2SO_4 leaching of niccolite. Gersdorffite under all conditions tested gave As(V) while rammelsbergite appears to give initially As(III) which is consecutively transformed gradually to As(V). The direct EMF measurements made during the pressure leaching of these minerals (Fig. 8) did not indicate any dependence of arsenic speciation to the prevailing oxidation potential. Other factors appear therefore to control the oxidative dissolution of the arsenide minerals and the resulting speciation of As. The fact that the overall solution potential does not play a decisive role in determining the oxidation state of arsenic in leaching is exemplified further with the results of Fig. 9. Here the distribution of As(III)/As(V) vs. time is compared for the three oxidation systems investigated at potentials > 650 mV (E_h).

Table 3. Pressure leaching of nickel arsenide minerals - the effect of temperature and pressure on arsenic speciation (4 hours).

Temp. (°C)	P_{O_2} (kPa)	% As(III) FORMATION					
		NiAs		$NiAs_2$		NiAsS	
		H_2SO_4	HCl	H_2SO_4	HCl	H_2SO_4	HCl
45	525	98	-	-	-	-	-
60	75	86	-	-	29	-	-
	525	87	32	52	12	-	-
	2100	86	31	-	-	-	-
75	525	85	-	-	-	-	-
90	525	92	-	24	-	n.d.	n.d.
	1050	-	-	-	-	n.d.	-
	2100	85	-	-	-	n.d.	-

n.d.: not detected

Table 4. Pressure oxidation of synthetically prepared As(III) solutions.

Temp. (°C)	P_{O_2} (kPa)	Acidity (N)	Additives (M)	$\lvert As(III)\rvert_{initial}$ (g/ℓ)	$\lvert As(III)\rvert_{4\ hrs.}$ (g/ℓ)
65	525	0.2 HCl	-	4.97	4.96
97	525	0.2 HCl	-	4.97	4.90
80	525	0.4 HCl	-	4.98	4.95
80	525	0.2 HCl	0.05 Fe^{3+}	4.97	5.04
80	525	0.2 HCl	0.05 Fe^{3+}	9.83	9.72
80	525	0.2 HCl	0.1 Ni^{2+}	5.02	4.98
80	525	0.2 HCl	0.1 Cu^{2+}	4.96	5.00
80	525	0.2 HCl	0.03 As^{5+}	5.00	4.88
100	525	0.4 HCl	0.05 Fe^{3+}	4.98	5.07
80	525	0.2 H_2SO_4	-	4.80	4.81
100	525	0.2 H_2SO_4	-	4.74	4.71
150	1050	0.5 H_2SO_4	0.05 Fe^{3+}	4.90	4.88

2.4 Discussion

According to the E_h-pH and oxidation state diagrams of Figs. 1 and 2 H_3AsO_4 is expected to form in the oxidative dissolution of the arsenide minerals. The experimental results though of this study show that this is not always the case. To account for these findings appropriate equations are proposed and deviations from theory are discussed in this section.

2.4.1 Ferric Ion Leaching System

Niccolite is dissolved in ferric ion media via the following reaction (eq. 1):

$$NiAs + 5Fe^{3+} + 3H_2O \rightarrow Ni^{2+} + H_3AsO_3(aq) + 5Fe^{2+} + 3H^+ \qquad (1)$$

Equation (1) holds for both chloride and sulphate media. The same reaction stoichiometry was also established for NiAs/$FeCl_3$ by Dutrizac and Morrison (26). Addition of $NaClO_3$ to the leach solution results in the formation of As(V). The following reaction sequence is believed to describe the action of $NaClO_3$.

(i) Fe(II) to Fe(III) oxidation (eq. 2)

$$6\ Fe^{2+} + ClO_3^- + 6H^+ \rightarrow 6\ Fe^{3+} + Cl^- + 3\ H_2O \qquad (2)$$

(ii) NiAs dissolution by Fe(III) ions (eq. 1)

(iii) As(III) to As(V) oxidation by $NaClO_3$ (eq. 3)

$$3\ H_3AsO_{3(aq)} + ClO_3^- \rightarrow 3\ H_3AsO_4(aq) + Cl^- \qquad (3)$$

Reaction (3) is of course independent of the arsenide mineral subjected to leaching. It can be expected then that in conventional uranium leaching practice where $NaClO_3$ is employed, any arsenic present in the ore would be oxidized to the pentavalent state having as a result precipitation of Fe(III) ion and thereby loss of the oxidizing leach power. The other commonly used oxidants in U leaching industry i.e. pyrolusite (MnO_2) and Caro's acid (H_2SO_5) can be tentatively assumed that will result in As(V) formation as well, in view of their strong oxidizing powers (1.224 and 1.81 V E^o respectively (30)). This view is supported further with some experimental evidence. Thus pyrolusite has been reported to oxidize As(III) to As(V) in acidic solutions (31), while the observation by Burkin and Monhemius (32) that leaching of the Key Lake U ore with Caro's acid results in relatively low iron and arsenic in solution might well be due to As(V) formation and subsequent Fe(III)-As(V) precipitation.

The respective ferric ion leaching reaction for rammelsbergite in both sulphate and chloride media is given below:

$$NiAs_2 + 8Fe^{3+} + 6H_2O \longrightarrow Ni^{2+} + 2H_3AsO_{3(aq)} + 8Fe^{2+} + 6H^+ \quad (4)$$

Again in this system As(III) enjoys a kinetic stability. Furthermore these results indicate that within the time scale of 6 hours no appreciable oxidation of As(III) by Fe(III) is observed. The oxidation of As(III) in ferric ion media was considered in two recent papers by Tan and Dutrizac (33 a,b). According to their studies no significant oxidation takes place in 6 hours reaction time thus confirming the findings of the present work. The same authors though found that prolonged retention times (measured by days and not by hours) result eventually in oxidation of As(III) by $FeCl_3$ (33 a). However, $Fe_2(SO_4)_3$ was found not to oxidize As(III) even after 28 days retention tie (33 b).

In contrast to NiAs and $NiAs_2$, NiAsS was found to confirm thermodynamic predictions yielding As(V) in both chloride and sulphate media. The respective reaction is given below (eq. 5).

$$NiAsS + 7Fe^{3+} + 4H_2O \rightarrow Ni^{2+} + H_3AsO_4(aq) + 7Fe^{2+} + S^o + 5H^+ \quad (5)$$

Elemental sulphur formation was clearly visible in all tests while the stoichiometry of reaction (5) was further confirmed by determining the Fe^{2+}/Ni^{2+} molar ratio. Apparently a different oxidation mechanism (most likely electrochemical) governs the dissolution of gersdorffite thus resulting in the formation of As(V).

2.4.2 Pressure Leaching System

Markedly different arsenic speciation picture is observed in pressure leaching as opposed to ferric ion leaching. Pressure leaching exhibits a strong tendency towards As(V) formation. The two leaching systems though differ only marginally (~50 mV) in oxidizing power as this was determined by the EMF measurements ($EMF_{Fe(III)}$ ~700-750 mV and EMF*O_2 ~800 mV). Appropriate reactions to account for the experimental findings for each mineral are proposed below. Eq. 6 represents the oxidation of NiAs by O_2.

$$2NiAs + 5/2\ O_2 + 4H^+ + H_2O \longrightarrow 2Ni^{2+} + 2H_3AsO_3\ (aq) \qquad (6)$$

No further oxidation of As(III) to As(V) is observed in the H_2SO_4 solution as the results of Fig. 8 show. This comes in direct contrast to the respective HCl solution in which oxidation of As(III) to As(V) (eq. 7) is indeed observed after the mineral has been completely dissolved via reaction 6.

$$2H_3AsO_{3(aq)} + O_2 \longrightarrow 2H_3AsO_{4(aq)} \qquad (7)$$

In the case of rammelsbergite, As(III) is also initially formed (eq. 8) followed subsequently by oxidation of As(III) to As(V) in both sulphate and chloride media (eq. 7). The oxidation of As(III) to As(V) is relatively faster in the chloride system (Fig. 8).

* The reasons for the large deviation of this value from the standard electrode potential value for the couple O_2/H_2O (1.23 V) have been discussed by Natarajan and Iwasaki (34).

$$NiAs_2 + 2O_2 + 2H^+ + 2H_2O \longrightarrow Ni^{2+} + 2H_3AsO_3\ (aq) \qquad (8)$$

In an attempt to confirm reaction (7) synthetic As(III) solutions were prepared by dissolving $NaAsO_2$ or As_2O_3 in HCl or H_2SO_4 solutions which were then subjected to pressure oxidation. The obtained results are summarized in Table 4. As can be seen for temperatures up to 150°C and O_2 pressures up to 1050 kPa no oxidation at all is observed. Also a number of cations added failed to catalyse the oxidation reaction. The results of Table 4 are in agreement with the results of Nishimura and Tozawa (35) who have also found out that reaction 7 does not take place in acid solution. The reasons for the differences observed in the oxidation of As(III) between sulphate and chloride solutions, on one hand, and natural mineral leach solutions and synthetic solutions on the other hand, are really not known. A plausible explanation for the latter difference might be the presence of some impurities in the natural minerals capable of catalysing reaction 7. In a recent study Harris and Monette (36) reported the successful oxidation of As(III) by oxygen sparging in a H_2SO_4-zinc dust leach solution. Although no mechanistic interpretation for this reaction was offered it is the opinion of the present authors that it is possible again to have some impurities present in the zinc dust material acting as catalysts for reaction 7.

Finally the pressure leaching of gersdorffite in both sulphate and chloride media can be represented by the following reaction (eq. 9). H_3AsO_4 appears to be the direct product of the heterogeneous oxidation reaction as was also the case for the

$$2NiAsS + 7/2O_2 + 4H^+ + H_2O \longrightarrow 2Ni^2 + 2H_3AsO_4 + 2S^{\circ} \qquad (9)$$

Fe(III) system and not the result of a consecutive homogeneous reaction (i.e. reaction 7). As(V) has also been observed to form in the high temperature pressure oxidation of arsenopyrite (FeAsS) (37). Thus it appears that differences in the physical-chemical properties of the various arsenide minerals result in markedly different arsenic oxidation chemistry. Undoubtedly detailed electrochemical studies for each arsenide mineral system are required, similar to those conducted in the past decade for common sulphide minerals, to elucidate the mechanisms of the various leaching reactions. It can be predicted though that these studies will be far more complicated due to the extensive mineral intergrowth, non-stoichiometry, and substitution phenomena observed in arsenide mineralization.

2.5 Summary

The ferric ion and pressure leaching of several arsenide minerals has been studied from the point of arsenic speciation. Niccolite and rammelsbergite were found to yield H_3AsO_3 in solution as opposed to H_3AsO_4 which is the thermodynamically expected species. Gersdorffite and arsenopyrite on the other hand were found to yield H_3AsO_4.

H_3AsO_3 appears to enjoy a considerable degree of metastability in the Fe(III) leaching system while in the pressure leaching system further oxidation to H_3AsO_4 is observed to take place. It appears that impurities present in the natural minerals subjected to leaching "catalyse" the oxidation of As(III) to As(V) by oxygen. This "catalytic" effect was found to be more pronounced in the chloride than the sulphate medium. No such oxidation reaction is observed in synthetically prepared solutions. $NaClO_3$ additions to the ferric ion leaching medium were found to effectively oxidize all As(III) to As(V).

From these findings it can be postulated that the arsenic precipitation problem will be more extensive in uranium leaching where $NaClO_3$ or O_2 are used. In ferric chloride leaching on the other hand which is presently advocated for the treatment of base metal sulphides, significantly less arsenic precipitation is expected. Finally the results of this study show that As(III)/As(V) formation is independent of the redox solution potential which in turn makes impractical, the possible stabilization of As(III) via potential control, as a means of avoiding the troublesome As(V) precipitations.

3. PRESSURE CHLORIDE LEACHING OF THE KEY LAKE URANIUM ORE

3.1 Scope

As the results of Chapter 2 have indicated, control of the oxidative leaching of the nickel arsenide minerals with proper adjustment of the prevailing solution redox potential in order to yield As(III) rather than As(V) proved not feasible in the present ore leaching system. The reasons being the presence of more than ore arsenide minerals with differing oxidation chemistry and the presence of impurities in the ore which "catalyse" the oxidation of As(III) to As(V). This avenue of improving the leaching of an arseniferous material via redox potential control remains though an option for systems involving leaching of high grade arsenical concentrates only.

Having considered the relevant oxidation chemistry of arsenic in phase I of this project then statistically designed leaching experiments on the actual uranium ore were performed to establish optimum conditions for the coextraction of U au Ra, and to study further the chemistry of the system. In particular a fractional 3-level factorial design involving four variables has been used. Mathematical models were derived by multiple regression analysis and 3-D graphs were generated with the aid of computer in order to estimate a number of response surfaces, - such as the extraction of U, Ra, and Ni acid consumption etc. - over the process design region of interest.

In view of the significance of the Key Lake Uranium Mill from economic (biggest uranium producing plant in the world) and ecological (production of large tonnages of highly radioactive tailings) considerations, the experiments reported here were carried out with ore samples from this mill.

3.2 Statistical Design and Modelling

3.2.1 Selection of Process Variables

In view of the large number and the complexity of the chemical analyses involved in this experimental programme it is understandable that only a select few of the process parameters could be investigated. In this section the parameters selected and the criteria used for this selection are described. Both data from the previous investigations conducted with the Midwest ore (22) and data from the current operation of the pressure leaching plant at Key Lake (6)(38) were the basis for this selection procedure.

The following parameters were considered: size distribution, temperature, oxygen pressure, slurry density, HCl concentration, $CaCl_2$ concentration, and time. The ore used in the present investigation was a sample cut directly from the leach feed of the Key Lake Uranium plant. So there was no need for further grinding. The size distribution of this sample is given in the subsequent Experimental section (3.3). No other size distributions were tested. Temperature was chosen to be kept constant at 68° for all the experiments conducted. Previous work with the Midwest ore (22) had identified 70°C as the best temperature while at Key Lake a 65°C temperature is applied (38). Furthermore as Sarkar (39)(40) has eloquently discussed a temperature just below 70°C is the preferred one from the standpoints of autogenous operation and construction material selection (rubber lining) for the autoclaves. Oxygen pressure was kept constant as well at 75 psi - the same level as that used in the previous work (22) and that applied at Key Lake (38).

Thus the parameters d_s (slurry density), HCl conc, $CaCl_2$ conc, and time were eventually selected for this investigation. The earlier work on the Midwest ore (22) had indicated that optimization is required as far as the addition levels of HCl and $CaCl_2$ (major economic parameters) are concerned on one hand. On the other due to the high acid consuming nature of the ore (6) slurry density and time were also thought of equal significance from the process optimization point of view and were investigated as well. In Table 5 the range of conditions tested in this experimental programme are summarized.

Slurry density is expressed in Kg solids/lit solution units instead of the usual units wt% because of the concentrated nature of the leach solution used (i.e. the density of the liquid is no longer 1). This range of conditions was chosen based on the results of the previous work on the Midwest uranium ore (22). The values given in Table 5 are the initial ones (time = 0) used. With the progress of the reaction the concentrations of HCl,

Table 5. Process variables investigated.

Process Variable	Range of conditions Low	Medium	High	
slurry density (ds)	0.33	0.66	1.0	kg l^{-1}
HCl conc (initial)	0.5	1.0	1.5	N
$CaCl_2$ conc (initial)	1.5	2.5	3.5	M
Time	2	4	6	hrs

Other parameters: Temp. = 68°C PO_2 = 75 psi

$CaCl_2$ and solids decrease with time. The drop in HCl conc was the most pronounced of all due to acid consumption by side actions (gangue dissolution). Detailed data of these changes are presented in section 3.4.

Although the principal objective of this work was optimization of the simultaneous extraction of U and Ra, apart these two responses, the extraction of Ni as monitored too in an attempt to identify conditions for the recovery of Ni as by-product. Moreover the behaviour of As and EMF were also of interest from the point of view of interlinking the work of phase 1 and the work of phase 2. Finally acid consumption was another major response which was closely studied as well.

3.2.2 Selection of Statistical Design

The difficulty in determining the fundamental relationships that affect the leaching of a complex ore, as is the case with the U-ore under investigation here, led to the adoption of statistical methods for the design of the experiments and the establishment of the necessary mathematical models needed for process optimization. In selecting an appropriate form of statistical design it was decided response surface methodology (i.e. three-level factorial design) to be adopted. The latter leads to second or higher order polynomial models that provide information regarding not only linear effects but interaction and curvature effects as well with respect to the independent variables selected. Among the various statistical designs reported in literature (41) a fractional three-level factorial design proposed by Box and Behnken (42) was chosen for the present work. Apart the advantage of describing each response surface by full quadratic polynomials, this type of experimental design requires a limited number of experimental trials (27) instead of 81 for the full 34 design) and still possess excelling statistical properties such as orthogonal blocking, rotatability, and boldness (43).

Each Box-Behnken design employs a subset of the points in the corresponding full three-level factorial, with two extra replicates at the center point which provide a measure of inherent experimental error. The four-variable Box-Behnken design used here is shown in Table 6 with high, medium, and low values of each continuous variable represented in coded form as "+", "O", and "-".

X_1, X_2, X_3 and X_4 represent respectively, slurry density, $[HCl]_o$, $[CaCl_2]_o$, and time. The experiments were arranged into these blocks of nine runs each and the order of execution was randomized to eliminate time effects as much as possible.

After execution of the statistically designed experiments the obtained data are subjected to preliminary inspection prior to model building (43). To this end the Data Matrix is formed and correlation coefficients (r) for each pair of dependent (Y_i,

Table 6. Four-variable Box-Behnken design.

Experiment Number	X_1	X_2	X_3	X_4	
1	+1	+1	0	0	
2	+1	-1	0	0	
3	-1	+1	0	0	
4	-1	-1	0	0	
5	0	0	+1	+1	Block 1
6	0	0	+1	-1	
7	0	0	-1	+1	
8	0	0	-1	-1	
9	0	0	0	0	
10	+1	0	0	+1	
11	+1	0	0	-1	
12	-1	0	0	+1	
13	-1	0	0	-1	
14	0	+1	+1	0	Block 2
15	0	+1	-1	0	
16	0	-1	+1	0	
17	0	-1	-1	0	
18	0	0	0	0	
19	+1	0	+1	0	
20	+1	0	-1	0	
21	-1	0	+1	0	
22	-1	0	-1	0	
23	0	+1	0	+1	Block 3
24	0	+1	0	-1	
25	0	-1	0	+1	
26	0	-1	0	-1	
27	0	0	0	0	

response) and independent variable, X_i (both types of variables are called Zi) are computed as follows:

$$r = \frac{\sum_{i=1}^{n} (Z_{i1}-\overline{Z}_1)(Z_{i2}-\overline{Z}_2)}{\left[\sum_{i=1}^{n} (Z_{i1}-\overline{Z}_1)^2 \sum_{i=1}^{n} (Z_{i2}-Z_2)^2\right]^{1/2}} \tag{10}$$

The magnitude of r $(-1 \leqslant r \leqslant 1)$ is a measure of the correlation of the casidered variable has with the measured response. This correlation is further inspected graphically by plotting Y_i vs X_i. In this manner a preliminary interpretation of the data is possible both in terms of statistical and metallurgical significance.

To build the appropriate models the experimental data generated with this design are fitted then with second-degree polynomials using multiple regression analysis (44). In other words the coefficients of each term of the fitted equation are estimated with the least squares method. For the four variables previously mentioned (Table 5) this polynomial has the following form:

$$\begin{aligned} y = {} & \beta_o + \beta_1 x_1 + \beta_2 x_2 + \beta_3 x_3 + \beta_4 x_4 \\ & + \beta_{11} x_1{}^2 + \beta_{22} x_2{}^2 + \beta_{33} x_3^2 + \beta_{44} x_4{}^2 \\ & + \beta_{12} x_1 x_2 + \beta_{13} x_1 x_3 + \beta_{14} x_1 x_4 + \beta_{23} x_2 x_3 \\ & + \beta_{24} x_2 x_4 + \beta_{34} x_3 x_4 + \varepsilon \end{aligned} \tag{11}$$

where y is the measured or calculated response (i.e. U extraction, Ra extraction etc.), X_i are the operating variables for the experimental study (i.e. Temp, HCl conc etc.), β_i, β_{ii}, and β_{ij} are the first-order, second-order, and interaction term coefficients, respectively, and ε is a random error term representing the discrepancy between the measured or calculated response and the corresponding value predicted by the polynomial model.

To permit direct comparisons to be made among coefficients of individual terms in a fitted model, without regard to the units in which the original operating variables are defined, the four variables are standardized. In this manner data analysis and model fitting is greatly facilitated. The formula used to standardize each independent variable is:

$$x_{ij} \text{ standardized} = \frac{X_{ij} - \overline{X}_j}{S_{xj}} \qquad (12)$$

where X_j = mean of X_{ij} observations

S_{xj} = standard deviation of X_{ij} observations

i = data point index

j = variable identification index

The fitted model in terms of standardized variables can be written as follows:

$$\begin{aligned}\hat{y} = \ & \hat{b}_o + \hat{b}_1 x_1 + \hat{b}_1 x_2 + \hat{b}_3 x_3 + \hat{b}_4 x_4 \\ & + \hat{b}_{11} x_1^2 + \hat{b}_{22} x_2^2 + \hat{b}_{33} x_3^2 + \hat{b}_{44} x_4^2 \\ & + \hat{b}_{12} x_1 x_2 + \hat{b}_{13} x_1 x_3 + \hat{b}_{14} x_1 x_4 + \hat{b}_{23} x_1 x_4 \\ & + \hat{b}_{24} x_2 x_4 + \hat{b}_{34} x_3 x_4 \qquad (13)\end{aligned}$$

where $\hat{y}$ denotes the predicted value of each response and $\hat{b}_{ij}$ the estimated coefficients.

Having established the full quadratic model in standardized variables (eq.13) with the aid of regression analysis then rigorous analysis of the model follows to verify its validity and determine the significance of each variable. This analysis involves the following steps:

1. The "augmented correlation matrix" is calculated to determine the degree of correlation among all terms in the model and all responses. This is useful for two purposes: (a) to verify the validity of the model as a whole by establishing that the independent variables (x_i) are uncorrelated among themselves and (b) by predetermining the relative significance of each variable x_i on the various responses (y_i) studied, i.e. U extraction, Ra extraction etc. Via this analysis the BOX-BEHNKEN design, used in the present leaching investigation proved to be statistically sound (correlation coefficients = 0 for x_i and x_{ij} and -0.2 for x_i^2).

2. Each of the terms in the fitted model is tested to establish its significance by analysing the variance. This test involves comparing the ratio

$$\frac{\text{mean square associated with the term}}{\text{residual mean square}}$$

with an appropriate value of the F-distribution (45). Whenever this ratio is greater than the F valve, then the corresponding term is significant and therefore is required in the model. If the ratio is smaller then correspondingly the respective term is not considered important and therefore is removed from the model. Thus eventually a model equation incorporating only the significant terms is retained for further testing.

3. The retained model is subjected to various diagnostic checks. These involve analysis of the residuals to reveal any nonrandom tendencies, and also to ensure that the assumptions upon which the least squares estimation is based are not violated. Plots of residuals against each predicted response (dependent variable) serve to locate possible deviation from random behaviour. Other residual plots such as plots of residuals against the independent standardized variables x_i can be used as well.

Finally, upon successful testing of the model equations, the latter are used to develop three-dimensional graphs with the aid of computer in order to visualize each response surface and determine the optimum conditions of operation over the selected process design region. Metallurgical discussion of the results then follows.

3.3 Experimental

3.3.1 Ore

The uranium ore used in the present investigation was obtained from the Key Lake Uranium Mill (Key Lake Mining Corp., Key Lake, N. Saskatchewan). This was derived directly, from the mill feed of the leach plant. The received slurry was subjected to agitation for homogenization and then the required ore sample (about 20 kg) was cut. This was dried up, blended and split into lots of 250 g, 500 g, and 750 g for the various experiments. Wet screening of a representative sample showed the ore to have the size distribution given in Table 7. That is approximately 30% -200 mesh. The chemical analysis of the ore used in this work is shown in Table 8. The high grade and complex ores of the Key Lake deposit are of vein type (46). Pitchblende (type I and II) and coffinite are the major uranium minerals present. Most of Ra^{226} is associated with pitchblende. Gersdorffite (NiAsS) is the most abundant nickel mineral within the Key Lake deposits, followed by millerite (NiS) and niccolite (NiAs). Accessory metallic minerals include pyrite, galena, chalcopyrite, baravoite

Table 7 Screen analysis of the leach feed

mesh size	wt. %
+ 35	2.20
−35 + 48	12.20
−48 + 65	20.00
−65 + 100	16.20
−100 + 150	10.70
−150 + 200	8.50
−200	29.70

Table 8 Chemical analysis of the leach feed.

Constituent	Weight, %
U	2.95
Ra^{226}	9,700 pCi/g
Ni	2.12
As	1.40
Fe	1.66
Co	0.06
S (total)	0.98
SiO_2	67.66
Al	3.76
Mg	1.14
Ca	0.37
K	0.29
Ti	0.21
CO_2	1.72

and pyrrhotite. The ore matrix consists mainly of silicates, carbonates and oxides. Major gangue minerals are quartz, chlorite, kaolinite, sericite, calcite and epidote.

3.3.2 Apparatus

Leaching tests were conducted in a 2-l titanium autoclave manufactured by Parr Instrument Company, Moline, IL. The autoclave was a floor stand model with a heavy duty magnetic-drive stirrer and a temperature-stirring speed controller. The autoclave was equipped with a serpentine cooling coil to control temperature overshoot caused by the exothermic nature of the leaching process. A definite improvement over the previous studies in which considerable overshoot was experienced (23). Also a specially adapted pressurized chamber allowed introduction of HCl at reaction temperature. The autoclave was connected throughout the course of a leaching test to the oxygen cylinder thereby allowing continuous supply of oxygen at the pre-set pressure level. Agitation was provided by two 6-bladed axial turbine impellers at a constant rate of 500 rpm. Temperature control was maintained at ± 2°C throughout the test. A special feature of the autoclave was an opening of a 1/2" NPT hole at the bottom of the bomb to accomodate a special EMF probe, with the aim of monitoring the slurry oxidation potential in situ. The probe was connected to an advanced microprocessor-based pH meter manufactured by Fisher Scientific, interfaced with an electrode switch and a printer.

3.3.3 Procedure

An aqueous slurry of $CaCl_2$ solution and ore, was heated to 68°C under slight (25 psi) nitrogen over-pressure (i.e. air was excluded). It is noteworthy here that the dissolution of $CaCl_2$ in water is highly exothermic, a very useful property in the case of continuous leaching. Hydrochloric acid (HCl) was introduced at reaction temperature to avoid commencement of the leaching at lower temperatures. Oxygen was also admitted at reaction temperature (time zero) under the slurry surface to ensure good gas dispersion. The oxygen pressure of 75 psi reported here is the difference between the total pressure measured after oxygen introduction (100 psi) and that before (25 psi).

At the end of the experiment a slurry sample was obtained through a 1/4" sampling port equipped with a ball valve, while the stirrer was kept going. The sample was filtered immediately after collection and the cake was transferred for repulping using 1.0 vol.% HCl at a ratio pregnant/wash around 1/2, for 15 minutes. Then the slurry was filtered again and washed repeatedly: twice with acidified distilled water (1.0 vol% HCl) and once with distilled water at room temperature. Pregnant solutions, combined wash solutions, and dried residues (90°C for at least 24 h) were analysed. The analytical solutions were acidified (20 v/o HCl) prior to their dispatch for analysis to ensure no post-precipitation. The suspension redox potential was monitored throughout the experiment, with the EMF probe. At the end of each experiment, after depressurization at room temperature, the EMF of the pulp was measured again, using a conventional combination-Pt electrode for comparison purposes. The acid concentration in the pregnant solution was measured by titration immediately after the first filtration, to obtain an estimate of the acid consumption occurred during leaching. The pregnant solutions of selected tests were also analysed for As(III) in an effort to correlate the solution chemistry of the actual U leaching with that of the simulated tests described in Chapter 2. Both analytical methods used for acid titration and As(III) determination are described in Appendix 6.1. An actual simulation of the industrial process would require the maintenance of a constant acid level (pH) throughout the experiment. This could have been accomplished with the continuous monitoring and control of the solution pH with the proper controller - a facility though not readily available.

Leaching efficiencies were determined based on the dried solids assays. Correction factors were applied to account for the solids weight losses during leaching. It should be mentioned that to reduce the loss of radium from the solution samples due to $RaSO_4$ precipitation and Ra adsorption onto the sample glass containers a predetermilned amount of HCl was added to these samples as a prevention measure.

3.4 Results and Discussion

In total 27 experiments were performed with the Key Lake uranium ore by following the BOX-BEHNKEN statistical methodology described in section 3.2.2. The independent variables investigated were slurry density, ds (kg solids/l solution), HCl concentration (N), $CaCl_2$ concentration (M) and time (hours). All the other variables were kept constant throughout this experimental program, namely temperature at 68°C, and O_2 pressure at 75 psi. The following responses were measured: U extraction (%), Ra extraction (%), Ni extraction (%), As extraction (%), acid consumption (Kg HCl/ton ore), and EMF (mV). All the experimental data are given in Table 9. The acid consumption data are given in Table 13 (p.48). From the replicate tests no. 11, 17, and 27 an estimate of the experimental error associated with each individual response was made. The results of these estimates are shown in Table 10. The values given in Table 9 for d_s, HCl, and $CaCl_2$ are the initial ones. During the course of leaching the levels of these variables dropped according to the extent of ore reaction. The extend of reaction for different ore components is discussed in the following section 3.4.1. After that (section 3.4.2) the statistical model equations are developed and eventually (section 3.4.3) the results are discussed from the standpoint of metallurgical significance.

Table 9 Pressure leaching of the Key Lake U ore in a $HCl-CaCl_2$ medium: Response surface four-variable design data.

n)	Ds (kg/l)	$\|HCl\|_o$ (M)	$\|CaCl_2\|_o$ (M)	Time (hrs)	Extraction (%)* U	Ra^{226}	Ni	As	EMF (mV)
	0.33	1.0	2.5	6	99.59 (0.012)	98.21 (174)	62.45 (0.796)	67.79 (0.451)	755
	1.00	1.0	1.5	4	55.49 (1.313)	33.18 (6482)	41.89 (1.232)	22.93 (1.079)	678
	1.00	0.5	2.5	4	45.15 (1.618)	38.19 (5996)	33.44 (1.411)	22.93 (1.079)	578
	0.66	0.5	3.5	4	53.39 (1.375)	52.55 (4603)	50.80 (1.043)	29.36 (0.989)	705
	0.66	1.0	1.5	6	82.61 (0.513)	59.51 (3928)	62.08 (0.804)	51.36 (0.681)	718
	0.33	1.5	2.5	4	99.59 (0.012)	98.32 (163)	65.24 (0.737)	67.29 (0.458)	774
	0.66	1.0	3.5	6	83.53 (0.486)	38.23 (5992)	60.80 (0.831)	42.57 (0.804)	757
	0.66	1.5	1.5	4	99.19 (0.024)	91.05 (868)	58.02 (0.890)	61.50 (0.539)	725
	0.33	1.0	1.5	4	99.56 (0.013)	97.74 (219)	64.39 (0.755)	64.07 (0.503)	749
	0.66	0.5	2.5	6	70.95 (0.857)	47.24 (5118)	64.15 (0.760)	30.57 (0.972)	723
	0.66	1.0	2.5	4	85.66 (0.423)	52.64 (4594)	62.69 (0.791)	44.14 (0.782)	749
	0.66	1.5	2.5	2	98.20 (0.053)	80.28 (1913)	49.29 (1.075)	48.57 (0.720)	706
	0.66	0.5	2.5	2	52.14 (1.412)	51.82 (4673)	44.15 (1.184)	21.93 (1.093)	705
	1.00	1.0	2.5	6	46.95 (1.565)	42.31 (5596)	52.45 (1.008)	17.93 (1.149)	679
	0.66	0.5	1.5	4	46.07 (1.591)	37.16 (6095)	49.53 (1.070)	22.93 (1.079)	668
	0.33	1.0	2.5	2	98.61 (0.041)	97.31 (261)	65.61 (0.729)	53.79 (0.647)	760
	0.66	1.0	2.5	4	87.80 (0.360)	53.10 (4549)	63.96 (0.764)	50.57 (0.692)	757
	0.33	0.5	2.5	4	92.37 (0.225)	89.25 (1043)	63.11 (0.782)	58.93 (0.575)	743
	0.66	1.0	1.5	2	72.51 (0.811)	81.88 (1758)	60.05 (0.847)	51.86 (0.674)	717
	1.00	1.0	3.5	4	62.51 (1.106)	38.37 (5978)	59.29 (0.863)	22.93 (1.079)	744
	1.00	1.5	2.5	4	76.85 (0.683)	25.11 (7264)	65.66 (0.728)	41.57 (0.818)	751
	0.66	1.0	3.5	2	85.19 (0.437)	70.23 (2888)	52.74 (1.002)	56.43 (0.610)	728
	0.66	1.5	3.5	4	99.05 (0.028)	98.18 (177)	65.66 (0.728)	69.14 (0.432)	798
	1.00	1.0	2.5	2	58.00 (1.239)	42.90 (5539)	52.74 (1.002)	39.50 (0.847)	750
	0.33	1.0	3.5	4	99.49 (0.015)	98.29 (166)	71.60 (0.602)	74.29 (0.360)	807
	0.66	1.5	2.5	6	99.12 (0.026)	93.22 (658)	71.23 (0.610)	69.07 (0.433)	755
	0.66	1.0	2.5	4	80.81 (0.566)	60.24 (3857)	63.11 (0.782)	55.07 (0.629)	732

The numbers in ( ) are the contents of the residue for each element in wt.% or pCi/g for Ra.

Table 10 Estimation of experimental errors

	Test No. 11	Test No. 17	Test No. 27	Average	Experimental Error
% Uranium Extraction	85.7	87.8	80.8	84.8	±3 %
% Radium Extraction	52.6	53.1	60.2	55.3	±3%
% Nickel Extraction	62.7	64.0	63.1	63.2	±0.5%
% Arsenic Extraction	44.1	50.6	55.1	49.9	± 5.5%
Acid Consumption (kg/ton)	24.1	20.7	22.7	22.5	±2 kg/ton
Slurry EMF (mV)	749	757	732	740	±12 mV

3.4.1 Ore Reactivity

The high grade uranium ores of N. Saskatchewan are known to be highly reactive resulting in considerable mass loss during the course of leaching (6). By weighing the final residues of tests #11, 19 and 26 the ore mass losses were established (Table 11). It can be seen that an average of 10% weight loss is observed with most of it occurring at the first 2 hours of the leach. Similar behaviour has been observed with the O_2-H_2SO_4 leaching system as well (6).

Percent extraction for U, Ra, Ni and As shown in Table 9 were calculated based on the analysis of residues. For mass balance purposes solution analyses were also done on a number of tests. The obtained results are listed in Table 12. The error for each test has been calculated using the following formula:

% Error = (mass of residue) x (% conc. of element in the ore) x 1/c.f.
- (mass of residue) x (% conc. of element in the residue)
- (vol. of preg. soln.) x (g l^{-1} conc. of element in the pregnant solution)
- (vol. of wash solution) x (g l^{-1} conc. of element in the wash solution)

where c.f. = correction factor for mass loss = 0.9 (see Table 11).

Table 11 Ore mass losses during O_2-HCl-$CaCl_2$ leaching

Test No.	Leaching conditions Time(hrs)	ds (kg/l)	HCl(M)	$CaCl_2$(M)	Ore mass Before (kg)	After	Mass loss (%)
19	2	0.66	1.0	2.5	0.500	0.455	8.9
11	4	0.66	1.0	1.5	0.500	0.450	10.0
26	6	0.66	1.0	2.5	0.500	0.442	11.6

Table 12 Mass balance calculations

Element	Test No.	Ore (wt.%)	Residue mass(g)	wt%	Pregnant Soln. Vol(l)	g/l	Wash Soln Vol(l)	g/l	Avg (%) Error
U	8	2.95	111.2	0.027	0.16	15.48	0.712	0.71	-4.5
	23		93.2	0.031	0.122	20.76	0.666	1.164	
Ra	8	9,700 pCi/g	111.2	966	0.16	5.99×10^6	0.712	3.34×10^5	+5.5
	23		93.2	197	0.122	$6{,}36\times10^6$	0.666	3.6×10^5	
Ni	8	2.12	111.2	0.99	0.16	7.15	0.712	0.36	+2.5
	23		93.2	0.81	0.122	10.48	0.666	0.58	
As	8	1.40	111.2	0.60	0.16	5.46	0.712	0.324	+4.5
	23		93.2	0.48	0.172	6.43	0.666	0.48	

In Table 12 the average error out of two tests is given. As can be seen the error varies from 2.5 to 5.5 percent units which is considered very good in view of the several samples and analyses involved in the calculation procedure.

As was mentioned previously the Key Lake U-ore is very reactive resultilng in considerable gangue mineral constitutent dissolution. As a result of this, acid consumption is several times larger than the stoichiometric requirements of the uranium dissolution reactions. The calculated acid consumption figures are shown in Table 13. Minimization of the acid requirements constitutes therefore one of the most critical aspects of the leaching optimization work. The effects of the various parameters on acid consumption will be discussed later with the use of a model developed for that purpose (see section 3.4.3). The increased acid consumption is attributed to the acid attack on the chlorite and the other clay minerals of the ore. A measure of the degree of gangue dissolution are the results of Table 14. In this table the deportment of certain key components of the ore is reported for a selected few tests. It can be seen that apart from SiO_2 the other gangue components dissolve to various degrees. For the conditions of Table 14 precipitation is observed as reaction time is extended to 6 hrs and this explains the decrease observed in the extraction of some elements. Comparison of the data of Table 14 with those of Table I-13 reported in Weir and Master's paper (6) indicate considerably higher levels of gangue dissolution in the present system.

Table 13 Acid consumption measurements

	Acid Concentration		
Test (#)	Initial (M)	Final (M)	Consumption (kg/ton)
1	1.0	0.55	49.773
2	1.0	0.565	15.878
3	0.5	0.25	9.125
4	0.5	0.255	13.549
5	1.0	0.635	20.186
6	1.5	1.095	44.795
7	1.0	0.57	23.780
8	1.5	1.035	25.716
9	1.0	0.81	21.015
10	0.5	0.31	10.508
11	1.0	0.565	24.057
12	1.5	0.92	32.076
13	0.5	0.17	18.250
14	1.0	0.51	17.885
15	0.5	0.305	10.784
16	1.0	0.80	22.121
17	1.0	0.625	20.739
18	0.5	0.36	15.485
19	1.0	0.665	18.527
20	1.0	0.535	16.973
21	1.5	0.91	21.535
22	1.0	0.55	24.886
23	1.5	0.78	39.818
24	1.0	0.47	19.345
25	1.0	0.66	37.606
26	1.5	0.775	40.095
27	1.0	0.59	22.674

Table 14 Deportment of some important ore components

Test No.	Leaching* Time (hrs)	Component Response											
		SiO$_2$(%)		Al(%)		Ti(%)		K(%)		Fe(%)		Ca(%)	
		C	E	C	E	C	E	C	E	C	E	C	E
original ore		67.7	Not measurable	3.76	-	0.21	-	0.29	-	1.66	-	0.37	-
22	2	67.16		2.8	25.5	0.02	90	0.26	10	0.88	47	0.13	65
17	4	68.6		2.6	37.7	0.02	90	0.26	10	0.93	44	0.15	60
7	6	79.3		3.5	18.0	0.02	90	0.27	8	0.98	41	0.23	38

* Other conditions: $d_s = 0.66$ kg/l, 1.0 M HCl, 2.5 M (3.5 M for test # 7) $CaCl_2$

C: Content E: Extraction

In an effort to correlate the findings of the arsenic chemistry work reported in Chapter 2 with the actual U leaching data the EMF of the pressure leach slurry was monitored in situ and certain solution samples were analysed for As(III)/As(V) and Fe(II)/Fe(III). The obtained results on arsenic and iron distribution are presented in Table 15. As can be seen at the early stages of leaching As(III) represents approximately 20% of the dissolved arsenic. At the later stages (6 hr - Table 15) arsenic (V) precipitation occurs which results in relatively higher $As(III)/As_{aq}^{tot}$ ratio (~30%). It is of interest to note that in the conventional $O_2-H_2SO_4$ leaching of the Key Lake ore the pressure leach solution contains about 35% As(III) per $As_{dissolved}^{tot}$ in other words somewhat higher than the present chloride system. The corresponding primary leach solution (atmospheric Fe^{3+} leach) of the Key Lake plant contains respectively 50% As(III) (38). The data of Table 15 along with those from the Key Lake plant (38) are in good agreement with the findings of Chapter 2. Thus according to Fig. 8 NiAsS yields As(V) under pressure leaching conditions while NiAs yields As(III) in sulphate solutions or mixed As(III)/As(V) in chloride solutions. Considering that NiAsS is the major nickel arsenide mineral in the Key Lake ore, this explains the observed As(III) distribution picture. The reason that the primary leach solution of the Key Lake plant contains relatively more As(III) than the secondary leach solution is the difference in reactivity between NiAs and NiAsS. Thus during primary leach (Fe^{3+} leaching) only NiAs dissolves yielding As(III) while during secondary leach

Table 15 Arsenic and iron distribution

Test No.	Leach* Time (hrs.)	Arsenic Extraction (%)	 As_{aq}^{tot} (g/l)	 As(III)	 $As(III)/As_{aq}^{tot}$ %	Iron Extr. (%)	 Fe_{aq}^{tot} (g/l)	 Fe(III) g/l	 Fe(III)/Fe(II) %	EMF(mV)
22	2	56.4	4.55	0.84	18.4	47	5.46	2.28	72	728
17	4	50.6	3.42	0.55	16.1	44	4.06	1.28	46	756
7	6	42.6	2.45	0.725	29.6	41	5.61	2.30	69.5	749

* Other conditions: same as in Table 15.

(pressure leaching) NiAsS primarily dissolves yielding As(V). The persistence of As(III) in the secondary leach (conventional system) can be attributed to NiAs grains encapsulated in NiAsS due to extensive mineral intergrowth. These grains are visualized to dissolve simultaneously with NiAsS during pressure leaching. The iron distribution data in the present work are similar to those of the O_2-H_2SO_4 system (38).

Finally, a typical EMF vs time curve recorded during actual leaching is shown in Fig. 10. As can be seen, for most of the leaching time, potentials in the range of 700 to 800 mV prevail. These potentials are in agreement with those of Fig. 8 of Chapter 2. Furthermore on Fig. 10 the terminal potentials of the leach slurry recorded after cooling and depressurization are shown. These potentials are 50 to 100 mV lower than the in-situ pressure leach potentials another indication of the oxidative dissolution strength of pressure leaching. While the terminal potentials (i.e. after depressurization) are mainly due to the Fe(III)/Fe(II) redox couple those of the presure leach are the mixed potentials of both the Fe(III)/Fe(II) and O_2/H_2O redox couples. The mixed potentials for these two redox couples have been discussed by Natarajan and Iwasaki (34) and Rando and Woods (47). In terms of chlorocomplexes uranium is known to form relatively weak positively charged complexes - a marked contrast with the respective sulphate system where extensive complexation occurs. The most important chlorocomplex expected to form under the applied leaching conditions is UO_2Cl^+ (stab. constant, 25°C = 0.88) (48).

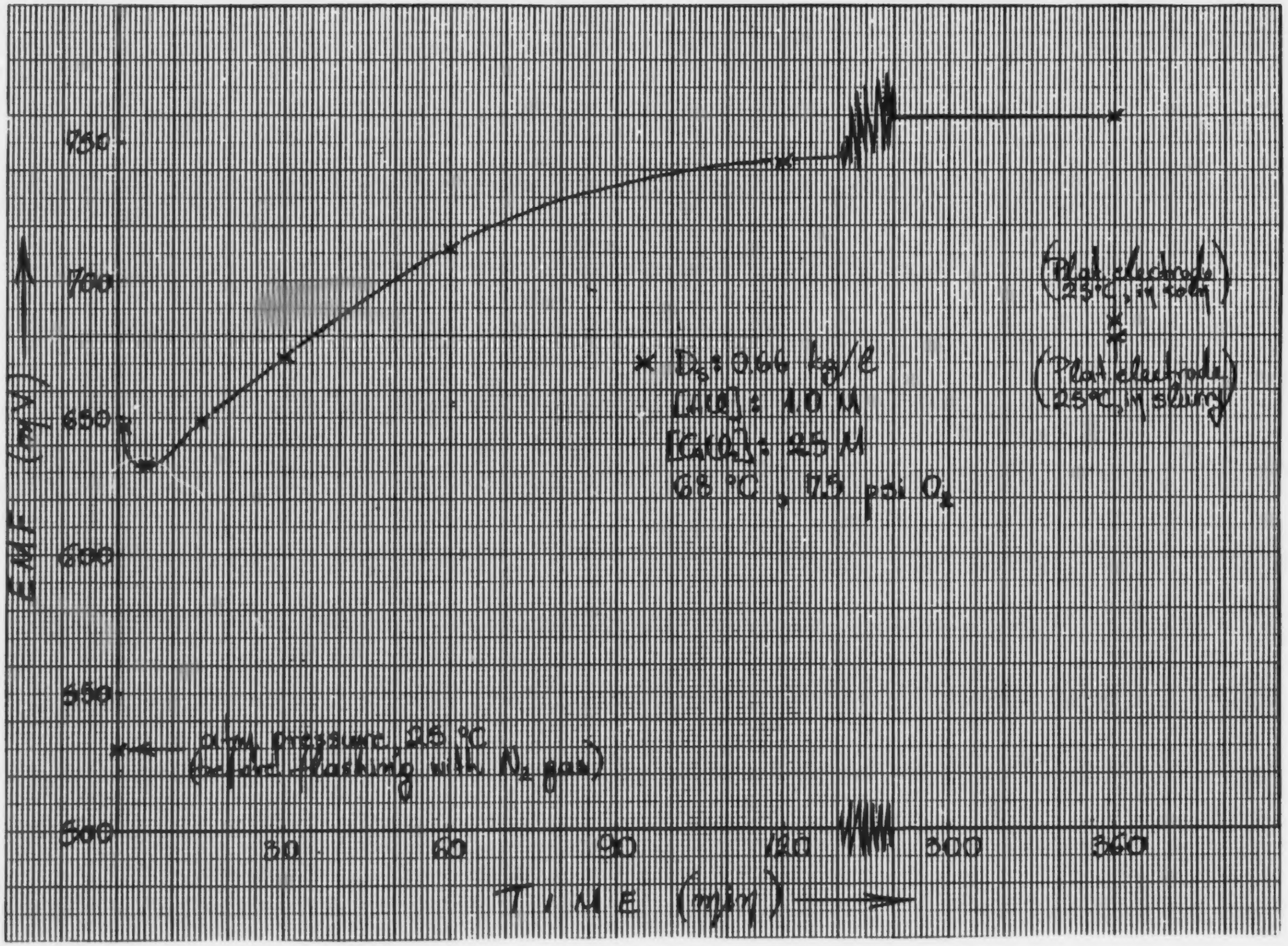

Fig. 10 Typical EMF vs time curve recorded during pressure chloride leaching.

Before this section on ore reactivity is concluded it is considered important to note that the dissolution process described here is highly exothermic. Thus in designing a plant based on this leaching approach, autogenous operation will have to be considered. Apart from the heat generated by the oxidative dissolution of several minerals present in the ore (U, Ni, etc.) the heat released by mixing HCl and $CaCl_2$ with H_2O will have to be accounted for. A good discussion of the problem of temperature control in pressure leaching of uranium ores has been given by Sarkar (39).

3.4.2 Model equations

As was discussed in section 3.2.2 the general second order polynomial (eq. 11) was fitted repeatedly to the experimental data of the design of Table 9 to get the model equation for each response. In this section the individual model equations are established and their statistical adequacy is tested. In section 3.4.3 the obtained results are discussed in terms of their metallurgical significance.

Following the statistical procedure described in section 3.2.2 the standardized model equations for U extraction, radium extraction, nickel extraction, arsenic extraction acid consumption and EMF were established to be those shown in Table 16.

Table 16 Standardized statistical model equations

Uranium extraction, eq. 14

$$\bar{Y}_u = 78.92 - 14.03x_1 + 12.01x_2 + 1.57x_3 + 2.84x_1x_2 - 2.08x_2x_4$$

Radium extraction, eq. 15

$$\bar{Y}_{ra} = 65.43 - 20.63x_1 + 9.63x_2 - 2.60x_4$$

Nickel extraction, eq. 16

$$\bar{Y}_{ni} = 59.73 - 4.99x_1 + 3.96x_2 + 1.41x_3 + 2.76x_4 - 1.41x_2^2 + 3.50x_1x_2$$

Arsenic extraction, eq. 17

$$\bar{Y}_{as} = 46.63 - 12.56x_1 + 9.67x_2 - 4.12x_1x_4$$

Acid consumption, eq. 18

$$\bar{Y}_{ac} = 0.411 + 0.059x_1 + 0.121x_2 + 0.038x_3 + 0.013x_4 - 0.019x_1^2 - 0.010x_3^2$$
$$+ 0.015x_4^2 - 0.009x_1x_2 - 0.014x_1x_3 - 0.034x_1x_4 + 0.033x_2x_4 + 0.024x_2x_3$$

Pressure leach EMF, Eq. 19

$$\bar{Y}_{emf} = 738.67 - 23.45x_1 + 21.94x_2 + 16.10x_3 - 8.99x_2^2 + 16.44x_1x_2 - 7.64x_1x_4$$

where $\hat{y}_u$ denotes the predicted value of the percentage of uranium extracted.

$\hat{y}_{ra}$ denotes the predicted value of the percentage of radium extracted.

$\hat{y}_{ni}$ denotes the predicted value of the percentage of nickel extracted.

$\hat{y}_{as}$ denotes the predicted value of the percentage of arsenic extracted.

$\hat{y}_{ac}$ denotes the predicted value of the acid consumption (moles/l).

$\hat{y}_{emf}$ denotes the predicted value of the pressure leach EMF (mV).

Acid consumption as it is predicted by eq. 18 is expressed in moles HCl consumed/lit solution. To obtain the more conventional expression of kg HCl/ton ore it is simply necessary to divide the model predictions by the appropriate d_s value (i.e. kg solids/l). Direct prediction of acid consumption in kg/ton was not statistically appropriate since this would mean apriori direct dependence of $\hat{y}_{ac}$ on x_1 (i.e. ds).

The statistical adequacy of these models is exemplified with the residuals plots shown in Figs. 11 to 16. The plots provide no evidence to suggest that the distribution of residuals is not random.

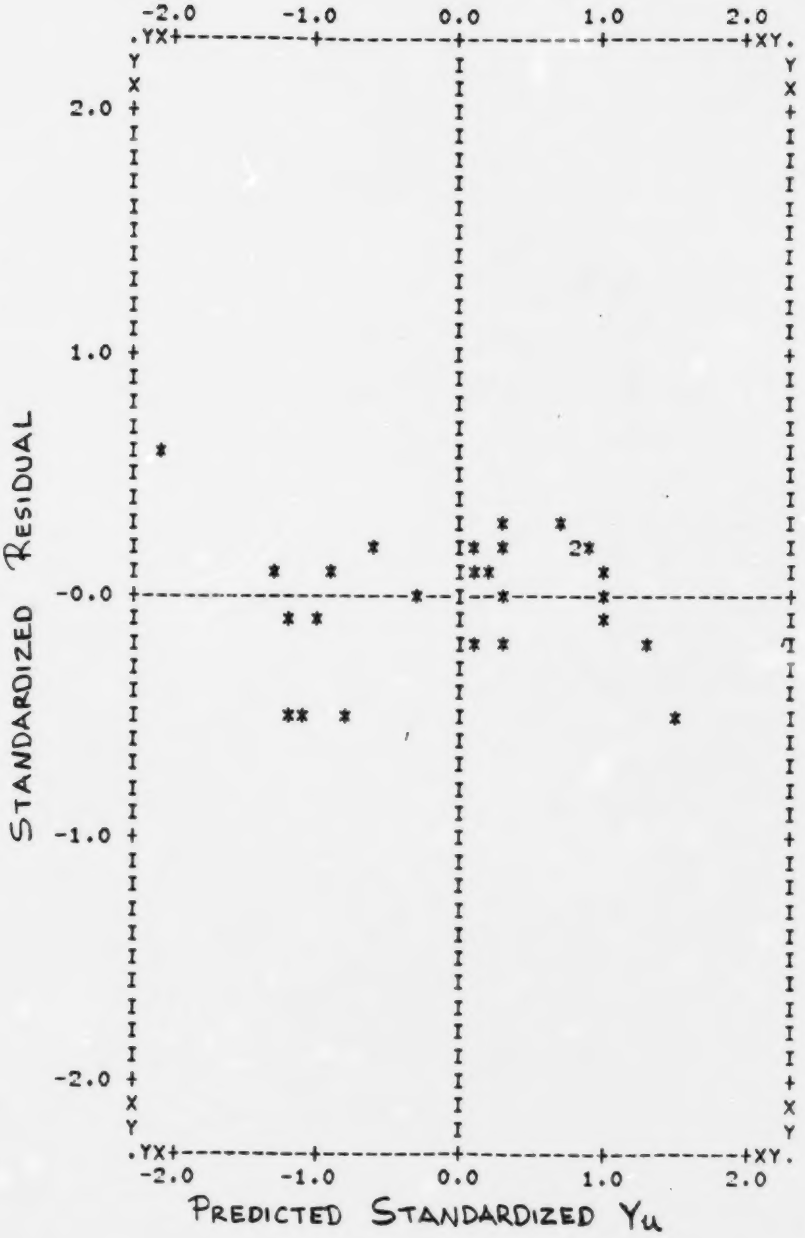

Fig. 11 Residuals vs predicted $\bar{Y}_u$ plot.

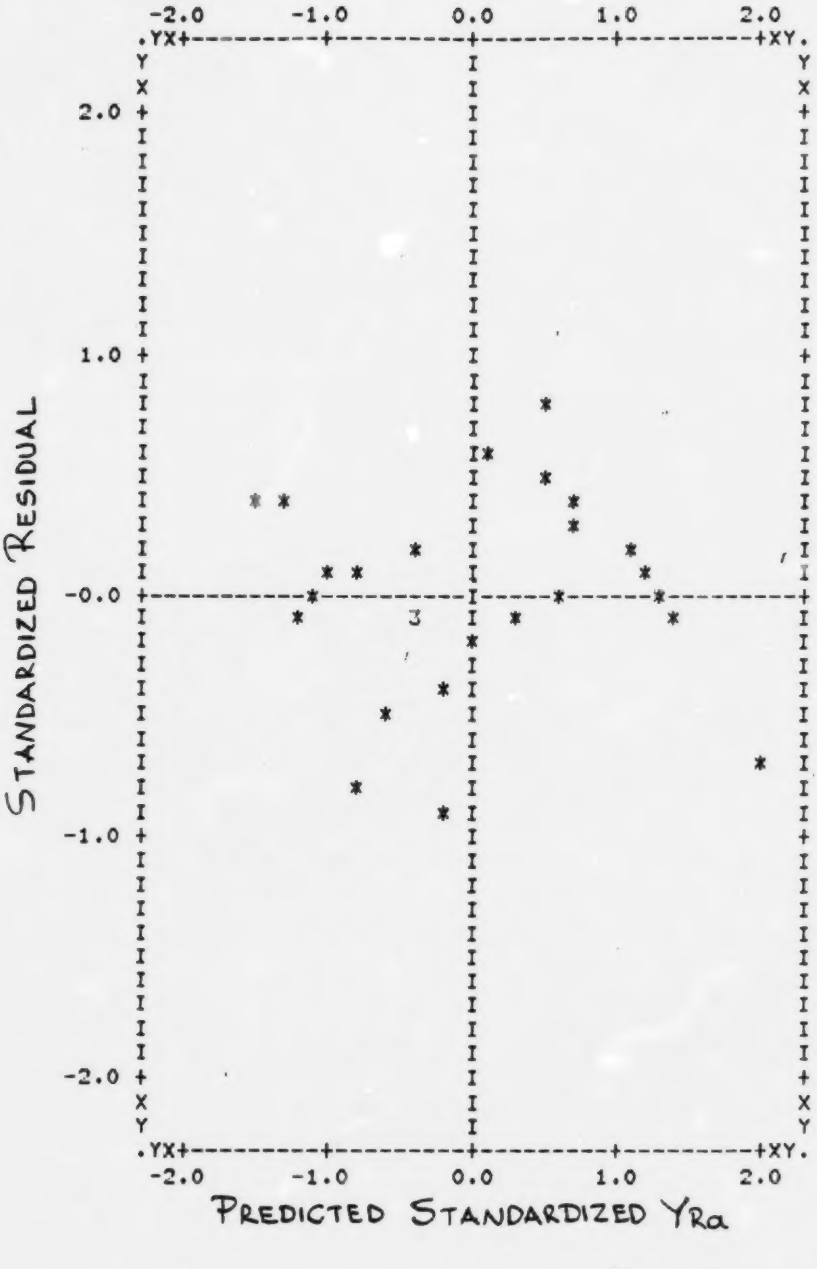

Fig. 12 Residuals vs predicted $\bar{Y}_{ra}$ plot.

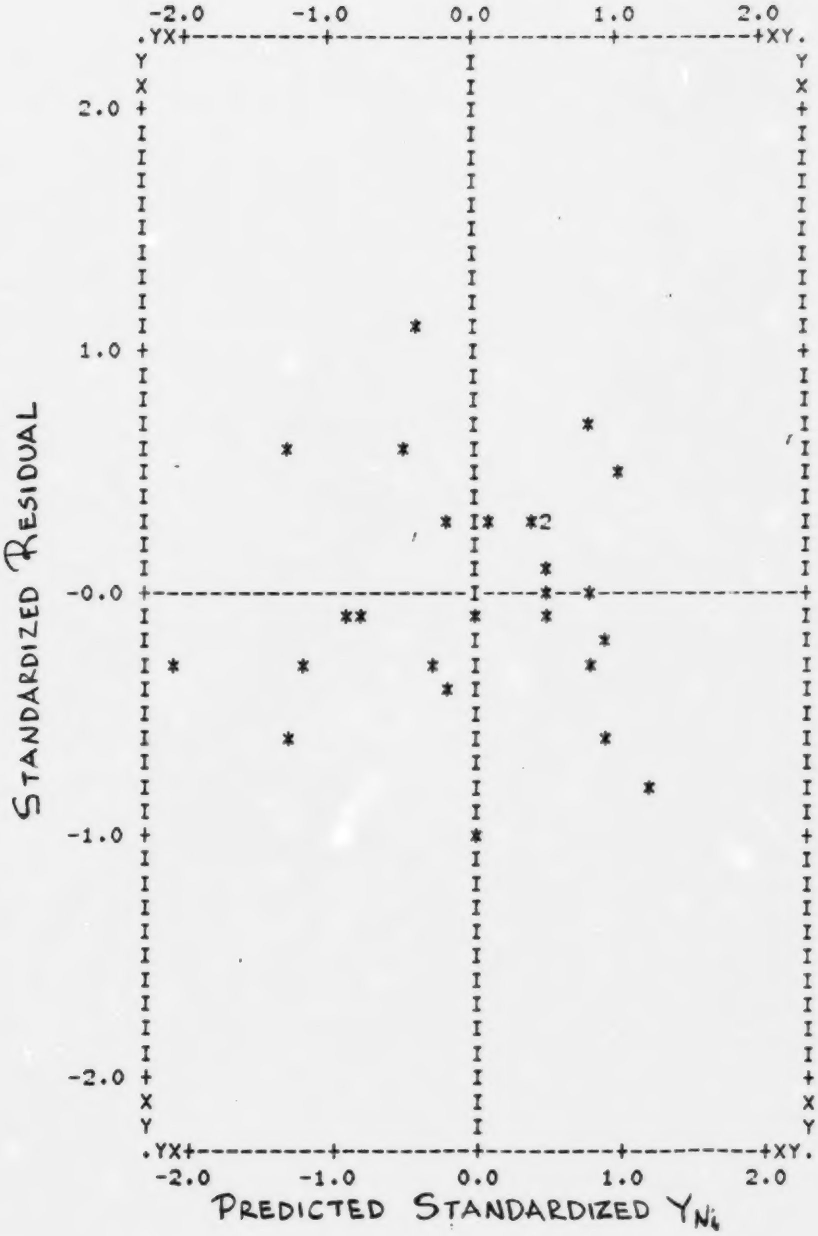

Fig. 13 Residuals vs predicted $\bar{Y}_{ni}$ plot.

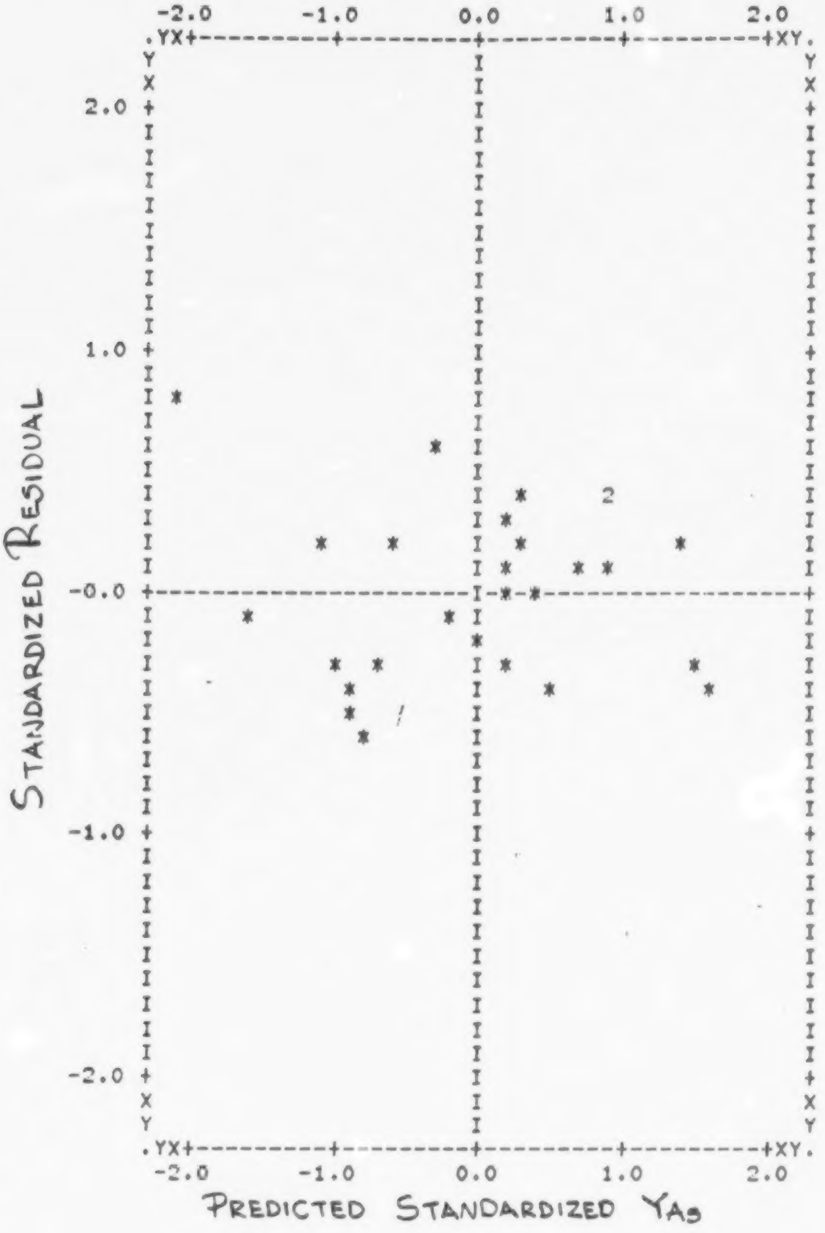

Fig. 14 Residuals vs predicted $\bar{Y}_{as}$ plot.

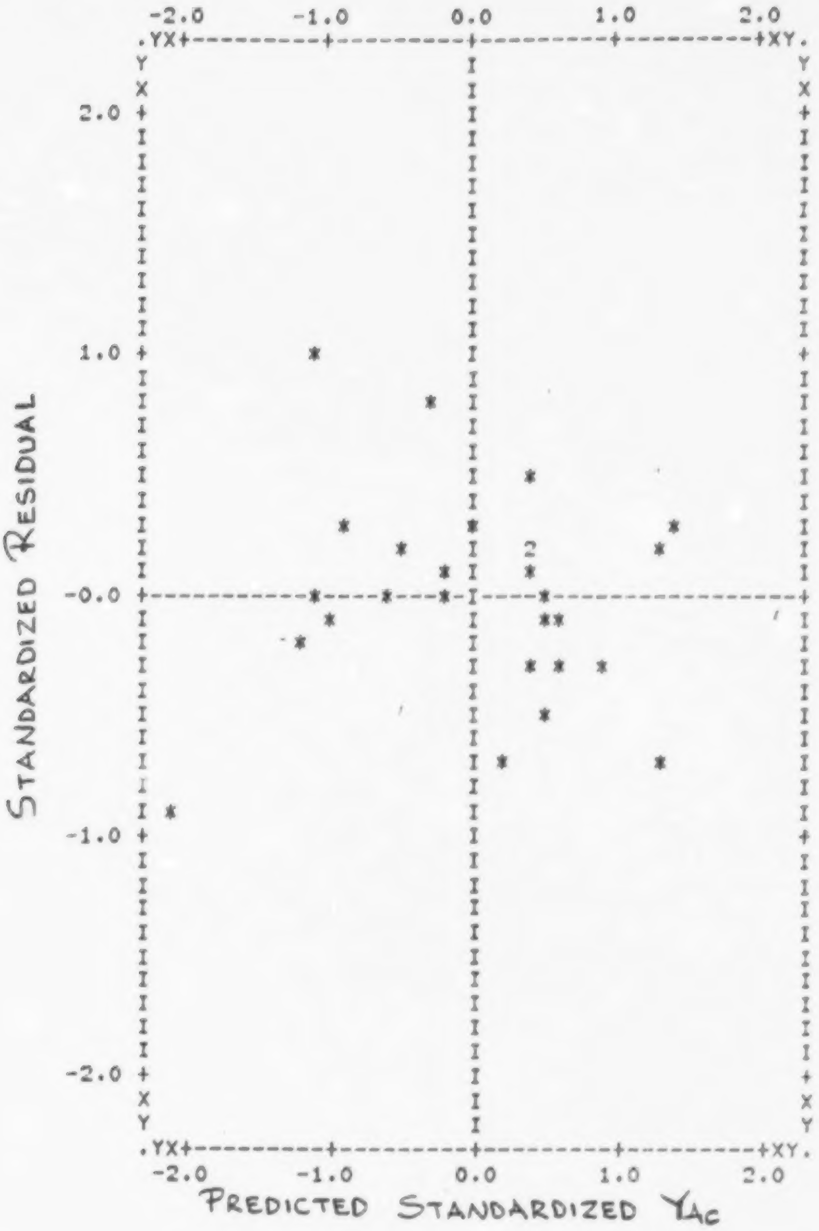

Fig. 15 Residuals vs predicted $\bar{Y}_{ac}$ plot.

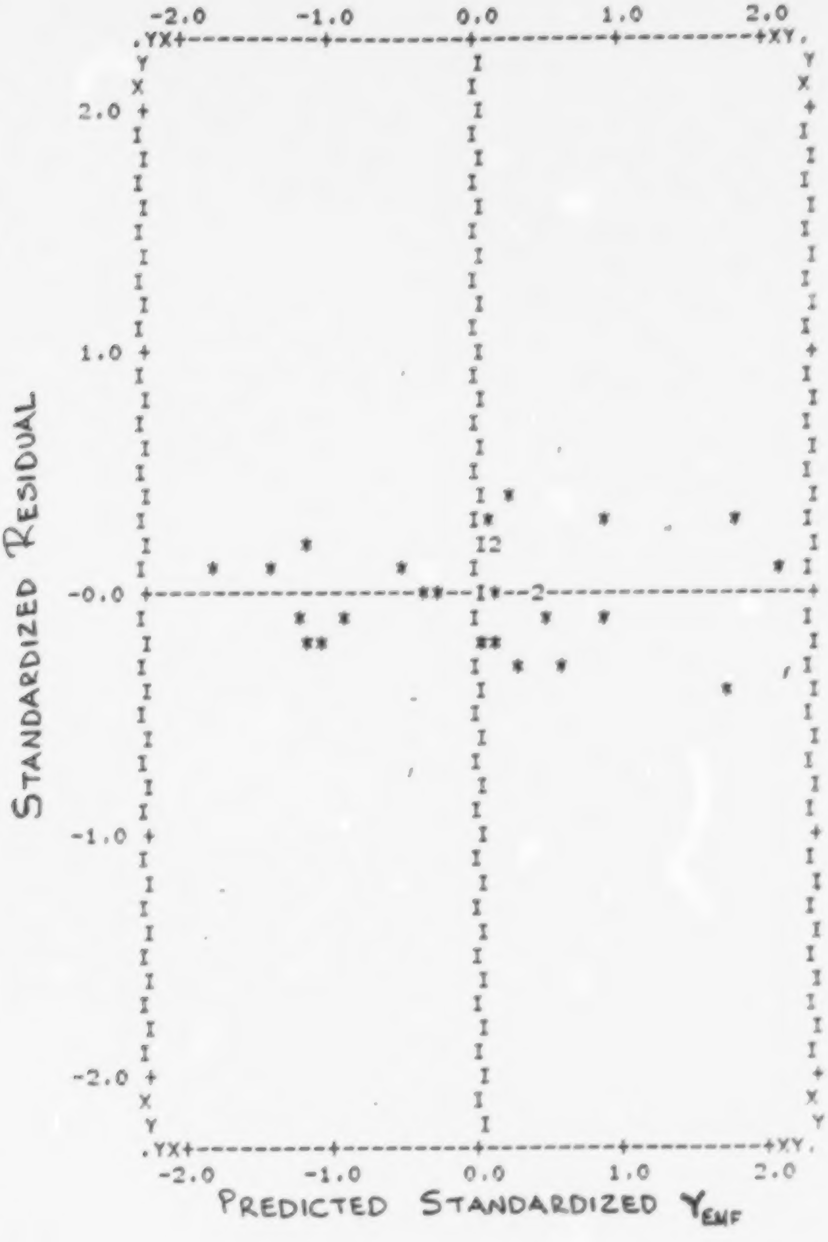

Fig. 16 Residuals vs predicted $\bar{Y}_{emf}$ plot.

For the purposes of statistical analysis all the model equations listed in Table 16 were expressed in terms of standardized values of the independent variables. In terms of the true physicochemical values of these variables the model equations are transformed to those shown in Table 17.

where D_S denotes slurry density in kg solids/l solution,
$[HCl]_o$ and $[CaCl_2]_o$ initial molar concentrations of acid and salt, and
T reaction time in hours.

3.4.2 Metallurgical Analysis

Statistical models as those developed in the present work (Table 17) do not usually provide an explanation of the underlying process mechanism but are rather an approximate mathematical description of the behaviour of the measured data. Consequently interpretation of these leaching models requires careful examination. Interpretation of the leaching results and the model predictions will be made with the aid of several 2-D and 3-D graphical representations. The simple 2-D graphs involve plotting each response, Y_j against the various process variables X_i. This type of plot can detect the most important effects and identify major trends among the experimental results. However, the 3-D graphs are actually those that allow the establishment of the dynamic correlations among the various process factors and identify avenues for process optimization. The latter type of graph can only be generated with the aid of computer by using the

Table 17 Model equations in terms of true physicochemical values

Uranium extraction, eq. 20

$$\bar{Y}_U = 84.54 - 98.14\ D_S + 29.22\ |HCl|_o + 2.3\ |CaCl_2|_o + 4.51\ T$$

$$+ 36.58\ D_S\ |HCl|_o - 4.51\ |HCl|_o\ T$$

Radium extraction, eq. 21

$$\bar{Y}_{Ra} = 104.46 - 90.49\ D_S + 28.33\ |HCl|_o - 1.91\ T$$

Nickel extraction, eq. 22

$$\bar{Y}_{Ni} = 66.78 - 66.99\ D_S + 6.26\ |HCl|_o + 2.08\ |CaCl_2|_o + 2.03\ T$$

$$- 12.18\ |HCl|_o^2 + 45.09\ D_S\ |HCl|_o$$

Arsenic extraction, eq. 23

$$\bar{Y}_{As} = 19.44 - 1.89\ D_S + 28.44\ |HCl|_o + 8.79\ T - 13.30\ D_S\ T$$

Acid consumption, eq. 24

$$\bar{Y}_{AC} = -0.275 + 1.290\ D_S - 0.267\ |HCl|_o + 0.120\ |CaCl_2|_o - 0.054\ T$$

$$- 0.365\ D_S^2 - 0.022\ |CaCl_2|_o^2 + 0.008\ T^2 - 0.116\ D_S\ |HCl|_o - 0.090\ D_S\ |CaCl_2|_o$$

$$-0.110\ D_S\ T + 0.104\ |HCl|_o\ |CaCl_2|_o + 0.071\ |HCl|_o\ T$$

Pressure leach EMF, eq. 25

$$\bar{Y}_{EMF} = 679.82 - 216.24\ D_S + 80.12\ |HCl|_o - 23.71\ |CaCl_2|_o$$

$$+ 16.27\ T - 77.76\ |HCl|_o^2 + 212.01\ D_S\ |HCl|_o - 24.65\ D_S\ T$$

proper model equation. In the following sections each response is discussed with the aid of these graphical representations.

3.4.2.1 Study of the response: % uranium extraction

The data of Fig. 17 (plots and $r = -0.703$) clearly indicate that uranium extraction deteriorates with increasing slurry density. This can be attributed to the acid consuming nature of the ore (see section 3.4.1). At high d_s more acid is consumed having as a result the acid tenor not being sufficient to maintain uranium soluble. This interpretation of the d_s effect on U extraction is supported by considering (in Fig. 17) the same effect at different HCl levels (broken lines on the graph). Moreover this interactive effect of d_s and HCl on U extraction is confirmed with the presence of the term $2.84\ x_1x_2$ in the U model equation (eq. 14, in Table 16).

Figure 18 (plots and $r = 0.61$) suggests that increasing HCl concentration results in increased U extraction which is again understandable from the standpoint of uranium leaching chemistry:

$$UO_2(s) + 2H^+ + 1/2\ O_2 \longrightarrow UO_2^{2+} + H_2O \qquad (26)$$

The broken lines of Fig. 18 suggest that an interaction between HCl and d_s seems plausible (i.e. the effect of HCl varies according to the d_s level).

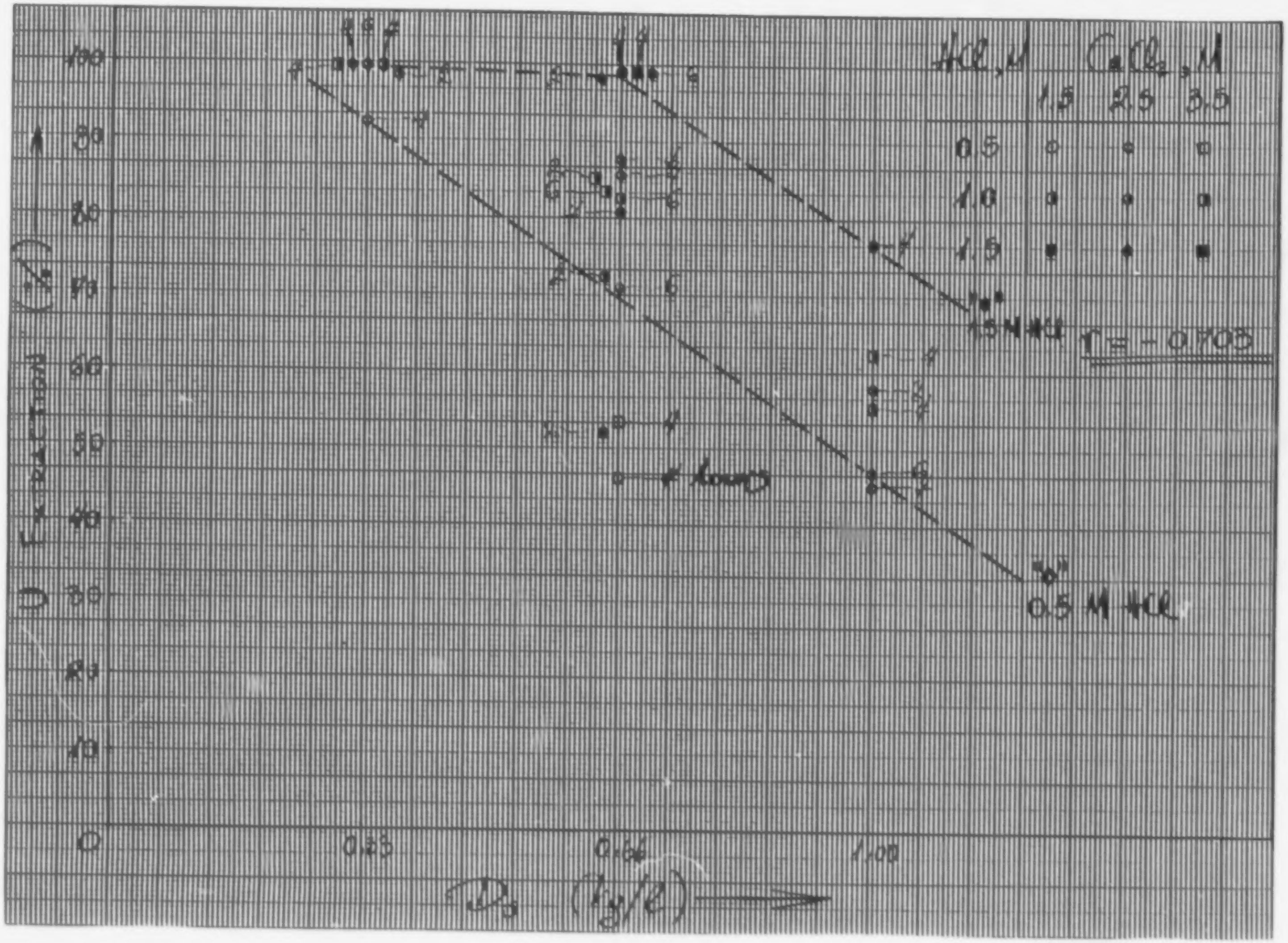

Fig. 17 Observed % U extraction vs slurry density.

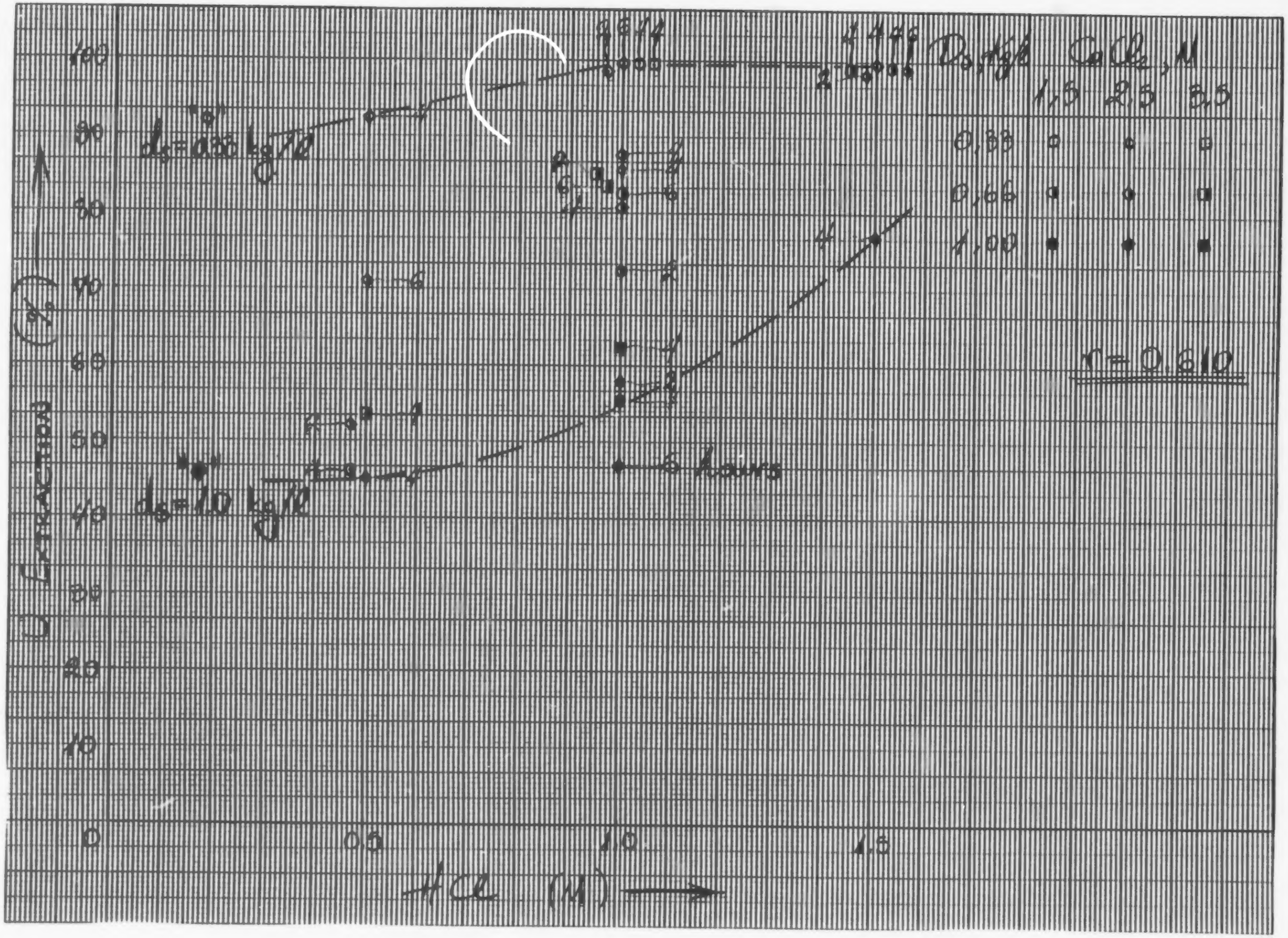

Fig. 18 Observed % U extracted vs $|HCl|_o$.

Finally, the data of Figs. 19 and 20 suggest that $CaCl_2$ conc and time have no apparent effect on U extraction.

Interaction effects as those of ds and HCl on U extraction are better understood by considering the model predictions represented by 3-D graphs generated with the computer. The 3-D graphs presented here were generated with the aid of the standardized model equations (Table 16) and thus the independent variables are given with coded units. Conversion of coded values to true physicochemical values is simple. Table 18 was constructed to give the coded and true values for each variable. The units of the dependent variables are not affected by the use of coded values.

Figs. 21 to 29 show 3-dimensional representation of the estimated response surface, that is % uranium extraction as a function of d_s and $[HCl]_o$. In Figs. 21 to 23 the response surface is estimated for reaction time kept constant at 2 hrs (in coded form -1.47) and various $[CaCl_2]$ concentrations. It can be concluded from these figures in accordance with Fig. 19 that $CaCl_2$ has practically no effect on U extraction. However, the same figures clearly show now the interactive effect of ds and $[HCl]_o$. Uranium extraction is very poor at high d_s (1.0 kg/l) and low $[HCl]_o$ (0.5 N). Only under strong acid conditions ($[HCl]_o \geqslant 1.0$ N) and dilute slurries (near 0.33 kg solids/l) complete uranium extraction is possible. Similar graphs to those of Figs. 21 to 23 have been constructed for 4 hrs ($X_T = 0.00$) (Figs. 24 to 26) and 6 hrs ($X_T = 1.47$) (Figs. 27 to 29)

Table 18 Conversion of coded values to true units for the four independent variables.

Coded Value	Slurry Density XDS (kg/l)	$\|HCl\|_o$ XHCL(M)	$\|CaCl_2\|_o$ XCACL2(M)	Time XT (hr)
-1.47	0.33	0.50	1.50	2.00
-1.00	0.43	0.66	1.82	2.64
-0.50	0.55	0.83	2.16	3.32
0.00	0.66	1.00	2.50	4.00
+0.50	0.77	1.17	2.84	4.68
+1.00	0.89	1.34	3.18	5.36
1.47	1.00	1.50	3.50	6.00

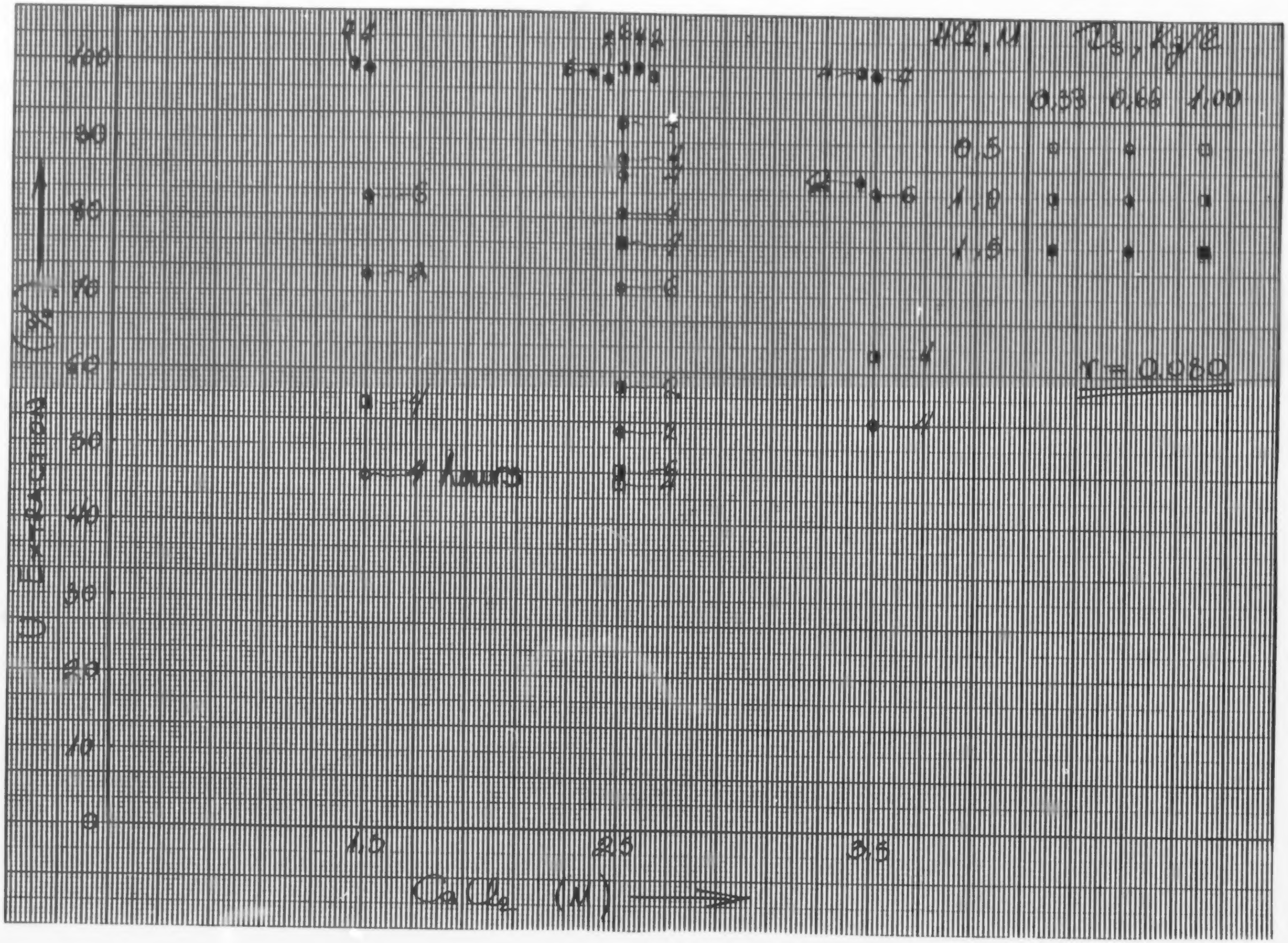

Fig. 19 Observed % U extraction vs $|CaCl_2|_o$.

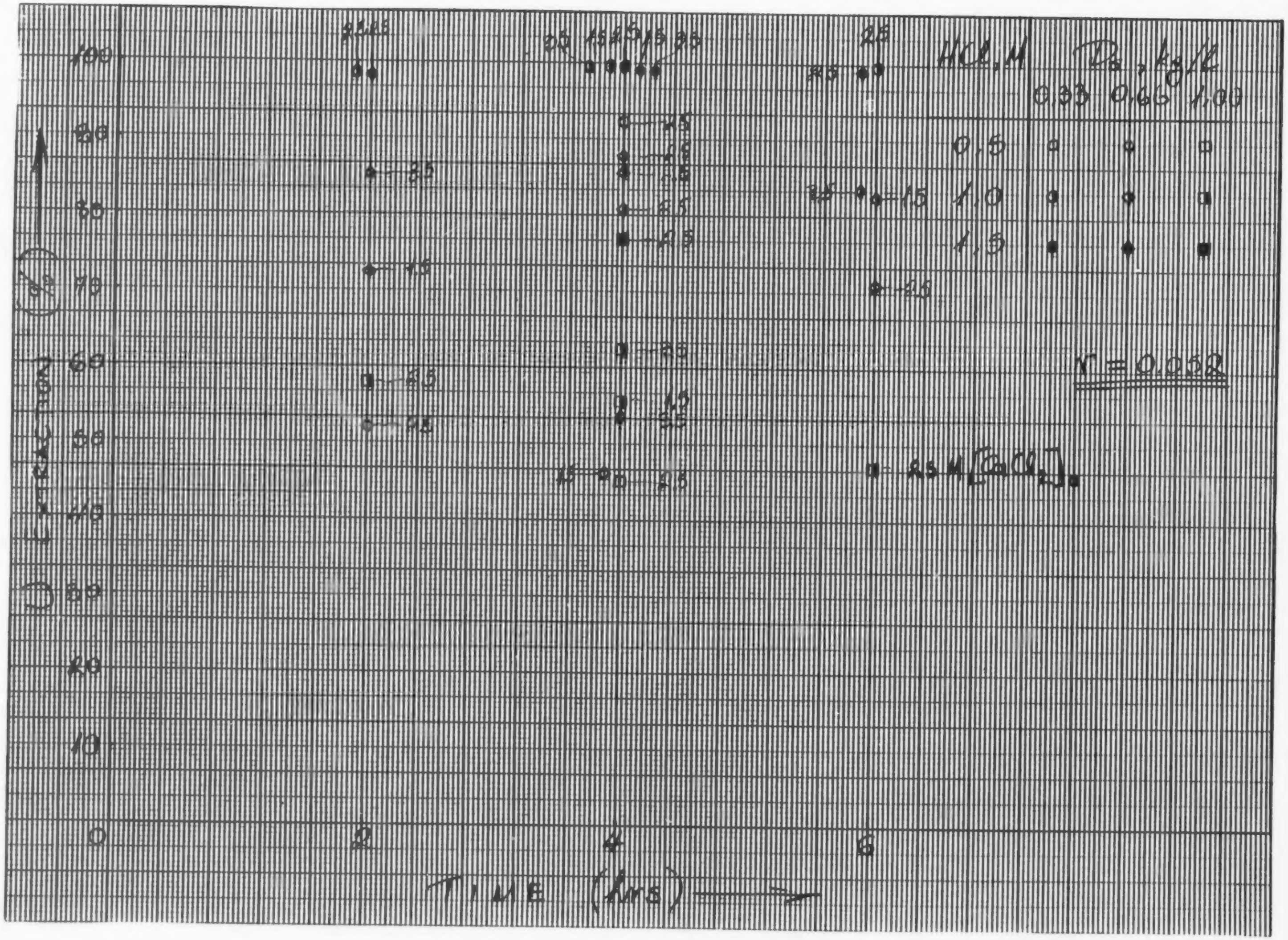

Fig. 20 Observed % U extraction vs time.

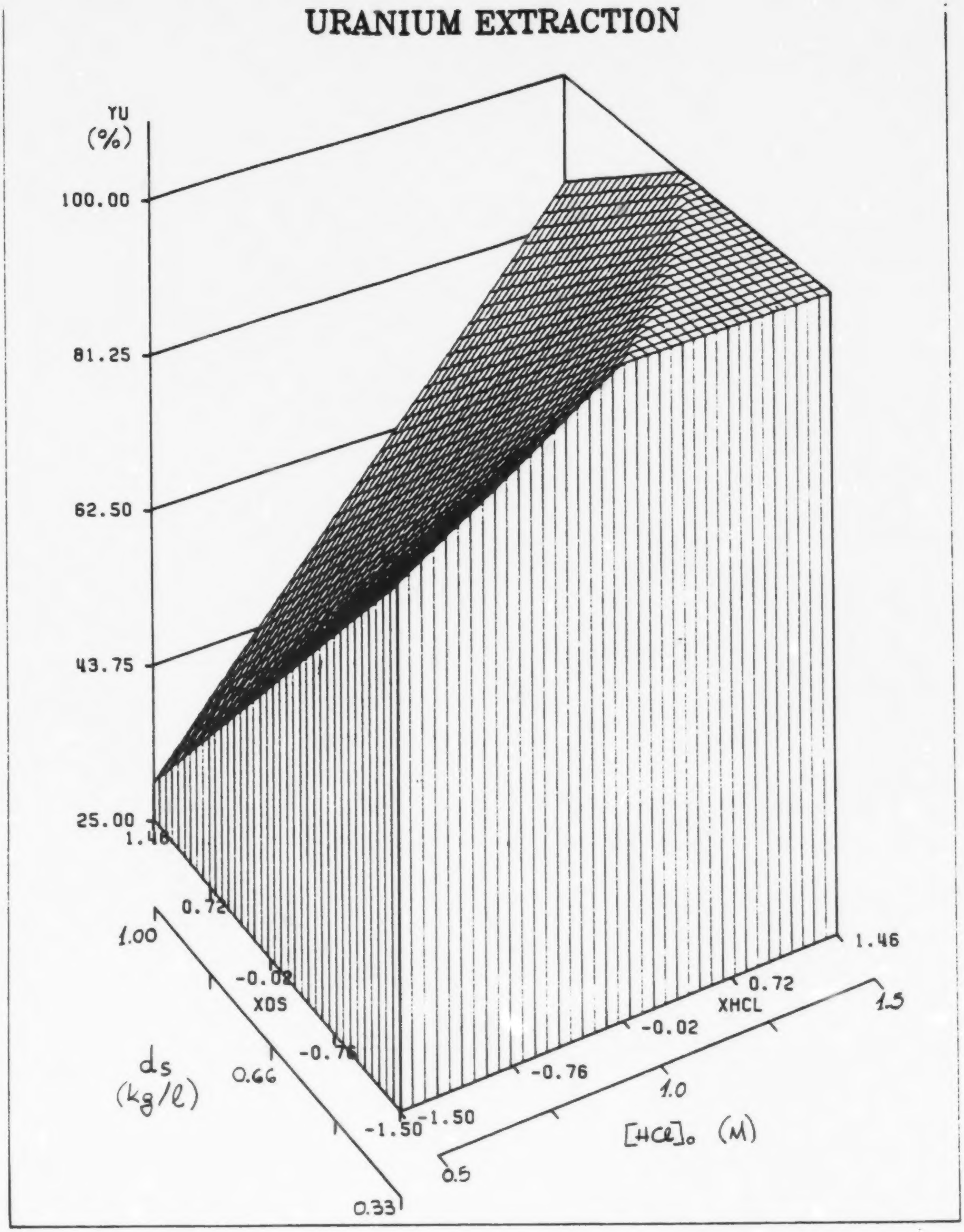

Fig. 21 Predicted % U extraction response surface as a function of slurry density (d_s) and $|HCl|_o$; $|CaCl_2|_o$ = 1.5 M and T = 2 hrs.

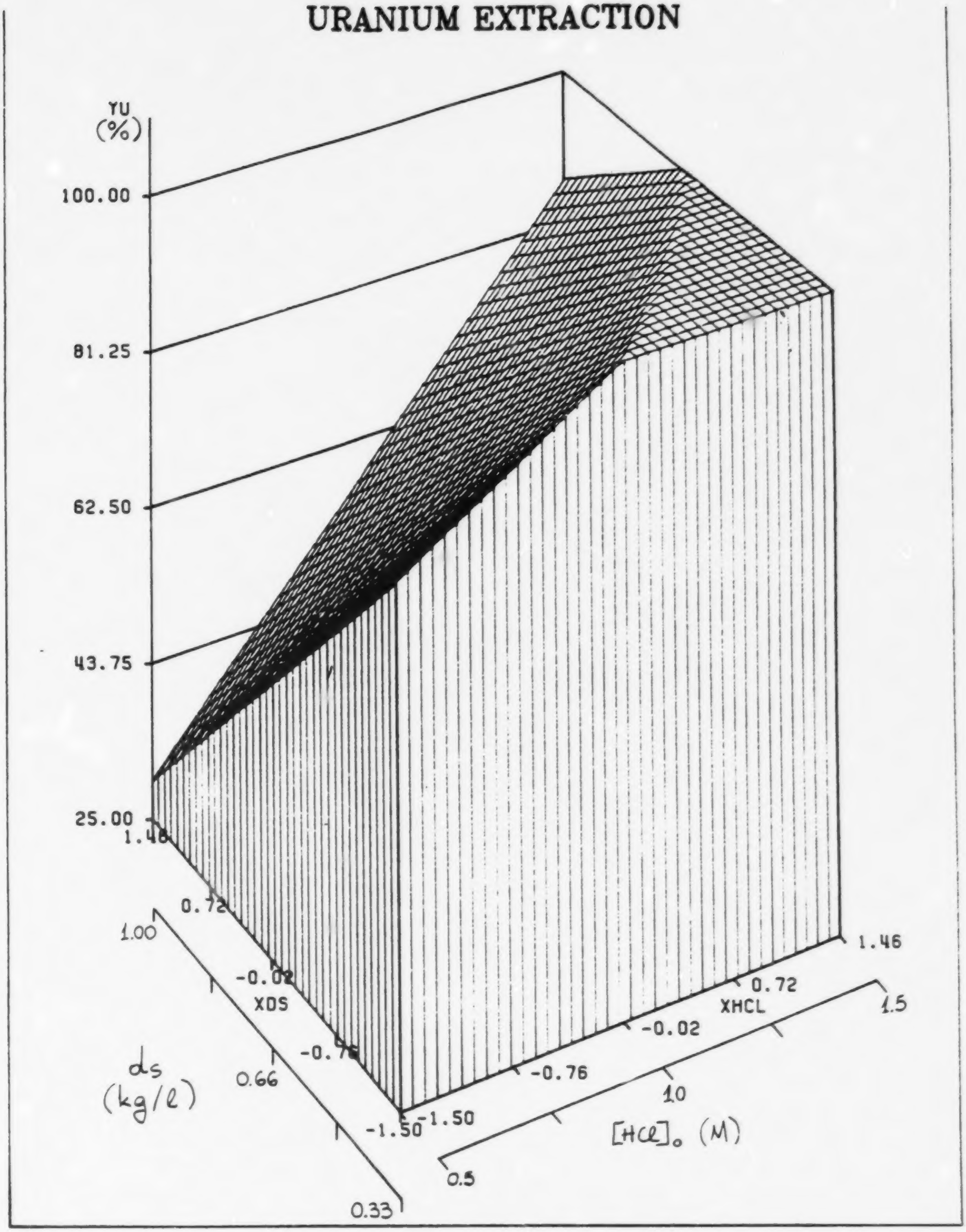

Fig. 22 Predicted % U extraction response surface as a function of slurry density (d_s) and $|HCl|_o$; $|CaCl_2|_o$ = 2.5 M and T = 2 hrs.

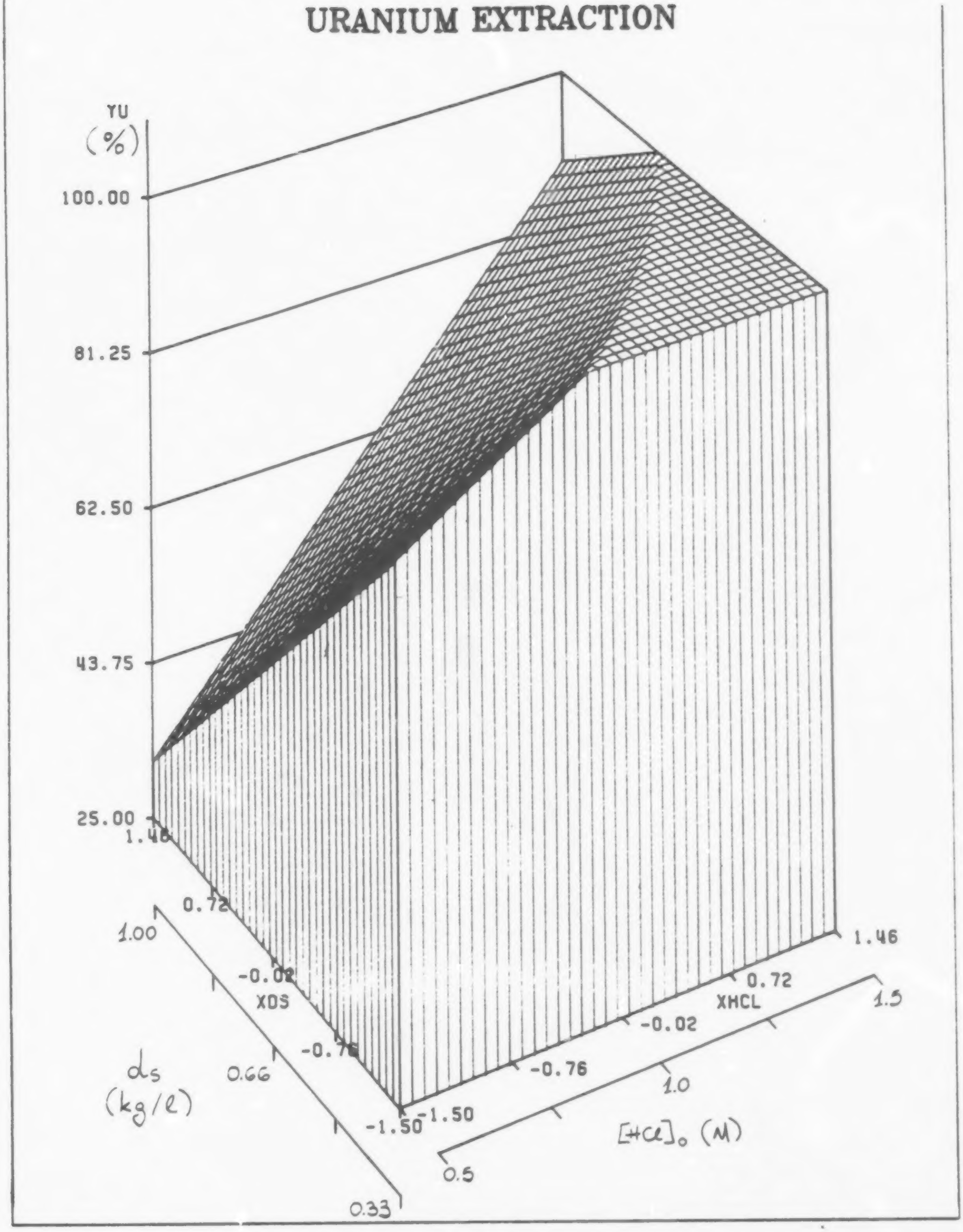

Fig. 23 Predicted % U extraction response surface as a function of d_s and $|HCl|_o$; $|CaCl_2|_o$ = 3.5 M and T = 2 hrs.

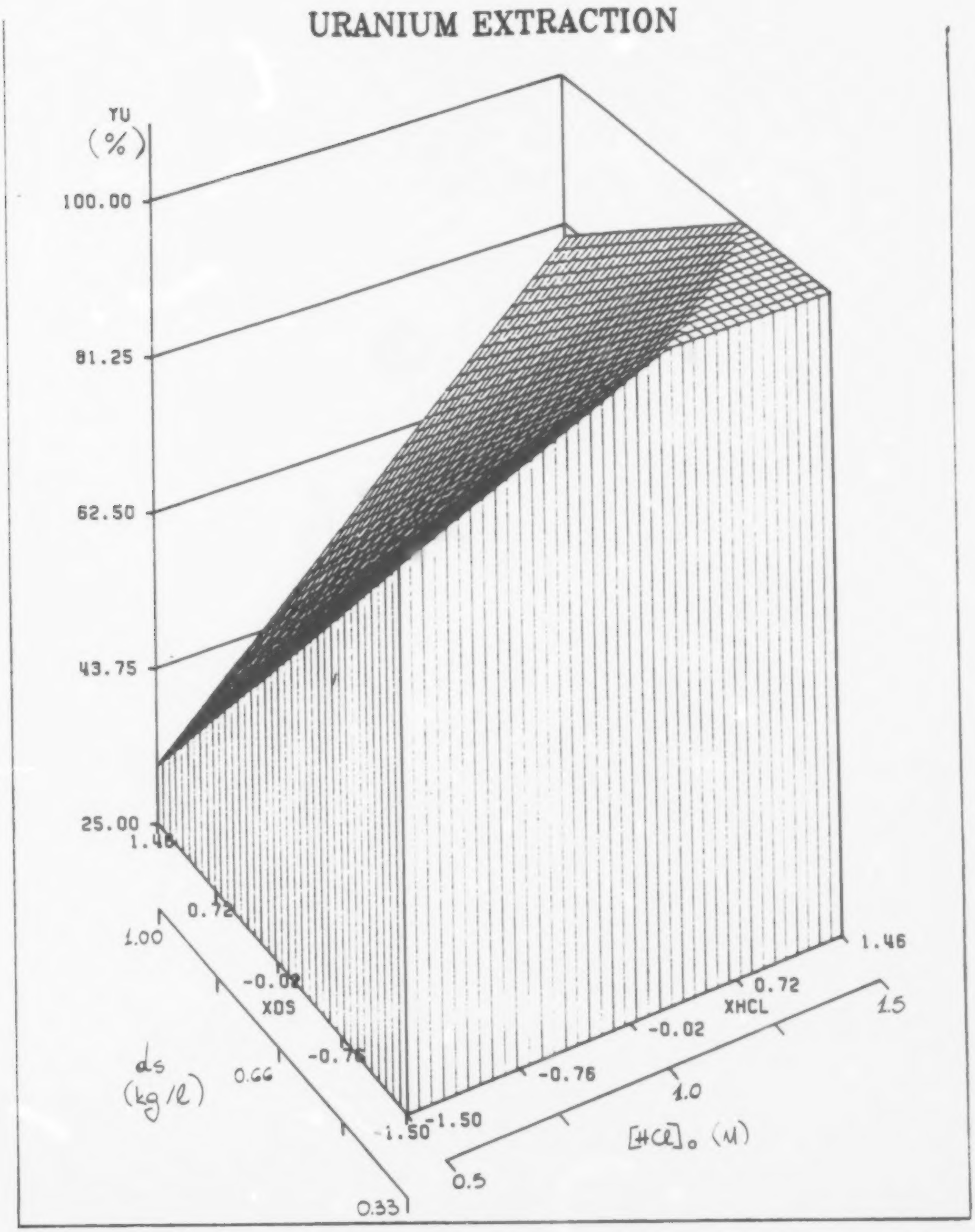

Fig. 24 Predicted % U extraction response surface as a function of d_s and $|HCl|_o$; $|CaCl_2|$ = 1.5 M and T = 4 hrs.

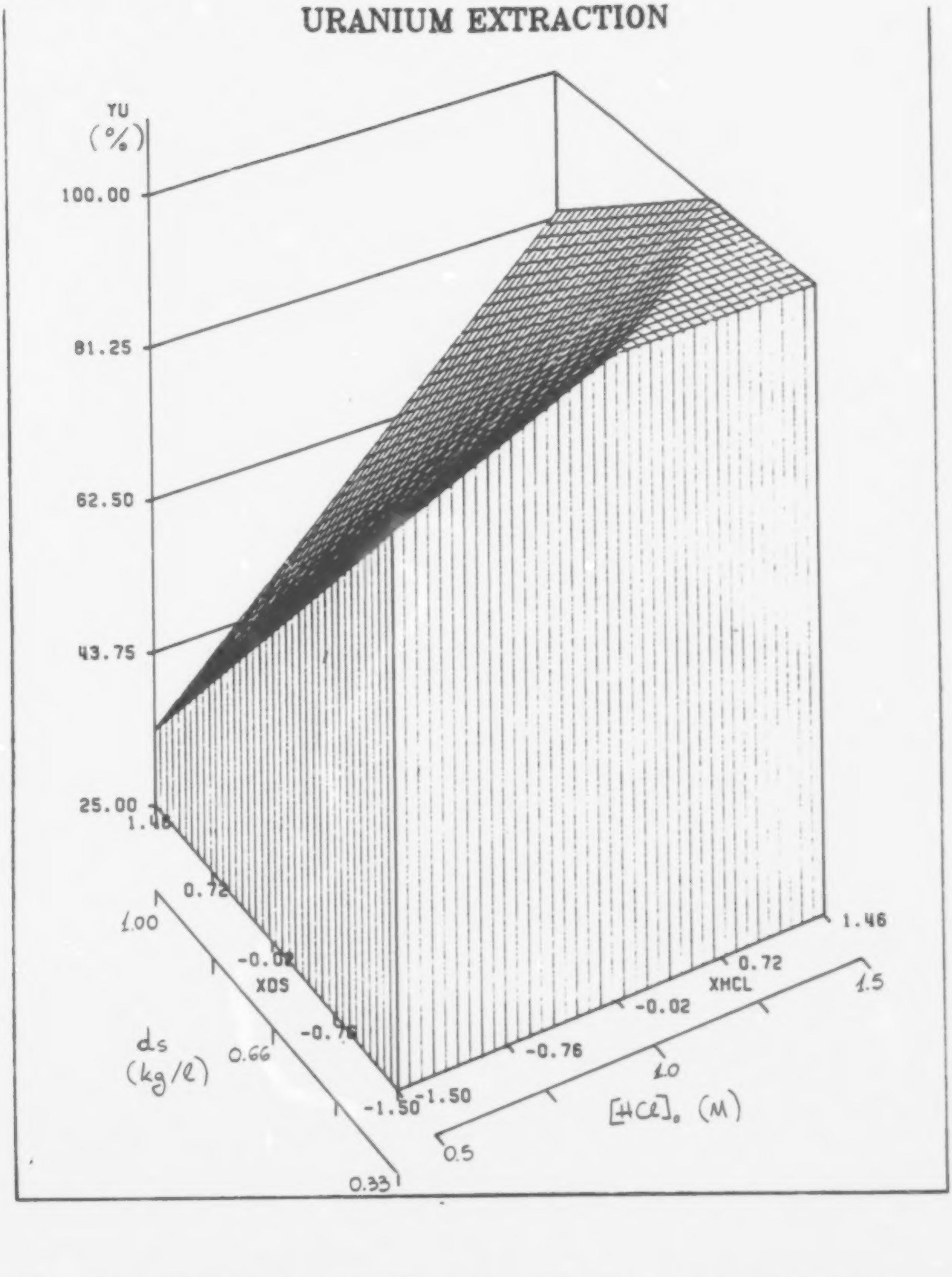

Fig. 25 Predicted % U extraction response surface as a function of d_s and $|HCl|_o$; $|CaCl_2|_o$ = 2.5 M and T = 4 hrs.

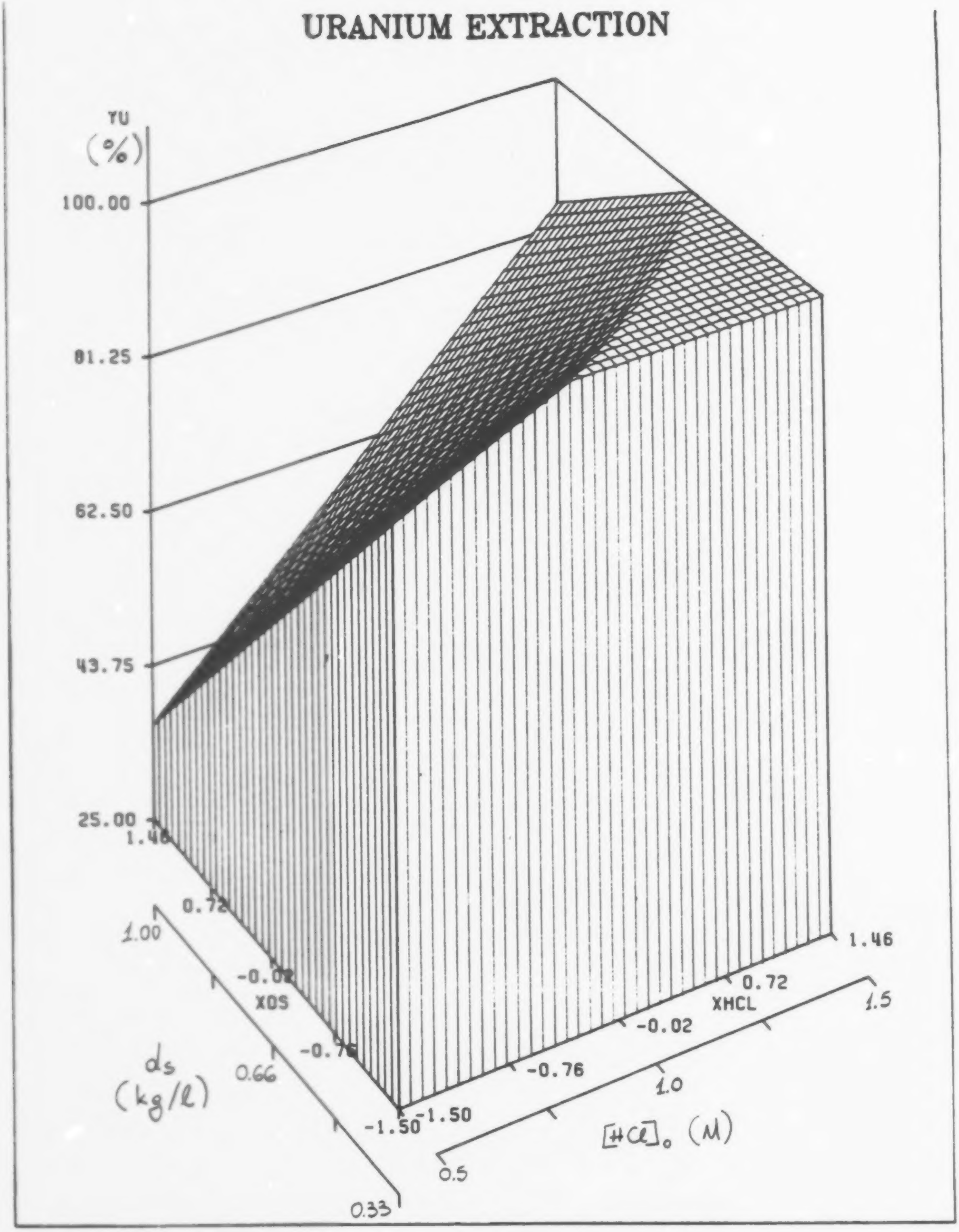

Fig. 26 Predicted % U extraction response surface as a function of d_s and $|HCl|_o$; $|CaCl_2|_o$ = 3.5 M and T = 4 hrs.

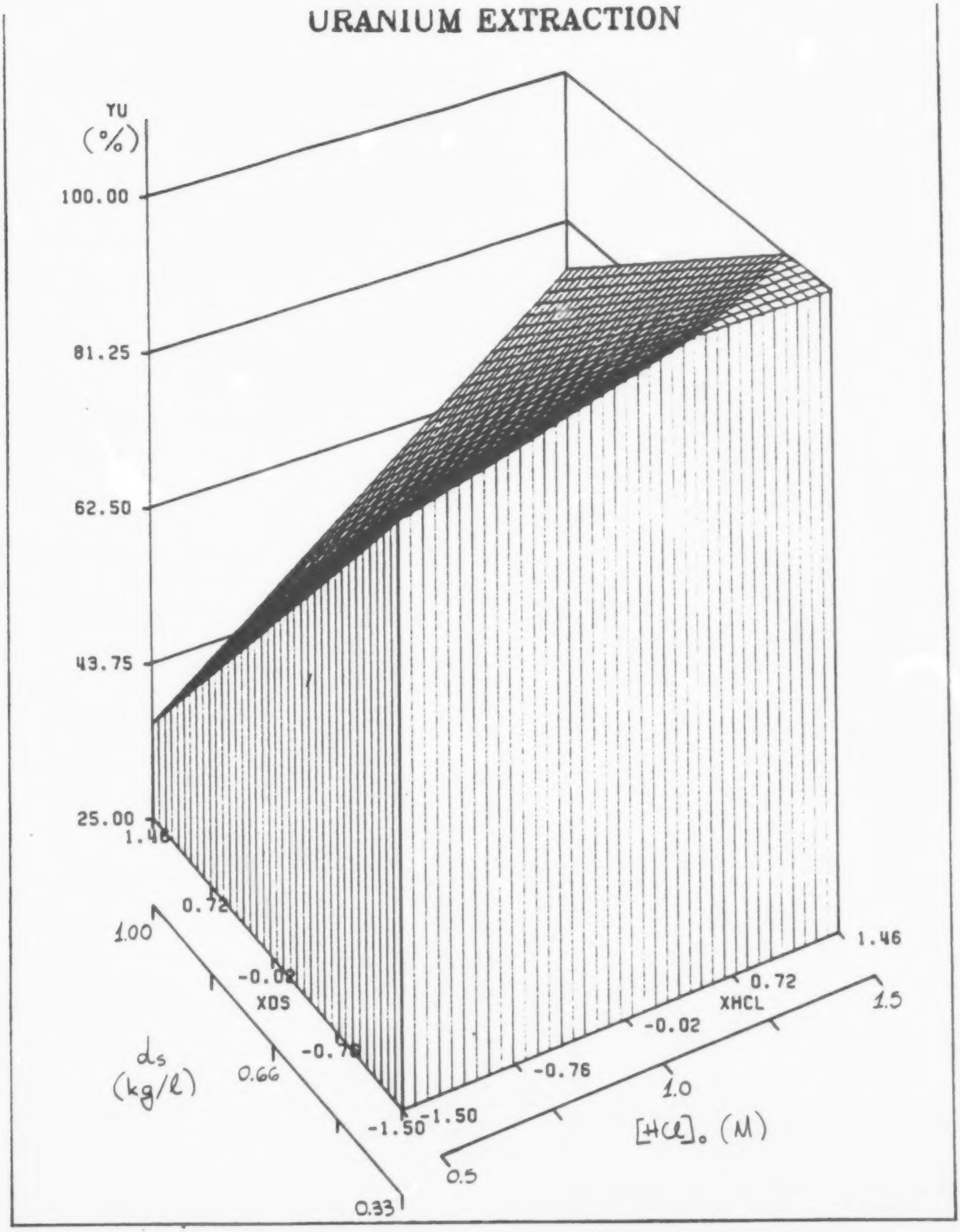

Fig. 27 Predicted % U extraction response surface as a function of d_s and $|HCl|_o$; $|CaCl_2|_o$ = 1.5 M and T = 6 hrs.

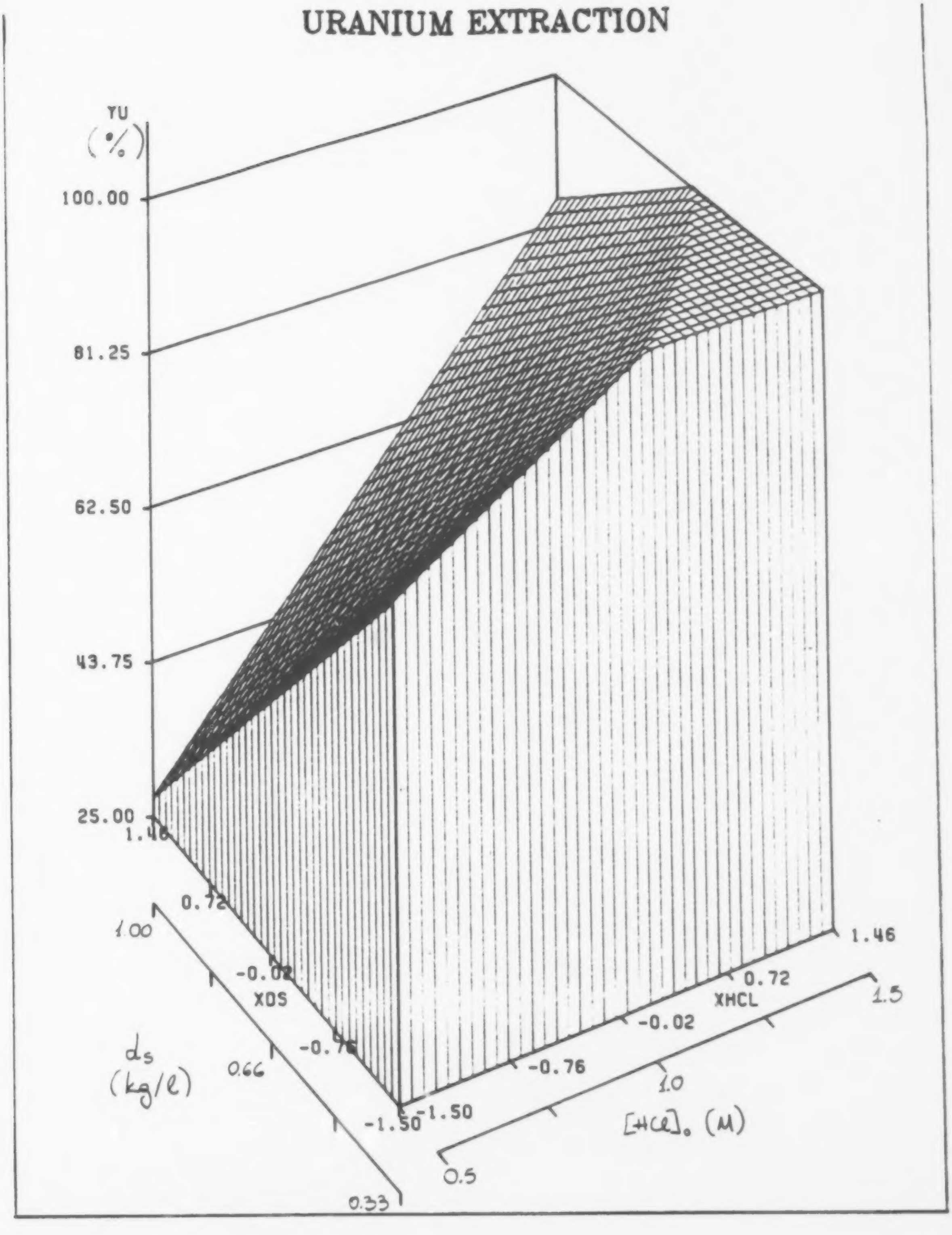

Fig. 28 Predicted % U extraction response surface as a function of d_s and $|HCl|_o$; $|CaCl_2|_o$ = 2.5 M and T = 6 hrs.

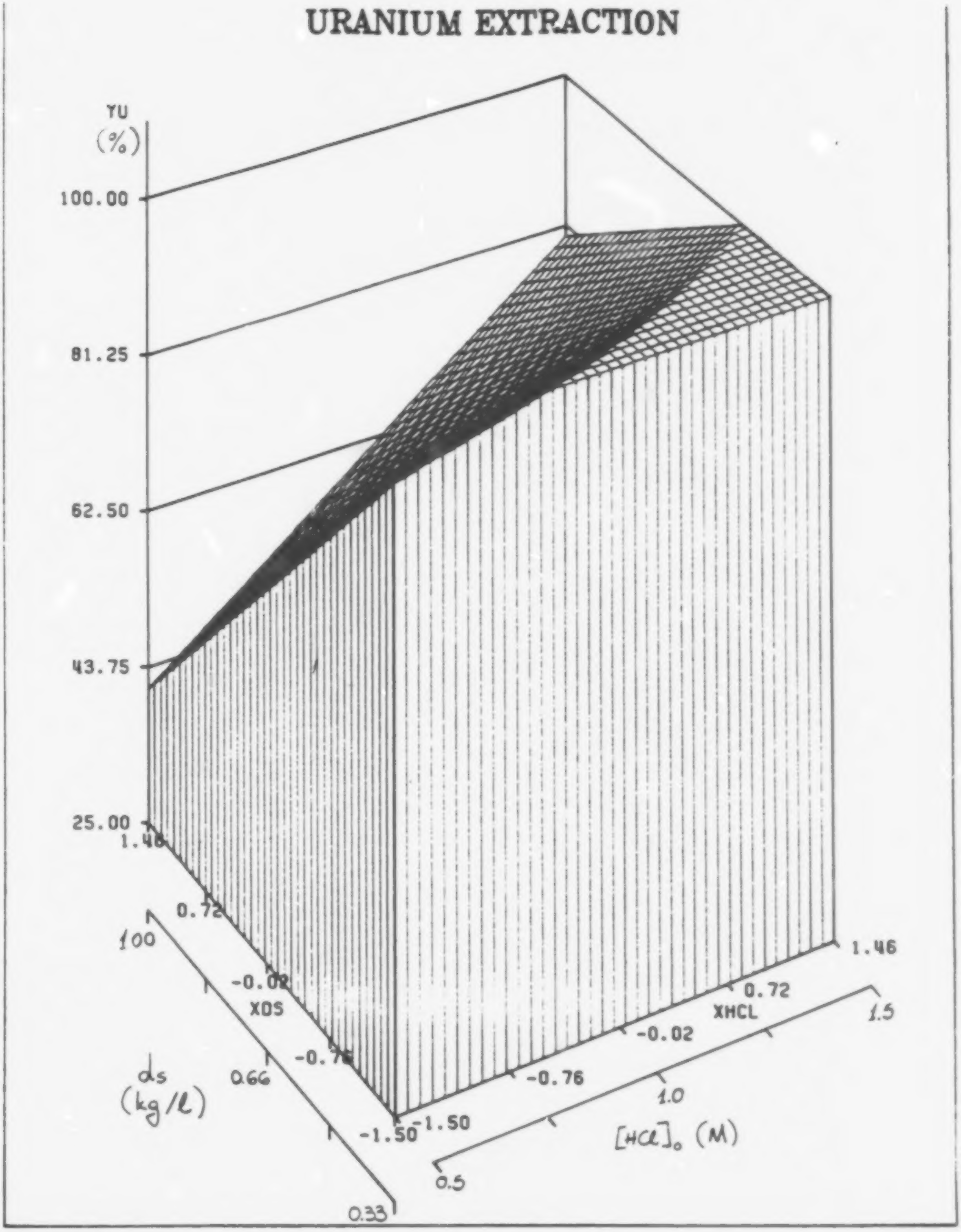

Fig. 29 Predicted % U extraction response surface as a function of d_s and $|HCl|_o$; $|CaCl_2|_o$ = 35 M and T = 6 hrs.

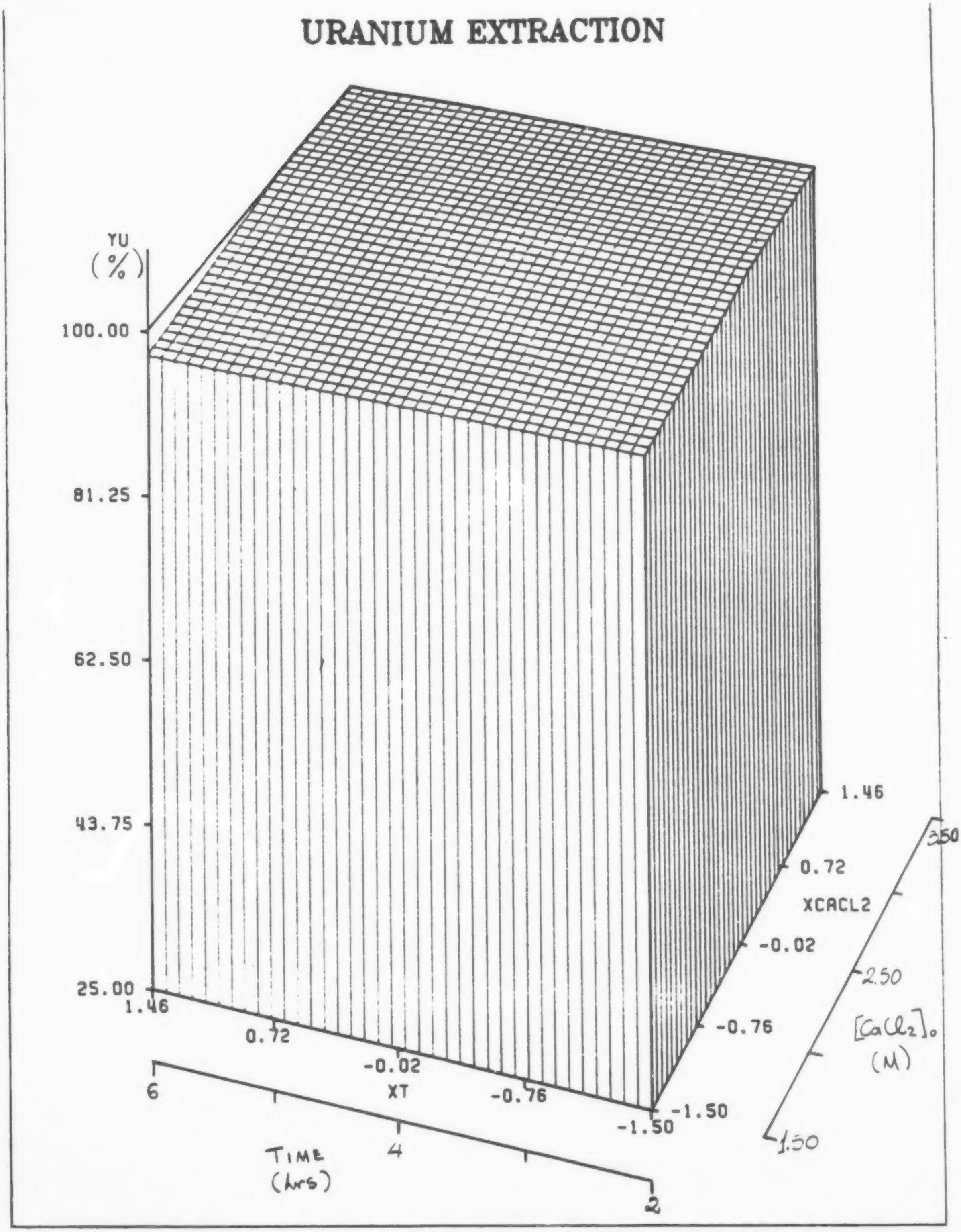

Fig. 30 **Predicted % U extraction response surface as a function of $|CaCl_2|_o$ and Time; d_s = 0. 33 kg/l and $|HCl|_o$ = 1.0 M.**

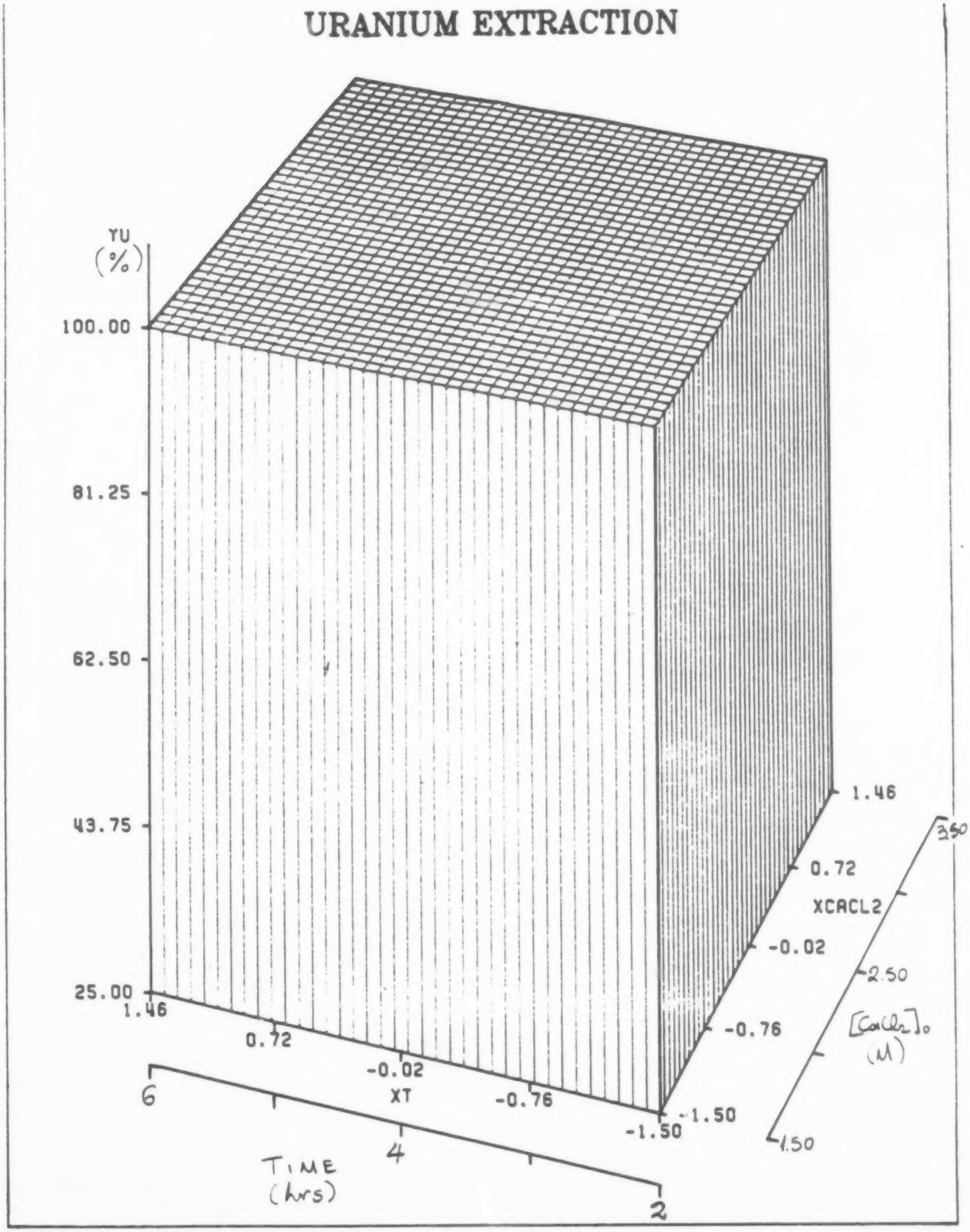

Fig. 31 Predicted % U extraction response surface as a function of $|CaCl_2|_o$ and Time; d_s = 0.33 kg/l and $|HCl|_o$ = 1.5 M.

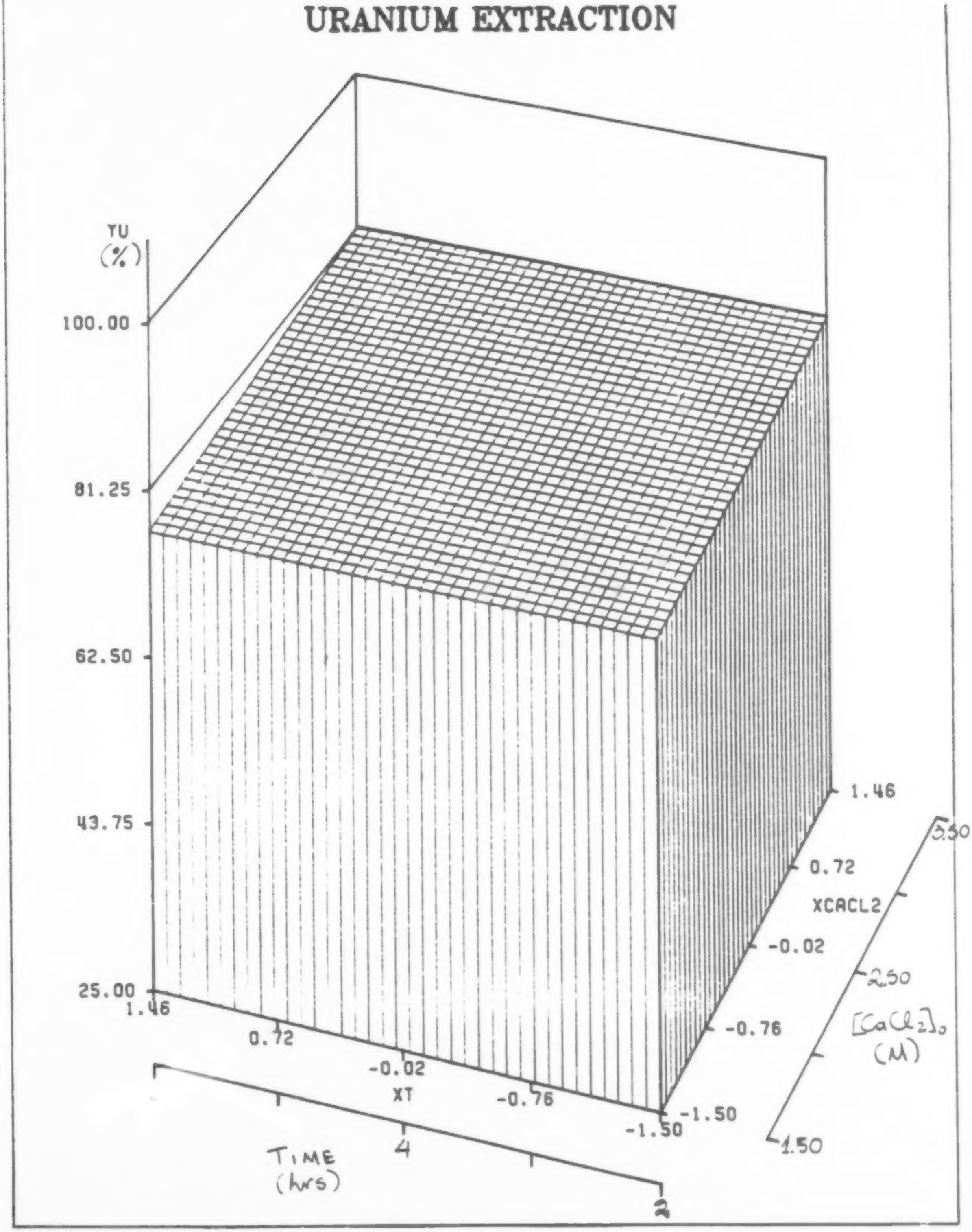

Fig. 32 Predicted % U extraction response surface as a function of $|CaCl_2|_o$ and Time; d_s = 0.66 kg/l and $|HCl|_o$ = 1.0 M.

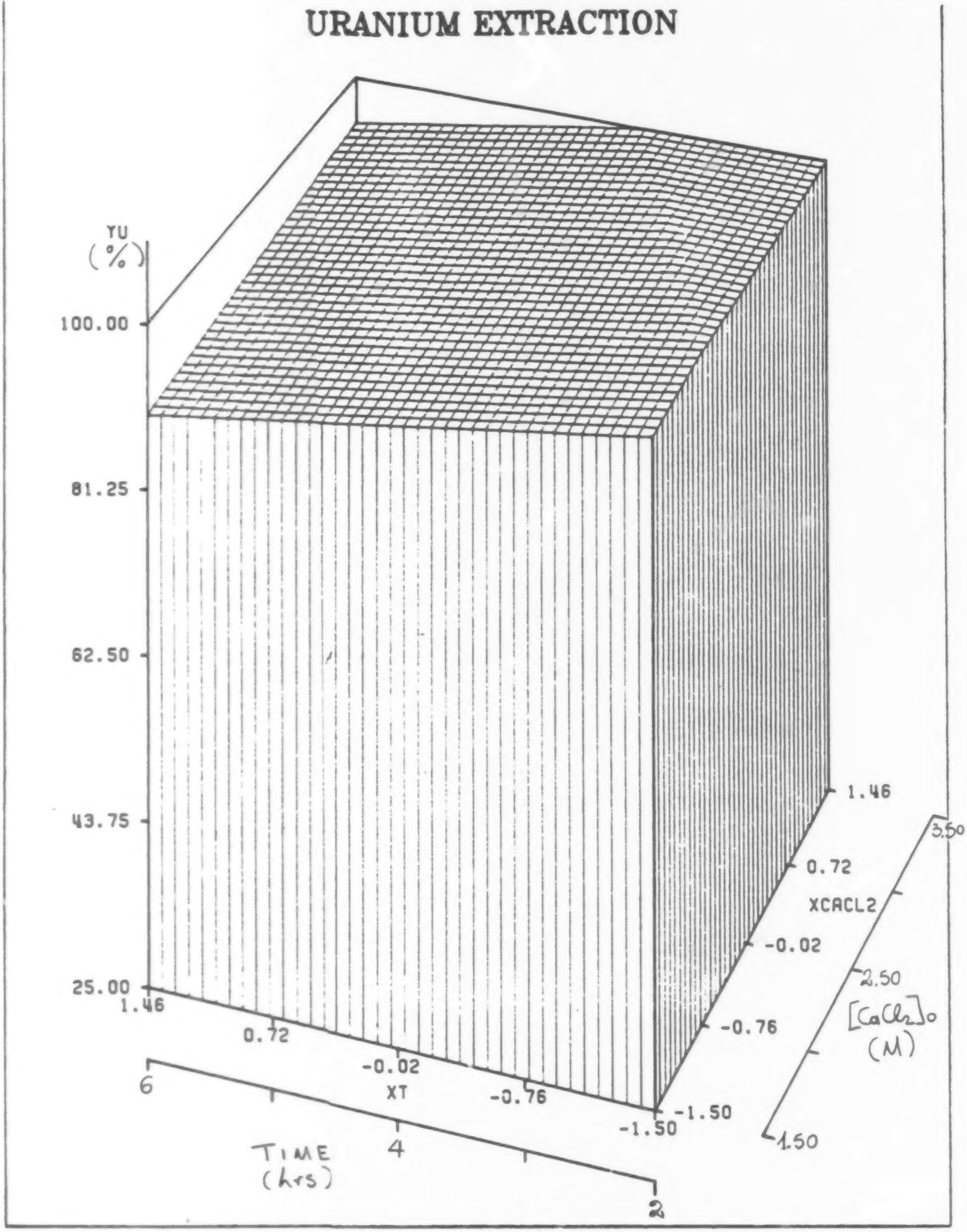

Fig. 33 Predicted % U extraction response surface as a function of $|CaCl_2|_c$ and Time; d_s = 0.66 kg/l and $|HCl|_o$ = 1.5 M.

respectively. Again the same observations are made. A slight shrinkage of the 100% extraction surface area is observed with longer reaction times. This might be attributed to uranium precipitation due to acid depletion. This is further exemplified by the presence of the term $-2.08\ x_2x_4$ in the U extraction model equation (14, Table 16). Apart from that these results confirm the notion that pitchblende and coffinite - the major U-bearing minerals in the K.L. ore - are readily leachable (49) and thus 2 hrs suffices for complete extraction.

Having identified from the above diagrams that $d_s = 0.33$ kg/l and $[HCl]_o = 1.5$ N offer complete uranium extraction, the next step was to optimize these values further by considering the combined effect of $[CaCl_2]_o$ and time in the process region near these conditions. Thus Figs. 30 and 31 were constructed by keeping d_s constant at 0.33 kg/l (coded value -1.47) and varying $[HCl]_o$ from 1.0 to 1.5 N (in coded form 0.00 to +1.47). For $d_s =$ 0.33 kg/l the optimum leaching conditions were identified to be 1.0 N HCl 2 hrs. reaction time and 2.5 M $CaCl_2$. If instead, the slurry density is raised to 0.66 kg/l (Figs. 32 and 33) complete uranium extraction is accomplished only by adding initially 1.5 N HCl and at least 2.5 M $CaCl_2$ while at the same time the leach time is kept at 2 hrs.

Thus from the standpoint of optimum uranium extraction the best operating conditions are summarized in Table 19. Before

Table 19 Best combinations of conditions for 100% uranium extraction

Combination No.	D_S (kg/l)	$\lvert HCl \rvert_o$ (M)	$\lvert CaCl_2 \rvert_o$ (M)	Time (hrs)	Source
1	0.33	1.0	1.5	2	Fig. 21
2	0.66	1.5	1.5	2	Fig. 21

though the overall optimum conditions are identified similar analysis of the other responses has to be performed as well.

3.4.3.2 Study of the Response: % Radium Extraction

Figure 34 shows the plot of pct Ra extraction observed against initial slurry density. Radium extraction is adversely affected by increasing d_s (r = -0.803). The observed effect might well be either due to increased acid consumption as d_s increases or to buildup of some troublesome component, i.e. SO_4^{2-} or H_3AsO_4 or even due to increased adsorption surface available for the retention of radium. Figure 35 is another manifestation of the favourable effect acid concentration has on radium extraction. This effect though is less pronounced (r = 0.380) than the respective negative d_s effect (r = -0.803). Within the range of conditions tested, i.e. 1.5 to 3.5 M, $CaCl_2$ appears not to influence radium extraction (Fig. 36; r = -0.011). Thus no $CaCl_2$ term appears in the radium extraction model equation (eq. 15, Table 16). Finally, reaction time can be seen (Fig. 37) to have a slightly negative effect on radium extraction. It appears in other words that radium solubilization is equally fast with that of uranium. This confirms the notion (22) that radium-226, as a daughter of the radioactive decay of U-238 occurs in the mineral lattice of the latter, therefore it is expected to be dissolved along with uranium during leaching. The small loss of radium extraction with the extention of leaching time from 2 to 6

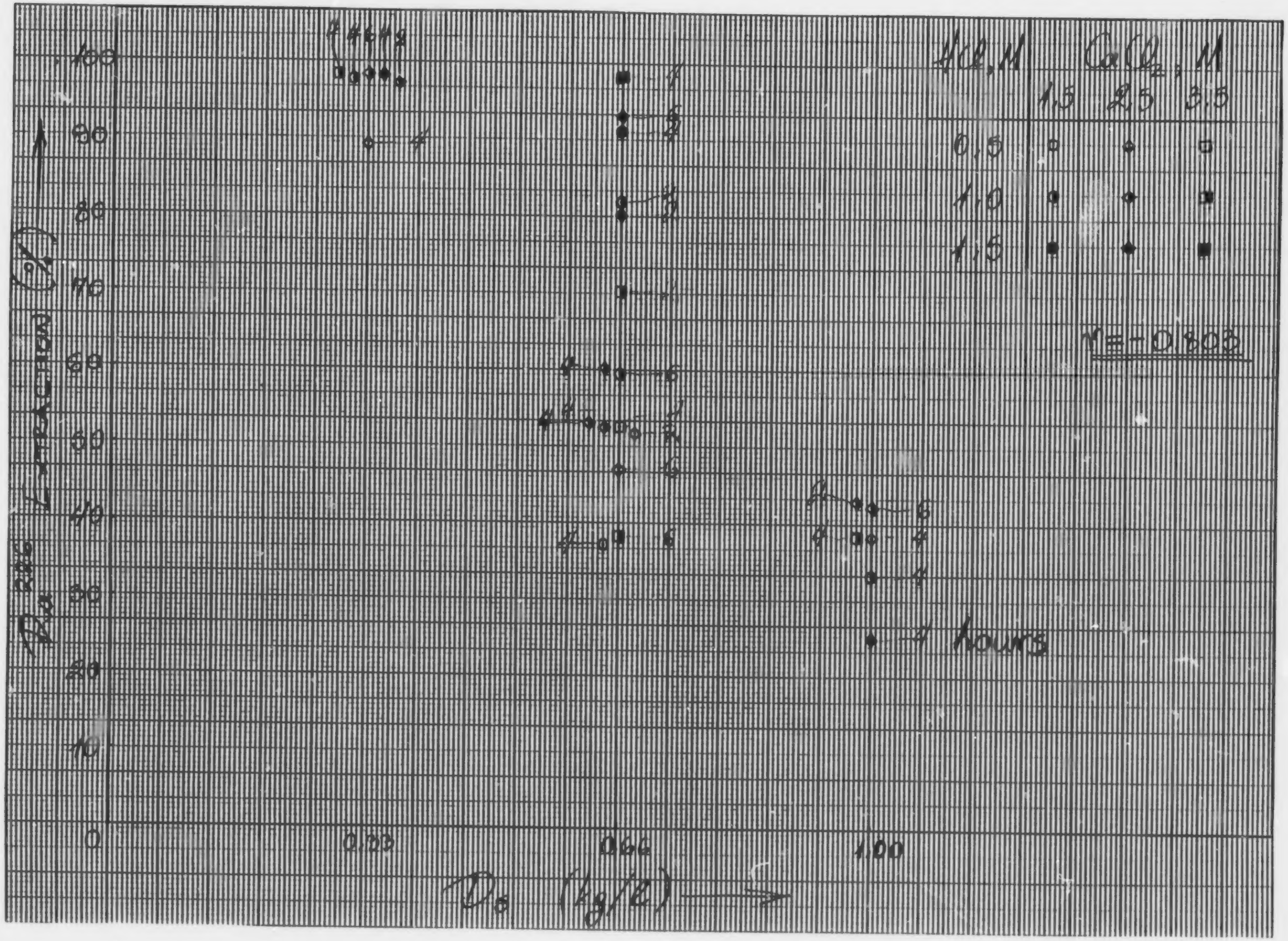

Fig. 34 Observed % Ra extraction vs slurry density.

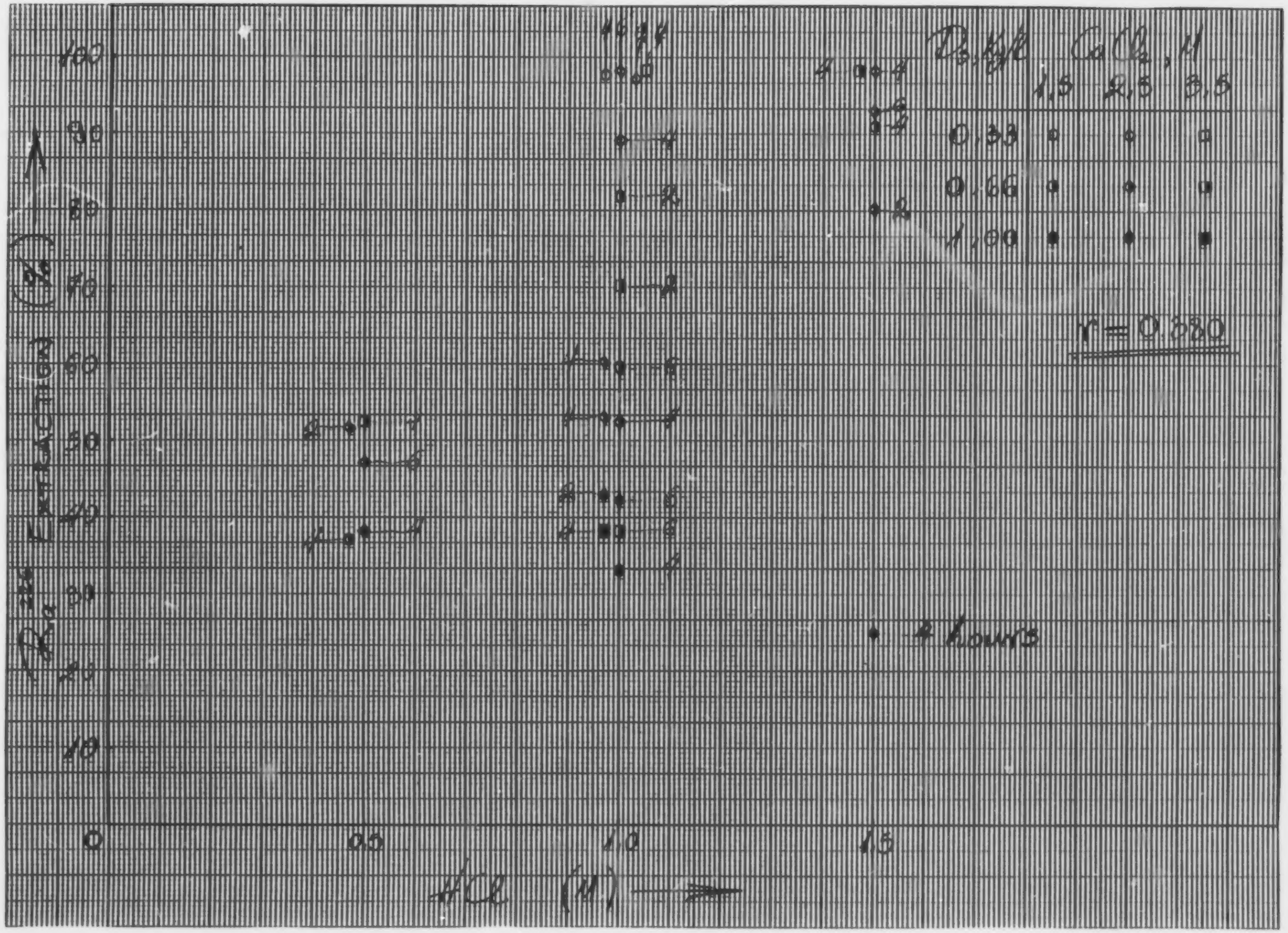

Fig. 35 Observed % Ra extraction vs $|\mathrm{HCl}|_o$.

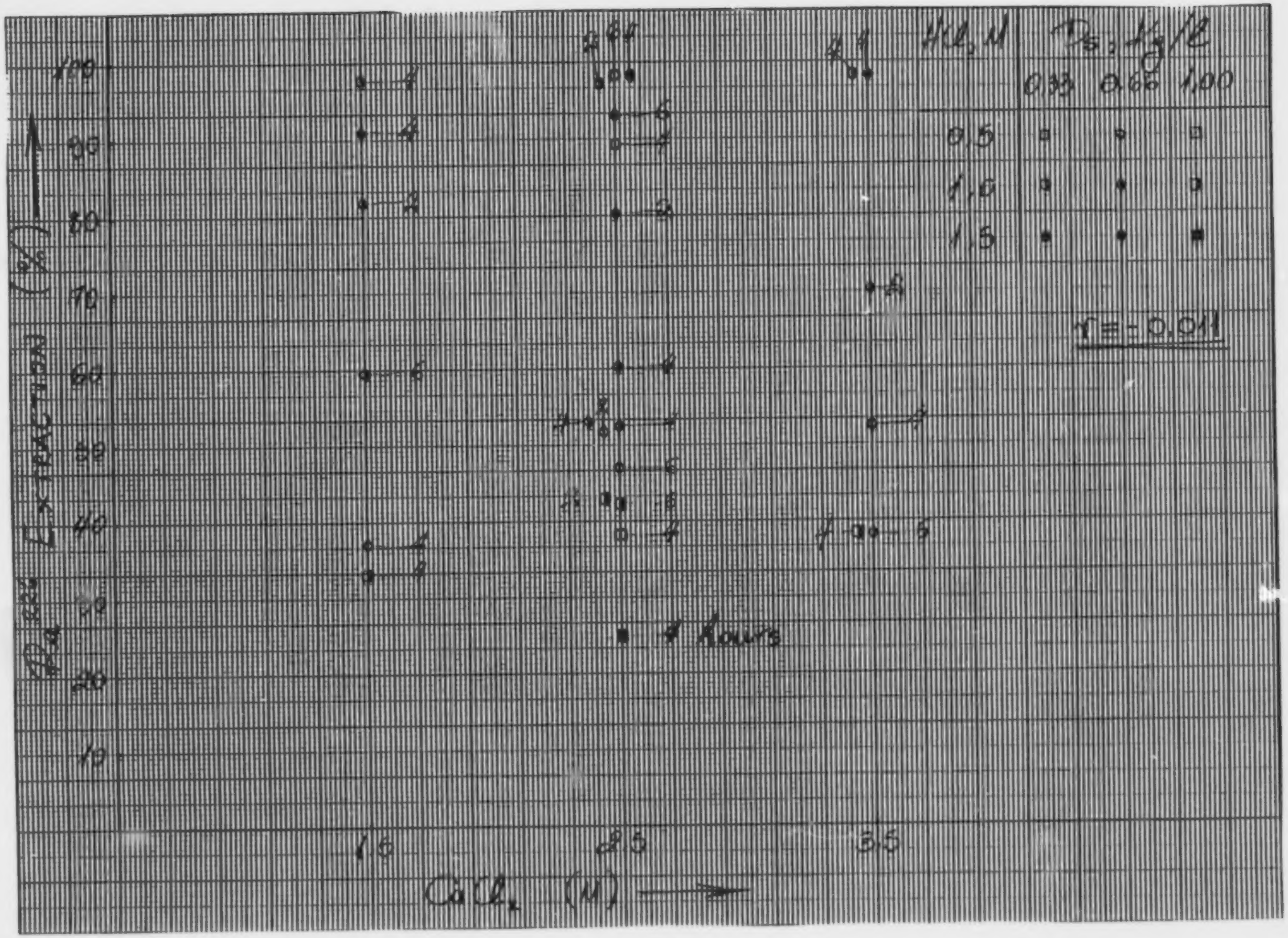

Fig. 36 Observed % Ra extraction vs $|CaCl_2|_o$.

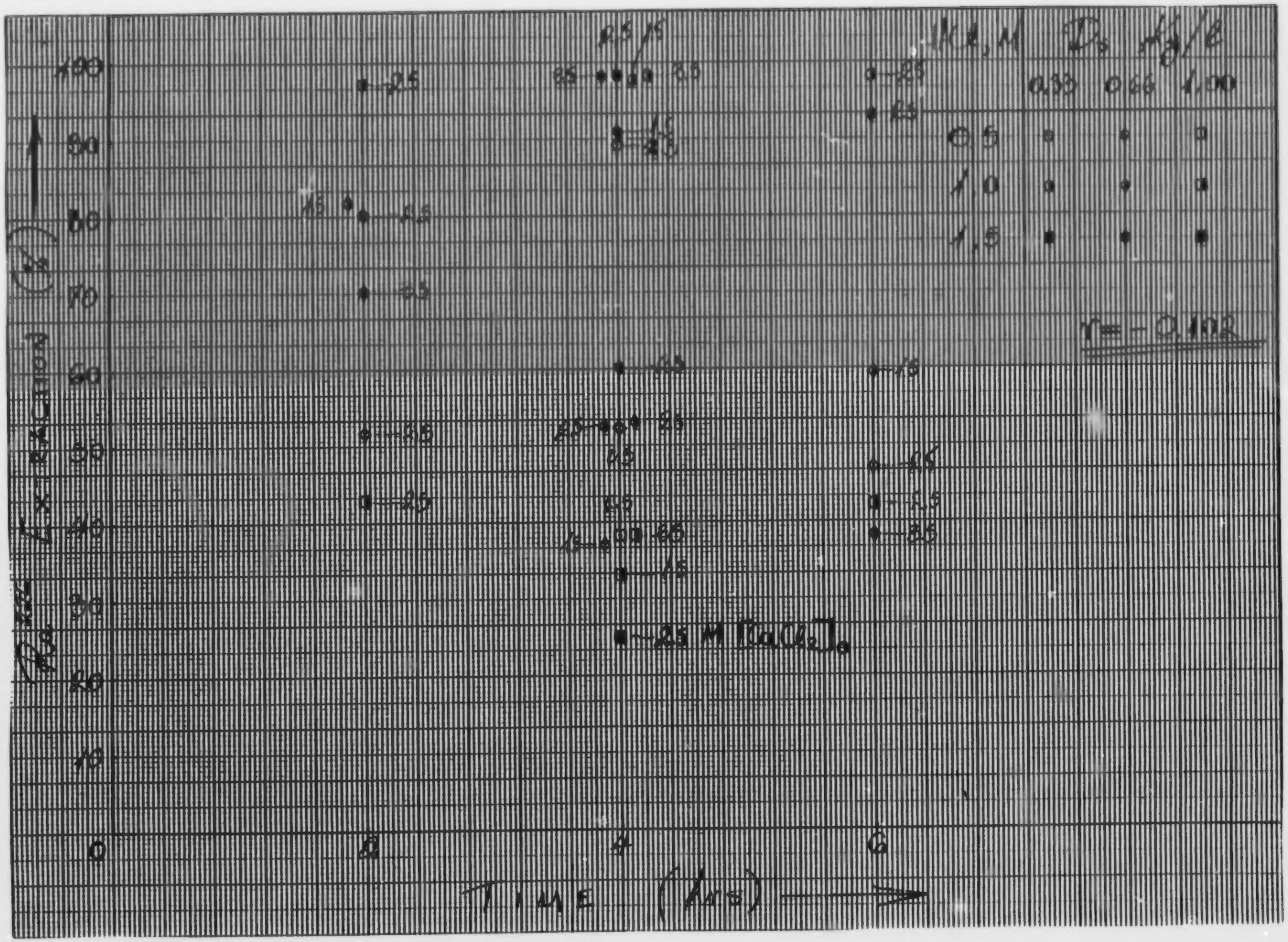

Fig. 37 Observed % Ra extraction vs Time.

hours might be the single or combined effect of either coprecipitation and/or adsorption mechanisms.

Several 3-dimensional representations of the radium extraction response surface have been generated using the model equation (eq. 15, Table 16) and they are shown in Figs. 38 to 44. Figures 38 to 40 represent the response surface as a function of d_s and $[HCl]_o$ at low (2 hr), medium (4 hr), and high (6 hr) time levels. From these graphs it can be concluded that 2 hrs reaction time is the optimum one while an initial acid concentration of at least 1.0 N (coded value: 0.00) is needed for a slurry density of 0.33 kg/l (coded value -1.50) to obtain complete Ra extraction. In Figs. 41 and 42 the response surface is determined as a function of d_s and time for $[HCl]_o$ = 1.0 N and 1.5 N respectively. These Figures indicate complete radium extraction to be obtained only at $[HCl]_o$ = 1.5 N, time = 2 hrs. and d_s = 0.5 kg.l ("-0.8"). Finally Figs. 43 and 44 were constructed at d_s = 0.33 kg/l ("1.47") and 0.66 kg/l ("0.00") slurry density levels respectively. It can be seen that an increase of d_s to 0.66 kg/l solids (Fig. 44) fails to yield 100% radium extraction. Thus from the examination of all these graphs, it can be concluded that optimum conditions for 100% radium extraction are those summarized in Table 20.

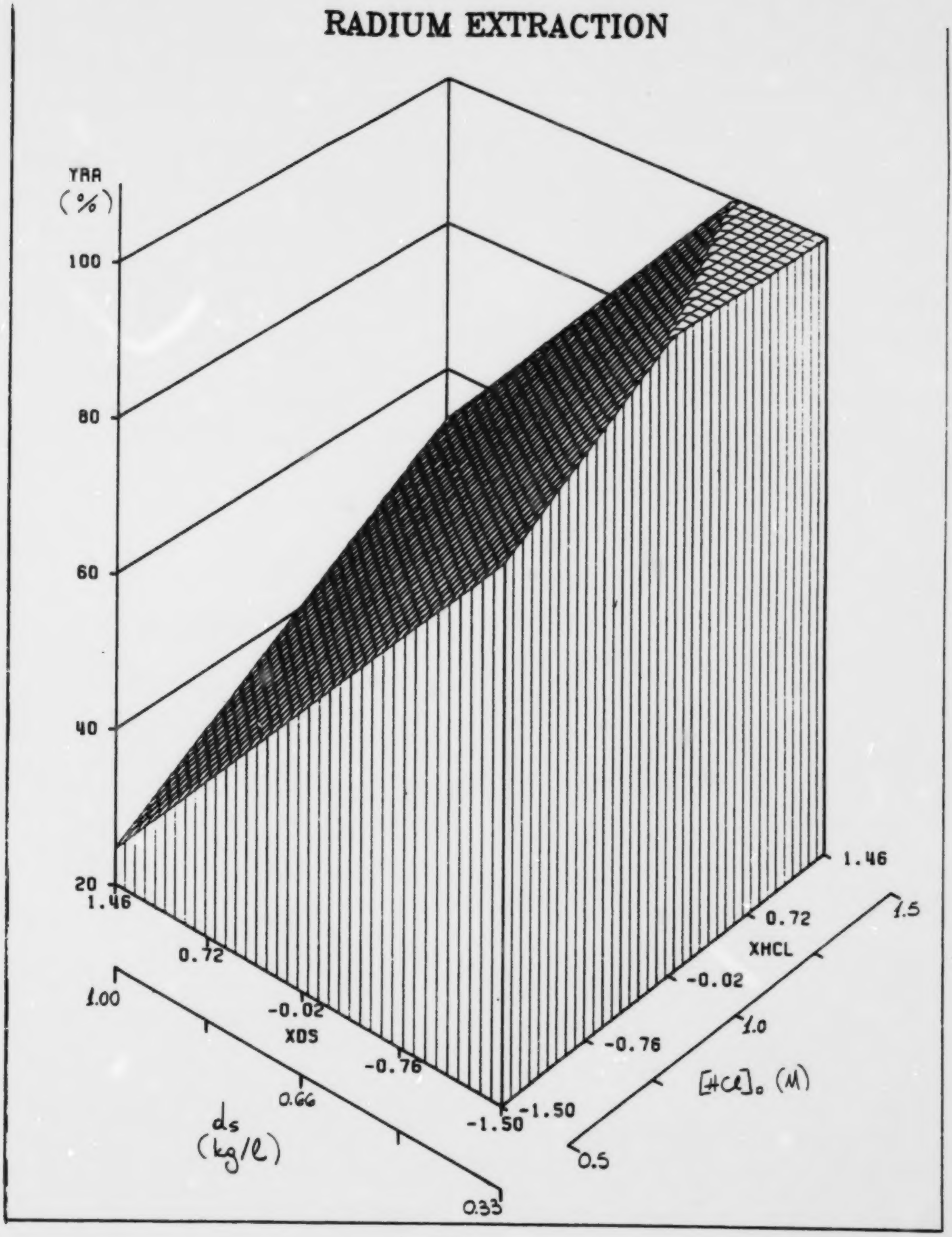

Fig. 38 Predicted % Ra extraction response surface as a function of d_s and $|HCl|_o$; $|CaCl_2|_o$ = 1.5 M and T = 2 hrs.

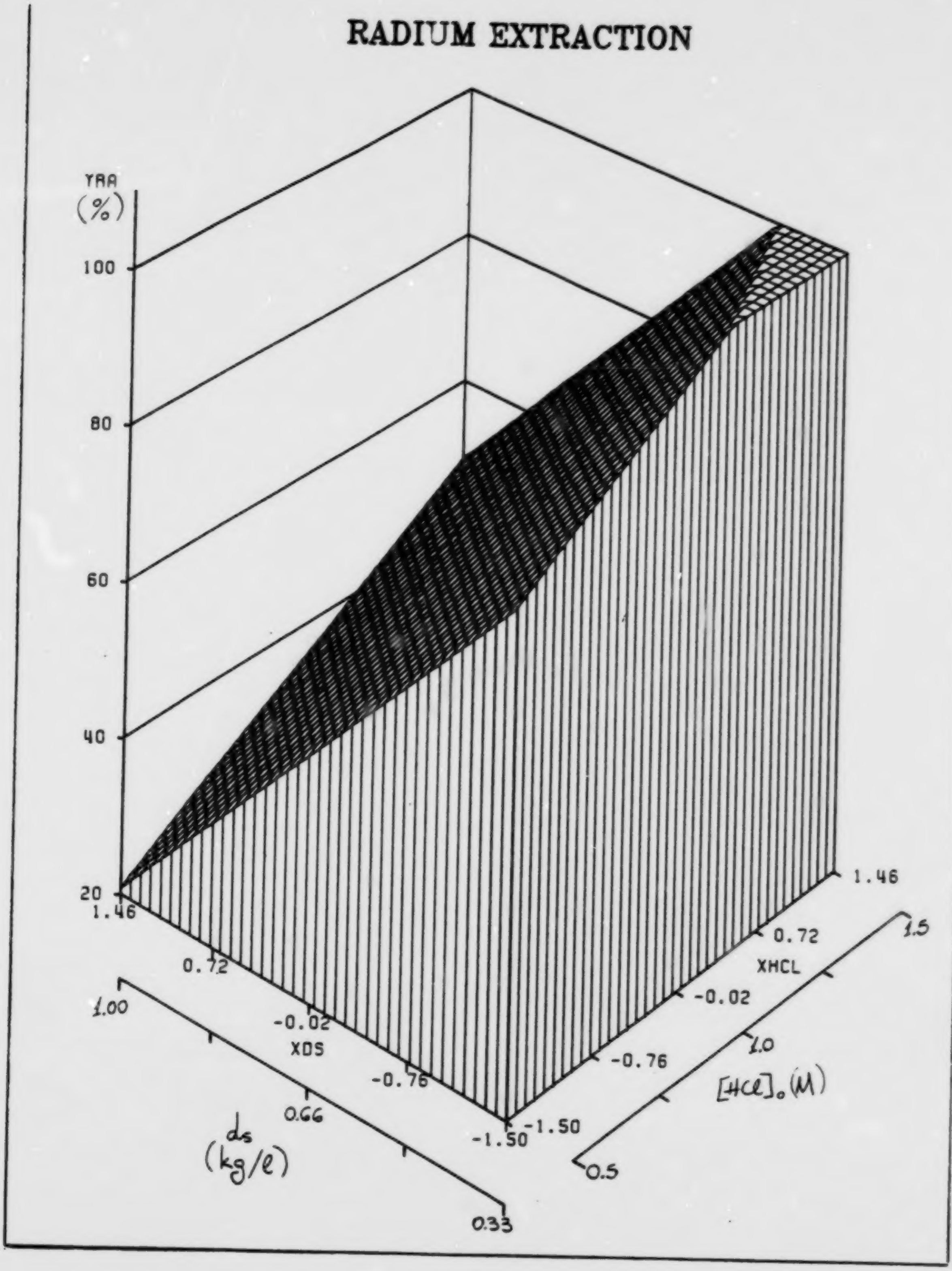

Fig. 39 Predicted % Ra extraction response surface as a function of d_s and $|HCl|_o$; $|CaCl_2|_o$ = 1.5 M and T = 4 hrs.

RADIUM EXTRACTION

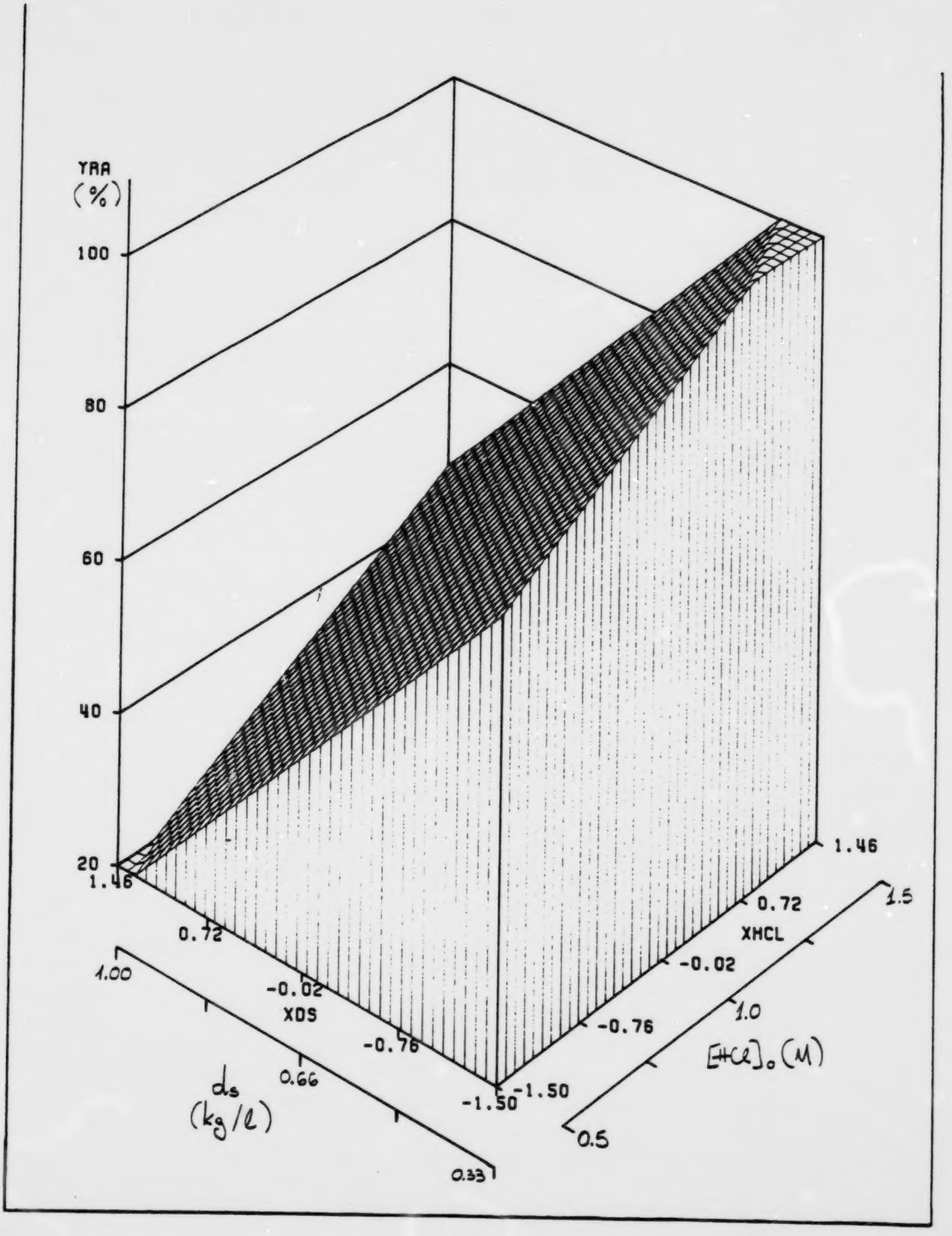

Fig. 40 Predicted % Ra extraction response surface as a function of d_s and $|HCl|_o$; $|CaCl_2|_o$ = 1.5 M and T = 6 hrs.

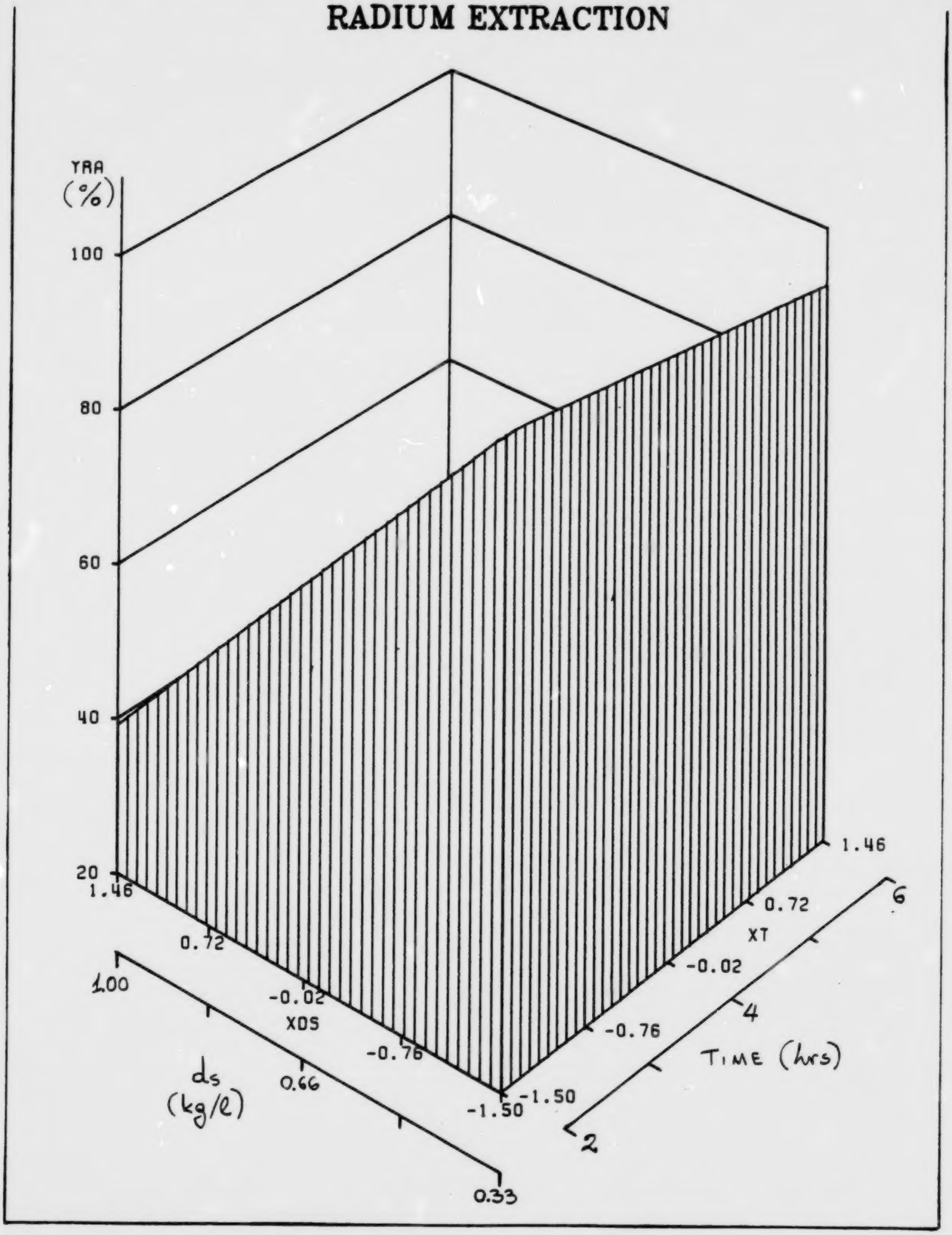

Fig. 41 Predicted % Ra extraction response surface as a function of d_s and Time; $|HCl|_o = 1.0$ M and $|CaCl_2|_o = 1.5$ M.

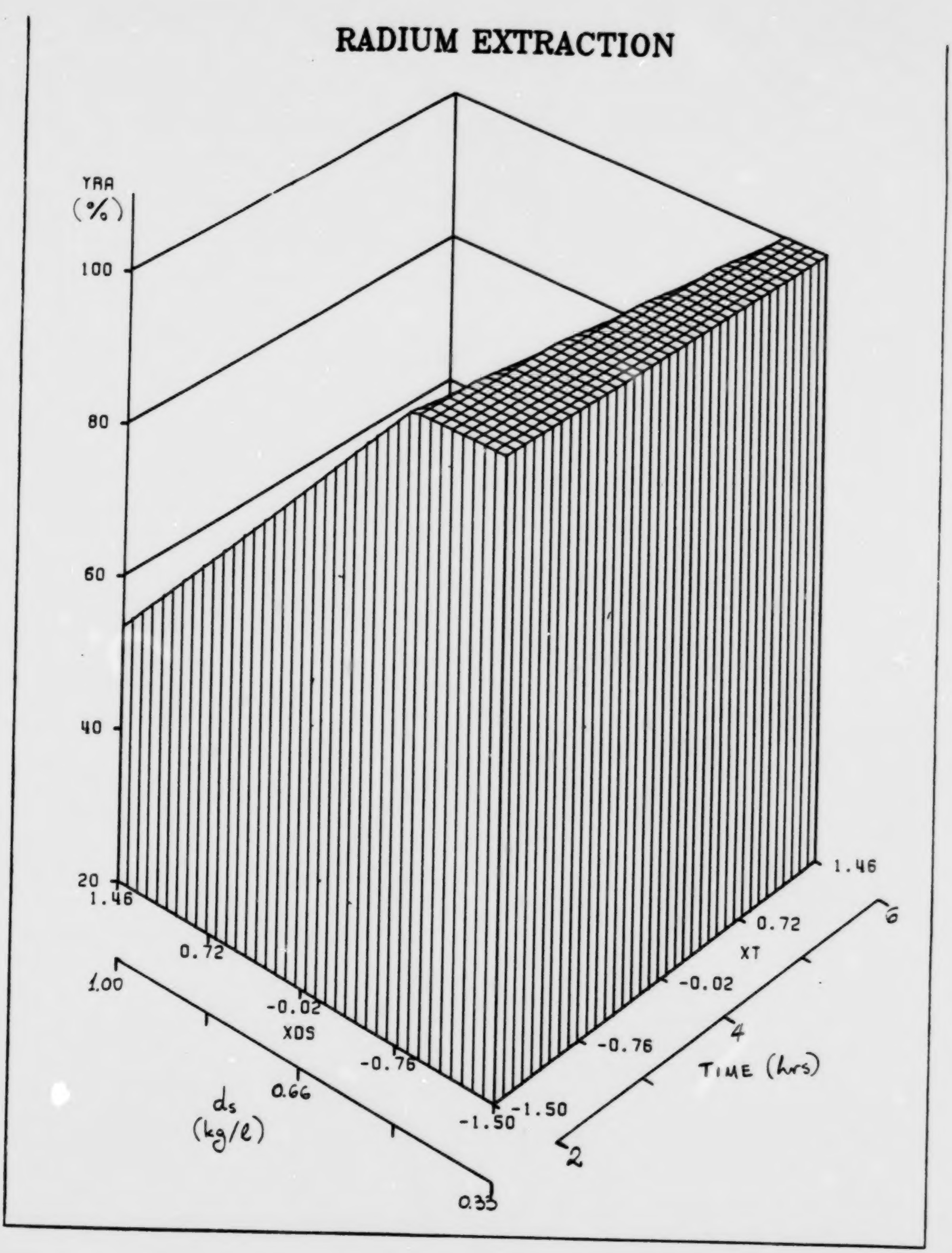

Fig. 42 Predicted % Ra extraction response surface as a function of d_s and Time; $|HCl|_o$ = 1.5 M and $|CaCl_2|_o$ = 1.5 M.

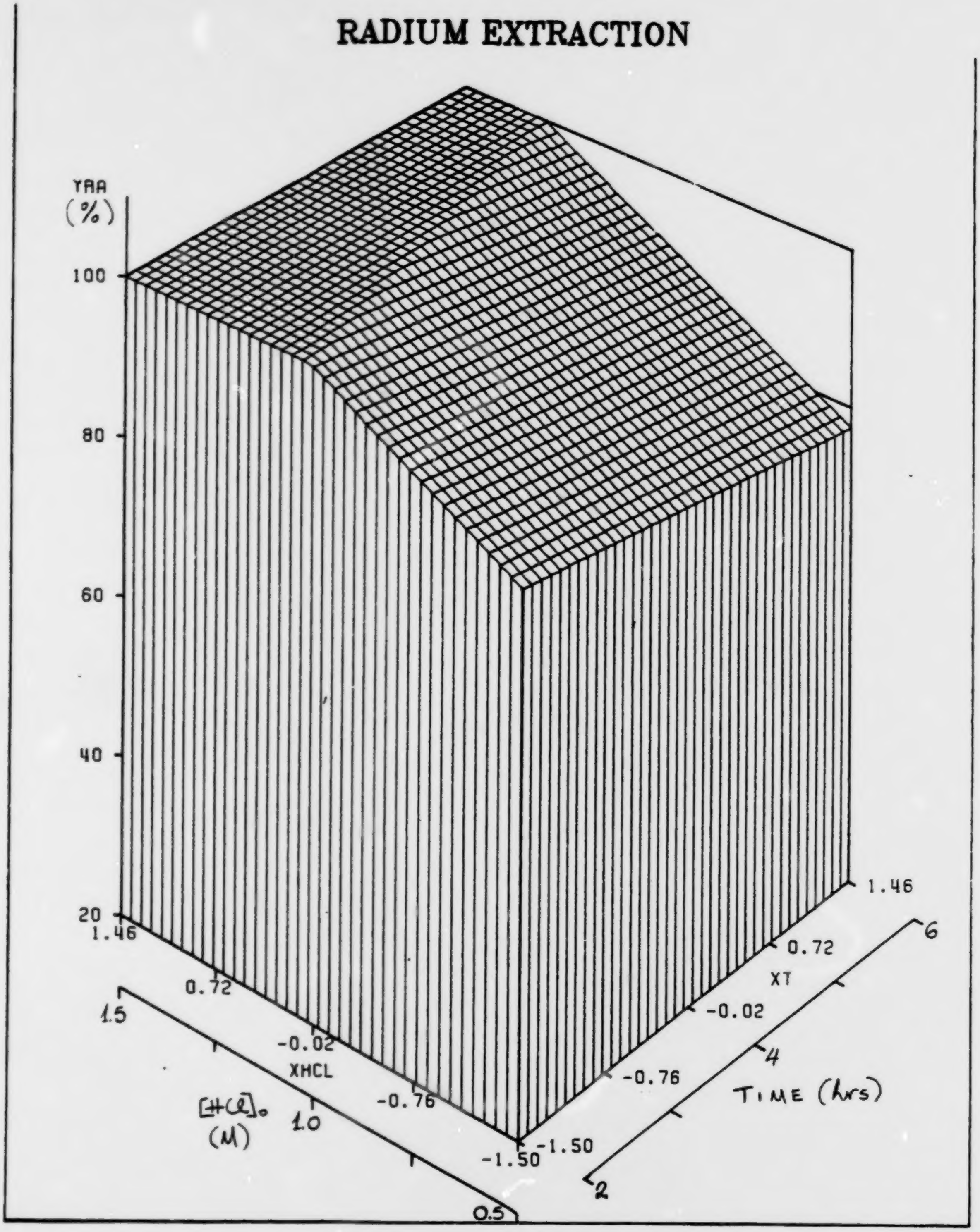

Fig. 43 Predicted % Ra extraction response surface as a function of $|HCl|_o$ and Time; $d_s = 0.33$ kg/l and $|CaCl_2|_o = 1.5$ M.

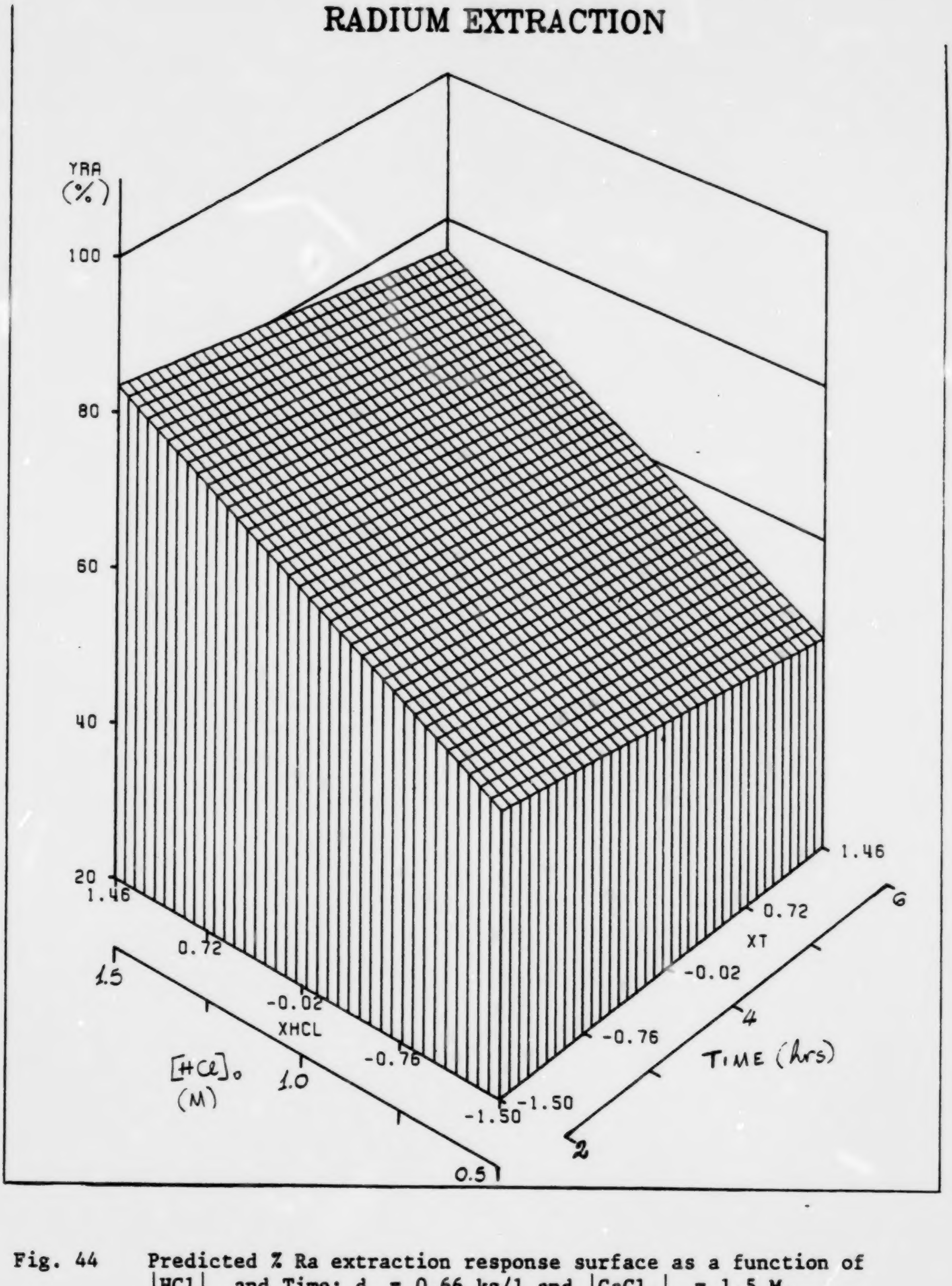

Fig. 44 Predicted % Ra extraction response surface as a function of $|HCl|_o$ and Time; d_s = 0.66 kg/l and $|CaCl_2|_o$ = 1.5 M.

Table 20 Best combinations of conditions for 100% radium extraction

Combination No.	D_S (kg/l)	$\lvert HCl \rvert_o$ (M)	$\lvert CaCl_2 \rvert_o$ (M)	Time (hrs)	Source
1	0.33	1.0	1.5	2.0	Figs. 38,43
2	0.5	1.5	1.5	2.0	Fig. 42

3.4.3.3 Study of the Response: % Nickel Extraction

Graphical inspection of the obtained experimental results in the form % Ni extraction versus each independent variable (Figs. 45 to 48) reveals that apart from slurry density ($r = -0.539$) all the other variables have a positive effect on nickel extraction (i.e. $r = 0.434$ for HCl; $r = 0.154$ for $CaCl_2$; and $r = 0.302$ for time). Of interest is the significant positive effect, time (Fig. 48) has on nickel extraction - a marked contrast in respect to U and Ra extraction behaviour. This might be interpreted as a manifestation of different leaching mechanisms characterizing the oxidative dissolution of the nickel arsenide minerals on one hand and the U-Ra minerals on the other. It has been determined in Chapter 2 (Fig. 7) that gersdorffite (NiAsS) (the major nickel arsenide mineral present in the Key Lake ore) dissolves at relatively slow rates. Thus at 90°C and 75 psi O_2 only 30% NiAsS dissolution was observed after 4 hours pressure leaching time. Apart from the slow leaching rate a relatively complex model (eq. 16, Table 16) represents nickel extraction incorporating both interaction (term $3.5x_1x_2$) and curvature effects (term $-1.41x_3^2$). The curvature and interaction effects of HCl conc and slurry density are indicated in Figs. 45 and 46 with the plotted broken lines (different slope at different levels).

These effects though (i.e. interaction and curvature effects) are better understood by considering the 3-D graphs shown in Figs. 49 to 51. The graphs represent % Nickel extraction (Y_{Ni}) as a function of initial slurry density (XDS)

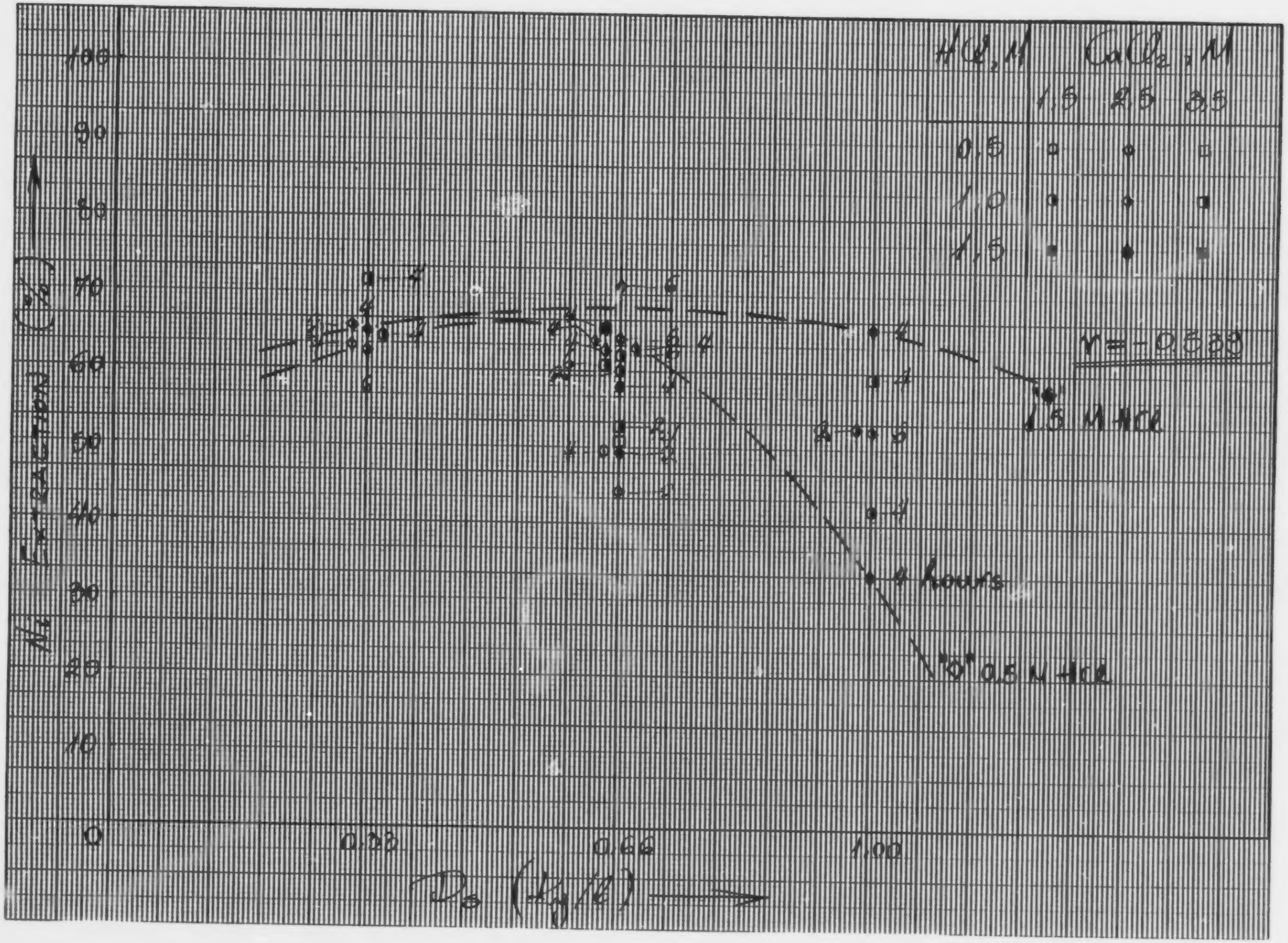

Fig. 45 Observed % Ni extraction vs slurry density.

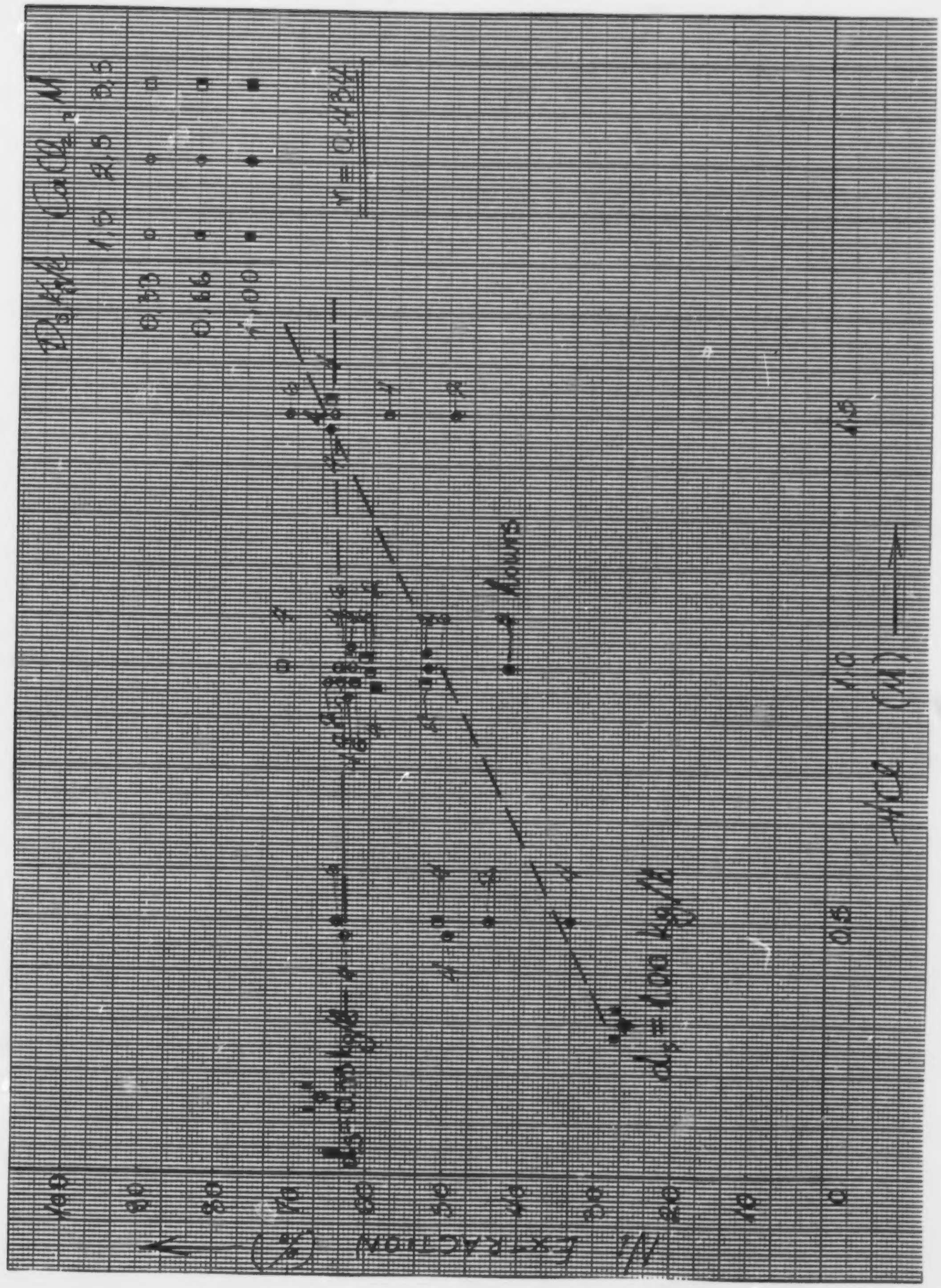

Fig. 46 Observed % Ni extraction vs $|HCl|_o$.

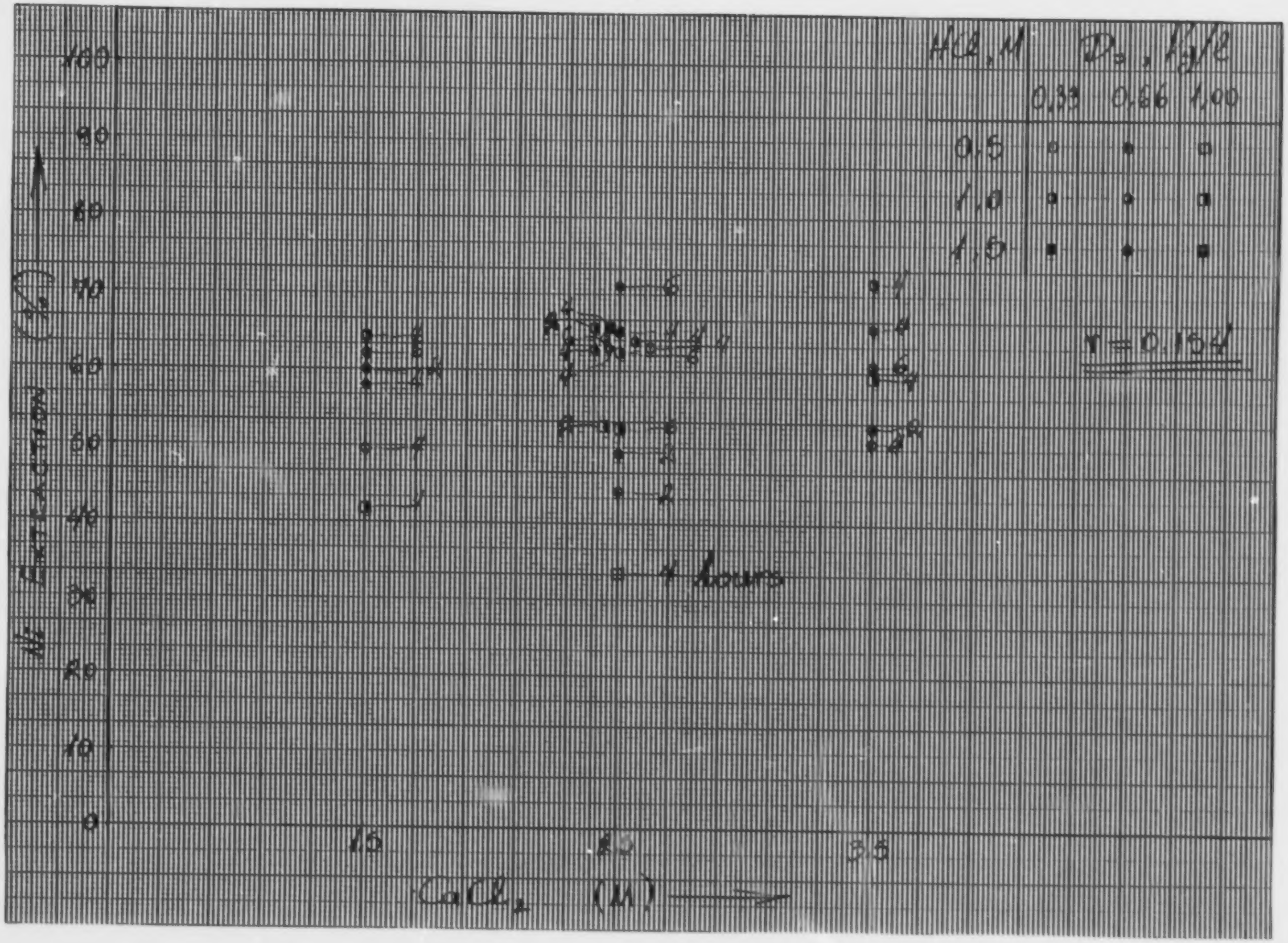

Fig. 47 Observed % Ni extraction vs $|CaCl_2|_o$.

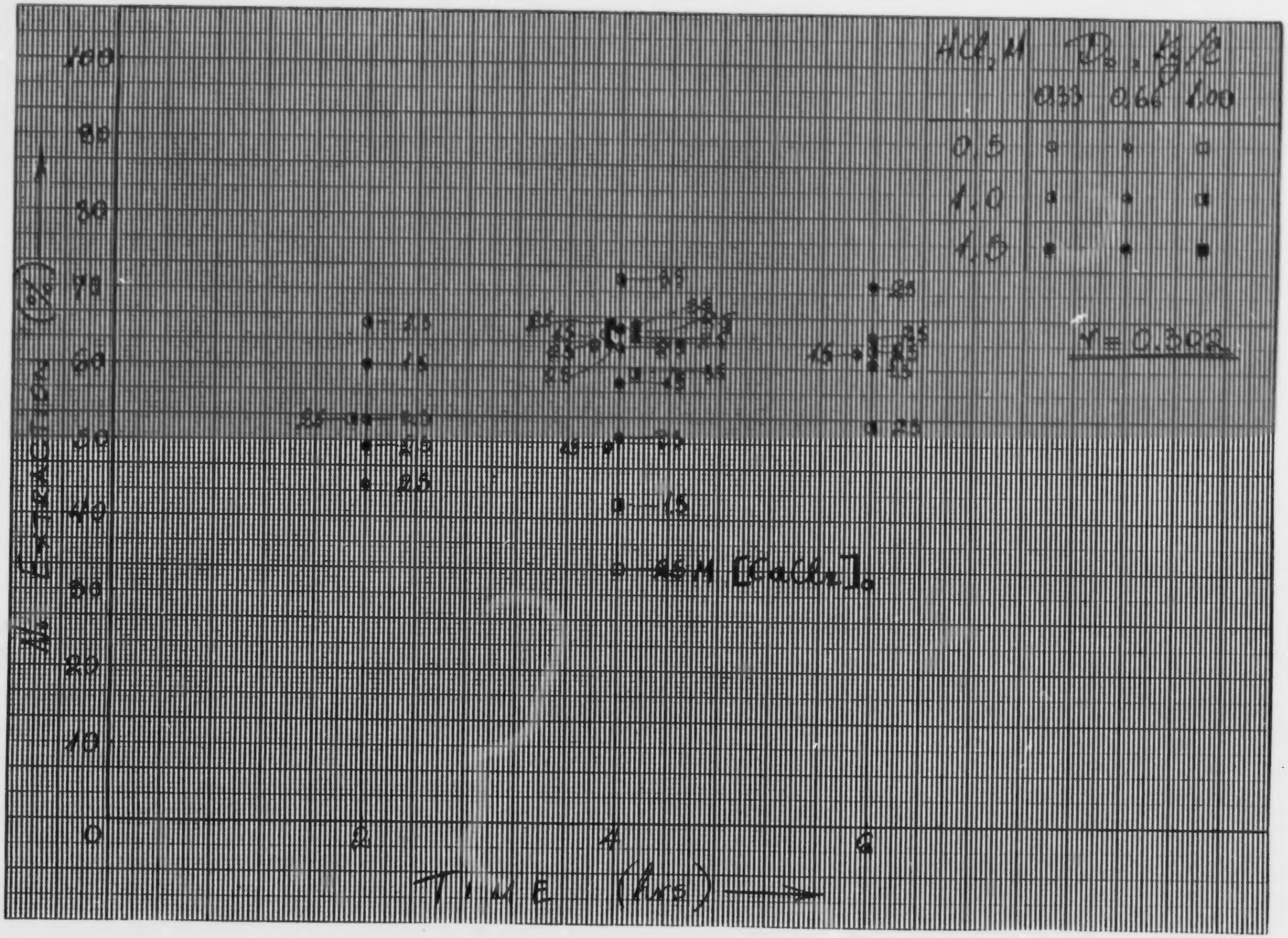

Fig. 48 Observed % Ni extraction vs Time.

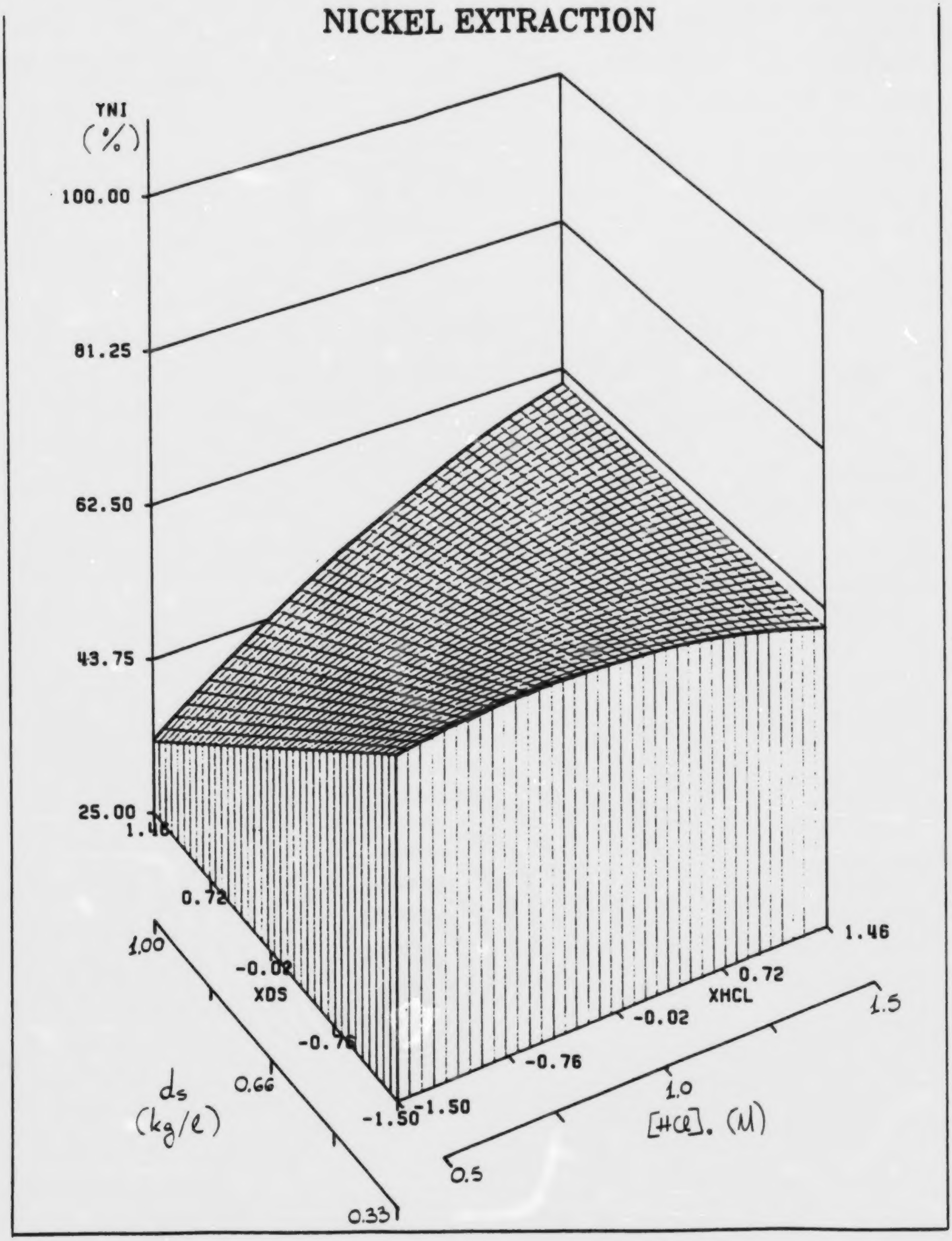

Fig. 49 Predicted % Ni extraction response surface as a function of d_s and $|HCl|_o$; $|CaCl_2|_o$ = 3.5 M and T = 2 hrs.

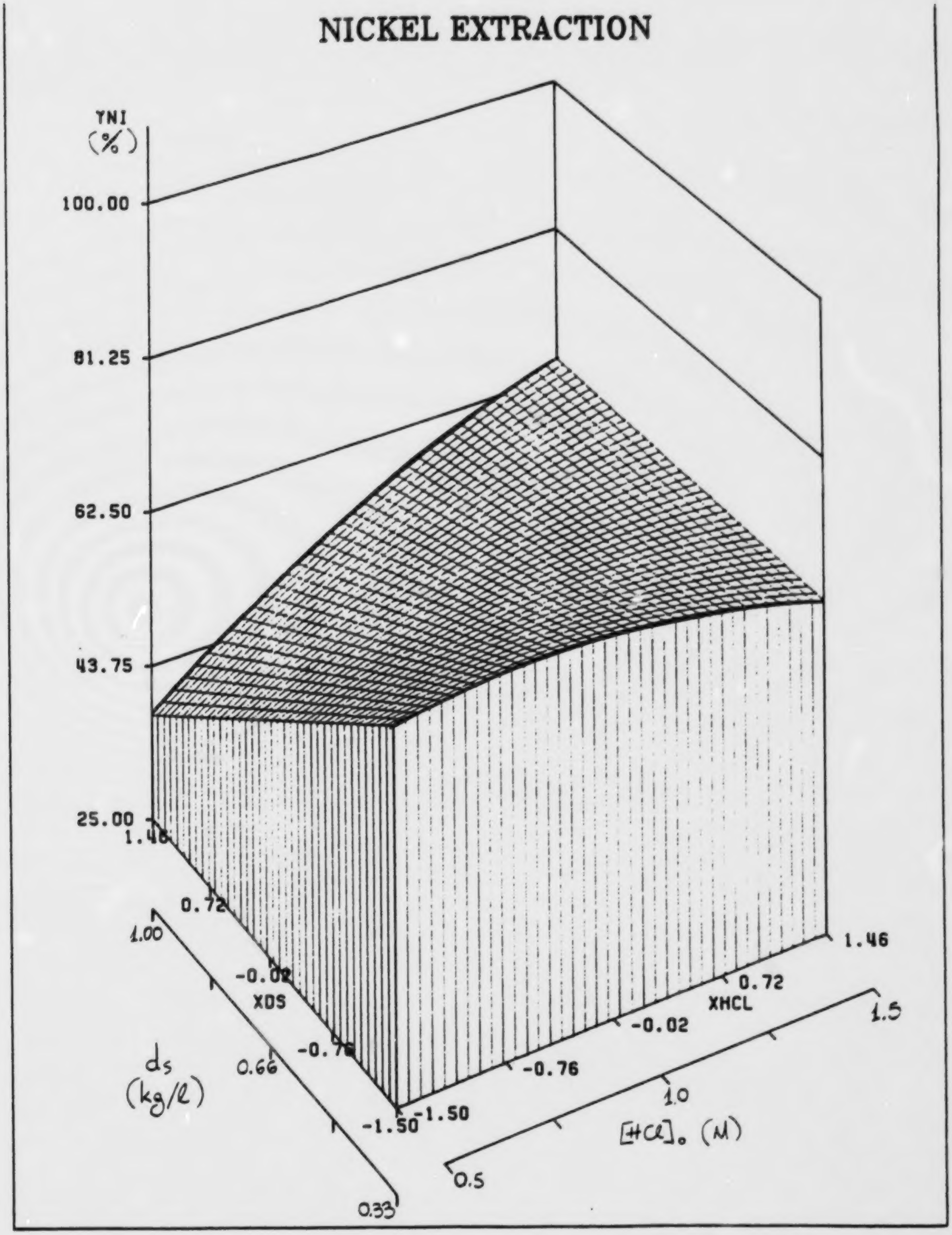

Fig. 50 Predicted % Ni extraction response surface as a function of d_s and $|HCl|_o$; $|CaCl_2|_o$ = 3.5 M and T = 4 hrs.

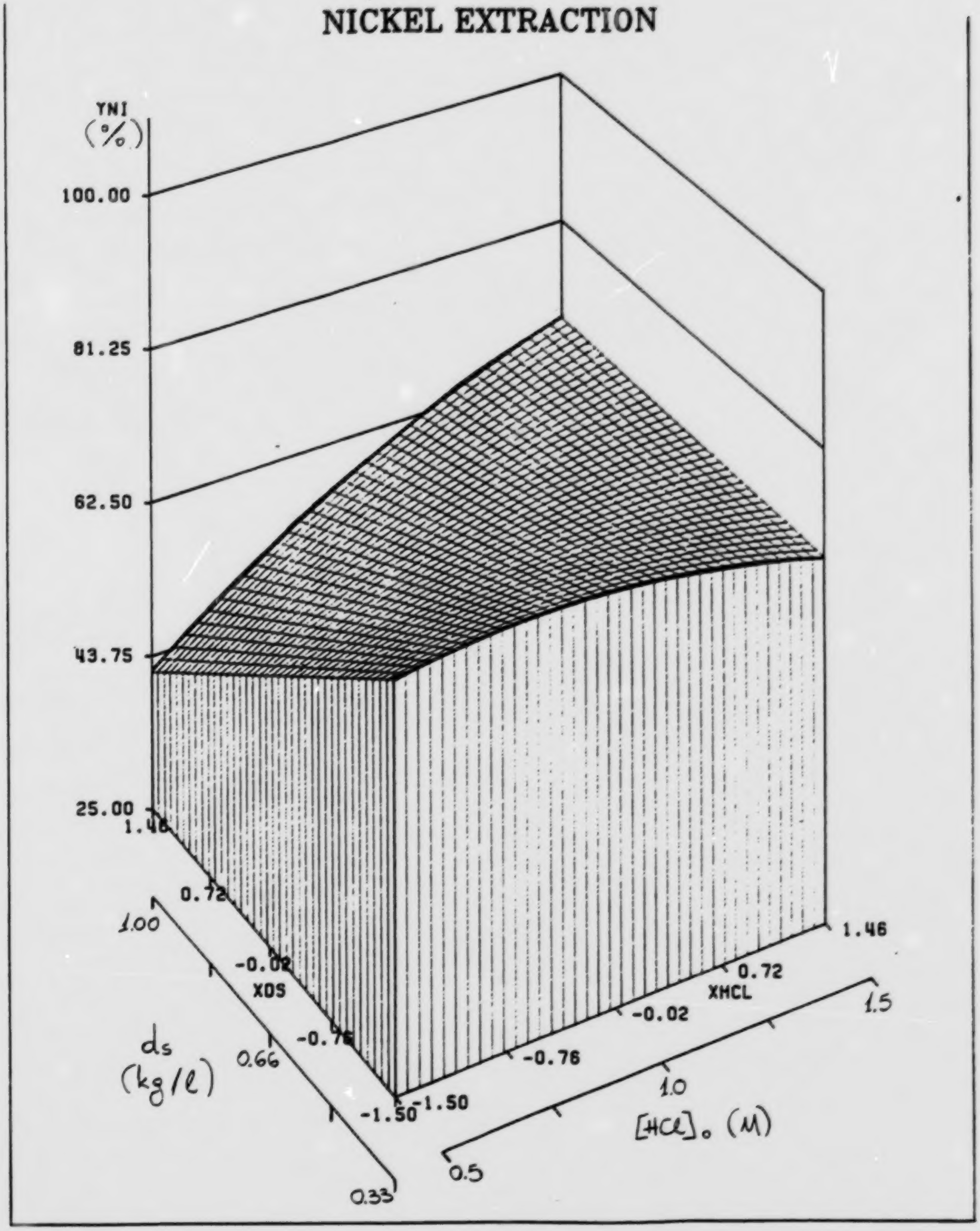

Fig. 51 Predicted % Ni extraction response surface as a function of d_s and $|HCl|_o$; $|CaCl_2|_o$ = 3.5 M and T = 6 hrs.

and HCl molar concentration (XHCl) at constant $[CaCl_2]_o$ (= 3.5 M; "1.47") and at low (2 hr; "-1.47"), medium (4 hr; "0.00"), and high (6 hr; "1.47") levels of reaction time respectively. The interaction effect is indicated by the difference in the slopes of the response lines at XDS = "1.46" and "-1.50" (thick lines on the graphs). In other words the effect of $[HCl]_o$ on % Nickel extraction is not the same at different slurry density levels. It is only through a statistical design and modelling experimental approach that someone can detect these variations and appropriately exploit the leaching conditions for best performance. Furthermore, the curfature effect of $[HCl]_o$ is indicated by the non-linearity of the thick lines. The implications of these two effects is that, at the low level of slurry density (XDS = "-1.50"; 0.33 kg/l) the optimum $[HCl]_o$ is at an intermediate level, i.e. 1.0 N; at the high d_s level though, i.e. 1.0 kg/l (XDS = "1.46") the optimum $[HCl]_o$ becomes now 1.5 N or (YHCl = "1.46"). The beneficial effect of HCl concentration on the extraction of nickel is in good agreement with the postulated reactions involved in the pressure leaching of the nickel arsenide minerals (i.e. eq. 6, 8 and 9 pp. -), and millerite

$$NiS + 1/2\ O_2 + 2H^+ \longrightarrow Ni^{2+} + S^o + H_2O \qquad (27)$$

On the other hand the negative effect of slurry density can be interpreted in terms of the increased acid consumption with high d_s which results in insufficient $[H^+]$ to drive reactions 6, 8, 9 and 27 to the right. However as the Figs. 49 to 51 show this negative effect of d_s is eliminated when a very large $[HCl]_o$ concentration is used, i.e. 1.5 N.

What remains not-understood from the above results (i.e. Figs. 49 to 51) is the drop in % Ni extraction observed when $[HCl]_o$ is increased from 1.0 to 1.5 N at constant d_s = 0.33 kg/l. This deterioration in Ni extraction under the said conditions can be better seen by considering Figs. 52 and 53. Here % Ni extracted is plotted against time and $[CaCl_2]_o$ at constant slurry density, 0.33 kg/l (i.e. X_{DS} = "-1.47") and at $[HCl]_o$ = 1.0 N ("0.00") and 1.5 N ("1.47") respectively. This effect is seen to persist for the whole range of reaction times (i.e. 2 to 6 hr) and $[CaCl_2]_o$ (i.e. 1.5 to 3.5 M) investigated in the present work. Finally the curvature effect of $[HCl]_o$ on Ni extraction is further illustrated in Figs. 54 and 55 as a function of time and $[CaCl_2]_o$ at d_s = 0.33 kg/l. Worth mentioning also, is the slight positive effect $CaCl_2$ concentration (Figs. 52, 53 and 55) has on % Ni extraction. This is believed to be due to increased activity of HCl with large additions of $CaCl_2$ salt to the leach solution (50, 51). The role of $CaCl_2$ in the present leaching system is discussed in the next chapter of the present report.

From the 3-D graphs of Figs. 49 to 55 the combination of conditions yielding the best % Ni extraction were identified and are summarized in Table 21.

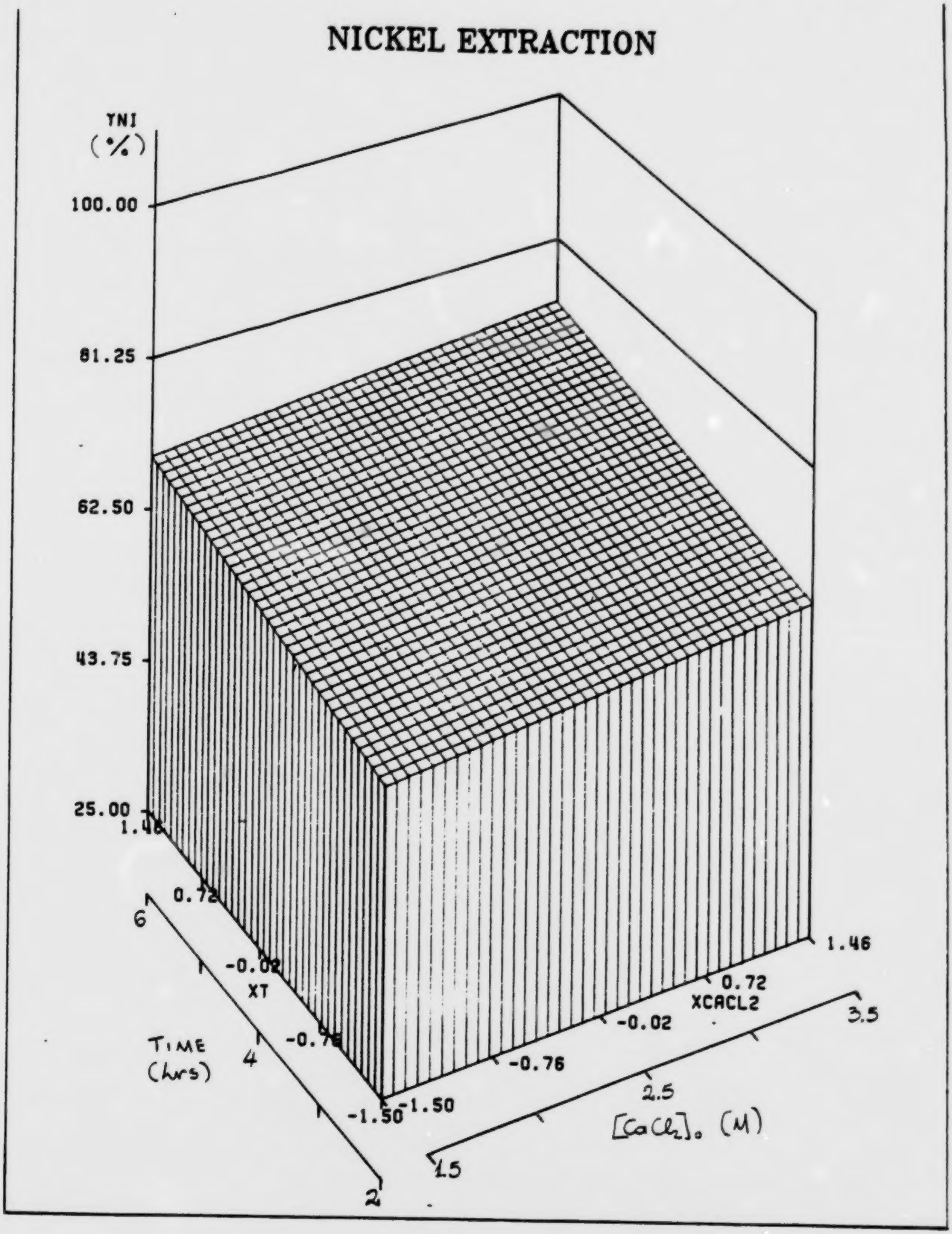

Fig. 52 Predicted % Ni extraction response surface as a function of $|CaCl_2|_o$ and Time; d_s = 0. 33 kg/1 and $|HCl|_o$ = 1.0 M.

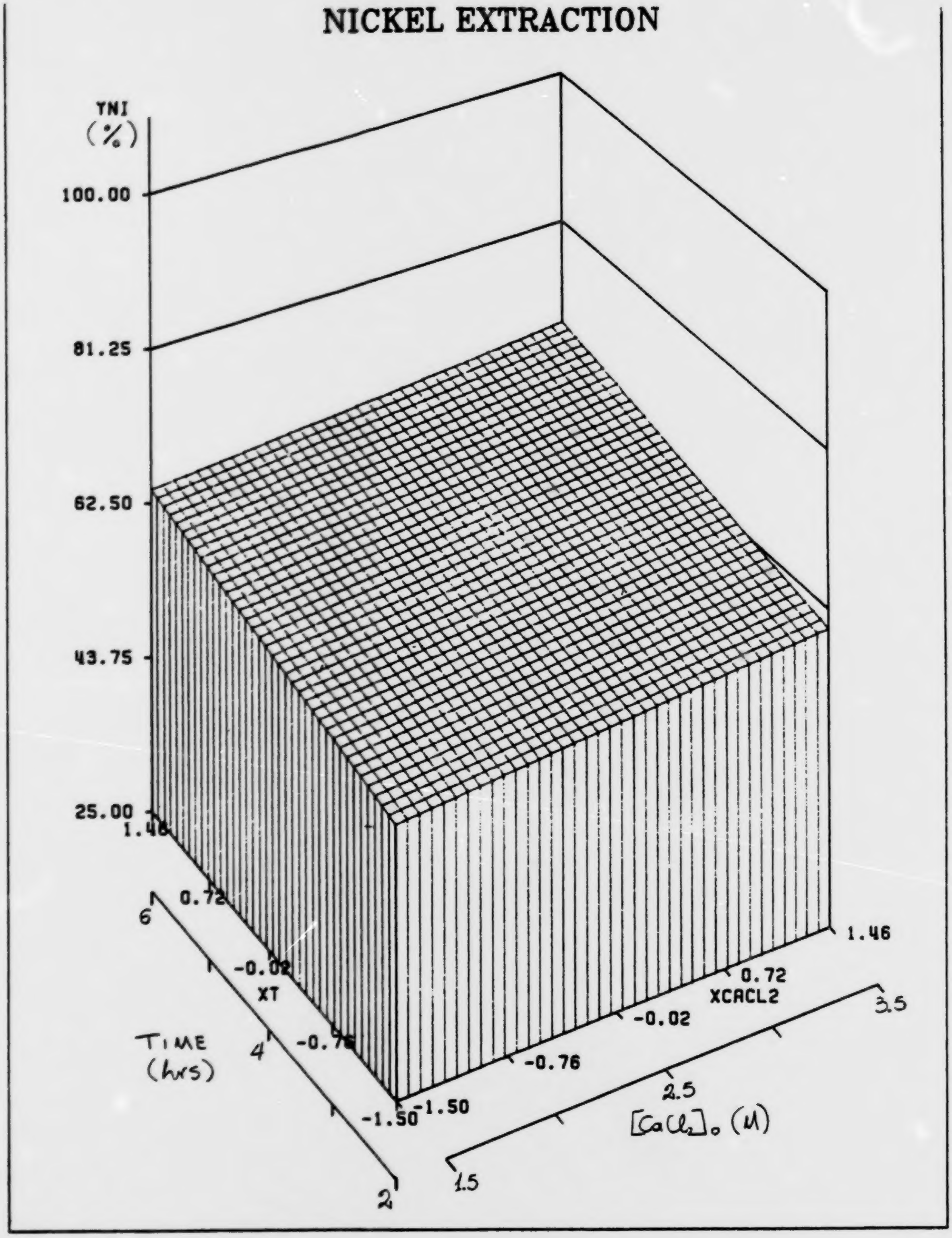

Fig. 53 Predicted % Ni extraction response surface as a function of $|CaCl_2|_o$ and Time; d_s = 0. 33 kg/1 and $|HCl|_o$ = 1.5 M.

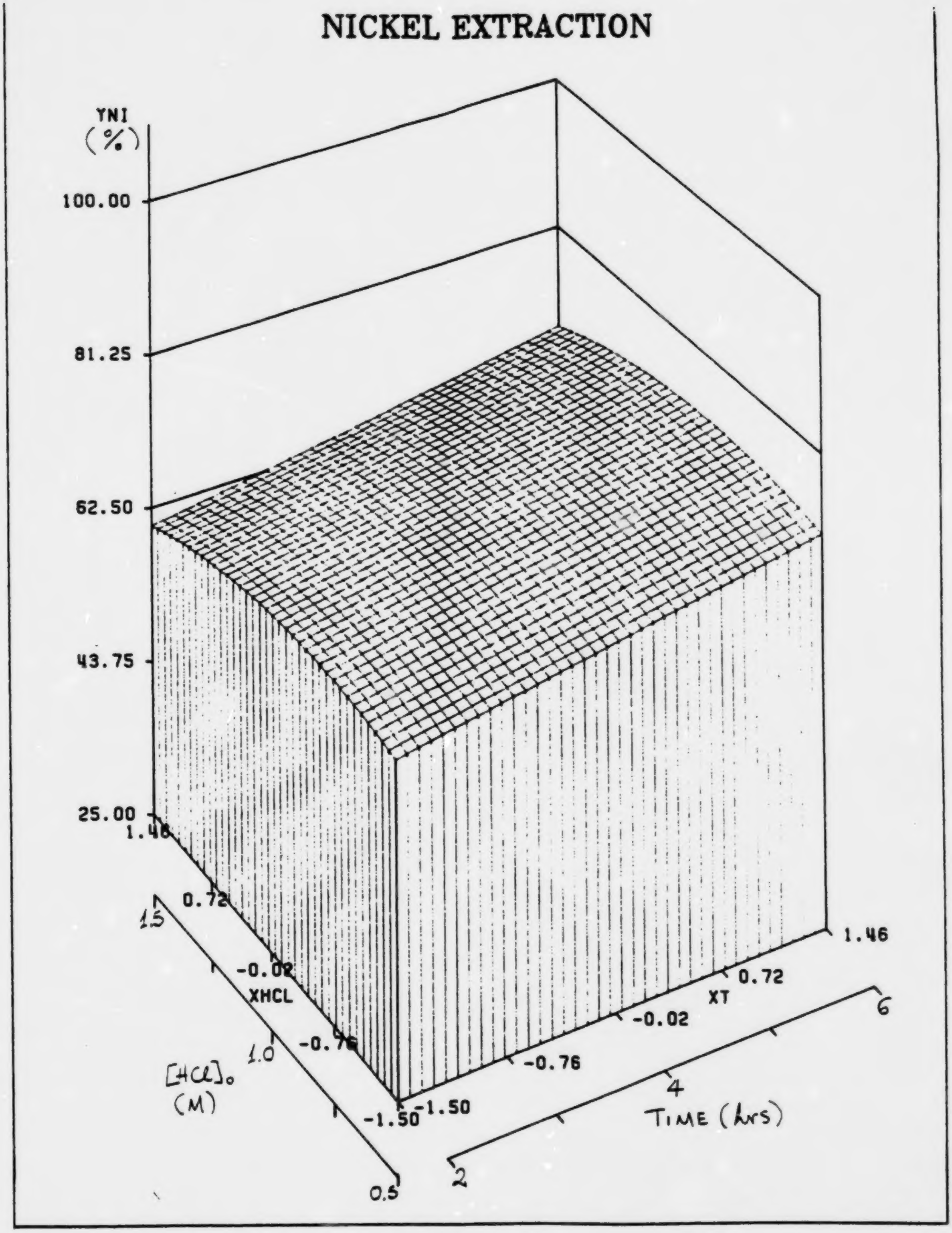

Fig. 54 Predicted % Ni extraction response surface as a function of $|HCl|_o$ and Time; d_s = 0. 33 kg/l and $|CaCl_2|_o$ = 3.5 M.

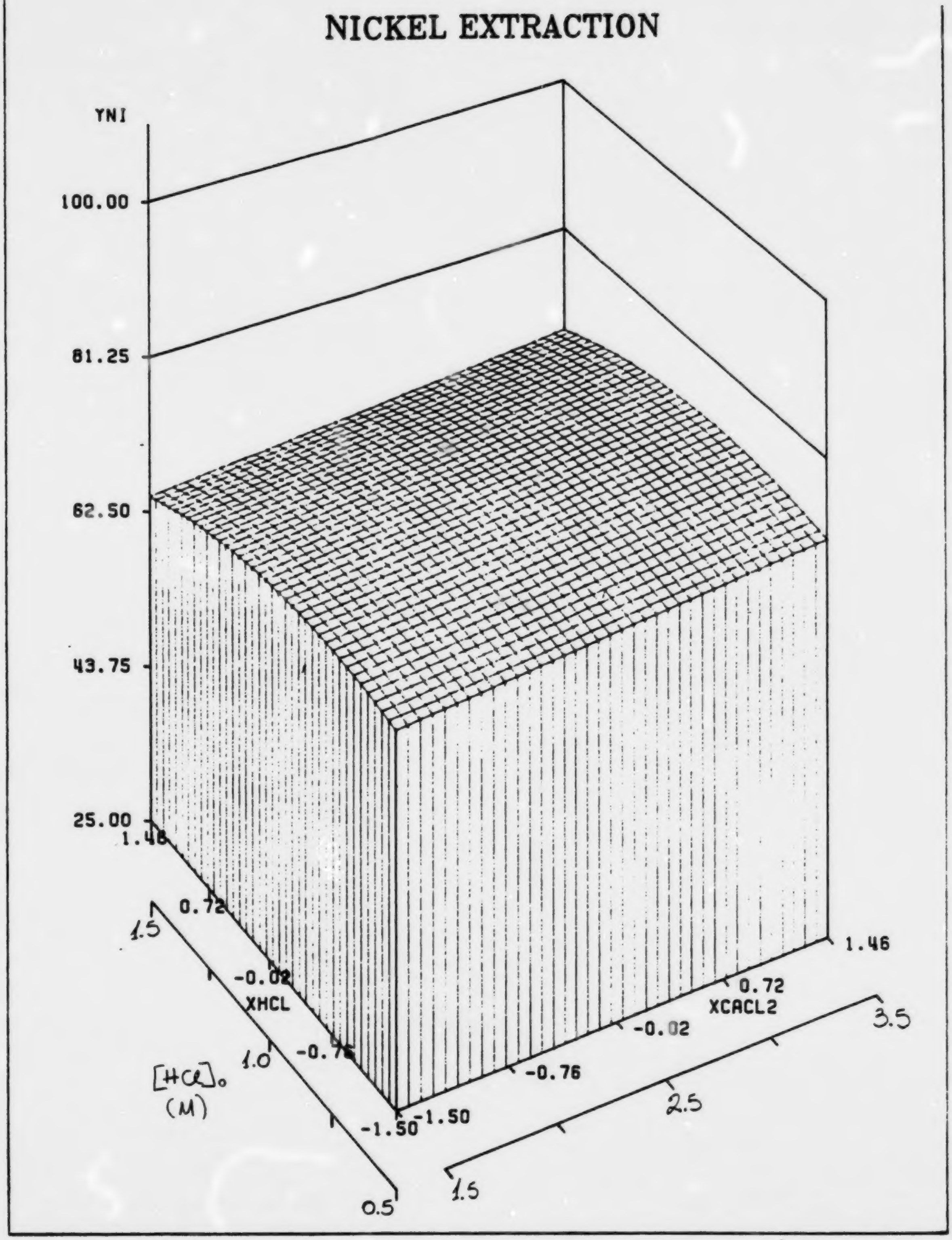

Fig. 55 Predicted % Ni extraction response surface as a function of $|HCl|_o$ and $|CaCl_2|_o$; d_s = 0. 33 kg/l and T = 6 hrs.

Table 21 Best combinations of conditions for maximum % nickel extraction

Combination No.	D_S (kg/l)	$\|HCl\|_o$ (M)	$\|CaCl_2\|_o$ (M)	Time (hrs)	Maximum % Ni Extraction	Source
1	1.0	1.5	3.5	6.0	70	Fig. 51
2	0.33	1.0	3.5	6.0	70	Figs. 52,53,54

3.4.3.4 Study of the Response: % Arsenic Extraction

The experimental data were inspected by constructing plots of % As extraction against each independent variable (Figs. 56 to 59) and calculating the respective correlation coefficients, r. From these data it can be clearly seen that slurry density (r = -0.707) and HCl concentration (r = 0.552) are practically the only parameters affecting arsenic extraction. $CaCl_2$ concentration and time, within the range of conditions tested, were found not to have any significant effect (r = 0.065 and 0.024 respectively). High slurry densities result in loss of arsenic extraction apparently due to build-up of As(V) in the solution which subsequently precipitates. In other words the loss of arsenic extraction with an increase in d_s is not due to difficulties with leaching but rather due to difficulties in keeping arsenic in solution after the latter has been solubilized. On the other hand with an increase in HCl concentration the solubility of the As(V) compounds increases and thereby arsenic extraction increases. The thermodynamic solubility of several arsenate compounds as a function of pH has been extensively studied by Robins (24, 25). In general all these compounds such as $Ca_3(AsO_4)_2$ and $FeAsO_4$, despite their very low solubility products (52) enjoy very high solubilities at pH < 1, especially the former one.

Three-D graphs representing the extraction of arsenic are presented in Figs. 60 to 62. In the first two graphs the

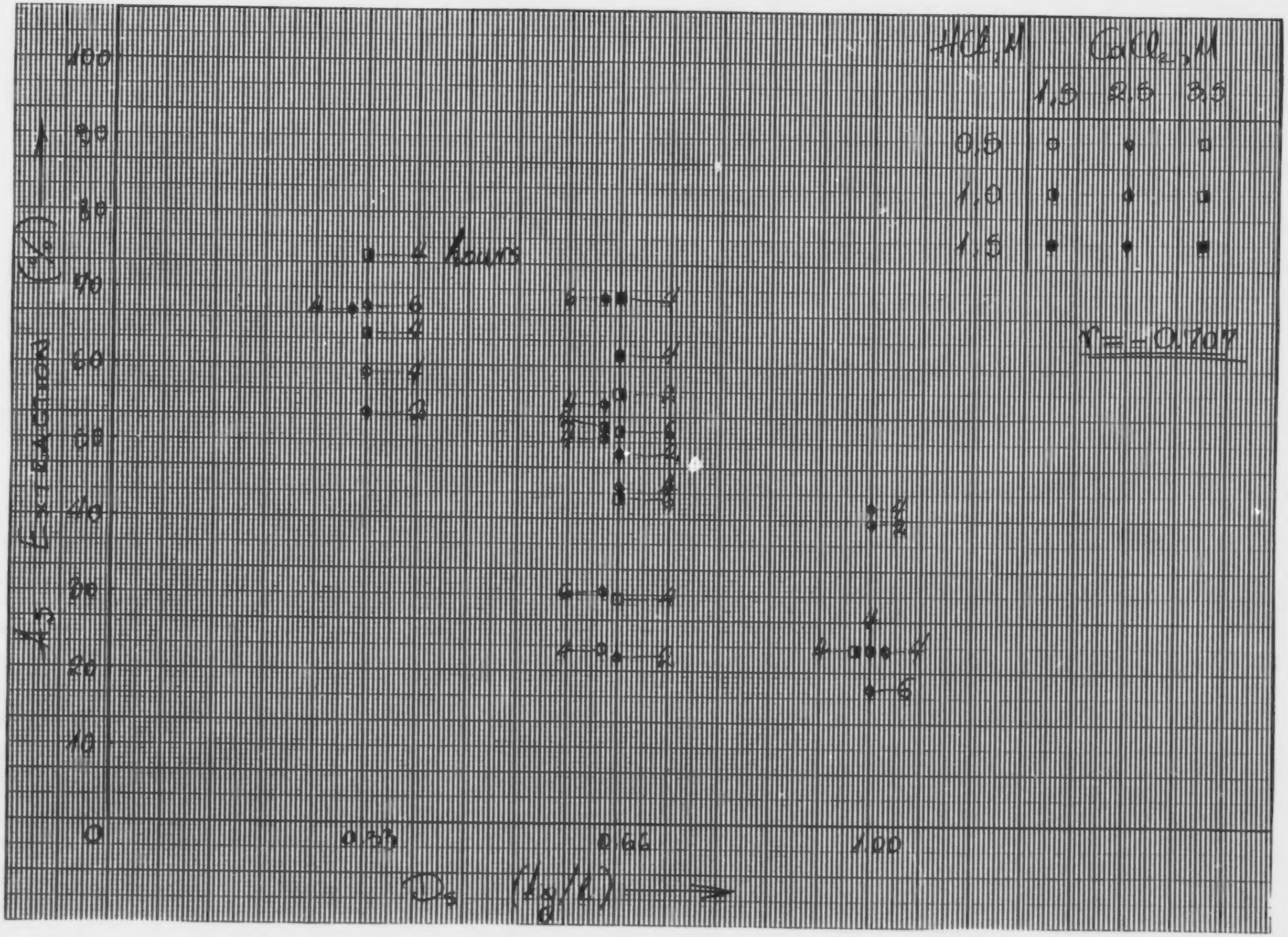

Fig. 56 Observed % As extraction vs slurry density.

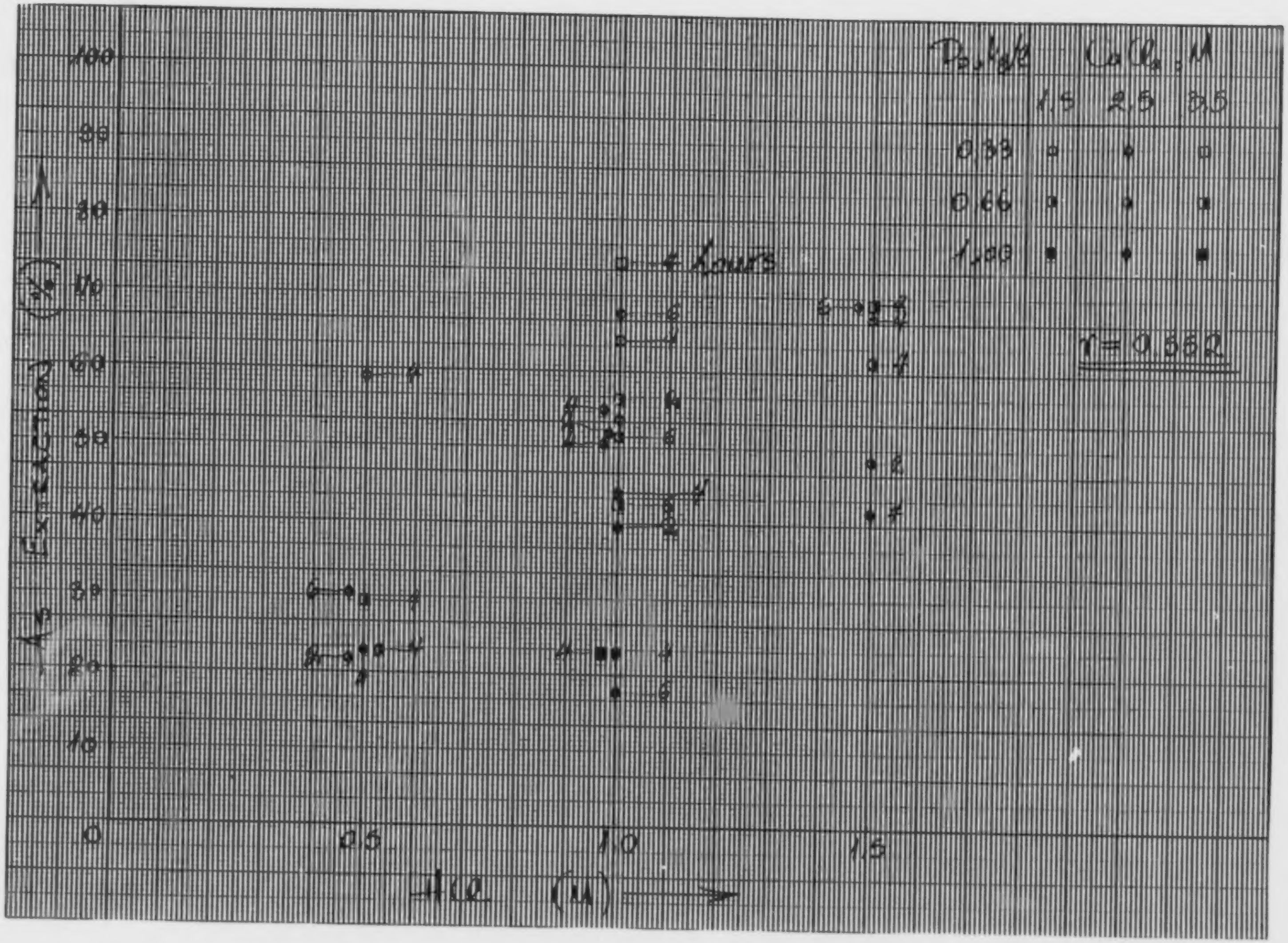

Fig. 57 Observed % As extraction vs $|HCl|_o$.

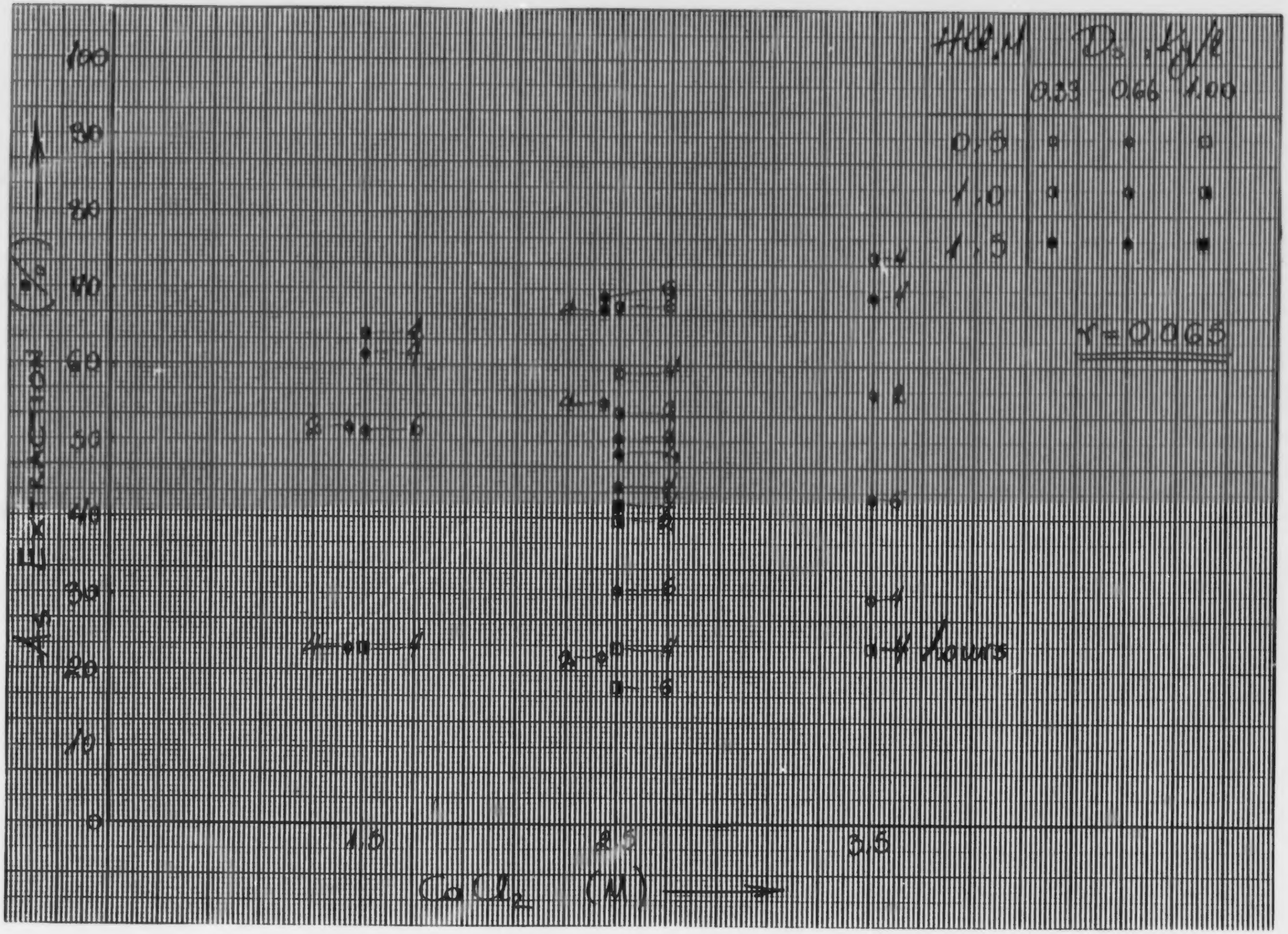

Fig. 58 Observed % As extraction vs $|CaCl_2|_o$.

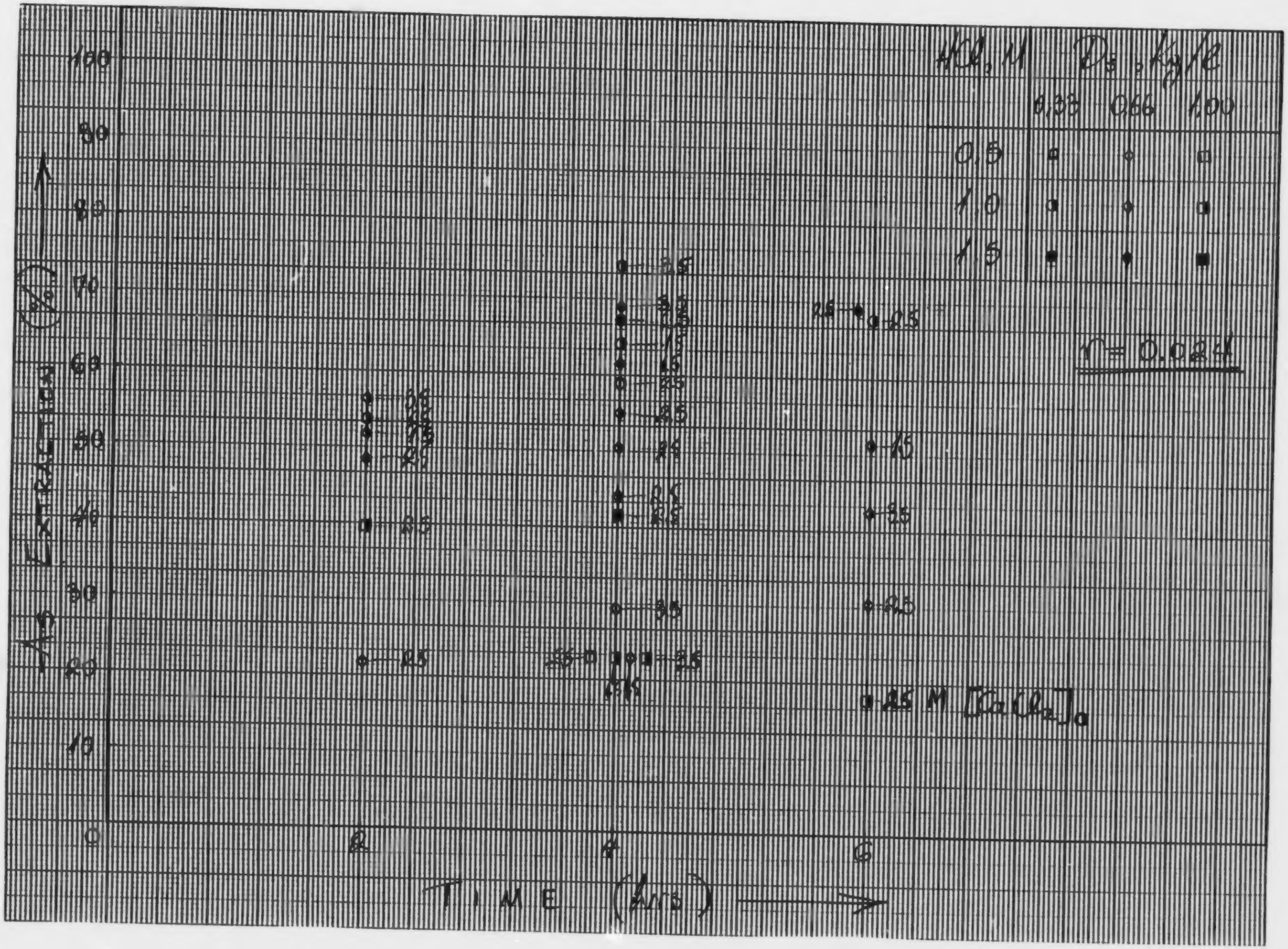

Fig. 59 Observed % As extraction vs Time.

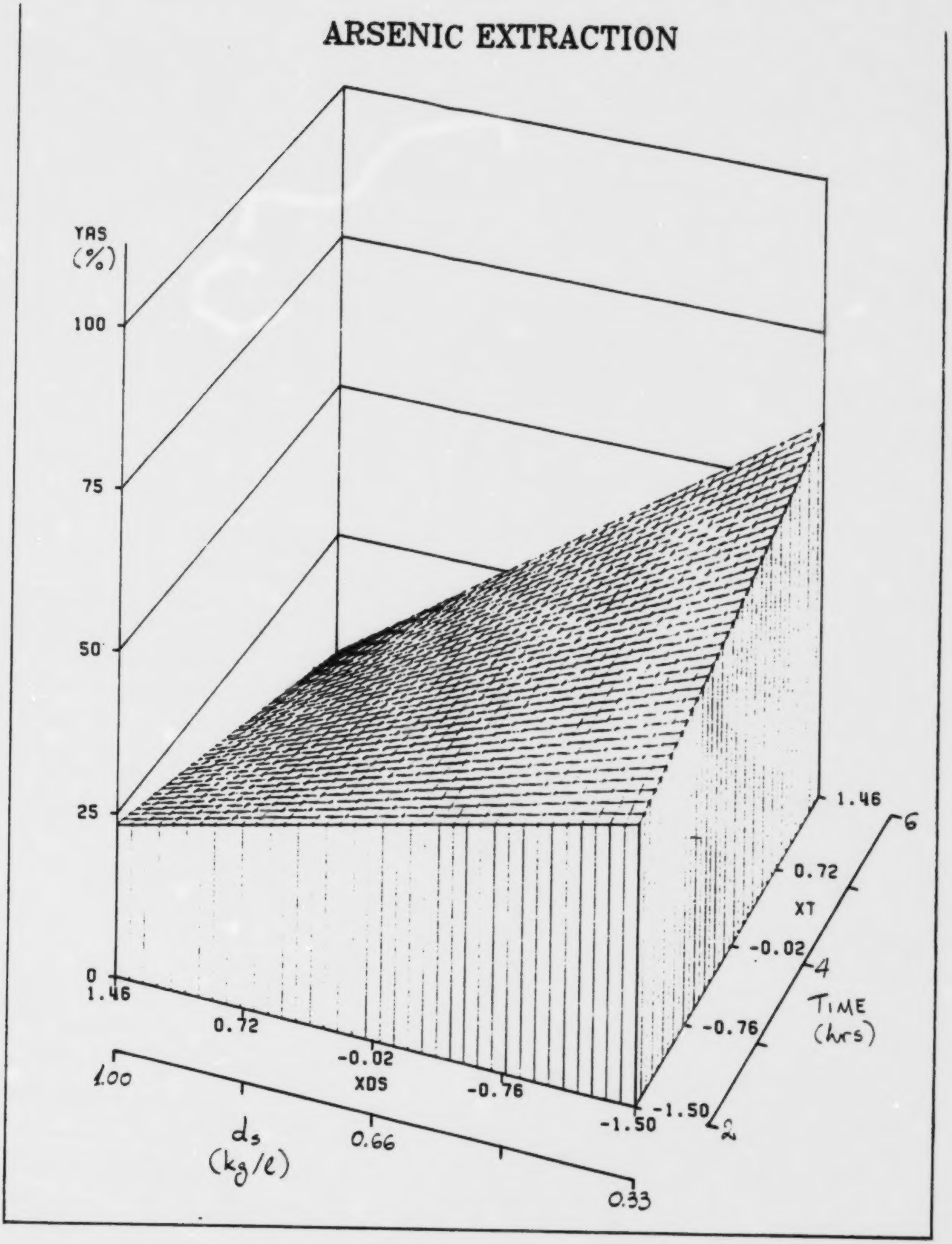

Fig. 60 Predicted % As extraction response surface as a function of d_s and Time; $|CaCl_2|_o$ = 1.5 M and $|HCl|_o$ = 0.5 M.

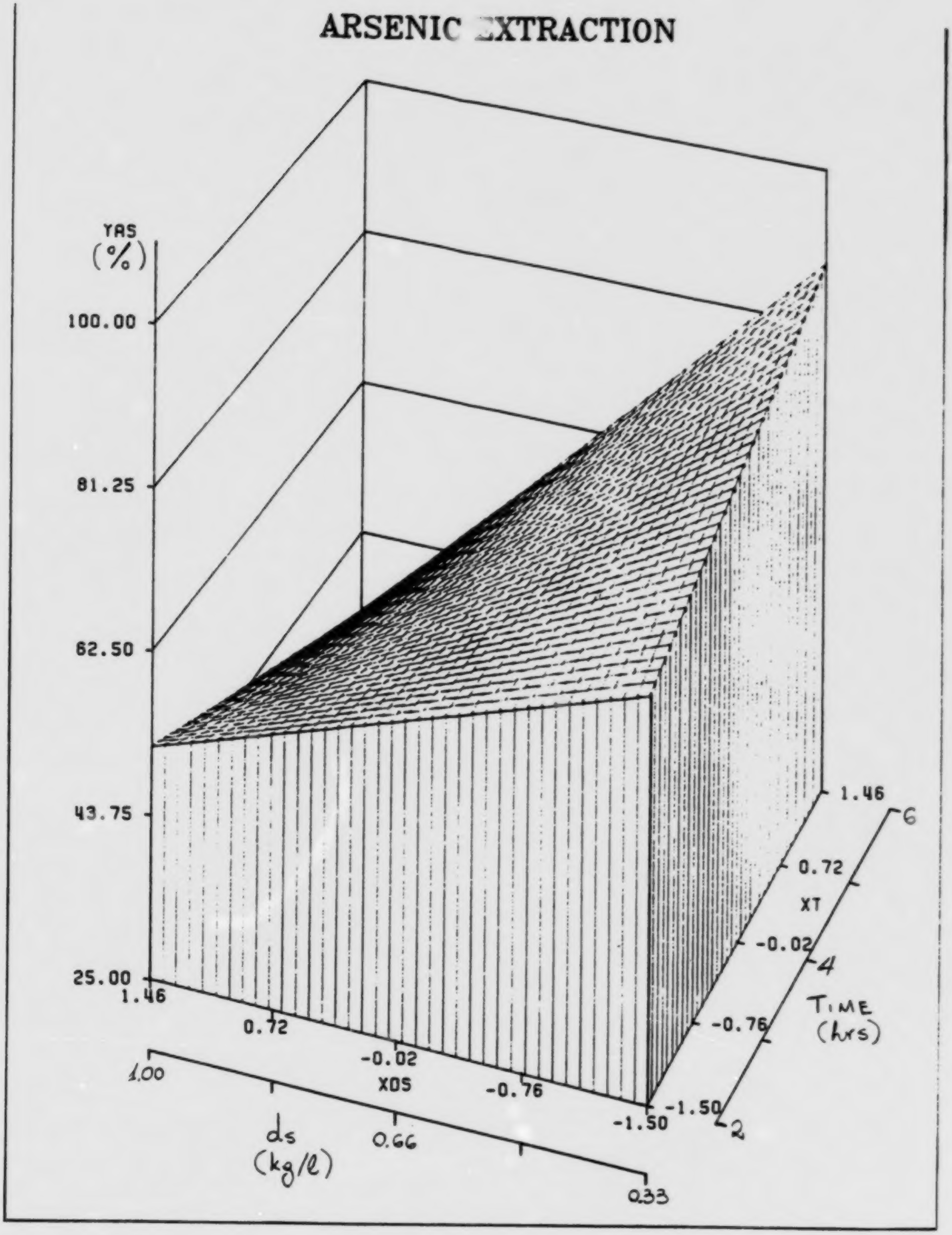

Fig. 61 Predicted % As extraction response surface as a function of d_s and Time; $|CaCl_2|_o$ = 1.5 M and $|HCl|_o$ = 1.5 M.

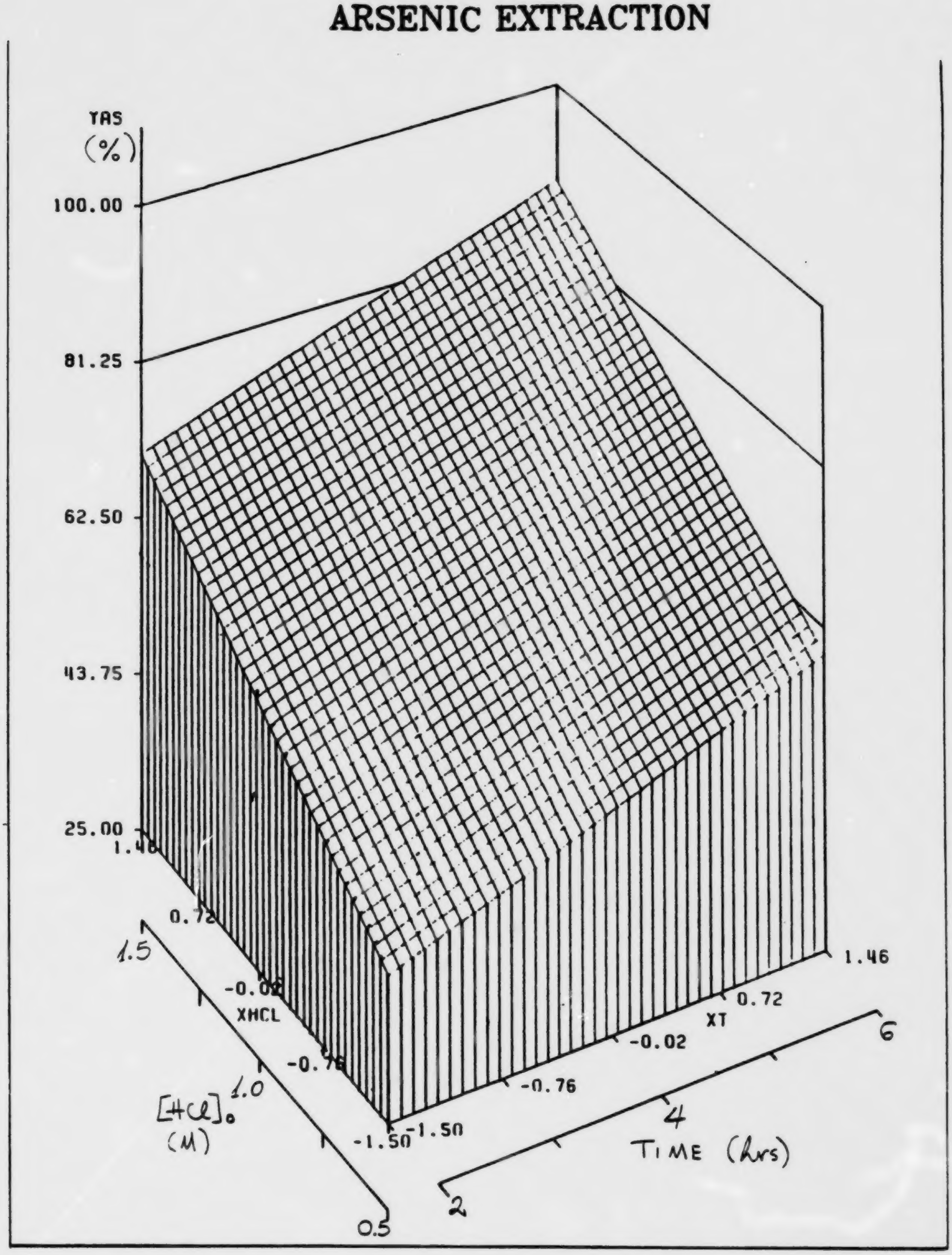

Fig. 62 Predicted % As extraction response surface as a function of $|HCl|_o$ and Time; d_s = 0. 33 kg/l and $|CaCl_2|_o$ = 1.5 M.

extraction of arsenic (%As) is plotted against slurry density and time for low (0.5 N; "-1.47") and high (1.5 N; "1.47") acid levels respectively. A strong negative interaction between slurry density and time is seen to operate. That is while time has a slightly positive effect on % As extraction at the low d_s level (0.33 kg/l; "-1.50"), this effect becomes strongly negative at the high d_s level (1.0 kg/l; "+1.46"). Apparently when high slurry densities are used the precipitation problem is more acute as reaction time progresses thereby resulting in loss of arsenic extraction. On the other hand with dilute slurries arsenic extraction increases with time since it is the leaching mechanism of the arsenide minerals becoming now more important than the precipitation mechanism. The negative interaction effect is reflected in the model equation for arsenic extraction (eq. 17, Table 16) by the presence of the term $-4.12X_1X_4$. Finally Fig. 62 represents arsenic extraction as a function of $[HCl]_o$ and time at the low slurry density level (0.33 kg/l; "-1.47"). It can be seen now time to have equivalent positive effects on arsenic extraction for both low and high HCl levels. That means that under these conditions of low d_s the leaching of the arsenide minerals is the controlling step of the arsenic extraction process and not precipitation. Thus for this regime of conditions arsenic extraction parallels the extracton of nickel (see Fig. 54). Moreover a closer comparison of Figs. 54 and 62 indicates arsenic extraction to be much higher than the respective nickel extraction (93% As vs. 70% Ni) under the same otherwise conditions. This is attributed to the relative refractoriness of millerite (NiS - the major non-arsenide nickel mineral present in

Table 22 Best conditions for maximum % arsenic extraction

D_S (kg/l)	$\lvert HCl \rvert_o$ (M)	$\lvert CaCl_2 \rvert_o$ (M)	Time (hrs)	Maximum % As Extraction	Source
0.333	1.5	1.5	6	93	Figs. 61,63

the ore) in comparison to the leaching of the arsenide minerals.

From the above analysis, the conditions shown in Table 22 were identified as the optimum ones for arsenic extraction within the process region of investigation.

3.4.3.5 Study of the Response: Acid Consumption (moles/l)

As has been discussed in section 3.4.1 the Key Lake ore is highly reactive resulting in considerable acid consumption. In an effort to minimize the acid requirements of the process a statistical model equation was developed with the aid of the data of Table 13 in order to generate 3-D graphs for optimization purposes. Before though the 3-D graphs being considered the obtained data are examined graphically in Figs. 63-66. In these graphs acid consumption (measured in moles /l) is plotted against each independent variable. It can be seen that all variables have a positive (i.e. detrimental) effect on acid consumption. Significant interaction and curvature effects are also indicated (see also the respective model equation (18)). To obtain acid consumption in terms of kg HCl/ton ore, the values given by the model equation and plotted in Fig. 63-70 have to be divided by the respective slurry density (i.e. d_s, kg solids/l).

Three-D graphs representing acid consumption as a function of slurry density and initial HCl concentration at various levels

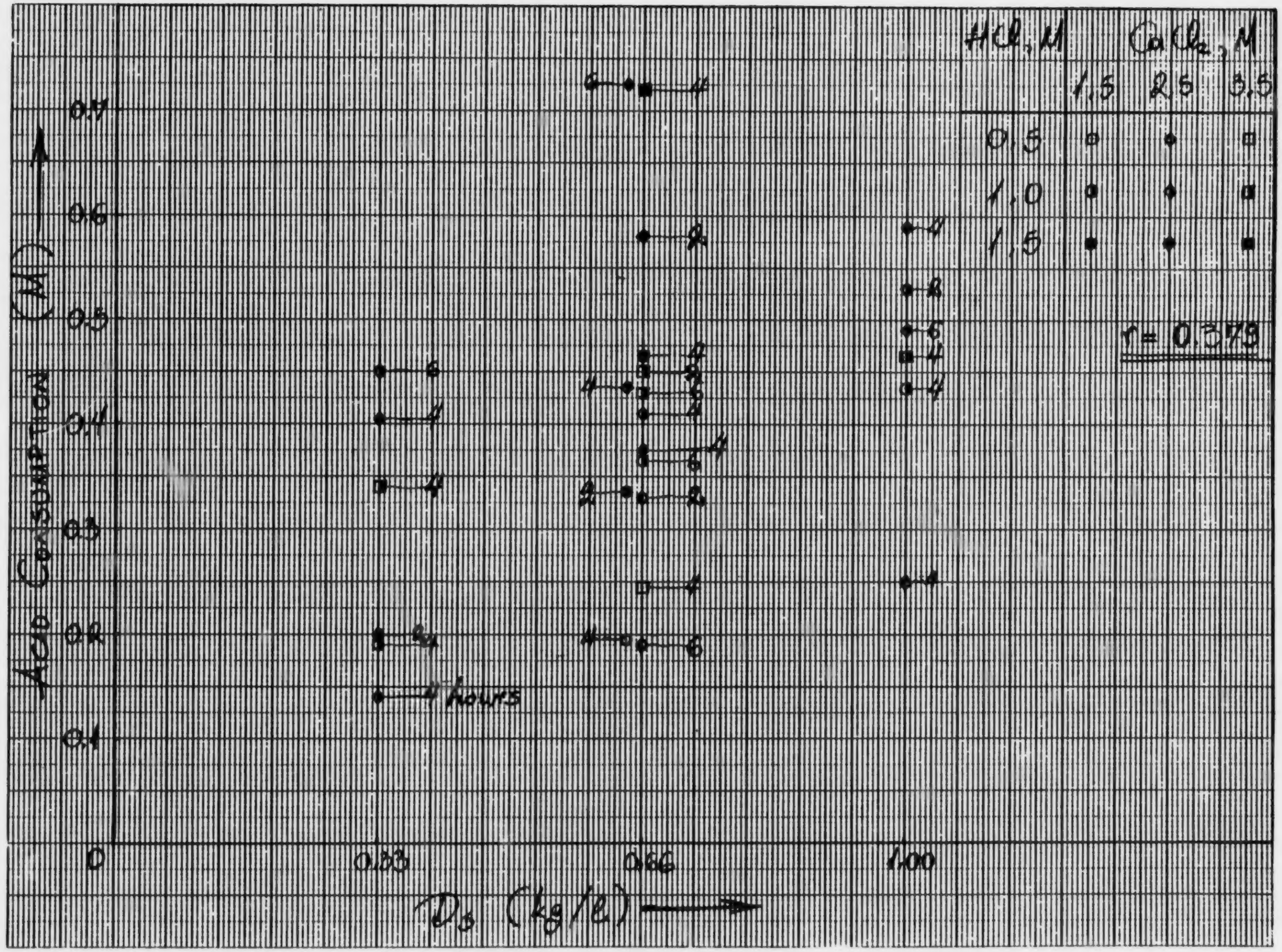

Fig. 6 3 Observed Acid Consumption (moles/1) vs d_s.

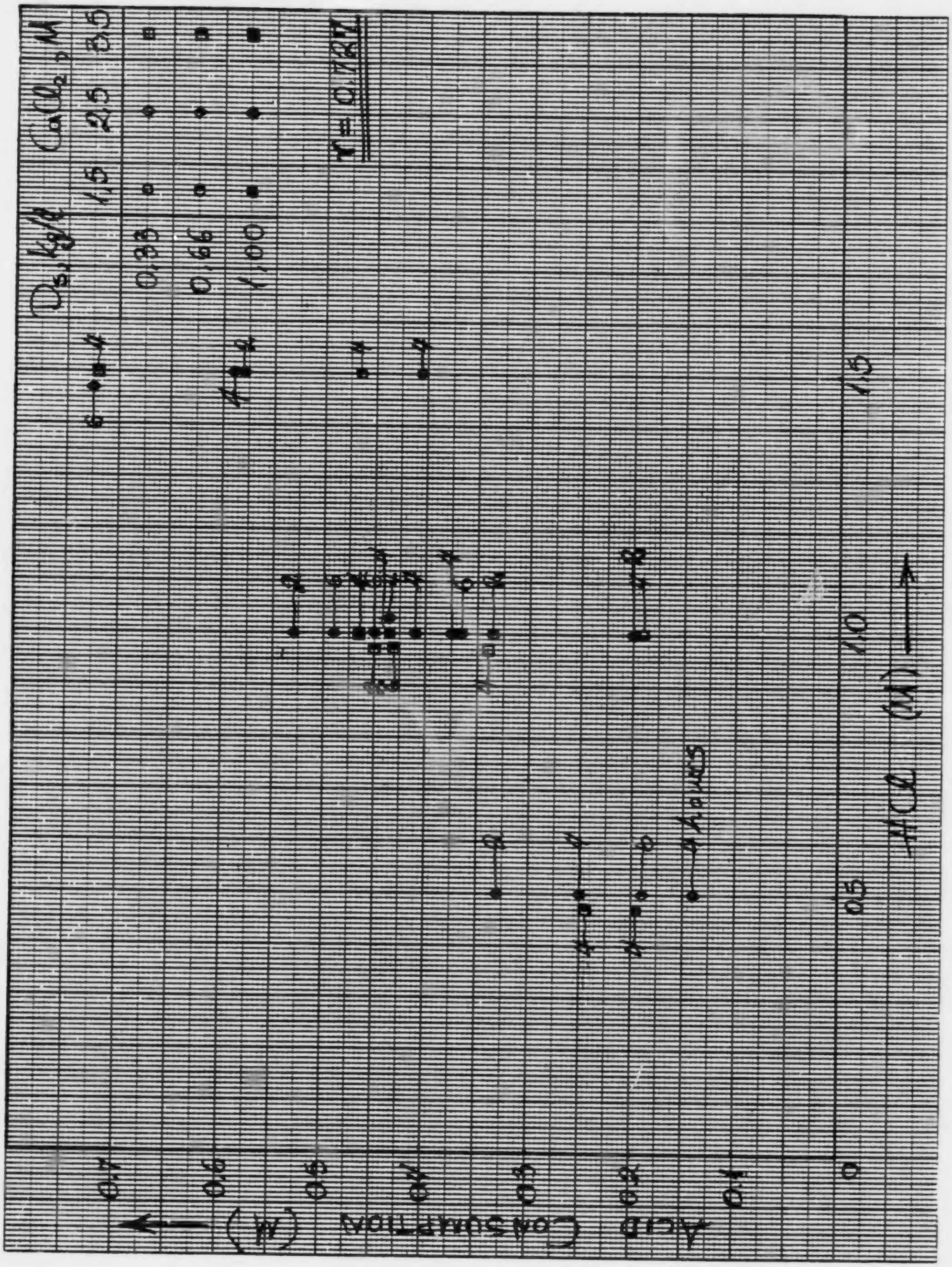

Fig. 64 Observed Acid Consumption (moles/l) vs $|HCl|_o$.

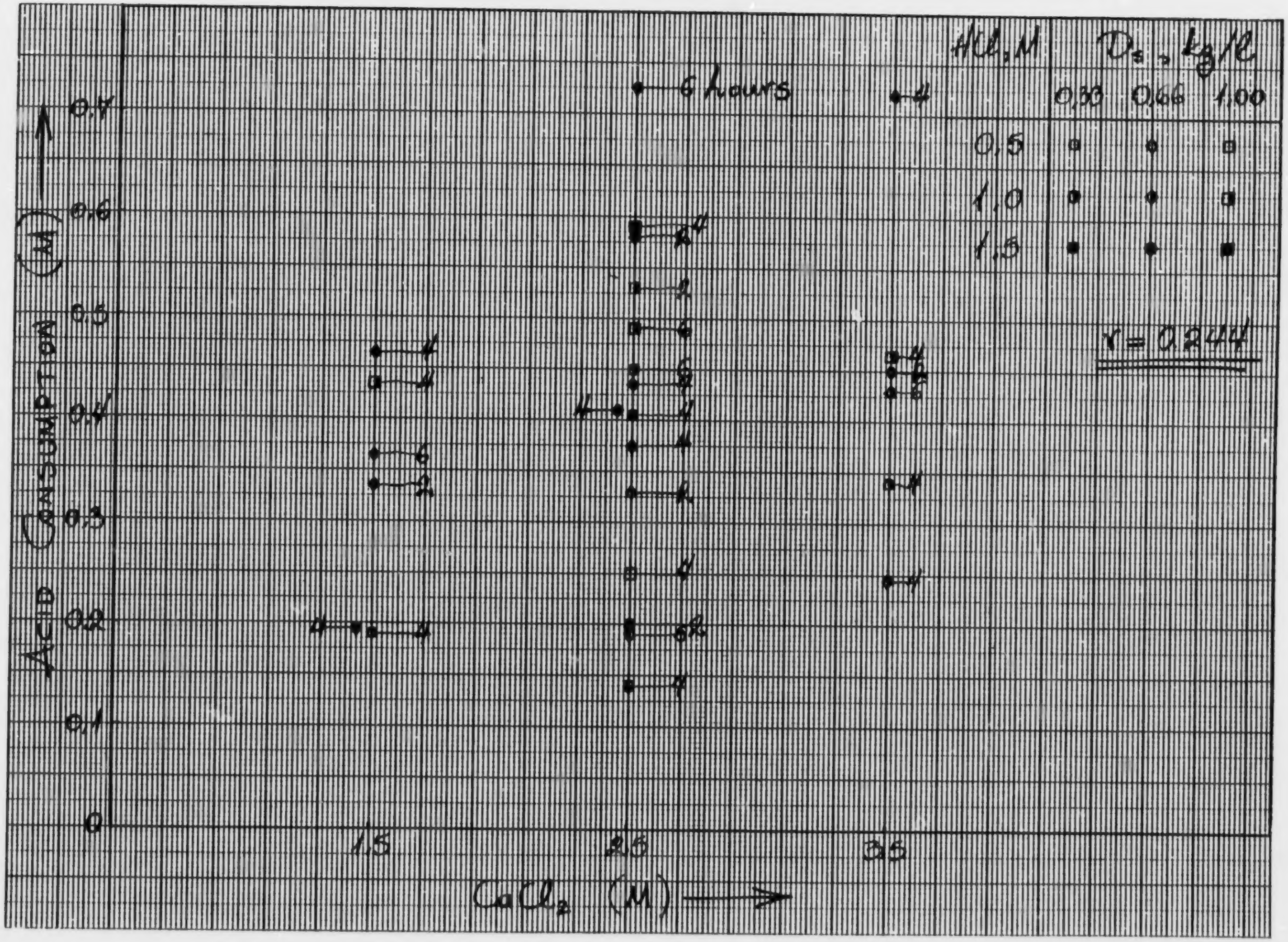

Fig. 65 Observed Acid Consumption (moles/1) vs $|CaCl_2|_o$.

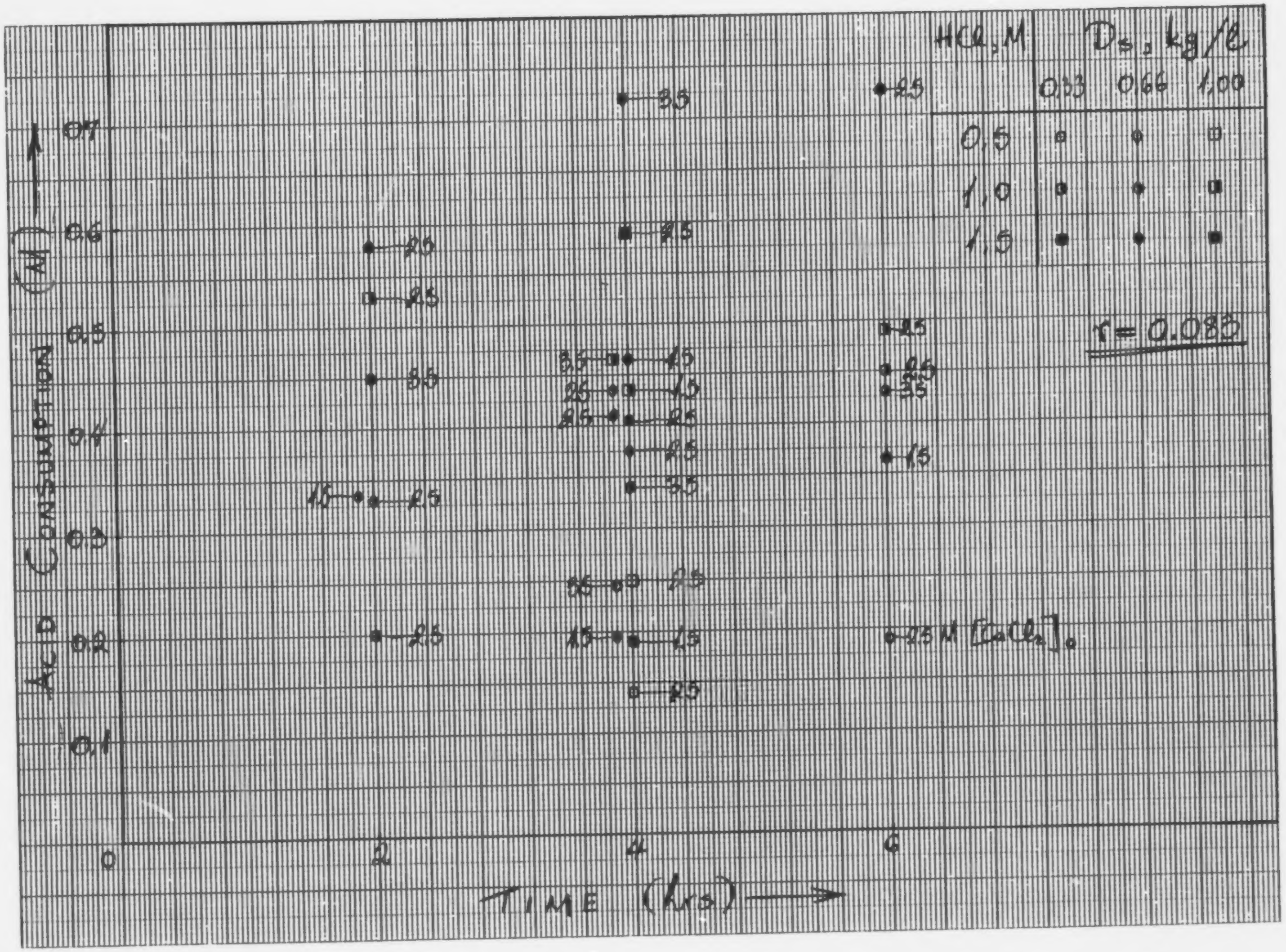

Fig. 66 Observed Acid Consumption (moles/1) vs Time.

of $CaCl_2$ concentration and time are shown in Figs. 67-70. Figs. 67 to 69 were generated by keeping time constant at 2 hr (X_T = "-1.47") and changing the $CaCl_2$ conc from low (1.5 M; "-1.47") to intermediate (2.5 M; "0.00") and high (3.5 M; "0.00") levels respectively. As is clearly seen from these Figures acid consumption increases dramatically by increasing $CaCl_2$ concentration. This is attributed to the increased activity of HCl in the presence of $CaCl_2$ (50, 51). Thus more extensive attack of the gangue mineralization takes place having as a consequence the augmented acid consumption observed. Acid consumption, according to Figs. 67 to 69 always increases also as the HCl concentration and/or the slurry density is increased for the same reasons.

To determine the optimum leaching conditions (i.e. minimum acid consumption on one hand and maximum (100%) coextraction of U and Ra on the other) the areas of the acid consumption response surface yielding 100% U and Ra extraction have been marked on Figs. 67 to 69. The broken line triangle represents the region for 100% uranium extraction and the solid line triangle the region for 100% radium extraction under the same experimental conditions as those indicated in each graph. From Fig. 67 (conditions $[CaCl_2]_o$ = 1.5 M and time = 2 hr) the best acid consumption value (shown by arrow "1" on the graph) was determined to be 11.8 kg HCl/ton ore. This is achieved for d_s = 0.33 kg/lit and $[HCl]_o$ =1.0 N. Alternatively operation with 0.5 kg/l slurry density and $[HCl]_o$ = 1.5 N results in 21 kg/ton acid consumption (arrow "2" on Fig. 67). The minimum acid consumption values have

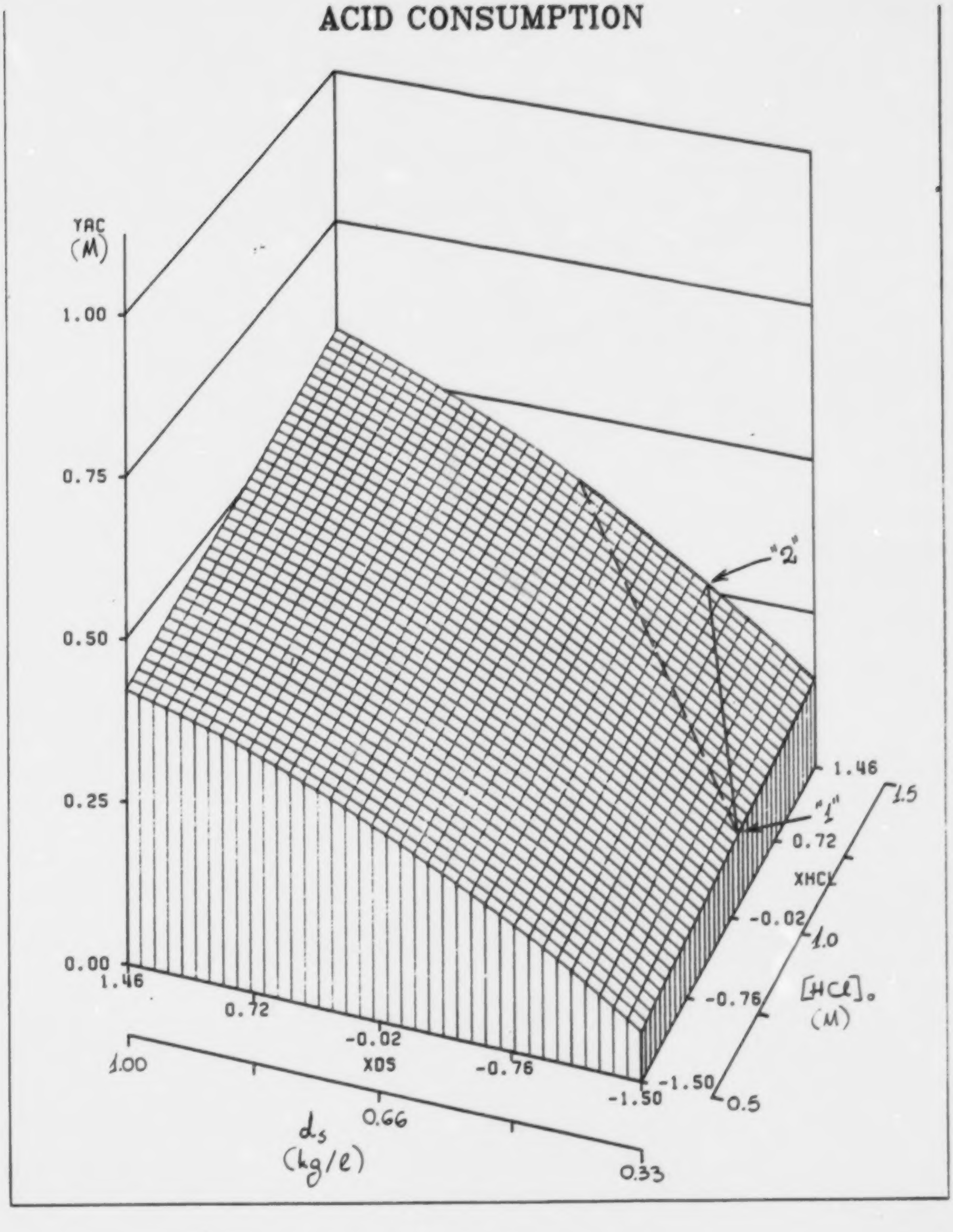

Fig. 67 Predicted Acid Consumption (moles/l) response surface as a function of d_s and $|HCl|_o$; $|CaCl_2|_o$ = 1.5 M and T = 2 hrs.; (The inner triangle represents 100% U/Ra co-extraction).

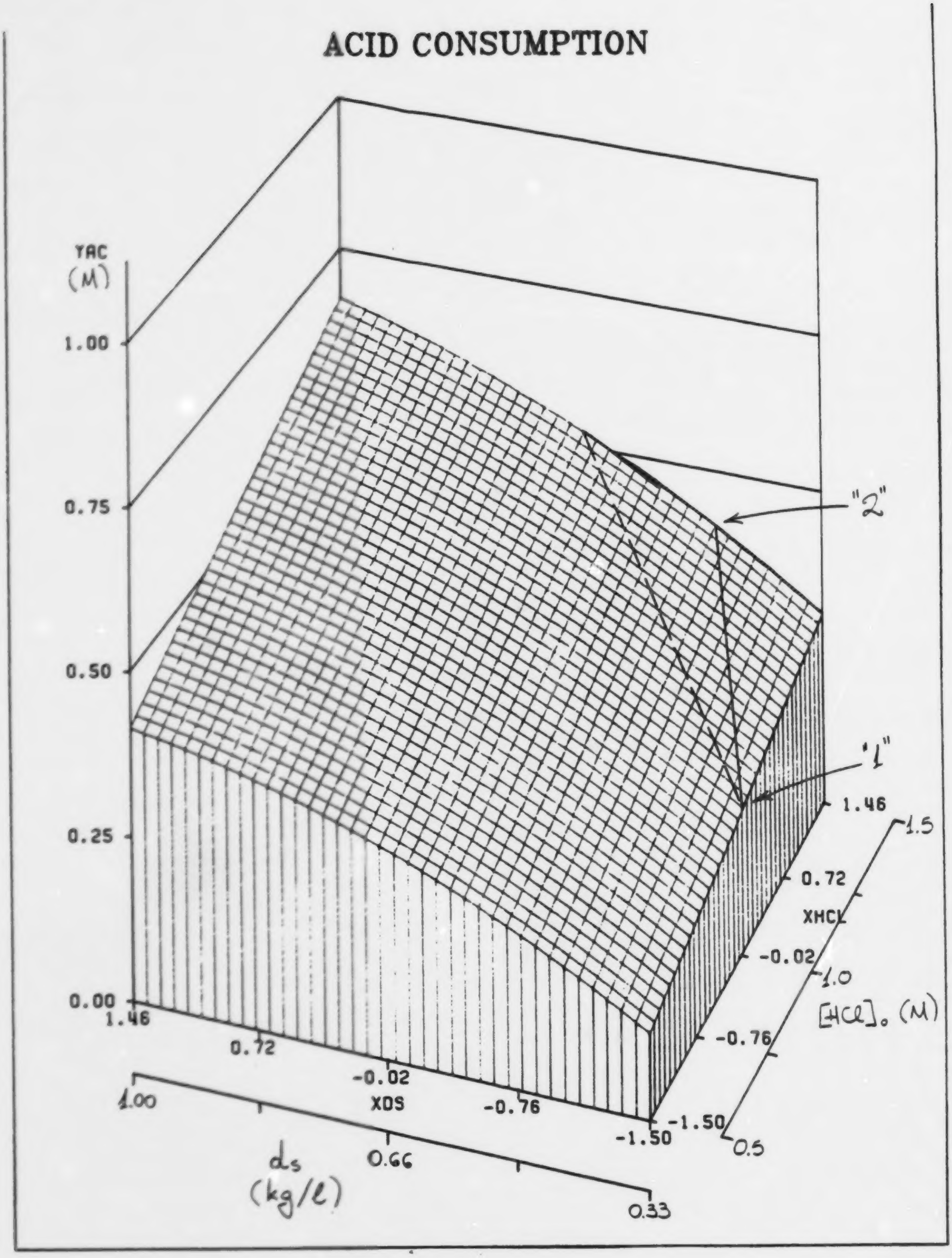

Fig. 68 Predicted Acid Consumption (moles/l) response surface as a function of d_s and $|HCl|_o$; $|CaCl_2|_o$ = 2.5 M and T = 2 hrs. (inner triangle: 100% U/Ra co-extraction).

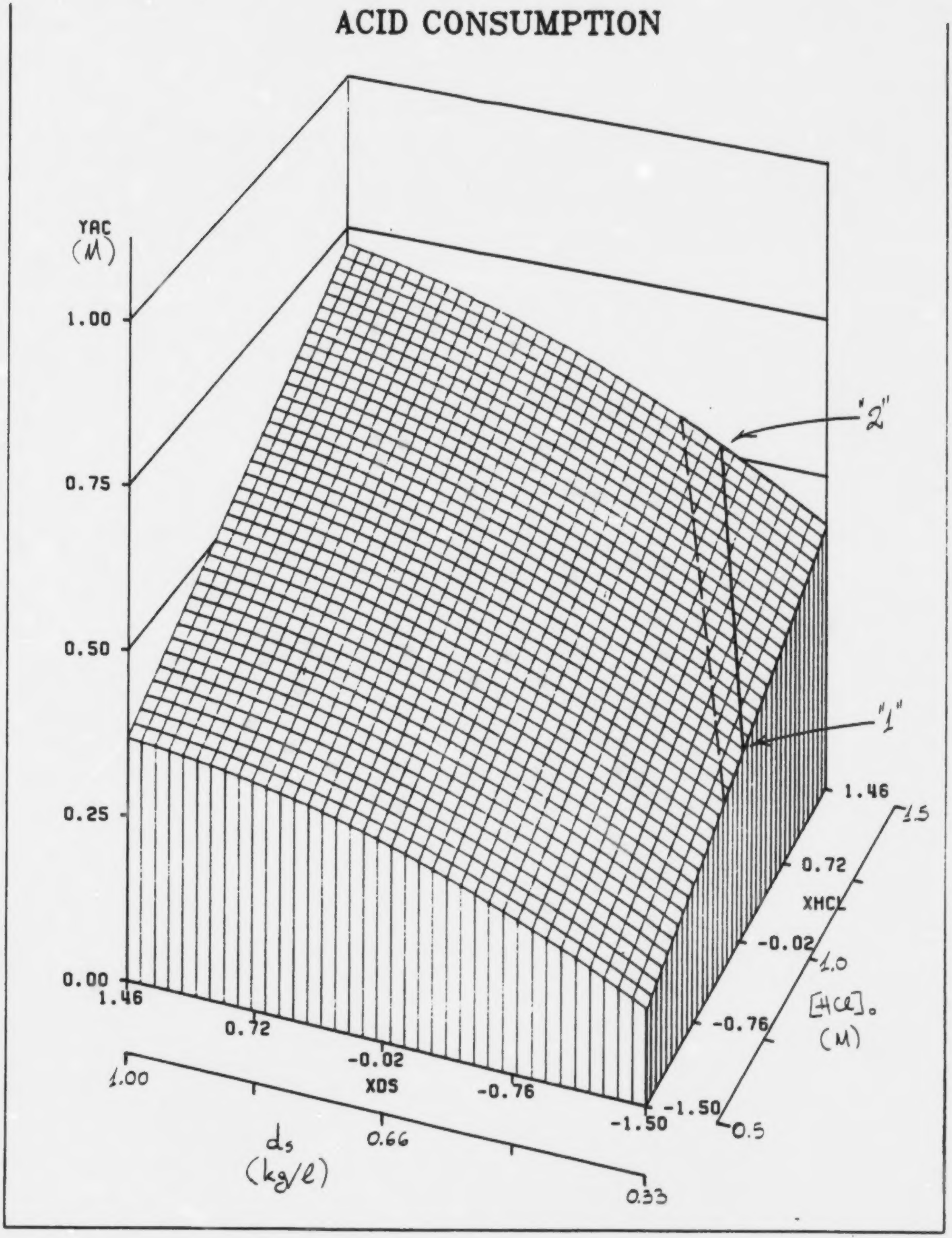

Fig. 69 Predicted Acid Consumption (moles/l) response surface as a function of d_s and $|HCl|_o$; $|CaCl_2|_o$ = 35 M and T = 2 hrs. (inner triangle = 100% U/Ra co-extraction).

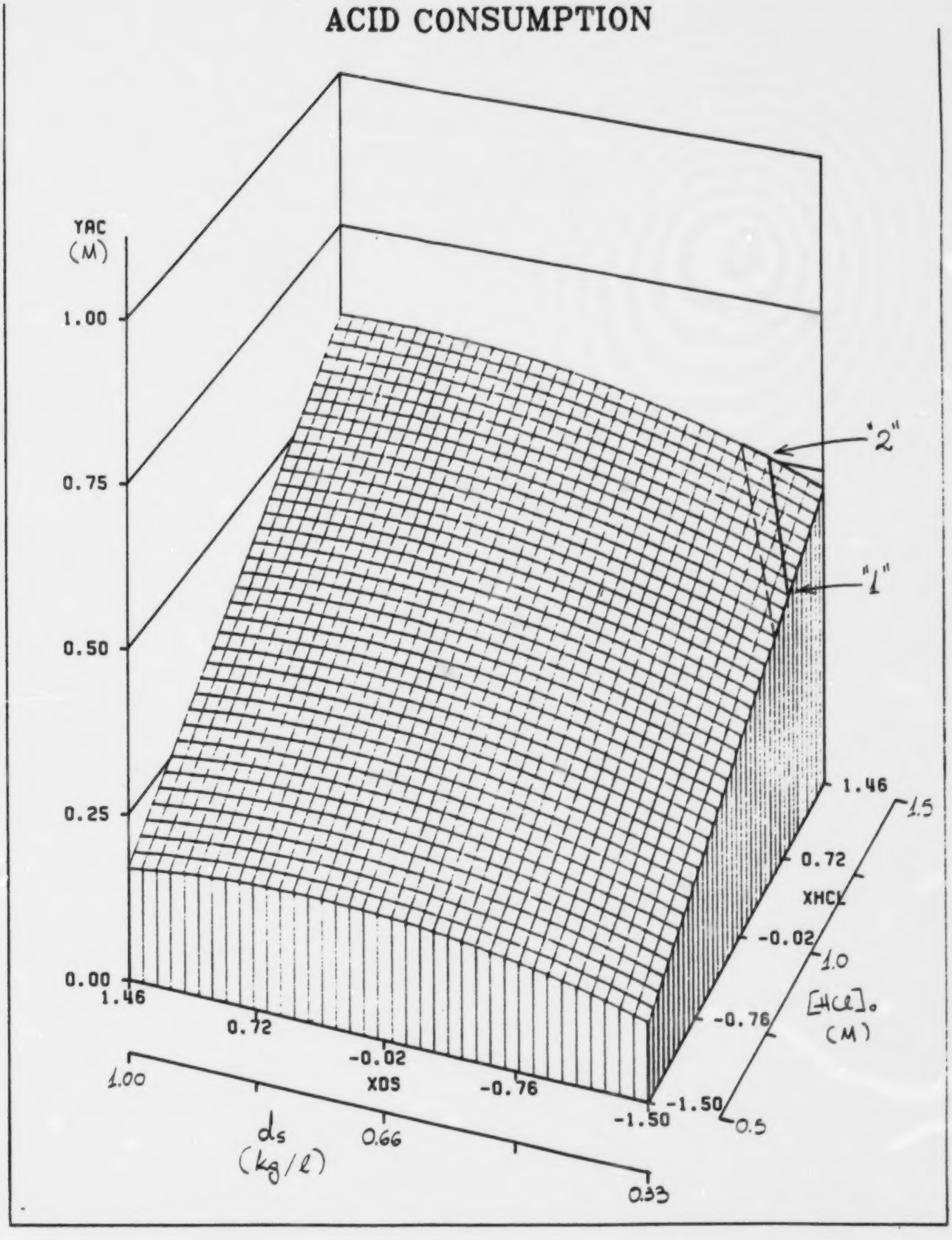

Fig. 70 Predicted Acid Consumption (moles/l) response surface as a function of d_s and $|HCl|_o$; $|CaCl_2|_o$ = 1.5 M and T = 6 hrs. (inner triangle = 100% U/Ra co-extraction).

Table 23 Minimum acid consumption for 100% U and Ra co-extraction as a function of $|CaCl_2|_o$ and Time

Fig. No.	d_s (kg/1)	$\|HCl\|_o$ (M)	$\|CaCl_2\|_o$ (M)	Time (hr)	Acid Consumption (kg/ton)	
67	0.33	1.0	1.5	2	11.8	← BEST SET
	0.47	1.5	1.5	2	20.7	
68	0.33	1.0	2.5	2	25.6	
	0.47	1.5	2.5	2	31.9	
69	0.33	1.0	3.5	2	32.2	
	0.47	1.5	3.5	2	39.9	
70	0.33	1.28	1.5	6	44.8	
	0.40	1.50	1.5	6	45.6	

also been determined for the data plotted in Fig. 68, 69, and 70 and they are given in Table 23. It can be clearly seen that severe deterioration of acid consumption is predicted for high $CaCl_2$ concentrations or equivalently longer leaching times (Fig. 70).

3.4.3.6 Study of the Response: Pressure leach EMF (mV)

Figures 71 to 74 were prepared by plotting the in situ oxidation potential (converted to E_h) as a function of the various independent variables. Figure 71 shows that d_s has an adverse effect on EMF ($r = -0.514$). However more careful examination of the data (compare the slopes of the two broken lines representing low and high acid levels) indicate possible interaction effect between d_s and HCl. HCl and $CaCl_2$ (Figs. 72 and 73) are shown to have a positive effect on the pressure leach EMF. These effects might be interpreted in terms of the increased solubility Fe(III) enjoys in strongly acid solutions, since it is the ratio Fe(III)/Fe(II) which mainly controls the oxidation potential. Finally time, despite its low correlation coefficient ($r = 0.020$), appears from the distribution of the data of Fig. 74 to have an either positive or negative effect on EMF depending on the levels of the other variables. The complex dependence of EMF on d_s, $[HCl]_0$ and time is reflected in the respective model equation (eq. 19, Table 16) by the existence of several interaction and curvature terms. It is with the aid of

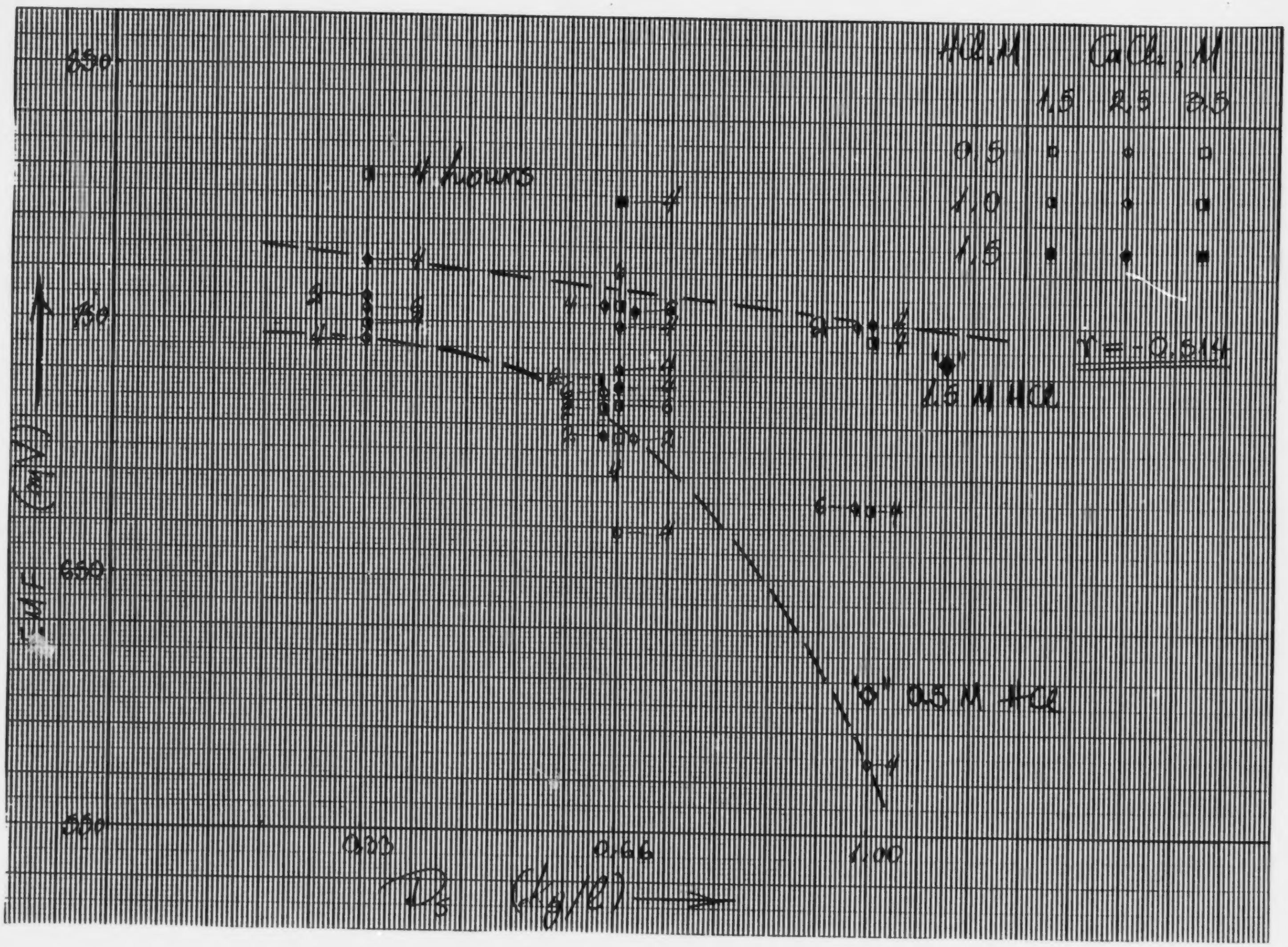

Fig. 71 Observed Pressure Leach EMF (vs SHE) vs d_s.

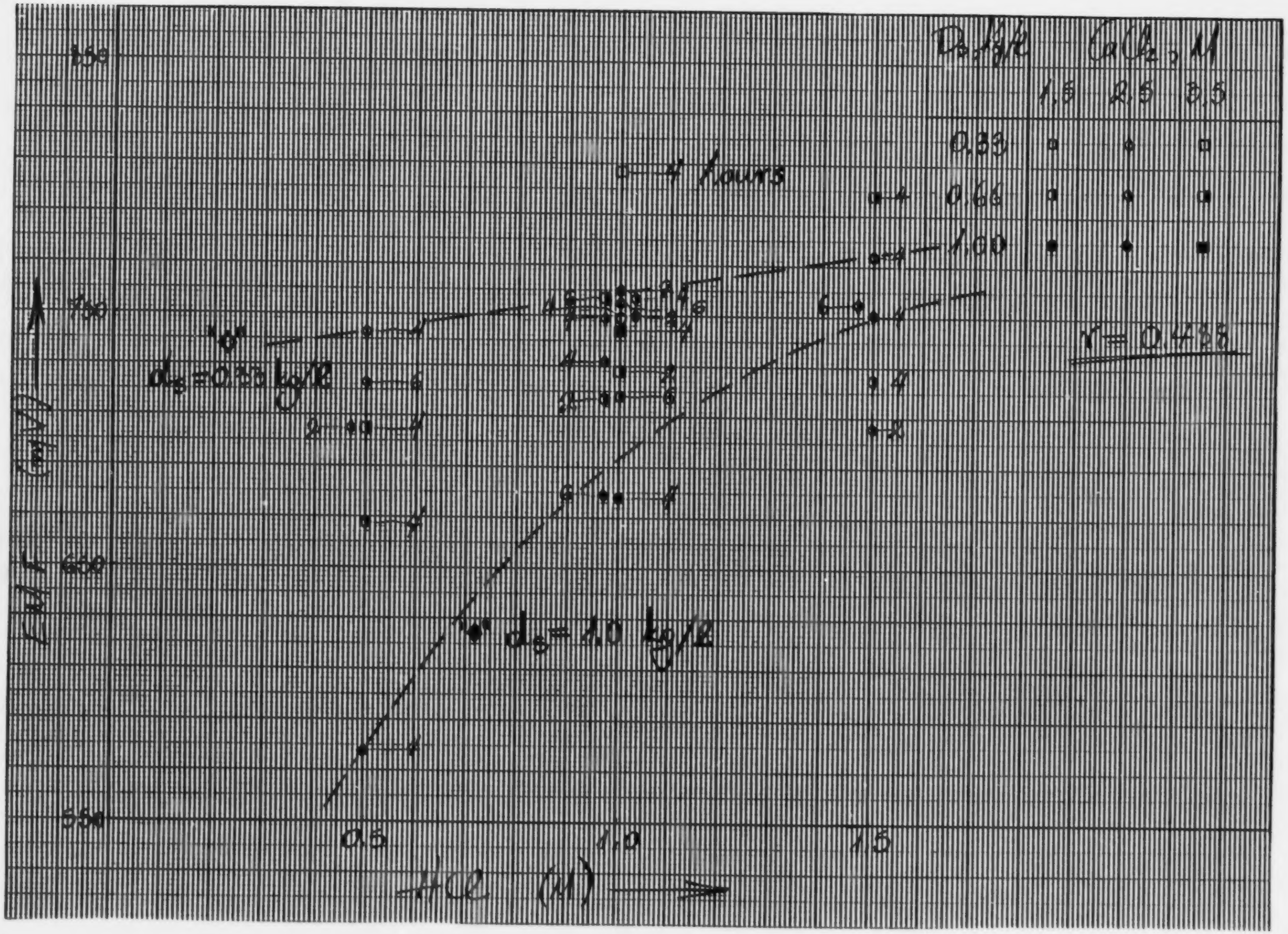

Fig. 72 Observed Pressure Leach EMF vs $|HCl|_o$.

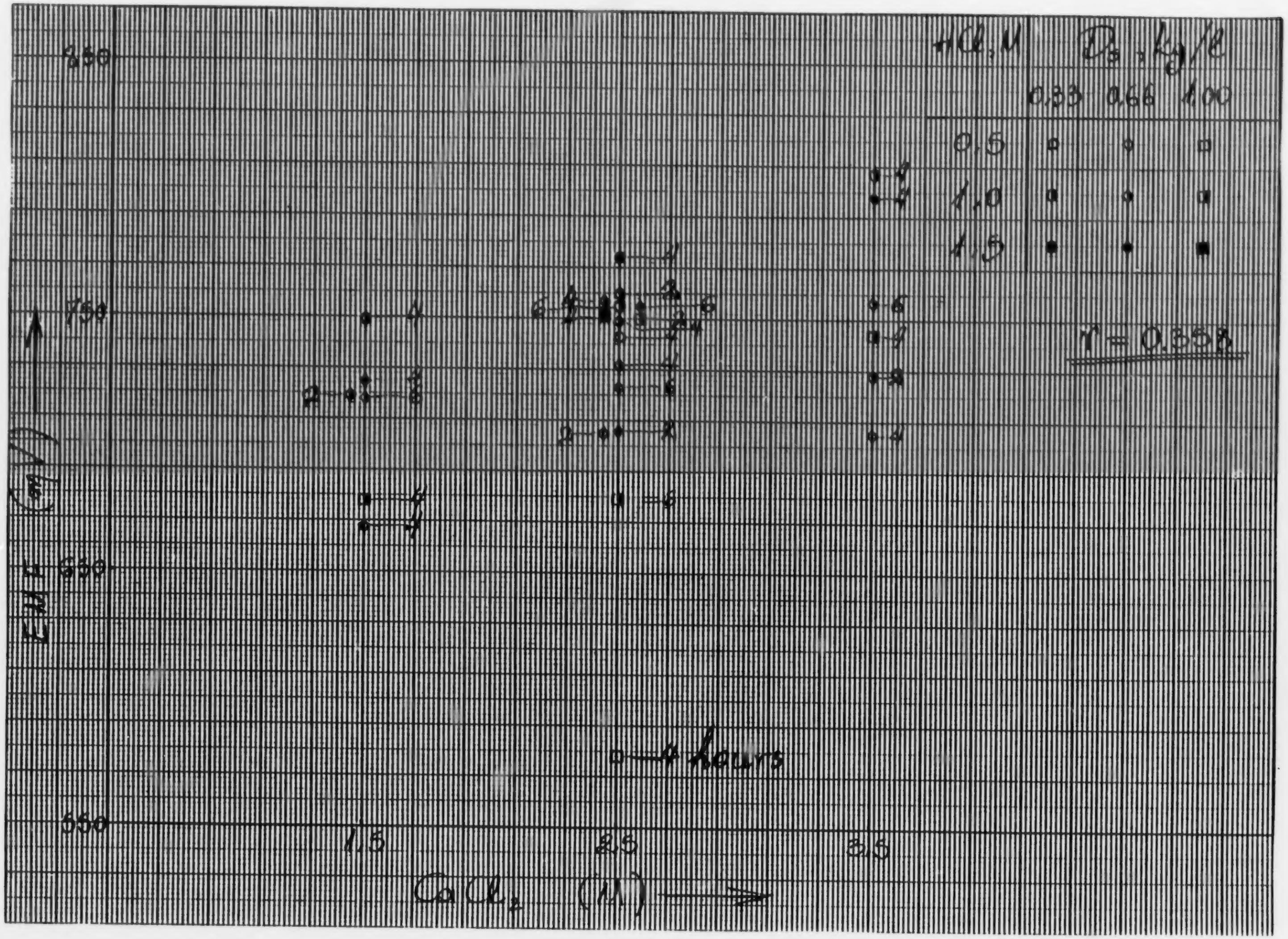

Fig. 7 3 Observed Pressure Leach EMF vs $|CaCl_2|_o$.

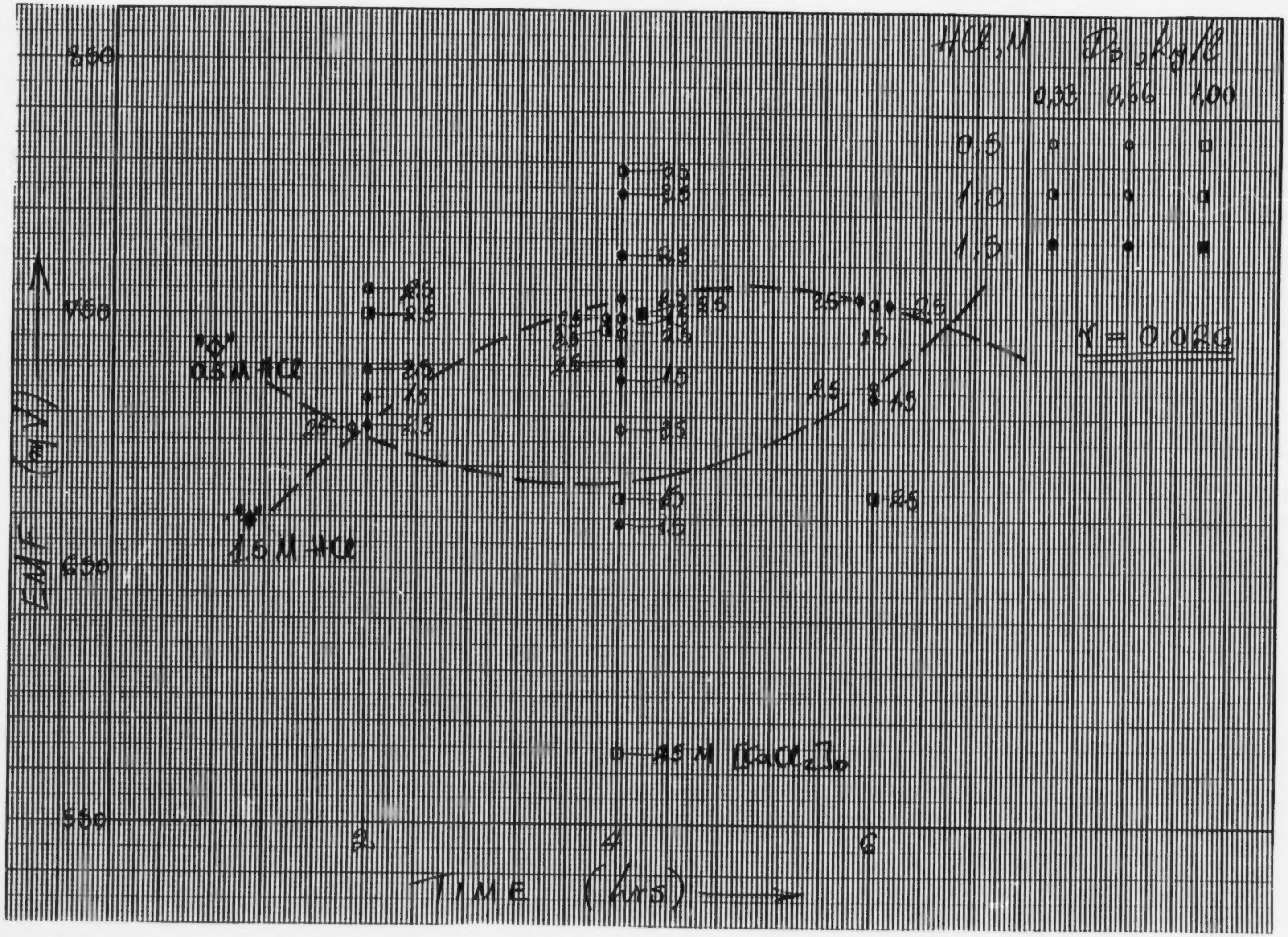

Fig. 74 Observed Pressure Leach EMF vs Time.

the 3-D graphs, shown in Figs. 75 to 78, that these effects can be better divulged.

In Figs. 75 and 76 EMF is plotted against slurry density and $[HCl]_o$, for 2 hrs constant time at low (1.5 M) and high (3.5 M) levels of $[CaCl_2]_o$ respectively. It can be seen now that while at low $[HCl]_o$ levels (= 0.5 N; "-1.50") d_s has a negative effect on acid consumption the reverse happens at high acid levels (= 1.5 N; "+1.46"). This behaviour can be interpreted as a result of the loss of Fe(III) under conditions of high d_s and low HCl which has a direct impact on the slurry EMF. Comparison of the Figs. 75 and 77 (2 hr and 6 hr respectively at $[CaCl_2]_o$ = 1.5 M) and Fig. 76 and 78 (2 hr and 6 hr respectively at $[CaCl_2]_o$ = 3.5 M) indicates that time has a positive effect at low d_s levels (i.e. "-1.50") but a negative effect at high d_s levels (i.e. "+1.40"). This interaction phenomenon between d_s and leach time is attributed to Fe(III) precipitation having as a consequence the observed loss in the EMF. According to Fig. 76 the best EMF value (+ 795 mV vs. SHE) is obtained under the following leaching conditions: d_s = 1.0 kg/l ("1.46"), $[HCl]_o$ = 1.5 N ("1.46"), $[CaCl_2]_o$ = 3.5 M ("1.47") and time = 2 hrs ("-1.47"). In principle a high EMF is desirable from the standpoint of extraction. However in the present case for the same conditions, uranium extraction is only 91% (Fig. 23) while simultaneously the acid consumption has reached the value of 26.3 kg/ton (0.72 mols/l in Fig. 69) - a clearly unacceptable performance. Apparently the complexity of the ore and the several reactions occurring simultaneously (oxidation, precipita-

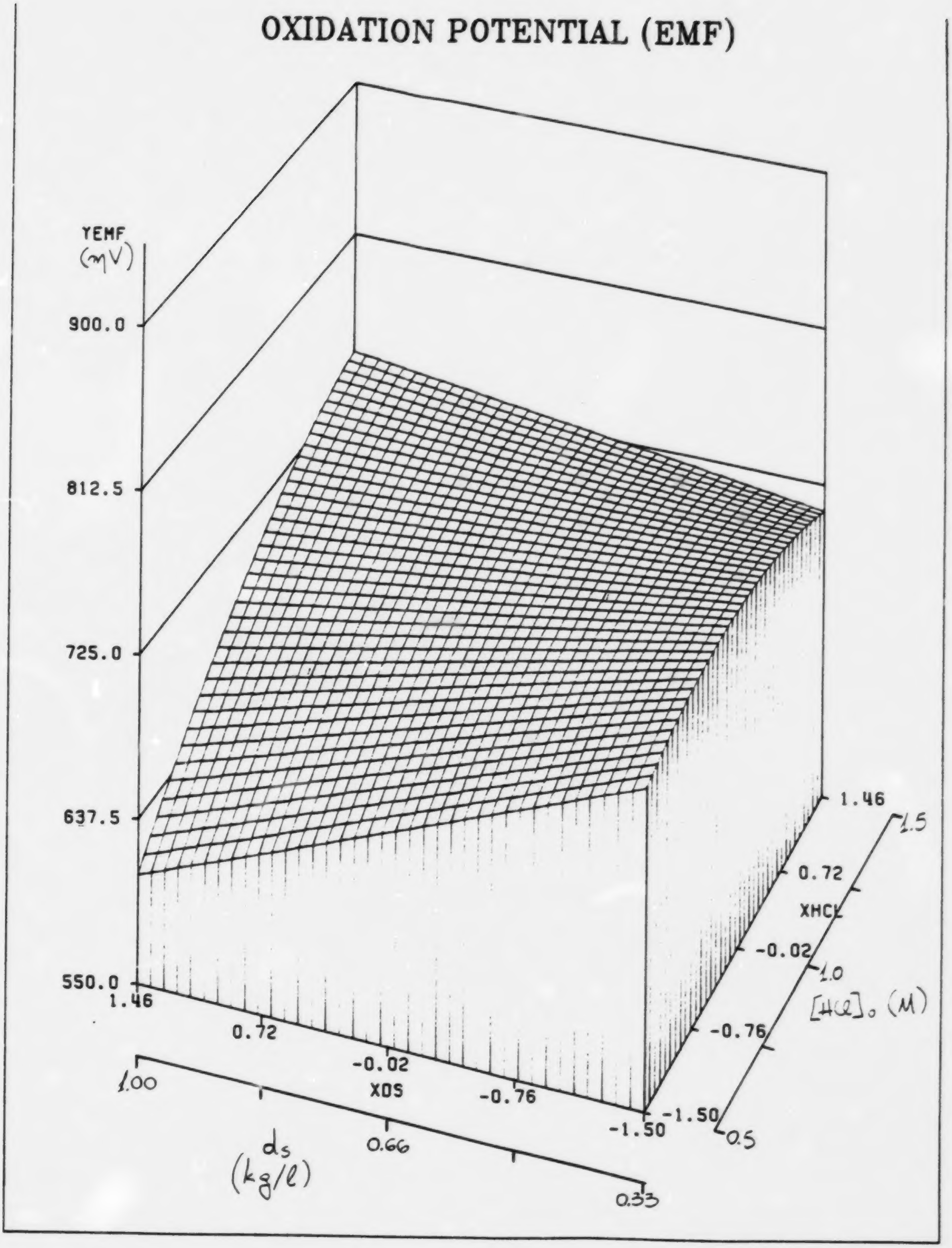

Fig. 75 Predicted EMF (vs SHE) response surface as a function of d_s and $|HCl|_o$; $|CaCl_2|_o$ = 1.5 M and T = 2 hrs.

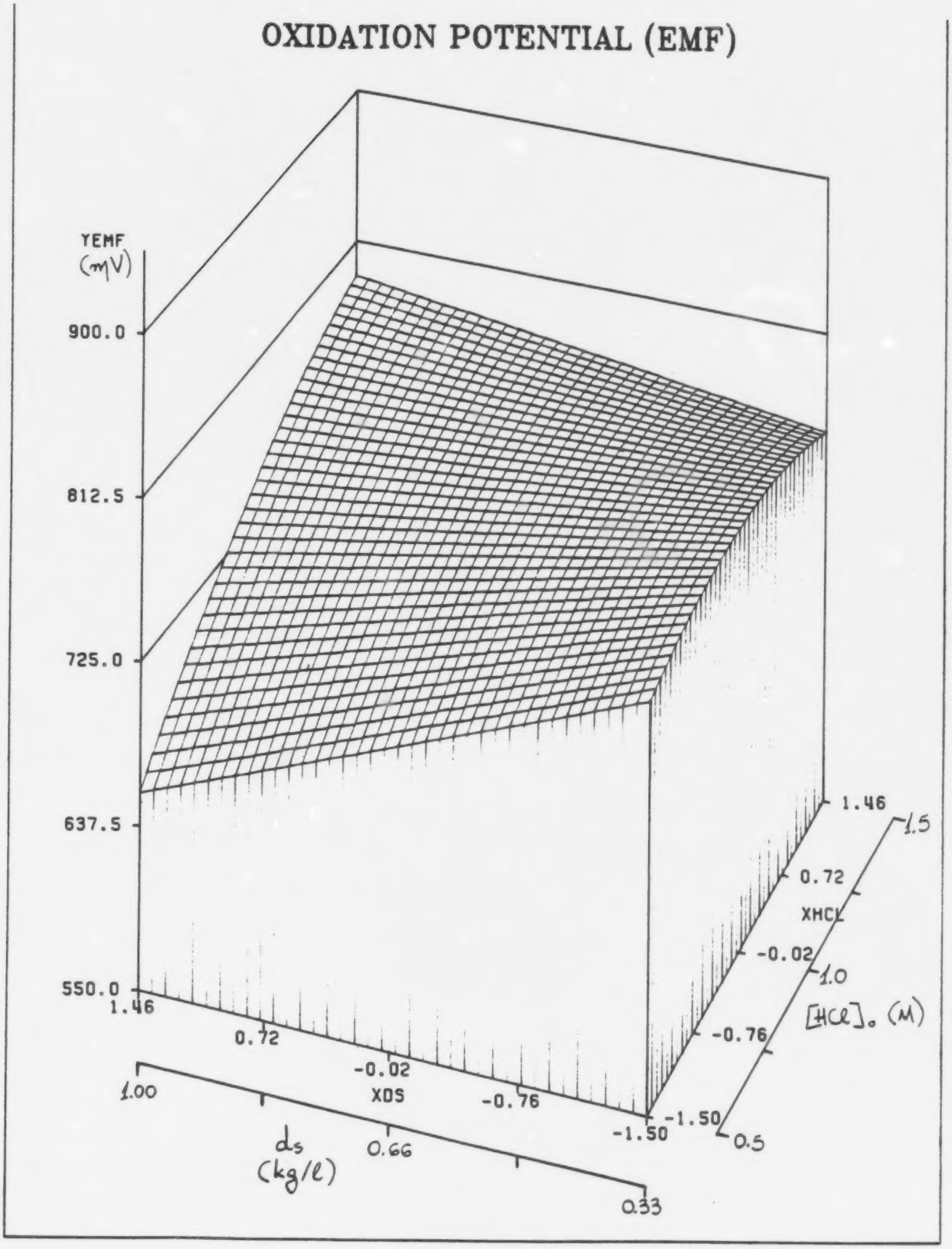

Fig. 76 Predicted EMF response surface as a function of d_s and $|HCl|_o$; $|CaCl_2|_o$ = 2.5 M and T = 2 hrs.

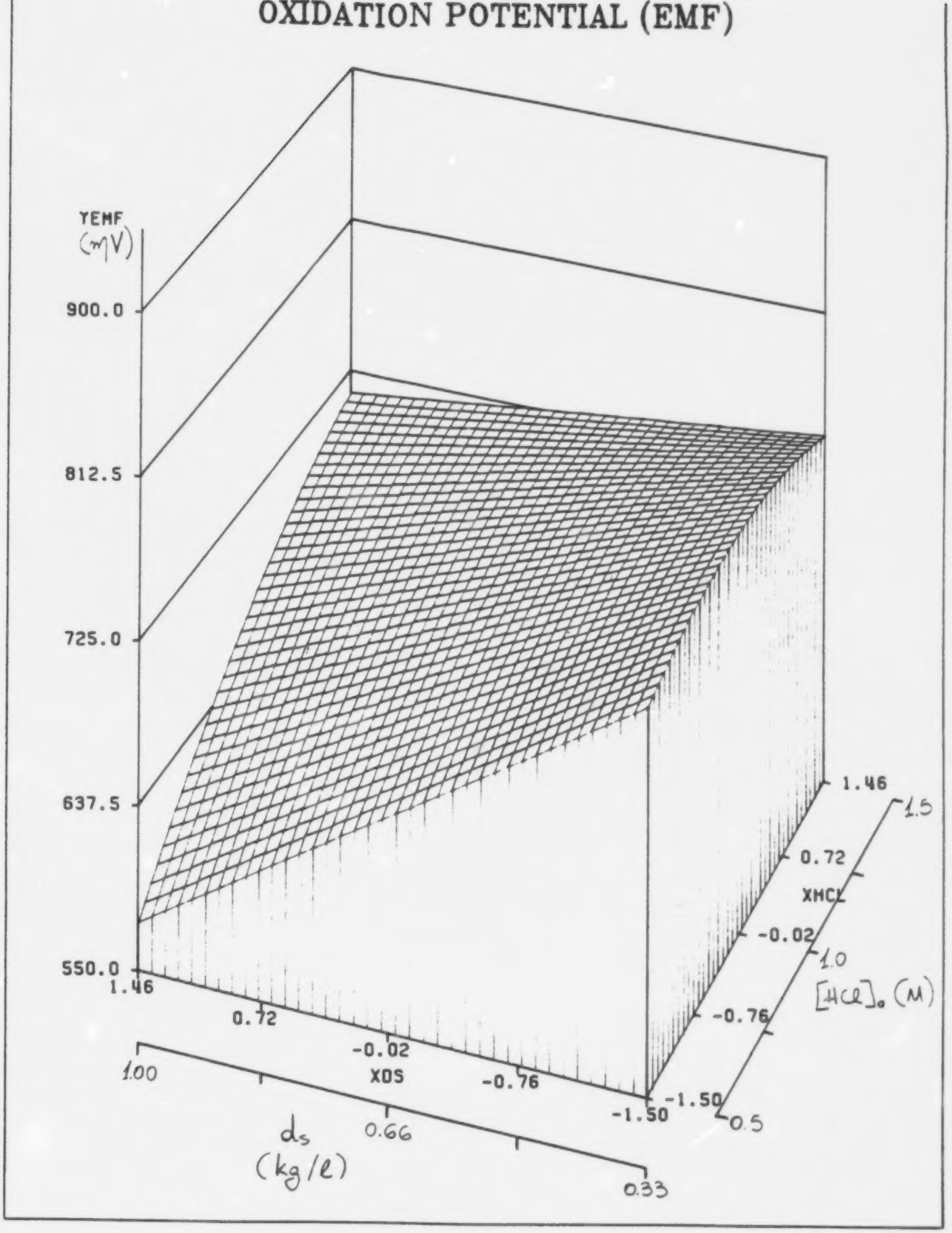

Fig. 77 Predicted EMF response surface as a function of d_s and $|HCl|_o$; $|CaCl_2|_o$ = 1.5 M and T = 6 hrs.

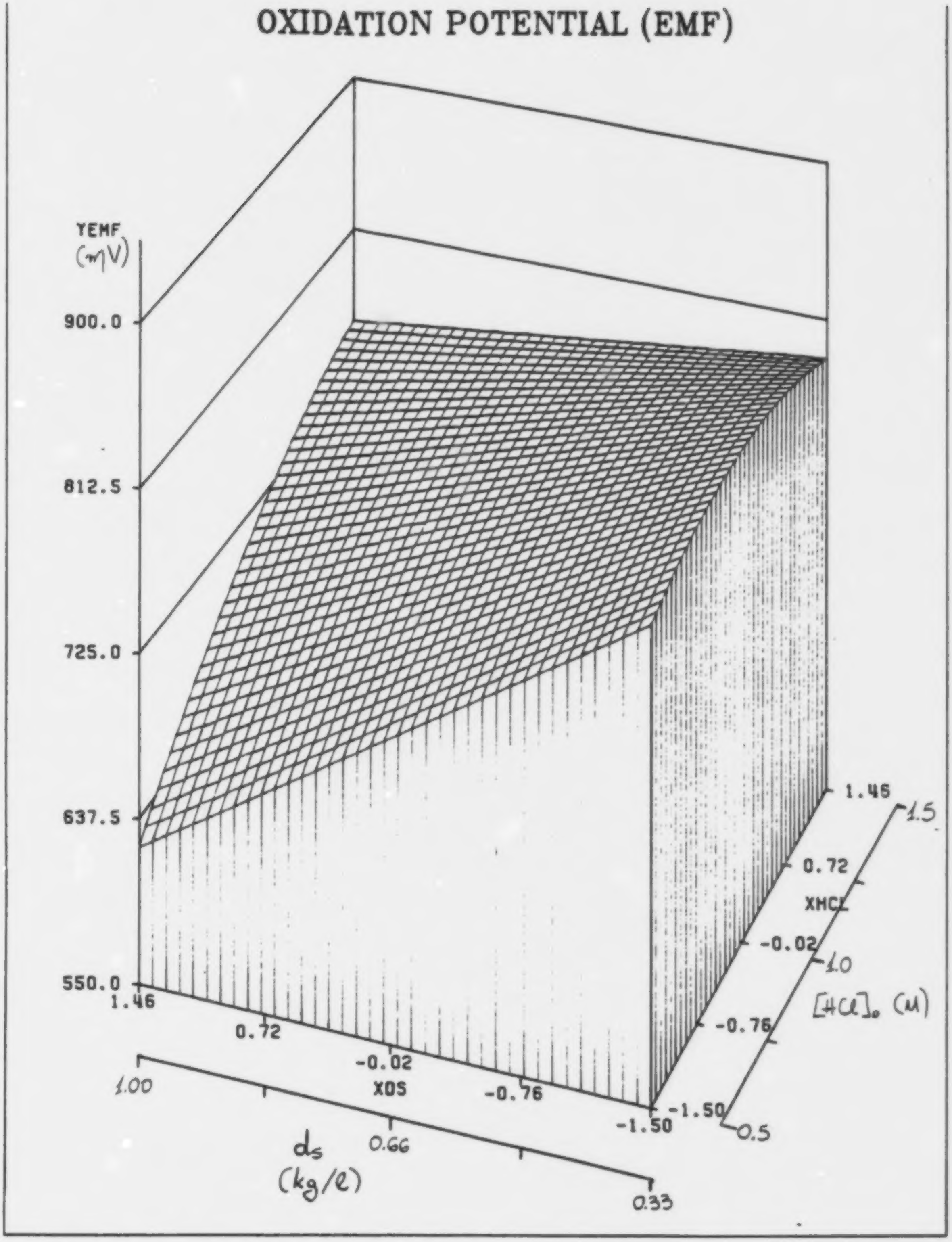

Fig. 78 Predicted EMF response surface as a function of d_s and $|HCl|_o$; $|CaCl_2|_o$ = 25 M and T = 6 hrs.

tion, etc.) do not allow a fundamental correlation between the slurry EMF and the various process parameters to be identified. It is exactly under these circumstances that statistical modelling is the best avenue to process optimization.

3.4.3.7 Optimum Leaching Conditions and Conceptual Flowsheet

The principal aim of the present work was to identify optimum leaching conditions for the simultaneous extraction of U and Ra from the Key Lake uranium ore. Possible maximization of nickel extraction under the same conditions would also be desired but not mandatory. It is implied that coextraction of U and Ra would have to be accomplished with the lowest possible reagent consumptions in terms of $CaCl_2$ and HCl - the latter being the most critical of the two. Thus using the data of Tables 19 to 23 the overall optimum leaching conditions were established to be those given in Table 24. Best results are obtained with 0.33 kg solids/lit slurry density, 1.0 N initial HCl if batch operation is used or alternatively controlling the HCl concentration at 0.9 M if continuous operation is adopted. $CaCl_2$ at 1.5 M concentration and 2 hrs retention time are indicated as the best levels for these two variables. For these conditions almost complete (100 % is predicted by the model; it is implied that in reality this would tend to be slightly lower i.e. > 99%) U and Ra extraction is obtained. Due to the "disequilibrium" phenomenon in Ra/U extraction discussed in previous papers (20)(22) the radium content in the final residues is expected to be slightly

Table 24 Overall optimum single-stage leaching conditions

d_s		$\lvert HCl \rvert_o$		$\lvert HCl \rvert_f$		$\lvert CaCl_2 \rvert_o$		Time	Extraction (%)				Consumption	
kg/1)	(wt %)*	(M)	kg/ton	(M)	kg/ton	(M)	kg/ton	(hr)	U	Ra	Ni	As	HCl (kg/ton)	Ca** (kg/ton)
0.33	25	1.0	110.6	0.89	98.8	1.5	504.5	2	100	100	64	58.3	11.8	~ 1.0
0.5	33	1.5	109.5	1.22	88.8	1.5	333	2	100	100	61	76.5	20.7	$\ll 3.0$

* assuming d_{saln} = 1 g/1, which is not true in the present work since a concentrated $CaCl_2$ medium is employed.

** Calcium consumption estimation is based on the assumption that 50% of the S content of the ore reports as SO_4^{2-} in the solution and that calcium is lost in the form of gypsum only.

higher than the amount expected from the secular equilibrium of U^{238} and Ra^{226}. Complete elimination (i.e. < 30 pCi/g Ra^{226} in residues) of radium could be brought upon by adding a second atmospheric leach stage using the same leaching medium in absence of oxygen overpressure. The effectiveness of this approach has been demonstrated previously in the case of the Midwest ore (22). Indicative data from that work is shown in Table 25. Nickel extraction under optimum U/Ra extraction conditions is only ~ 65%. Higher nickel extraction can only be achieved at prohibitively high reagent cost (HCl and $CaCl_2$) which will be difficult to justify. For these optimum conditions given above, acid consumption of about 12 kg/ton is expected while less tha 1 kg (Ca/ton) is expected to be consumed in the form of $CaSO_4$ precipitate. This amount of Ca will have to be replenished prior to recycling of the $CaCl_2$ medium. This can be done by adding CaO to the solution. In this way no significant build-up of Cl^- ions is expected to occur.

A simplified conceptual flowsheet incorporating pressure chloride leaching for the simultaneous extraction of U and Ra (and possibly Ni as byproduct) is shown in Fig. 79. The present work has established the best leaching conditions for single stage co-extraction of U and Ra. Depending on the specifications set for radium content in disposed solid residues, a second stage atmospheric leach using the same medium could be added as well (refer to data of Table 25). A critical aspect of the proposed flowsheet apart from the recovery stages which are investigated in house at CANMET is the removal of arsenic from the final leach solution (to avoid its build-up and thereby undesirable precipitation problems in the circuit) and its recycling back to the leaching operation. The first could be accomplished with the use of pressurized H_2S which would stabilize arsenic as As_2S_3 and the latter by evaporating the excess water which enters the circuit (from the comminution and solid washing operations) and replenishing the HCl and $CaCl_2$ losses. These two aspects of the flowsheet, that is As_2S_3 precipitation and $CaCl_2$/HCl recycling will have to be studied more thoroughly before a pilot plant is designed to test this new leaching approach.

Table 25 Second stage $CaCl_2$/HCl of Midwest ore pressure leach residues (23).

	First Stage Pressure Leach				Second Stage Atmospheric Leach		
Conditions:	70°C, 75 psi O_2, d_s=0.33 kg/l $\lvert HCl\rvert_o$=1 M $\lvert CaCl_2\rvert_o$=2M, 4 hrs				70°C, air, d_s=0.33 kg/l, $\lvert HCl\rvert_o$ = 1.0 M $\lvert CaCl_2\rvert_o$= 3.0 M, 4 hrs.		
Residue		Extraction		Residue		Overall Extraction	
U, wt.%,	Ra pCi/g	U (%)	Ra	U, wt.%,	Ra pCi/g	U (%)	Ra
0.016	111	99.2	98.3	0.004	21	99.8	99.7

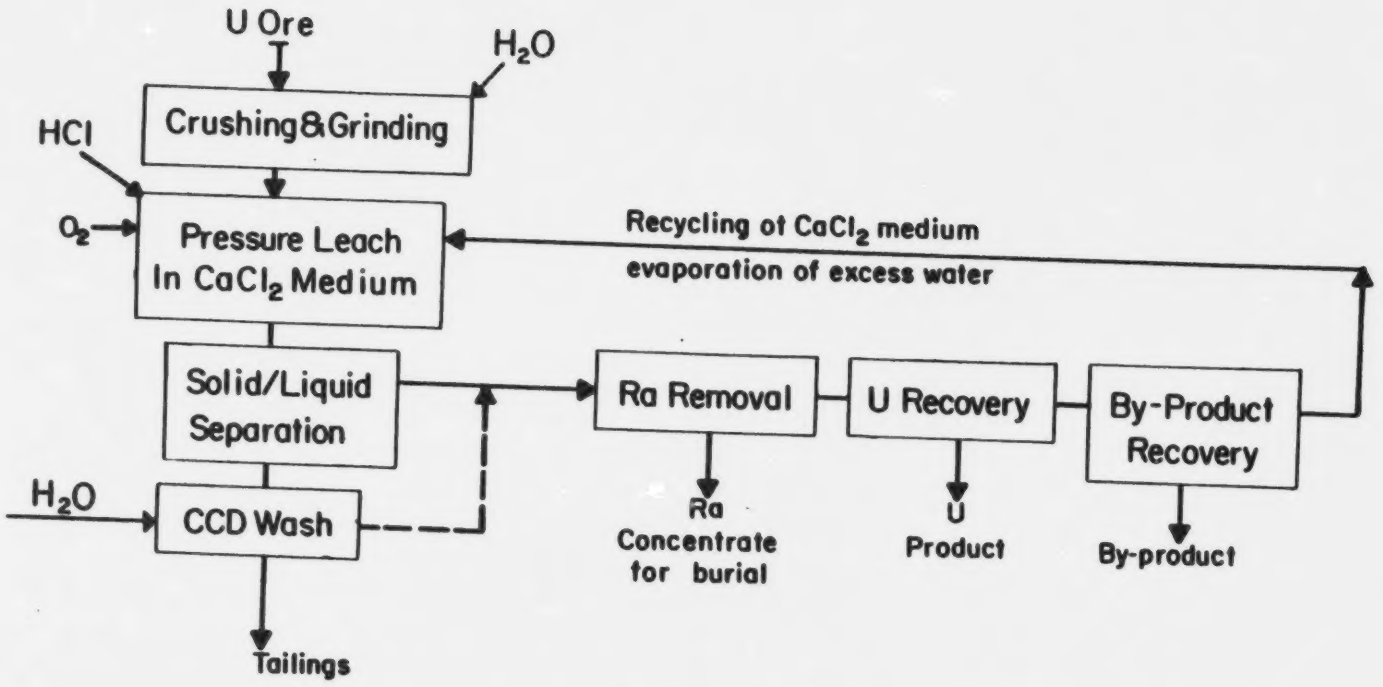
U Ore
H_2O
HCl
Crushing&Grinding
O_2
Pressure Leach In $CaCl_2$ Medium
Recycling of $CaCl_2$ medium
evaporation of excess water
Solid/Liquid Separation
Ra Removal
U Recovery
By-Product Recovery
H_2O
CCD Wash
Ra Concentrate for burial
U Product
By-product
Tailings

Fig. 79 A simplified flowsheet incorporating pressure chloride (O_2-$CaCl_2$-HCl) leaching for the co-extraction of uranium and radium from complex ores.

4. RADIUM EXTRACTION: THE ROLE OF CALCIUM CHLORIDE

4.1 Scope

In an earlier investigation involvilng pressure chloride leaching of Midwest ore samples (22) it was tentatively concluded that by adding $CaCl_2$ to the leach solution the limitations imposed by the solubility product of $RaSO_4$ are overcome and radium becomes significantly more soluble. This was attributed to the following triple action of $CaCl_2$: (i) by removing the excess SO_4^{2-} ions via $CaSO_4$ precipitation (ii) by decreasing the activity of SO_4^{2-} and (iii) by increasing the activity of HCl. Furthermore it was tentatively concluded that AsO_4^{3-} ions are not involved in removing Ra^{2+} from the solution via radium arsenate precipitation (either as $Ra_3(AsO_4)_2$ $RaHAsO_4$. Finally adsorption mechanisms were held responsible for the observed difficulty in removing residual trace amounts of radium (< 50 pci/g) from the ore solids. In other words it was tentatively assumed that solubility phenomena are mostly responsible for the increased extraction of radium in $CaCl_2$ brines.

We decided to test this hypothesis and determine quantitatively the solubility of $RaSO_4$ and divulge thus the true mechanism involved in radium extraction. To this end we have adopted a method developed by Meissner (53) which allows the estimation of the activities of the components of the leach solution which control the solubility of $RaSO_4$. The predicted solubility of $RaSO_4$ data are then compared with the actual extraction data obtained in the present work and discussed accordingly.

4.2 Estimation of the Solubility of $RaSO_4$

Predicting the solubilities of the various components in a concentrated aqueous system as the one employed in the present work requires information on the activity coefficient of each electrolyte. The Debye-Huquel equation (54) for estimating such activity coefficients unfortunately applies only to dilute solutions having concentrations far below those encountered in the present sytem. In the last decade, however, several significant advances have been made in the estimation of activity coefficients in concentrated aqueous solutions of interest to hydrometallurgists (55). Among these methods the "reduced activity coefficient" approach introduced by Meissner (53) has been used here to predict the solubility of $RaSO_4$. This method along with the algorith developed for the prediction of the solubility of $RaSO_4$ are described in Appendix 6.2.

Before the developed mathematical model (= algorithm)is used for the prediction of the solubility of $RaSO_4$ it is mandatory to check the validity of its prediction power for a well known system. As such, the solubility of gypsum in NaCl solutions was chosen. The obtained results are plotted in Fig. 80. Here the continuous line (—— x ——) represents the model predictions while the points (o and ●) represent experimental data

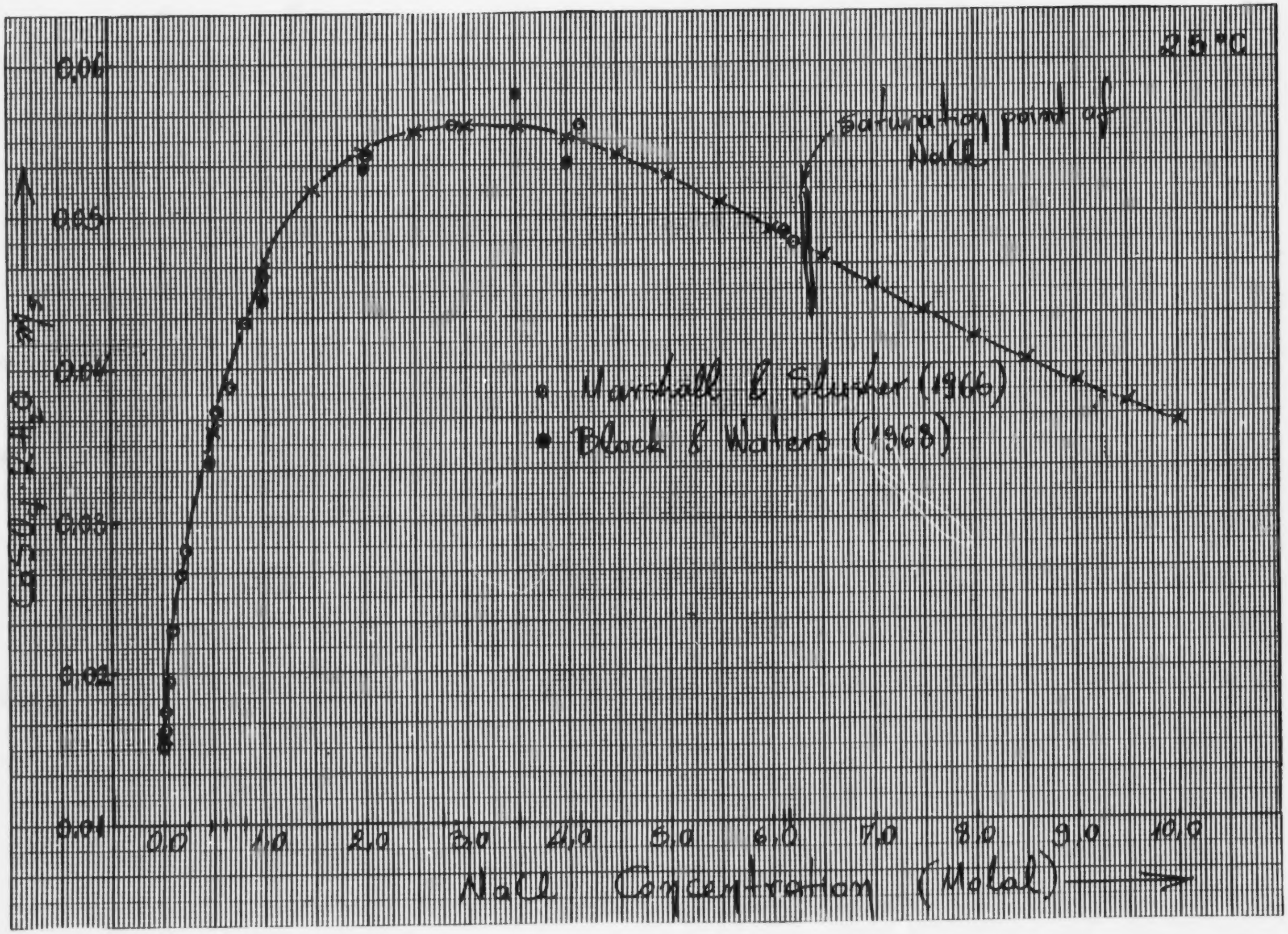

Fig. 80 Comparison of predicted and experimentally determined solubility of $CaSO_4.2H_2O$ in NaCl solutions.

published previously in the literature (56 ,57). As can be seen excellent predictions are made which confirm the validity of the assumptions and equations used to develop the present algorithm (Appendix 6.2).

Using the said algorithm the solubility of Ra^{2+} in a 1.0 M HCl solution as a function of the initial SO_4^{2-} concentration was established first (Fig. 81). It is obvious that increasing SO_4^{2-} concentrations, Ra^{2+} solubility dramatically decreases as it would be expected. No $CaCl_2$ is present in these simulation runs.

The addition of $CaCl_2$ in the solution has a very significant effect in Ra^{2+} solubility, as is shown in Fig. 82. There is about one order of magnitude increase in solubility, and it is due to the combined effec of an increase in the ionic strength and, the formation of gypsum ($CaSO_4.2H_2O$). The formation of gypsum results in the removal of most of the SO_42- ions from the solution, which allows more Ra^{2+} ions to remain soluble. As is seen in the same graph HCl does not have any significant effect on Ra^{2+} solubility in the range 0.5 to 1.5 N conc. The data of Fig. 82 were obtained for free SO_4^{2-} concentration determined by the solubility product of gypsum ($CaSO_4.2H_2O$) and 25°C temperature. The initial SO_4^{2-} concentration level (i.e. indirectly the S content of the ore) affects the solubility of $RaSO_4$ only in the absence of $CaCl_2$. This is better illustrated with the results - model predictions - plotted in Fig. 83. Two initial SO_4^{2-} concentrations namely 0.05 M and 0.3 M were tested.

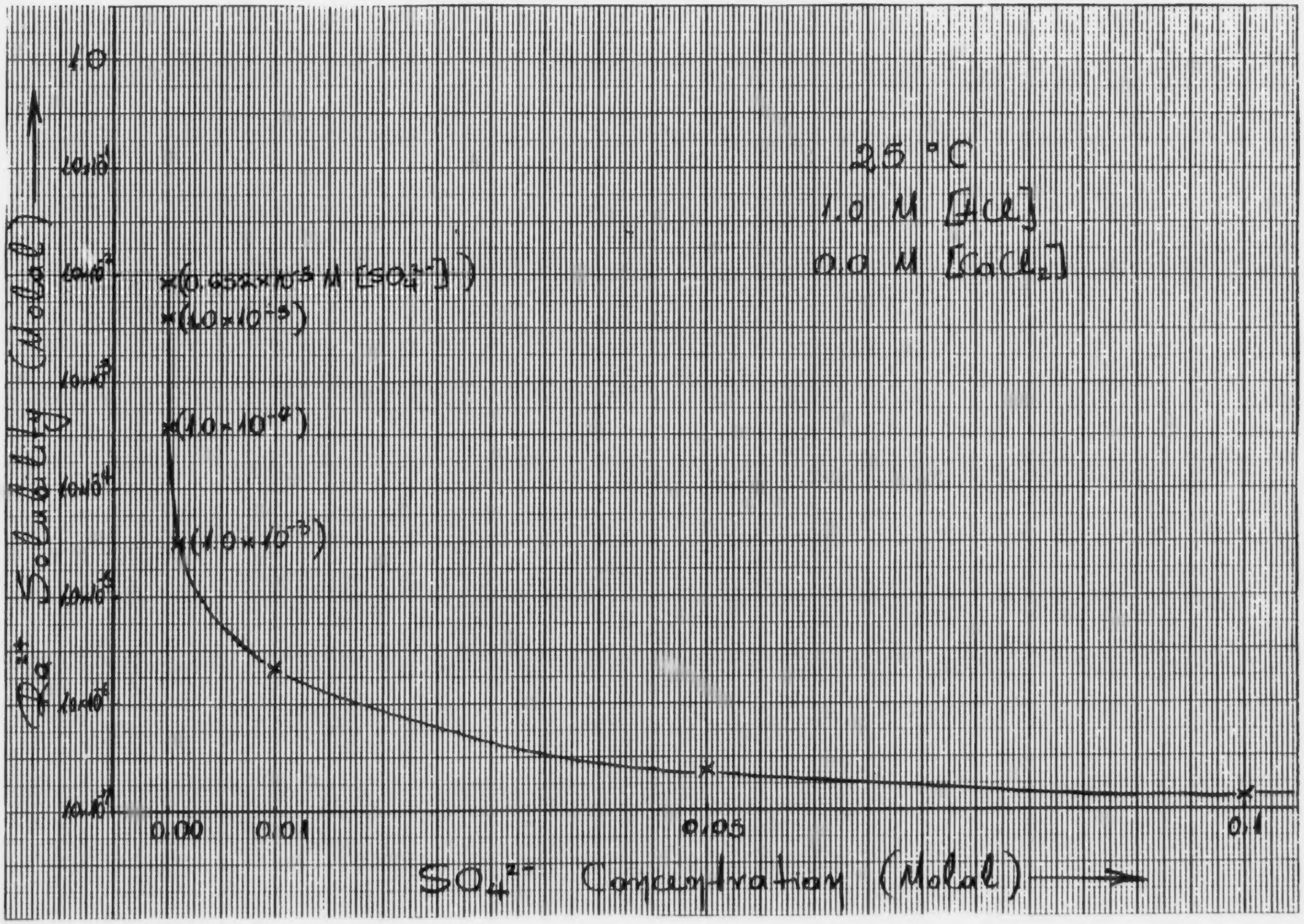

Fig. 81 Estimation of Ra^{2+} solubility in 1 molar HCl solution as a function of free SO_4^{2-} concentration.

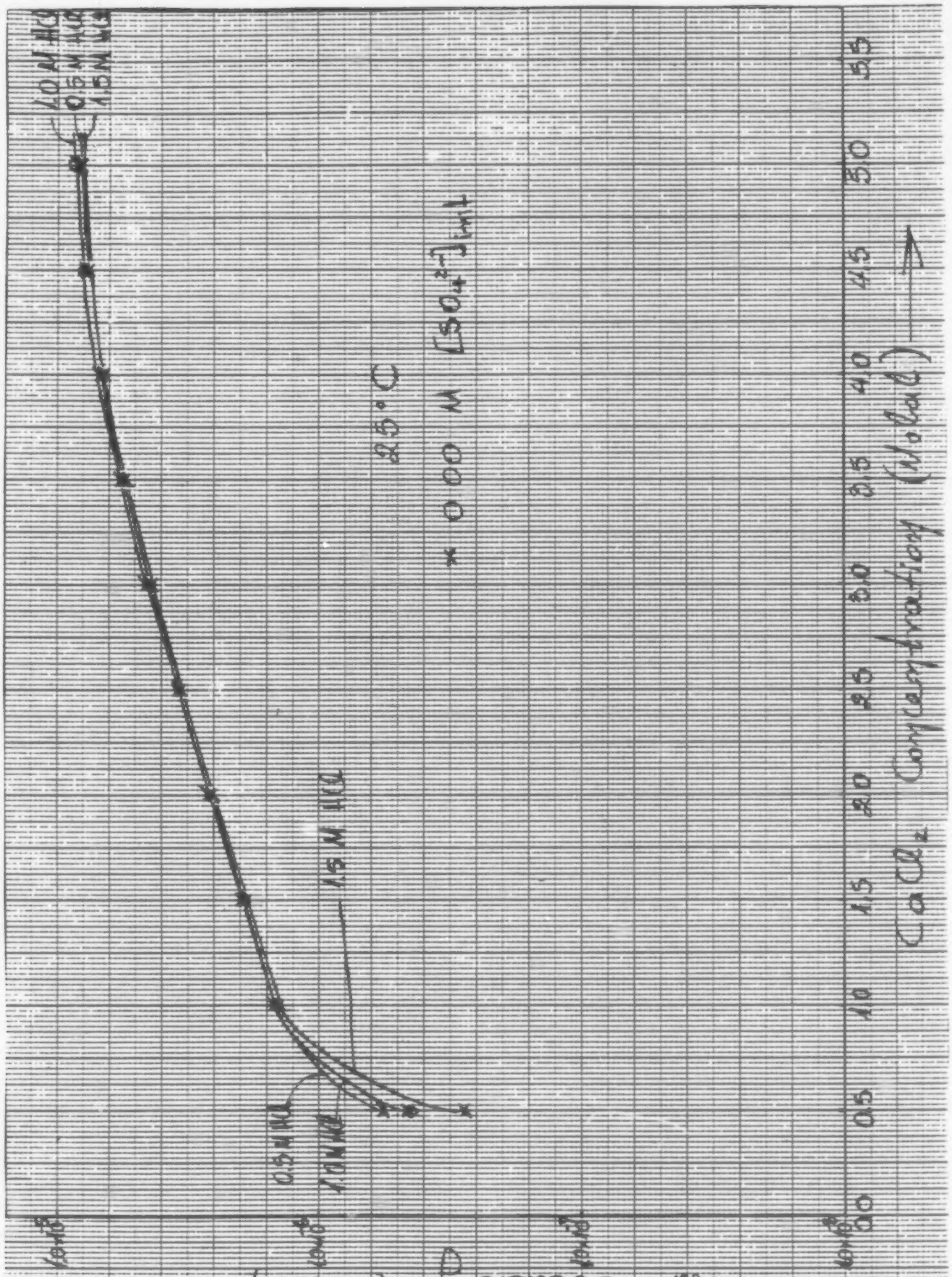

Fig. 82 Estimation of Ra^{2+} solubility in $CaCl_2$/HCl media.

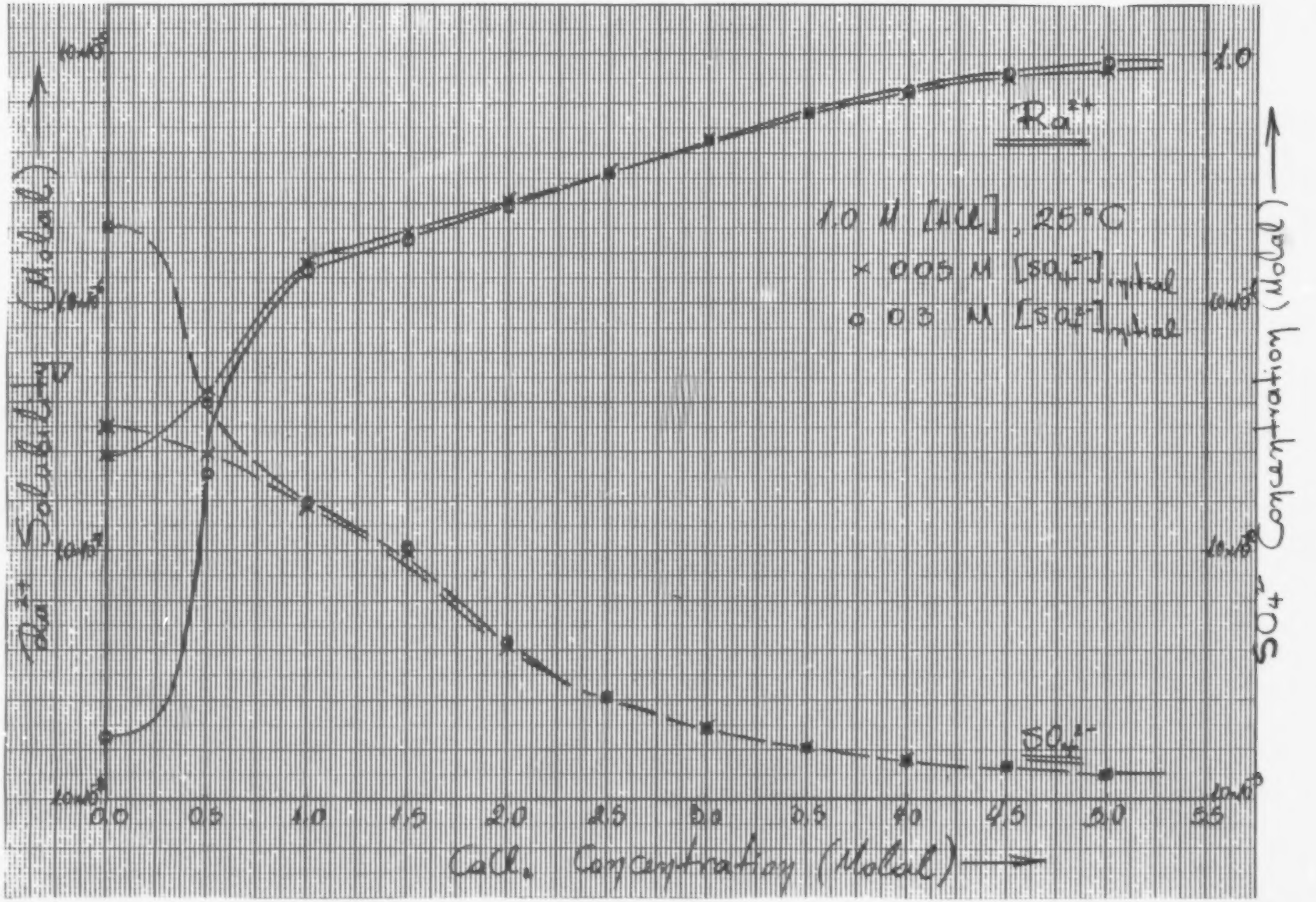

Fig. 8 3 Estimation of Ra^{2+} solubility and $SO_4{}^{2-}$ concentration in $CaCl_2/HCl$ media.

It can be seen that for a $CaCl_2$ conc. > 1.0 M practically the same Ra^{2+} solubility is estimated since the free SO_4^{2-} conc. is determined by the solubility of gypsum. The model was used further to establish the solubility of Ra^{2+} at higher temperatures (100° C) and other leaching media, i.e. NaCl/HCl and KCl/HCl. The obtained results are plotted in Fig. 84. From these data it can be seen that temperature does not have any measurable effect on the solubility of Ra^{2+} in $CaCl_2$/HCl media. On the other hand, the predicted solubility of Ra^{2+} in monochloride salt media is far less than that in the $CaCl_2$/HCl medium used in the present work. Apparently the formation of gypsum in the latter medium ties up the free SO_4^{2-} and this greatly enhances the solubility of Ra^{2+}, while in the case of NaCl and KCl-based media only marginal improvement is obtained via the ionic strength effect on the activity of Ra^{2+}. These calculations have not considered the possibility of jarosite formation with the monovalent cations which could lead to SO_4^{2-} removal as well and thus higher Ra2+ solubility.

4.3 The Role of $CaCl_2$

Assuming that all the sulphur content of the K.L. ore will report upon leaching in the solution then the maximum SO_4^{2-} would be 0.3 M. For that amount of SO_4^{2-} the maximum solubility of Ra^{2+} was estimated and the data are plotted in Fig. 85. In the same Figure apart from the predicted solubility data, actual radium extraction values are shown as well. These extraction values were obtained under average experimental conditions (i.e.

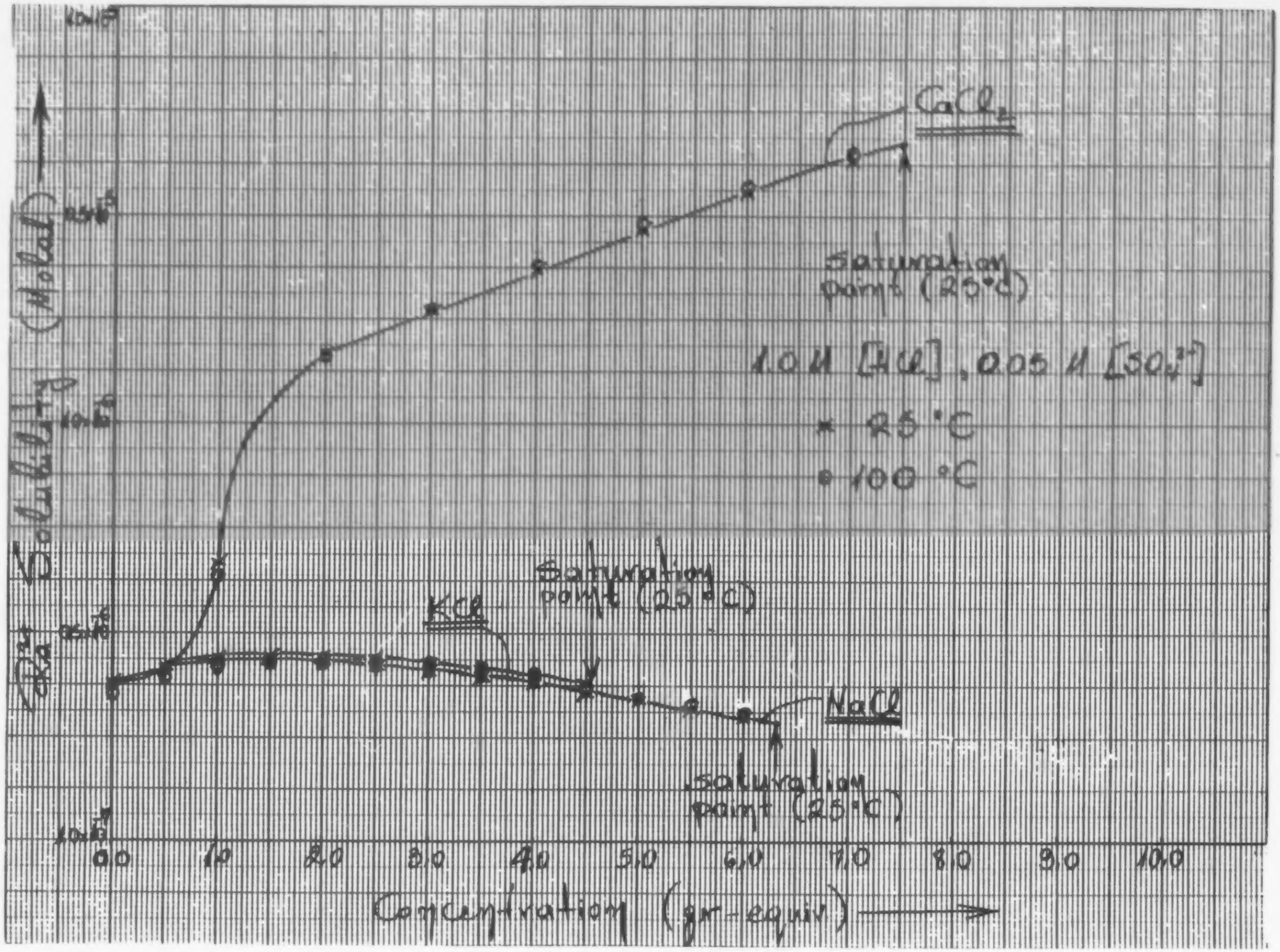

Fig. 84 Estimation of Ra^{2+} solubility in $CaCl_2$/HCl, NaCl/HCl, and KCl/HCl media at 25° and 100°C.

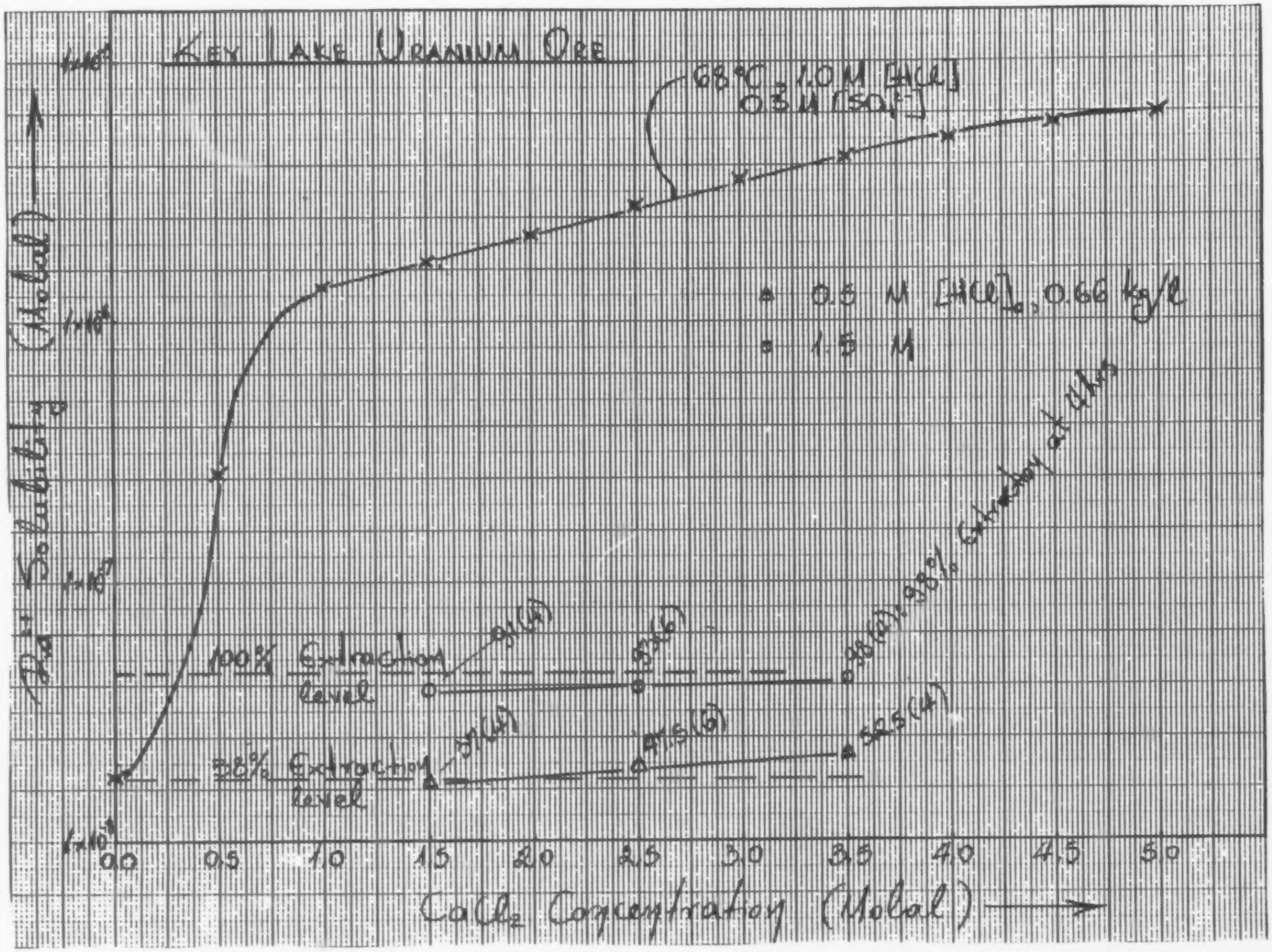

Fig. 85 Observed and estimated solubilities of Ra^{2+} in the Key Lake ore pressure leach solution.

68°C, 0.66 Kg/l slurry density, 4 - 6 hours retention time). On the same graph the maximum levels of radium extraction for the given ore composition (Ra and S content) and experimental conditions are indicated. It is seen from these data that the use of the $CaCl_2$ medium allows an ample solubility window to open which allows complete radium extraction from the Key Lake U ore, provided of course that all radium is effectively liberated and leached from the host mineral structure and no other mechanisms apart from solubility of $RaSO_4$ operate. However there is not a perfect matching of U and Ra extraction as the results of Table 26 show. This indicates that apart from the precipitation of $RaSO_4$, supplementary mechanisms result in further removal of Ra^{2+} from the leach solution. These mechanisms could be: (i) the precipitation of Ra^{2+} as $RaHAsO_4$ or $Ra_3(AsO_4)_2$ (ii) the coprecipitation of Ra^{2+} along with gypsum and (iii) the adsorption of Ra^{2+} by surface active solid components of the leach residue.

Mechanism (i): Solubility data on radium arsenate are not available in the literature but its behaviour can be inferred from that of barium arsenate instead. Both radium and barium have divalent cations and similar ionic radii, 1.57 Å and 1.42 Å respectively (58) and hence their solubility characteristics should be similar. The solubility of Barium arsenate has been studied by Robins (59). Assuming that all the arsenic content (1.4 wt.%) of the ore goes into solution as As(V) then the maximum arsenic concentration (for 1 kg/l slurry density) will be

Table 26 Mismatch of U and Ra extraction

	Experimental Conditions				Extraction	
Test	d_s(kg/l)	$\|HCl\|_o$(M)	$\|CaCl_2\|_o$	Time (h)	U %	Ra
15	0.66	0.5	1.5	4	46.0	37.1
10	0.66	0.5	2.5	6	71.0	47.2
4	0.66	0.5	3.5	4	53.4	52.5
8	0.66	1.5	1.5	4	99.2	91.0
26	0.66	1.5	2.5	6	99.1	91.2
23	0.66	1.5	3.5	4	99.1	98.2

0.19 M or log $[As^{5+}] = -0.7$. For this As(V) concentration and pH < 2 barium arsenate is highly soluble (59). It is implied therefore that no radium arsenate precipitation is responsible for the observed discrepancy in radium-uranium extraction. Furthermore no calcium arsenate precipitation is possible under the same conditions (59) which confirm the assumption made earlier (Table 24) that calcium losses are associated with gypsum formation only.

Mechanism (ii): Coprecipitation of radium along with gypsum is not expected to play a role in removing radium from the leach solution since $CaSO_4$ is known not to be a good radium carrier (60).

Mechanism (iii): Adsorption of Ra^{2+} by active solid components present in the leach residue appears to be an important mechanism of radium removal from the leach solution. Radium is known to adsorb on various solid materials (61) even on glass and other container walls (62). Description of already adsorbed Ra prior to leaching or suppression of adsorption during leaching can be affected by using strong acidic conditions (61). As a matter of fact the great effect HCl has on Ra extraction (Fig. 38) can be partly explained in the grounds of this phenomenon. (HCl is needed of course for U leaching and thereby radium liberation as well). $CaCl_2$ appears to act in two ways in suppressing radium adsorption: (1) by ion-exchange reactions similar to the one outlined below:

$$CaCl_2 + Ra - clay_{solid} \rightarrow Ca\text{-}clay_{solid} + RaCl_2 \qquad (28)$$

(2) by increasing the activity of HCl and thereby suppressing the adsorption process.

The dramatic effect of $CaCl_2$ on increasing the activity of HCl is exemplified with the data of Fig. 86 (52).

It can be therefore concluded that by conducting the leaching of the Key Lake U ore in concentrated $CaCl_2$ solutions the solubility of $RaSO_4$ increases several times and thus high Ra extraction levels are obtained. Additionally high acid activity levels are obtained in the mixed $CaCl_2$/HCl medium which further improve Ra extraction by suppressing the adsorption of Ra^{2+} by solid components of the leach residue. The theoretically predicted solubility of $RaSO_4$ in other brine solutions shows that NaCl/HCl or KCl/HCl are not equally effective media to render radium soluble.

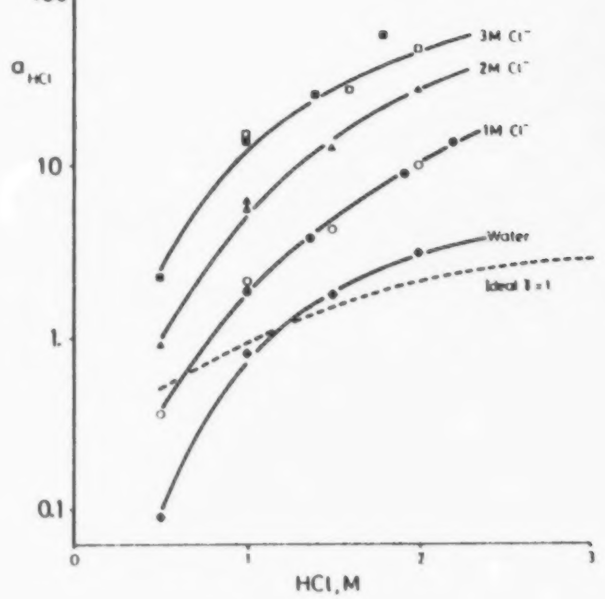

Fig. 86 Effect of added Cl^- on the activity of HCl (o Δ □ added as NaCl; ● ▲ ■ added as $CaCl_2$) (from ref. 51).

5. CONCLUSIONS-RECOMMENDATIONS

The present study has allowed a number of conclusions to be drawn concerning the technical feasibility of coextraction of U and Ra from the high grade arseniferous U ores of N. Saskatchewan by pressure chloride leaching. In addition to those some conclusions of broader significance are drawn as well. Finally recommendations are made for further developmental work on this novel O_2-$CaCl_2$-HCl leaching system.

5.1 Conclusions

1. The oxidative leaching chemistry of NiAs, $NiAs_2$ and NiAsS - the major arsenic carriers in the high grade ores of N. Saskatchewan - is very complex. The results of the present study show that As(III)/As(V) formation is independent of the redox solution potential which in turn makes unfeasible the possible stabilization of As(III) via potential control, as a means of avoiding the troublesome As(V) compound precipitation problem occurring during leaching.

2. The results of the study on leaching chemistry of arsenic (Chapter 2) helped to interpret the arsenic speciation picture observed in the present pressure chloride system ($\sim$20% As(III) as well as that of the current Key Lake Mill circuit (50% As(III) in primary (Fe^{3+}) leach and 33% As(III) in secondary (O_2-H_2SO_4) leach)..

3. The pressure chloride leaching of the Key Lake ore is highly exothermic and proper reactor design is needed.

4. The ore is more reactive in the chloride medium than in the conventional sulphate medium. Its reactivity increases with the addition of $CaCl_2$.

5. The present system, due to its complex leaching rection behaviour (several ore components reacting via sequential and parallel reactions) does not render itself to fundamental reaction analysis and optimization. It was due to this fact that a computer-aided statistical methodology was employed as an experimental strategy.

6. The employed statistical design (BOX-BEHNKEN) has allowed us to develop model equations simulating the leaching response of the ore in the following process region: $0.33\ kg/l \leqslant d_s \leqslant 1.0\ kg/l$; $0.5\ N \leqslant [HCl]_o \leqslant 1.5\ N$; $1.5\ M \leqslant [CaCl_2]_o \leqslant 3.5\ M$ and $2\ hrs \leqslant Time \leqslant 6\ hrs$. Temperature and oxygen pressure were kept constant throughout this experimental programme at 68^oC and 75 psi respectively.

7. Uranium and Radium were found to dissolve simultaneously and rapidly (99% extraction in 2 hrs) provided that the solution conditions prevent their re-precipitation.

8. Nickel dissolution (maximum extraction 70%) was found to be relatively slow this being attributed to the refractory nature of gersdorffite (NiAsS) and millerite (NiS) - the major nickel carriers in the ore

9. Due to their different leaching mechanisms U/Ra vs Ni, maximization of the simultaneous extraction of the three elements is not feasible. The latter could by only achieved at the cost of extremely high acid consumptions and long reaction times which cannot be justified.

10. Optimization of the obtained results with the aid of computer generated 3-D graphs identified the following batch leach conditions offering almost complete coextraction (> 99%) of U and Ra: 0.33 kg ore/1 (or ∿ 25% solids), $[HCl]_o$ = 1.0 M (or 110 kg HCl/ton ore); $[CaCl_2]_o$ = 1.5 M (or 500 kg $CaCl_2$/ton ore) and 2 hours retention time. Simultaneously the extraction levels of Ni and As obtained were respectively 64% and 58%. For the same conditions the following reagent consumption values were estimated: 12 kg HCl/ton ore and 1.4 kg CaO/ton ore. For continuous operation the steady state [HCl] concentration needed is 0.9 M (or 100 kg HCl/ton ore) for the same otherwise conditions and performance.

11. The solubility of $RaSO_4$ has been estimated using the "reduced activity coefficient" method and the role of calcium chloride in enhancing radium extraction has been

quantified. It has been shown that radium arsenate precipitation does not occur under most of the experimental conditions. Adsorption phenomena though limit the extraction of residual trace amounts of radium from the leach solids ("disequilibrium" phenomenon). Monochloride salts (i.e. NaCl and KCl) have been shown not to be equally effective in solubilizing radium.

12. Recycling of the leach medium ($HCl/CaCl_2$) is considered mandatory for both economic and ecological reasons.

5.2 Recommendations

1. The aspects of arsenic removal by H_2S precipitation and recycling of the $HCl/CaCl_2$ medium will have to be addressed before a pilot-plant is designed and operated based on the present leaching approach.

2. The impact of $CaCl_2$ on the downstream solution purification operations (ion exchange removal of radium; solvent extraction of uranium and possibly nickel; yellowcake precipitation) should also be assessed.

3. The O_2-$CaCl_2$-HCl leaching system possesses excellent chemical properties that can be proven very useful in the treatment of a number of other primary and secondary materials, such as (i) auriferous refractory pyritic

concentrates (63), (ii) arsenical sulphide concentrates (64), and (iii) hot acid leach zinc residues (65).

4. The statistical modelling with the aid of response surface methodology is a powerful tool in leaching experimentation and its use should be encouraged.

6. APPENDICES

6.1 Innovations in Chemical Analysis

During the course of this work a number of chemical analysis difficulties were encountered and methods described in literature had to be modified and tested before they were applied for quantitative analysis of the produced liquors. Pertinent information of the method used to determine As(III) and HCl concentrations in the leach solutions are described below.

6.1.1 Determination of Arsenic (III)

The method consists of two steps: step (i) separation of As(III) and As(V) species from the metal cations with the aid of a cation exchange resin. This is needed to be done prior to titration in order to avoid interferences by the presence of other oxidizable species in the liquor, such as Fe^{2+}.
(ii) Titration of the purified liquor with potassium bromate to determilne directly As(III). This method was adopted from analytical procedures published elsewhere (66,67,68).

Ion Exchange Separation

A strong cation exchange resin (available as Dowex 50W-X8) of acid form was used to retain the metal cations. The IX column was prepared by contacting 10 g of the resin with water for 1 - 2 hours and then transfering this medium to a 50 ml ordinary bruette having a bed of glass wool at the bottom. The column was washed with 350 ml of 2 N HCl and then with 200 ml of distilled water. The liquid was never allowed to fall below the upper end of the resin bed.

The liquor sample for analysis did not contain more than 100 mg total metal content (i.e. As(III) + As(V) + Fe(II) + Fe(III) + ...) The volume of the liquor sample was adjusted to 40 ml and its acidity level approximately at 0.3 N HCl. The solution was let to percolate through the IX column and then the column was washed first with 20 ml of 0.1 N HCl and then with 400 ml of the same. The combined solution was subsequently used for titration of As(III) with $KBrO_3$. The rate of percolation was kept between 5 - 10 ml/min. Finally the resin was regenerated (prepared) for another analysis by percolating through the column 350 ml of 2 N HCl, followed by 200 ml of distilled water.

Titration

The obtained solution after IX separation of the interfering metal cations was acidified with HCl to 2 - 4 N level. Then 3 drops of 0.1% aqueous methyl orange indicator was added. Titration was done with a 0.01 N $KBrO_3$ solution until the end point was reached - colorless solution.

The method was successfully tested using synthetic solutions of known As(III)/As(V)/Fe(II)/Fe(III) compositions prior to its applications to the leach solutions of the present work.

6.1.2 Free Acid Determination

Free acid titration with NaOH in actual U chloride leaching solutions is complicated by the presence of $CaCl_2$ on one hand and several metals originating from the ore dissolution (such as Fe, Mg, Ni, Al etc.) on the other. The former affects the end point of the titration curve since it increases considerably the activity of HCl (see Fig. 86) while the latter undergo hydrolysis upon neutralization thus generating additional protons which interfere with the determination of free acid. Rolia and Dutrizac (69) have dealt with the problem of acid determination as this is related to zinc processing solutions. Salts of EDTA were proposed by these investigators to overcome the hydrolusis problem. This method was also adopted here after certain modifications to accomodate the change of the end-point due to the presence of $CaCl_2$. The procedure eventually adopted is described below.

Procedure

(i) Blank solution testing: A quantity of 2 moles Na_2 EDTA/mole metal was added in a beaker containing 100 ml distilled water. Titration of this solution followed with 0.1 N NaOH till a pH ~ 6.3 (potentiometrically monitored). Then the corresponding to the specific leach solution under analysis, molarity of $CaCl_2.2H_2O$ was added and titration was repeated again till pH ~ 6.3.

(ii) Free acid determination: A quantity of 2 moles Na_2 EDTA/mole metal was added in a beaker containing 100 ml distilled water. This solution was titrated with a 0.1 N NaOH standardized solution till pH = 6.3. Then, 1 mol of the pregnant solution was added and the solution was titrated again till pH = 6.3. This measurement was corrected for the blank solution reading in order to determilne the actual free acid concentration in the leach solution.

6.2 The "Reduced Activity" Method (53)

General

The method is based on predicting at any concentration, the mean ionic-activity coefficient of an electrolyte, ij, which for a single electrolyte solution, is written as γ^{o}_{ij}. At any constant temperature, the term $(\gamma^{o}_{ij})^{1/zizj}$, plotted against the total ionic strength, I_T, forms a curve which generally falls quite well into a curve family (zi, zj are the valencies of the cation and anion of the electrolyte respectively). Concentrations are expressed both in molalities and in ionic strength units, related as follows for ions:

$$I_i = 1/2\ m_i\ z_i^2 \qquad (29)$$
$$I_j = 1/2\ m_j\ z_j^2$$

The total ionic strength of solutions is defined as I_T, where

$$I_T = 1/2\ m_i z_i^2 \qquad (30)$$

where m_i is the molality of the designated ion, and z_i is its charge.

Defining $(\gamma^{\circ}_{ij})^{1/z_i z_j}$ as Γ°_{ij}, the reduced activity coefficient, an analytical expression for these curves is found to be:

$$\Gamma^{\circ}_{ij} = [1 + B(1 + 0.1\ I)^{q^{\circ}_{ij}} - B]\ \Gamma^{*}_{ij} \qquad (31)$$

where

$B = 0.75 - 0.065\ q_{ij}^{\circ}$

$\log_{10} \Gamma_{ij}^{*} = -0.5107\ \sqrt{I}/(1 + C\ \sqrt{I})$

$C = 1 + 0.055\ q_{ij}^{\circ} \exp(-0.023\ I^3)$

By inspection, Γ°_{ij} is a unique function of I and of a characteristic constant q_{ij}° for each dissolved electrolyte. Values of q_{ij}° calculated from experimental γ°_{ij} data, for electrolytes in pure solution at 25°C, available in the literature for 120 different strong electrolytes have been compiled (70). Existing methods of determining q°_{ij} involve use of solution vapour pressures (71), solubilities in mixed solutions, or published estimation methods (72). Meissner's estimation method is applicable to a number of electrolytes in predicting γ_{ij}^{c} at an ionic strength of 2, from which the q_{ij}° can be calculated, using equation 31.

Suitable q_{ij}° values for use in equation (31) at temperatures other than 25°C are estimated using the following formula (53,73)

$$q_{ij}^{\circ},T = q_{ij}^{\circ},25^{\circ}C\,[1-0.0027\,(T-25)/(z_i z_j)] \qquad (32)$$

where T is in °C. Equation 32 is an empirical equation, following the observation that the isotherms of all electrolytes at any temperature between 25°C and 120°C fall into the same curve family (53), and so conform to equation 31. However, an electrolyte's isotherm generally shifts somewhat in position as temperature changes, and this is accomodated by equation 32.

The activity of water ($a_w = p/p^{\circ}$) over pure solutions can be directly evaluated from equation 31 in conjunction with the Gibbs-Duhem equation, written for convenience in integrated form as:

$$\log_{10}(a_w^{\circ})_{z_i z_j} = -0.0156\, I_{ij}/z_i z_j - 0.036 \int_{1.0}^{\Gamma_{ij}} I_{ij}^{\circ}\, d\log_{10}\Gamma_{ij}^{\circ} \qquad (33)$$

Furthermore, in developing the integral:

$$\int_{1.0}^{\Gamma_{ij}} I_{ij}^{\circ}\, d\log_{10}\Gamma_{ij}^{\circ} = \int_{1.0}^{\Gamma_{ij}} I_{ij}^{\circ} \log_{10}(e)\, 1/\Gamma_{ij}^{\circ}\, d\Gamma_{ij}^{\circ} \qquad (34)$$

By using equation 31, the result is:

$$d\Gamma_{ij}^{o} = \Big(\big((1-B)\, 10^{\frac{D\sqrt{I}}{1+(1+Ee^{FI^3})\sqrt{I}}} \ln 10 \, \frac{\frac{1}{2} D I^{-1/2} - 3DEFI^3 e^{FI^3}}{(1+(1+Ee^{FI^3})\sqrt{I}} + {}$$

$$+ E(1+0.1I)^{q}\, 10^{\frac{D\sqrt{I}}{1+(1+E e^{FI^3})\sqrt{I}}} \ln 10 \, \frac{\frac{1}{2} D I^{-1/2} - 3DEFI^3 e^{FI^3}}{(1+(1+Ee^{FI^3})\sqrt{I}} + {}$$

$$+ B\, 10^{\frac{D\sqrt{I}}{1+(1+Ee^{FI^3})\sqrt{I}}} \, q\,(1+0.1I)^{(q-1)}\, 0.1\, dI \qquad (35)$$

where $B = 0.75 - 0.065\, q$

$D = -0.5107$

$E = 0.055\, q$

$F = -0.023$

$I = I_{ij}^{o}$

$q = q_{ij}^{o}$

$I = I_{ij}^{o}$, $q = q_{ij}^{o}$

The new integral limits for the ionic strength being now zero and I_{ij}. These equations can be handily solved by computer for a_w^{o}. Also, a graphical solution of the equation is available.

In the case of mixed solutions, where more than one strong electrolyte is present, the value of the activity coefficient $\gamma_{ij,mix}$ for each dissolved electrolyte can be determined at any value of I_T. As before, $\Gamma_{ij,mix}$ is equal to $(\gamma_{ij,mix})^{1/z_iz_j}$.

Addition or removal of water only from a mixed solution leaves the solution's "dry composition" unchanged. At any constant dry composition and constant temperature, $\Gamma_{ij,mix}$ for any component plotted against I_T, forms again a curve falling into the same family of curves. Equation 31 applies therefore again provided that q_{ij}° is replaced by $q_{ij,mix}$ which is calculated as follows:

$$q_{12,mix} = B_{12} + D_{12} \tag{36}$$

where B_{12} is the interaction of anion 2 with each of the cations present:

$$B_{12} = I_1/I_T q_{12}^{\circ} + I_3/I_T\, q_{32}^{\circ} + I_5/I_T\, q_{52} + \ldots$$

while D_{12} is the interaction of cation 1 with each of the anions present:

$$D_{12} = I_2/I_T\, q_{12}^{\circ} + I_4/I_T\, q_{14}^{\circ} + I_6/I_T\, q_{16}^{\circ} + \ldots$$

A mixed solution of total ionic strength I_T is made by adding N_{12},N_{32}, N_{52}, etc. moles of the indicated electrolytes to 1000 g water. Considering these electrolytes to exist in "pure" form, then the respective initial ionic strengths of each would be I_{12}^{in}, I_{32}^{in}, I_{52}^{in}, etc. By defining $a_{12} = I_{12}^{in}/I_T$, $a_{32} = I_{32}^{in}/I_T$, etc., the water vapor pressure over this mixed solution then becomes:

$$a_{w,mix} = A_{12}^{a12}\, A_{32}^{a32}\, A_{52}^{a52} \ldots \tag{37}$$

The quantity A_{12} is the activity of water in a hypothetical pure solution whose q_{12}^{o} value equals $q_{12,mix}$ at the total ionic strength of the mixture.

The activity of a dissolved electrolyte in solution is expressed as $m_i^{v_i} m_j^{v_j} \quad {}_{ij}^{v_{ij}}$, where $v_{ij} = v_i + v_j$. On the other hand, the activity $(a_{ij}^{o})_{sat}$ of a solid electrolyte (generalized as $A_{v+}B_{v-}.nH_2O$) in equilibrium with its pure saturated solution becomes:

$$SP_{12}^{o} = a_{12}^{o}{}_{,sat} = (m_1^{o})_{sat}^{v_1}(m_2^{o})_{sat}^{v_2}(\gamma_{12}^{o})^{v_{12}}(a_w^{o})_{sat}^{n} \quad (38)$$

To avoid confusion, $(a_{12}^{o})_{sat}$ is here also called SP^{o}, the "thermodynamic solubility product". For this same solid electrolyte in equilibrium with any one of its saturated mixed solutions:

$$SP_{12,mix} = a_{12,mix,sat} = (m_1)_{sat}^{v_1} m_2)_{sat}^{v_2}(\gamma_{12,mix})^{v_{12}} a_w)_{sat}^{n} \quad (39)$$

Development of the Algorithm

For the efficient use of the previously presented method it is necessary to develop a computer algorithm for the solution of the given equations, under different applied conditions.

The developed algorith for the $CaCl_2/HCl/RaSO_4$ system is presented in Fig. 87 . A brief description of this flowchart is essential.

In the beginning of the program the concentrations of $CaCl_2$, HCl and SO_4^{2-} are introduced as well as the solution temperature. A convenient way to supply a series of values to these variables is with the use of appropriate DO loops.

The next step is to calculate the various ionic strength's components ($I_{Ca^{2+}}$, I_{Cl^-}, I_{H^+}) and the total ionic strength (I_T) of the solution. The equations 29 and 30 are used.

Now, if the $CaCl_2$ concentration is zero or not will determine the next step. For $CaCl_2$ concentrations different than zero, the characteristic constant $q_{CaCl_2,mix}$, for the $CaCl_2/HCl$ mixture is estimated with the use of equation 36 assuming that SO_4^{2-} concentration is negligent. Then this constant is corrected for higher temperatures by introducing equation 32.

To calculate the activity of the water, as a function of $CaCl_2$, integral 34 has to be solved. This was succeeded with the utilization of Simpson's rule, a numerical analysis method. So, using I_T and q_{CaCl2,mix,T^oC} and equations 31,33,34 and 35 the $A_{w,CaCl2}$ value was obtained.

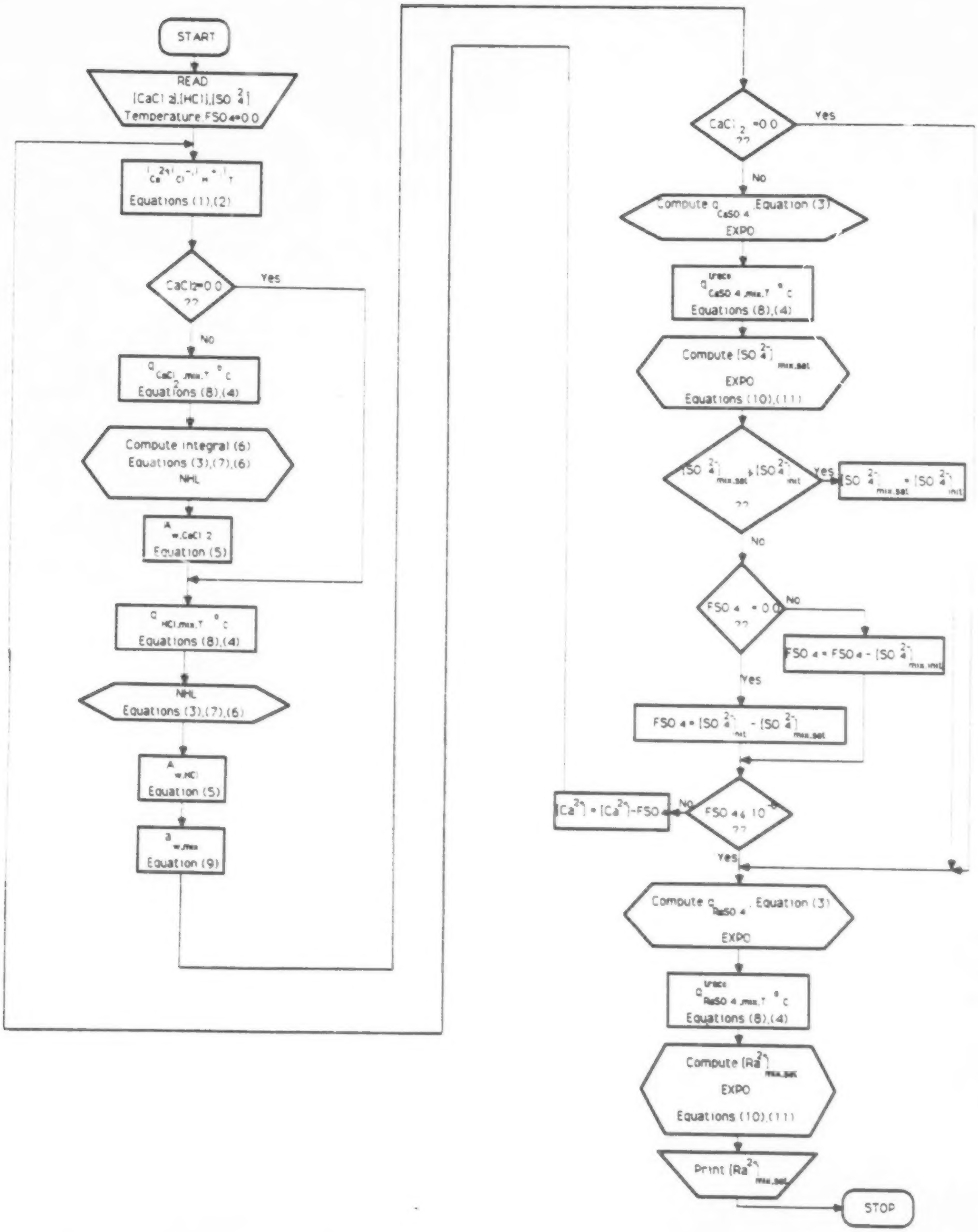
START
READ
[CaCl2],[HCl],[SO 2 4]
Temperature,FSO4=0.0
Equations (1),(2)
CaCl2=0.0 ??
Yes
No
Equations (8),(4)
Compute integral (6)
Equations (3),(7),(6)
NHL
Equation (5)
Equations (8),(4)
NHL
Equations (3),(7),(6)
Equation (5)
Equation (9)
Compute q CaSO4 Equation (3)
EXPO
Equations (8),(4)
Compute [SO 2- 4] mix,sat
EXPO
Equations (10),(11)
FSO4 = 0.0 ??
FSO4 = FSO4 - [SO 2- 4] mix,init
FSO4 = [SO 2- 4] init - [SO 2- 4] mix,sat
[Ca2+] = [Ca2+] - FSO4
FSO4 ≤ 10
Compute q RaSO4 Equation (3)
EXPO
Equations (8),(4)
Compute [Ra2+] mix,sat
EXPO
Equations (10),(11)
Print [Ra2+] mix,sat
STOP

Fig. 87 The flowchart of the algorithm used to estimate the solubility of $RaSO_4$ in $CaCl_2$/HCl media.

The same approach is followed in the estimation of $q_{HCl,mix}$, $q_{HCl,mix,T^{o}C}$, and $A_{w,HCl}$. Finally, equation 37 gives the water activity of this mixed solution.

In an aqueous chemical solution, where Ca^{2+} and SO_4^{2-} ions exist in significant concentrations, the formation of gypsum ($CaSO_4.2H_2O$) is eminent. The computer program takes into account gypsum's solubility in order to determine the SO_4^{2-} concentration in the solution and, subsequently, the maximum Ra^{2+} concentration in solution.

In the case of $CaCl_2$ concentration not equal to zero, the characteristic constant q_{CaSO4} has to be estimated. This is done through Meissner's estimation method (72). According to this method, the reduced activity coefficient (Γ^{o}_{CaSO4}) is estimated first at an ionic strength of 2, and subsequently q_{CaSO4} is estimated from equation 31 with the help of a numerical analysis method (Secant). Using this value, the quantity $q_{CaSO4,mix,T^{o}C}$ is calculated from equations 36 and 32, having in mind that $CaSO_4$ exists in traces in the $CaSO_4/CaCl_2/HCl$ system.

From this point on, equations 31,38 and 37 are used to obtain the maximum SO_4^{2-} concentration in the solution. This SO_4^{2-} concentration is then compared with the initial SO_4^{2-} concentration and accordingly is corrected, till the equilibrium value is reached.

To proceed with the estimation of q_{RaSO4}, an assumption was made, that $BaCl_2$ and $RaCl_2$ have similar chemical characteristics and so their q constants are equal. Based on this assumption q_{RaSO4} was estimated with Meissner's method, as previously, and with equation 31. Furthermore, q_{RaSO4,mix,T^oC} is calculated with equations 36 and 32, with the justified simplification that $RaSO_4$ exists in traces in the $RaSO_4/CaCl_2/HCl$ system. Also, due to lack of information, it was assumed that solid $RaSO_4$ has no waters in its crystal structure.

Finally, using equations 31,38 and 39 the maximum Ra^{2+} concentration in solution is obtained under $RaSO_4$ saturation conditions.

A similar, but much simpler, approach was used to estimate the solubility of $RaSO_4$ in the case of NaCl/HCl and KCl/HCl systems. This was done in an effort to compare the effectiveness of the different leaching media, that is $CaCl_2$/HCl used in the present work and NaCl/HCl and KCl/HCl employed by other investigators.

The pertinent q^o values used for the calculation of $RaSO_4$ solubility are summarized in Table 27. It is worthy to note here that H_2SO_4 does not follow closely the behaviour of the other electrolytes present in the system due to its incomplete dissociation. Thus a single q^o value cannot be assigned to it. Instead the formula (38)

$$\log(-q^{o}_{H2SO4}) = 0.8803 - 0.4316\sqrt{I} \tag{38}$$

reported recently by Tozawa and Sasaki (74) has been applied.

Table 27 Electrolytes and pertinent parameters used for the estimation of $RaSO_4$ solubility.

Electrolyte	q^o (at 25°C)	m^o_{sat}
HCl	6.69	-
H_2SO_4	$-10^{0.8805-0.4316\sqrt{I}}$	-
$CaCl_2$	2.40	7.462 ($CaCl_2.2H_2O$)
$CaSO_4$	0.108 (estimated)[1]	0.0156 ($CaSO_4.2H_2O$)
$BaCl_2$	1.48	1.157 ($BaCl_2.2H_2O$)
$RaCl_2$	1.48 (assumed)[2]	-
$RaSO_4$	0.049 (estimated)[3]	0.652×10^{-5} ($RaSO_4$)
NaCl	2.23	6.146 (NaCl)
Na_2SO_4	-0.19	1.971 ($Na_2SO_4.10H_2O$)
KCl	0.92	4.794 (KCl)
K_2SO_4	-0.25	0.617 (K_2SO_4)

1. Estimation based on $q^o_{CaCl_2}$, Ref. 72

2. Assumed $q^o_{RaCl_2} = q^o_{BaCl_2}$

3. Estimation based on $q^o_{RaCl_2}$, Ref. 72

7. REFERENCES

1. Technical Reports Series No. 196: International Atomic Energy Agency; Vienna; Significance of mineralogy in the development of flowsheets for processing uranium ores, 23-26, 1980.

2. Itzkovitch, I.J. and Ritcey, G.M. "Removal of radionuclides from process streams - a review", CANMET Report 79-21, CANMET, Energy, Mines and Resources Canada, Ottawa, 1979.

3. Proc. OECD/NEA Sem. on Management, Stabilization and Environmental Impact of Uranium Mill Tailings, Albuquerque, New Mexico, July 1978.

4. Proc. OECD/NEA Workshops on Uranium Mill Tailings Management, Ft. Collins, Colorado, Oct. 1981.

5. Report of the National Technical Planning Group on Uranium Tailings Research; CANMET, Energy, Mines and Resources Canada, Ottawa, Sept. 1981.

6. Weir, D.R. and Masters, I.M. Key Lake project process development - Part I - uranium extraction, paper presented at the 19th Ann. Conf. Metallurgists, CIM, Halifax, N.S., August 1980, 9-48.

7. Scales, M. Key Lake uranium mill largest in the world, Can. Min. J., 105, 1984, 10-20.

8. Borrowman, S.R. and Brook, S.P.T. Radium removal from uranium ores and mill tailings, RI-8099, U.S. Bureau of Mines 1975.

9. Nirdosh, I., Mathuswami, S.V. and Baird, M.H.I. Radium in uranium mill tailings - some observations on retention and removal, Hydrometallurgy, 12, 1984, 151-176.

10. Ritcey, G.M. Treatment of radioactive ores at CANMET, Division Report ERP/MSL 77-139 (OP), CANMET, Energy, Mines and Resources Canada, Ottawa, 1977.

11. Phillips, C.R. and Poon, Y.C. Status and future possibilities for the recovery of uranium, thorium, and rare earths from Canadian ores with emphasis on the problem of radium, Miner. Sci. Eng., 12, 1980, 53-72.

12. Pigford, T. Geological disposal of radioactive wastes, *Chem. Eng. Progr*. March 1982, 18-26.

13. Seeley, F.G. Problems in the separation of radium from uranium ore tailings, *Hydrometallurgy*, *2*, 1976/77, 249-263.

14. Ryon, A.D., Hurst, F.J. and Seeley, F.G. Nitric acid leaching or radium and other significant radionuclides from uranium ores and tailings, *ORNL/TM-5944*, Oak Ridge National Laboratory, 1977.

15. Skeaff, J.M. "Proposed route for nitric acid leaching of uranium ore and removal of Ra^{226} by EDTA, *Internal Report MSL-INT 78-101*, CANMET, Energy, Mines and Resources Canada, 1979.

16. Nirdosh, I. Ferric nitrate leaching of uranium and radium from uranium ores, *Hydrometallurgy*, *15*, 1985, 63-76.

17. Haque, K.E., Lucas, B.H. and Ritcey, G.M. Hydrochloric acid leaching of Elliot Lake uranium ore, *CIM Bull*. *73* (819), 1980, 141-147.

18. Haque, K.E. Chlorine-assisted leaching of typical Canadian uranium ores, Report *ERP/MSC* 80-167 (J), CANMET, Energy, Mines, and Resources Canada, 1980.

19. Torma, A.E., Gündiler, I.H., Kirby, D.J., Sandana, J.J. and Yen, S-Y. Hydrochloric acid leaching of a low-grade New Mexico Uranium Ore, *METALL* *37*, 1983, 148-152.

20. Nirdosh, I., Baird, M.H.I., Muthusurami, S.V. and Banergee, S. Co-extraction of uranium and radium from ore with ferric chloride , *Hydrometallurgy*, *10*, 1983, 265-283.

21. Demopoulos, G.P. Acid pressure leaching of a sulphidic uranium ore with emphasis on radium extraction, *Hydrometallurgy*, *15*, 1985, 219-242.

22. Demopoulos, G.P. Pressure leaching of uranium ores in a calcium chloride medium with simultaneous solubilization of radium , *Trans. IMM*, (Sect. C) March 1987 (in press).

23. Demopoulos, G.P. and G.M. Ritcey. Pressure leaching of uranium ores in a chloride medium, *Can. Pat. Appl*. No. 265-7826-2, June 28, 1985.

24. Robins, R.G., *Hydrometallurgy: Research, Development and Plant Practice*, Eds. K. Osseo-Asare and J.D. Miller, AIME, Warrendale, Pa, 1983, pp. 291-310.

25. Impurity Control and Disposal, Ed. A.J. Oliver, CIM, Vancouver, B.C., August 1985.

26. Dutrizac, J.E. and Morrison, R.M., Hydrometallurgical Process Fundamentals, R.G. Bautista, Ed. Plenum Press, New York, N.Y., 1984, pp. 77-112.

27. Arnold, J.P. and Johnson, R.M., Talanta, 16, 1969, pp. 1191-1207.

28. Kedzierzowski, P. and Szkarska-Smialowska, Z., J. Electroanal. Chem. 122, 1981, pp. 269-278.

29. Papangelakis, V.G., Berk, D. and Demopoulos, G.P., "Hydrometallurgical Reactor Design and Kinetics", Eds. R.G. Bautista, R. Wesely and G.W. Warren, AIME, Warrendale, Pa, 1986, pp. 209-225.

30. Burkin, A.R., Manning, G.D. and Monhemius, A.J., Hydrometallurgy 81, SCI, Manchester, U.K., 1981, paper B5.

31. Pustovalov, N.N. et al., in Chemical Abstracts V. 87, No. 43600j (1977); 87, No. 28423k (1977); V. 86, No. 1280086 (1976).

32. Burkin, A.R. and Monhemius, A.J., Acid Leaching of Uranium Ores Using Hydrogen Peroxide and Caro's Acid , paper presented at the 8th CIM Hydrometallurgical Meeting, Montreal, Que., Aug. 1978.

33. Tan, L.K. and Dutrizac, J.E., Anal. Chem. 57, 1985, (a) pp. 1027-1032; (b) 2615-2620.

34. Natarajan, K.A. and Iwasaki, I., Minerals Sci. Engng., 6, No. 1, 1974, pp. 35-44.

35. Tozawa, K. and Nishimura, T., Nippon Kogyo Kaishi, 92 (1066), 1976, pp. 809-814.

36. Harris, G.B. and Monette, S., Complex Sulfides: Processing of Ores, Concentrates and By-Products , Eds. A.D. Zunkel, R.S. Boorman, A.E. Morris and R.J. Wesely, AIME, Warrendale, Pa, 1985, pp. 361-375.

37. Papangelakis, V.G. and Demopoulos, G.P., Aqueous pressure oxidation of arsenopyrite , to be submitted to Canadian Metallurgical Quarterly.

38. Neven, M., Steane, R. and Becker, J., Arsenic Management and Control at Key Lake , in Impurity Control and Disposal, Proc. 15th Ann. Hydromet. Meeting, CIM, Vancouver, B.C., August 1985, paper 6.

39. Sarkar, K.M. Temperature control of acid pressure leaching of uranium ores, *Trans. Inst. Min. Metall.* (Sect. C: Mineral Process Extr. Metall.), *93*, 1984, C23-C29.

40. Sarkar, K.M., Selection of Autoclaves in Hydrometallurgical Operations , *Trans. IMM (Section C)*, *94*, 1985, C184-C194.

41. Box, G.E.P., Hunter, W.G. and Hunter, J.S., *Statistics for Experimenters:* An Introduction to Design Data Analysis and Model Building , J. Wiley and Sons, N.Y., 1978.

42. Box, G.E.P. and Behnken, D.W., Some New Three Level Designs for the Study of Quantitative Variables , *Technometrics*, 1960, *2*, pp. 455-75.

43. Anon, *Strategy of Experimentation* , E.I. du Pont de Nemours and Co. (Inc.), Applied Technology Division, Wilmington, Delaware (1984).

44. Daniel, C. and Wood, F.S., *Fitting Equations to Data* , 2nd Edition, J. Wiley and Sons, New York, N.Y., 1980, pp. 5-18.

45. Bacon, D.W., Making the Most of a "one-shot" Experiment , *Ind. Eng. Chem*., 1970, *62*, no. 7, pp. 27-34.

46. Gatzweiler, R., Lehyert-Thiel, K., Chasey, D., Tay, B., Voutsidis, V., Strnad, J.G. and Rich, J., The Key Lake Uranium-Nickel Deposits , *CIM Bulletin*, July 1979, pp 73-79.

47. Rand, D.A.J. and Woods, D., E_h Measurements in Sulphide Mineral Slurries , *Int'l. J. Min. Proc*., *13*, 1984, pp 29-42.

48. Maj H., Awakura, Y., Sato, K. and Hirono, S., Calculation of Equilibrium Species for the Aqueous Solution Systems of UO_2SO_4-$U(SO_4)_2$ - H_2SO_4 - HF and UO_2Cl_2 - UCl_4 - HCl - HF at 298 K , *Metall. Trans. B*, March 1987, *18B*, pp. 49-57.

49. Gasparrini, C. and R.G. Williamson, The mineralogy of the uranium ores with some considerations of their significance in metal extraction and mineral exploration , *Process Mineralogy: Extractive Metallurgy, Mineral Exploration, Energy Resources*, TMS-AIME, Warrendale, PA, 1981, 325-337.

50. Peters, E. Application of chloride hydrometallurgy in treatment of sulphide minerals , in *Chloride Hydrometallurgy*, Benelux Metallurgie, Brussels, Sep. 1977.

51. Muir, D.M. and Senanayake, G., Principles and Applications of Strong Salt Solutions to Mineral Chemistry , Extraction Metallurgy '85, Australasian I.M.M., 1985, pp. 65-91.

52. Monhemius, A.J. Precipitation diagrams for metal hydroxides, sulphides, arsenates and phosphates, Trans. Inst. Min. Met. (Sect. C: Mineral Process. Extr. Metall.) 86, 1977, C202-C206.

53. Meissner, H.P., Prediction of Activity Coefficients of Strong Electrolytes in Aqueous Systems , ACS Symposium Series, No. 133, 1980, pp. 495-511.

54. Barrow, G.M. Physical Chemistry , 4th edition, McGraw Hill, N.Y., 1979, pp.593-612.

55. Demopoulos, G.P., Kondos, P. and Papangelakis, V.G., Prediction of Solubilities in Chemical Compound Precipitation Systems , paper to be presented at ISCAP, Saskatoon, Sask., October 1987.

56. Marshall, W.L. and Slusher, R., Thermodynamics of Calcium Sulfate Dihydrate in Aqueous Sodium Chloride Solutions, 0-110,011 , J. Phys. Chem., 70(12), 1966, pp. 4015-4027.

57. Block, J. and Waters, O.B., The $CaSO_4$-Na_2SO_4-NaCl-H_2O System at 25° to 100°C , J. Chem. Eng. Data, 13(3), 1968, p. 336.

58. Cotton, F.A. and G. Wilkinson, Advanced Inorganic Chemistry , 4 Ed., John Wiley and Sons, New York, N.Y., 1980, p. 271.

59. Robins, R.G. The Solubility of Barium Arsenate: Sherritt's Barium Arsenate Process, Metall. Trans. B, 16B, 1985, 404-406.

60. Sedlet, J. Radon and radium, in: I.M. Kolthoff and P.J. Elving (Eds) Treatise on Analytical Chemistry, Part II, Wiley-Interscience, New York, 1960, 4, pp. 297-298.

61. Sedlet, J. Radon and radium, in: I.M. Kolthoff and P.J. Elving (Eds) Treatise on Analytical Chemistry, Part II, Wiley-Interscience, New York, 1960, 4, pp. 163-205.

62. Tsezos, M., Walker, C. and Keller, D., Adsorption of Radium-226 from Solution by the Container Walls , The Con. J. of Chem. Eng., 64, April 1986, pp. 346-348.

63. Demopoulos, G.P., Development of a Single-Stage Pressure Chloride Leaching System for Gold Extraction from Refractory Concentrates , work under investigation, EMR Research Agreement 191, 1986-87.

64. Smyres, G.A., Kral, R.L., Lei, K.P.V. and Carnahan, T.G., Calcium Chloride-Oxygen Leaching of an Arsenical Cobalt-Copper Concentrate , Complex Sulfides: Processing of Ores, Concentrates and By-Products, eds A.D. Zunkel, R.S. Boorman, A.E. Morris and R.J. Wesely, The Metallurgical Society, Inc., 1985, p. 359.

65. Van Ceulen, A. and C. Eusebe Traitement de résidus de l'hydrometallurgie du zinc, Memoires et Etudes Scientifiques Rev. Métall., Octobre, 1982, p. 569-576.

66. Odencrantz, J.T. and Rieman, W. Determination of As in Insecticides , Anal. Chem., 1950, 22, 1066.

67. Charlot, G., Potentiometry and Titration , Bull. Soc. Chim. Fr., 1941, 8, 222.

68. Charlot, G. and Bézier, D., Quantitative Inorganic Analysis , London: Methuen, New York: John Wiley, 1957, p. 337-338.

69. Rolia, E. and Dutrizac, J.E., The Determination of Free Acid in Zinc Processing Solutions , Can. Met. Q., 23, No. 2, pp. 159-167, 1984.

70. Kusic, C.L. and Meiss er, H.P., Electrolyte Activity Coefficients in Inorganic Processing , AIChE Symp. Ser. No. 173, 1978, pp. 14-20.

71. Kusik, C.L., Meissner, H.P., Vapor Pressures of Water Over Aqueous Solutions of Strong Electrolytes , Ind. Eng. Chem., Proc. Des. Dev., 1973, 12, pp. 112-115.

72. Meissner, H.P., Tester, J.W., Activity Coefficients of Strong Electrolytes in Aqueous Solutions , Ind. Eng. Chem., Proc. Des. Dev., 1972, 11, pp. 128-133.

73. Meissner, H.P., Manning, M.P., Prediction of Solubilities and Activity Coefficients in Sodium-Potassium-Magnesium Chloride Brines , Chem. Eng. Thermod., 1983, ch 28, pp. 339-348.

74. Tozawa, K. and Sasaki, K., Effect of Coexisting Sulphates on Precipitation of Ferric Oxide from Ferric Sulphate Solutions at Elevated Temperatures , Iron Control in Hydrometallurgy, eds. J.E. Dutrizac and A.J. Monehmius, Ellis Horwood, 1986, pp. 454-476.